

ERNEST ORLANDO LAWRENCE
BERKELEY NATIONAL LABORATORY

Capture Efficiency of Cooking-Related Fine and Ultrafine Particles by Residential Exhaust Hoods

Melissa M. Lunden, William W. Delp, Brett C. Singer

Environmental Energy Technologies Division

June 2014

This work was supported by the California Energy Commission PIER-Environmental Program via Contract 500-09-024; the U.S. Department of Energy Building America Program via Contract DE-AC02-05CH11231; the U.S. Department of Housing and Urban Development, Office of Healthy Homes and Lead Hazard Control via Agreement I-PHI-01070; and the U.S. Environmental Protection Agency Indoor Environments Division via Agreement DW-89-9232201-0

DISCLAIMER

This document was prepared as an account of work sponsored by the United States Government. While this document is believed to contain correct information, neither the United States Government nor any agency thereof, nor The Regents of the University of California, nor any of their employees, makes any warranty, express or implied, or assumes any legal responsibility for the accuracy, completeness, or usefulness of any information, apparatus, product, or process disclosed, or represents that its use would not infringe privately owned rights. Reference herein to any specific commercial product, process, or service by its trade name, trademark, manufacturer, or otherwise, does not necessarily constitute or imply its endorsement, recommendation, or favoring by the United States Government or any agency thereof, or The Regents of the University of California. The views and opinions of authors expressed herein do not necessarily state or reflect those of the United States Government or any agency thereof, or The Regents of the University of California.

Ernest Orlando Lawrence Berkeley National Laboratory is an equal opportunity employer

PUBLICATION NOTE

The main body of this report and Appendix A present the content that is included in a scientific paper bearing the same title and authors that was published online 24-May-2014 by the journal Indoor Air (DOI: 10.1111/ina.12118). Appendices B-H of this report provide additional information and details that are not included in the Indoor Air journal paper.

Table of Contents

Abstract	2
Key Words	2
Practical Implications.....	2
Introduction.....	2
Materials and Methods.....	4
Overview.....	4
Range Hoods.....	4
Experimental Setup.....	4
Airflow and Mixing Verification Experiments.....	5
Pollutant Measurements.....	7
Cooking Procedures.....	7
CO ₂ -Based Capture Efficiency	8
Experimental Schedule	8
Capture Efficiency Calculations	9
Uncertainty in Calculated Capture Efficiencies.....	11
Results and Discussion	12
Measured Concentrations.....	12
Capture Efficiency Results	14
Airflow and Mixing Verification Experiments.....	17
Comparisons to Published Studies on Cooking Hood Effectiveness.....	18
Conclusions.....	19
Acknowledgements	19
Literature Cited	20
Appendix A: Supporting Information.....	0
Appendix B: Detailed Cooking Protocols.....	8
Appendix C: Summary of Experiments.....	17
Appendix D: Results of Experiments Conducted without Exhaust.....	20
Appendix E: Results of Experiments Conducted with Hood L1	53
Appendix F: Results of Experiments Conducted with Hood E2	73
Appendix G: Results of Experiments Conducted with Hood M1.....	103
Appendix H: Results of Experiments Conducted with Hood P1	123

List of Figures

Figure 1. Experimental configuration of the room used to measure gas and particle phase capture efficiency.....	6
Figure 2. Concentrations of CO ₂ in the hood exhaust and particles in room measured by the CPC and OPC resulting from (a) pan-fry and (b) stir-fry cooking activities.....	13
Figure 3. Concentration of particles ≥ 6 nm as measured by the CPC from a sampling point near the exhaust outlet of room. Data shown for pan-frying experiments with no hood present (black dashed line) and with hood E2 operating on low (red) and high (blue) fan speeds.	15
Figure 4. Capture efficiencies (CE) calculated using CO ₂ measured in hood exhaust and particles measured in room for pan-frying hamburger.	16
Figure 5. Capture efficiencies (CE) calculated using CO ₂ measured in hood exhaust and particles measured in room for stir-frying green beans.	17
Figure 6. Capture efficiencies (CE) calculated using CO ₂ and particle measurements for stir frying on the front or back burners.....	18

List of Tables

Table 1. Summary results for hamburger pan-frying experiments.....	14
Table 2. Summary results for green bean stir-frying experiments.....	14

Capture Efficiency of Cooking-Related Fine and Ultrafine Particles by Residential Exhaust Hoods

Melissa M. Lunden^{1,2}, William W. Delp¹, Brett C. Singer^{1*}

¹Indoor Environment Group and Residential Building Systems Group, Environmental Energy Technologies Division, Lawrence Berkeley National Laboratory, Berkeley CA, USA

²Aclima Inc., San Francisco, CA, USA

*Corresponding author contact information:

1 Cyclotron Road, MS90-3058, Lawrence Berkeley National Lab, Berkeley CA 94720, USA

Email: bcsinger@lbl.gov; Tel: 1-510-486-4779

Abstract

Effective exhaust hoods can mitigate the indoor air quality impacts of pollutant emissions from residential cooking. This study reports capture efficiencies (CE) measured for cooking generated particles for scripted cooking procedures in a 121-m³ chamber with kitchenette. CEs also were measured for burner produced CO₂ during cooking and separately for pots and pans containing water. The study used four exhaust hoods previously tested by Delp and Singer (Environ. Sci. Technol., 2012, 46, 6167-6173). For pan-frying a hamburger over medium heat on the back burner, CEs for particles were similar to those for burner produced CO₂ and mostly above 80%. For stir-frying green beans in a wok (high heat, front burner), CEs for burner CO₂ during cooking varied by hood and airflow: CEs were 34–38% for low (51–68 L s⁻¹) and 54–72% for high (109–138 L s⁻¹) settings. CEs for 0.3–2.0 μm particles during front burner stir-frying were 3–11% on low and 16–70% on high settings. Results indicate that CEs measured for burner CO₂ are not predictive of CEs of cooking-generated particles under all conditions, but they may be suitable to identify devices with CEs above 80% both for burner combustion products and for cooking-related particles.

Key Words

Cooker hood; Extractor fan; Kitchen ventilation; PM_{2.5}; Range hood

Practical Implications

This study reinforces previous findings that exhaust hoods can be much more effective in capturing pollutants when cooking occurs on the back burners, compared to the front cooktop burners. Results indicate that capture efficiency (CE) measured for burner produced CO₂ is not predictive of CE for cooking-generated particles under all conditions, but results of a CO₂-based CE test may be suitable to identify devices with CEs above 80% for both burner combustion products and cooking-related particles. Development of a standard test method for pollutant capture efficiency is an important step to providing effective kitchen ventilation in residences.

Introduction

Pollutant emissions from cooking burners and the cooking of food can substantially and adversely impact air quality in homes. Natural gas burners commonly emit nitrogen dioxide

(NO₂) and under some conditions emit substantial quantities of carbon monoxide (CO), formaldehyde (HCHO) and ultrafine particles (UFP) (Wallace et al., 2004; Singer et al., 2010; Dennekamp et al., 2001; Moschandreas and Relwani, 1989). Electric coil resistance burners produce UFP (Dennekamp et al., 2001). Cooking activities produce fine and ultrafine particles and a wide range of irritant and other potentially harmful gases including acrolein (Abdullahi et al., 2013; Fortmann et al., 2001; Buonanno et al., 2009; Fullana et al., 2004; Seaman et al., 2009; Zhang et al., 2010). Gas burners and cooking also release substantial quantities of water vapor that can contribute to moisture related indoor air quality problems (Parrott et al., 2003). Individual cooking events can produce short-term PM_{2.5} concentrations exceeding 300 µg m⁻³ and UFP concentrations exceeding 10⁵ cm⁻³ in homes (Abdullahi et al., 2013; Buonanno et al., 2009; Wallace et al., 2004; Zhang et al., 2010; He et al., 2004; Afshari et al., 2005). A recent study estimated that among Southern California homes that cook with natural gas on a weekly basis, >5% have acute CO and >50% have 1-h NO₂ concentrations that exceed the corresponding concentration thresholds for health-based ambient air quality standards (Logue et al., 2013).

Indoor concentrations of pollutants generated during cooking can be reduced through use of an exhaust hood positioned above the cooktop or an exhaust fan in the kitchen. Exhaust hoods remove some fraction of the emitted pollutants before they mix into the general air volume of the kitchen with additional removal as air from the kitchen is exhausted outdoors. Exhaust fan effectiveness can be described as a capture efficiency (Li and Delsante, 1996; Li et al., 1997; Singer et al., 2012) that quantifies the fraction of generated pollutants removed either directly or over the duration of exhaust fan operation. Alternately, effectiveness can be framed as the reduction in pollutant concentrations in the kitchen or other location in the home (Rim et al., 2012; Zhang et al., 2010). Direct removal without mixing into the kitchen is termed first-pass CE; including removal from the exhaust provided by the fan gives total CE.

Published studies conducted in laboratories, test homes and in the field have reported CE or other metrics of exhaust hood removal effectiveness for gases, particles, or moisture produced by natural gas burners (Farnsworth et al., 1989; Delp and Singer, 2012; Singer et al., 2012; Rim et al., 2012). Performance has been shown to vary with airflow; hood geometry and height with respect to the cooktop; whether front, back or oven burners were used; and hood design, which is most prominently differentiated by the collection volume offered by the hood. A few studies have reported on the effectiveness of range hoods at reducing concentrations of particles generated by cooking activities (Sjaastad and Svendsen, 2010; Zhang et al., 2010).

Currently in the US there is no direct information available to consumers about the pollutant removal effectiveness of cooking exhaust hoods. The Home Ventilating Institute (HVI) provides third party certification of airflows and sound levels determined using standard test methods (HVI, 2013b; HVI, 2013a). Rated airflows and sound levels are listed in a catalog that is updated monthly by HVI (<http://www.hvi.org/proddirectory/index.cfm>). Standard IEC-61591 (IEC, 2005) quantifies grease removal effectiveness for an oil-drop heating event by pre- and post-weighing of the hood and filters and includes a test for odor removal; but this test is not commonly used to rate products sold in the US.

A relatively simple test method was used recently by Delp and Singer (2012) to characterize CE of seven exhaust hoods in a controlled laboratory study and by Singer et al. (2012) to quantify CE for 13 exhaust hoods and two downdraft systems installed in residences. The method calculates CE as the ratio of incremental CO₂ mass removal through the exhaust hood to CO₂ generation by the burners. Incremental CO₂ exhaust flow is calculated as the product of the measured airflow rate through the exhaust hood and the measured increase in CO₂

concentration in the exhaust flow during burner use. The method looks at incremental CO₂ flow because there is a baseline flow of CO₂ from ambient air and from additional CO₂ exhaled by the cook and other building occupants. The method uses CO₂ as a surrogate for all combustion products emitted by a gas burner. The test method incorporates pots of water on the cooktop burners to simulate the impact of cooking vessels on the dynamics of the exhaust plumes.

The work described in this paper was initiated with the dual objectives of (1) quantifying CE for particles generated during typical cooking events and (2) conducting a preliminary assessment of the applicability of the simple, CO₂-based test method as an indicator of capture efficiency for cooking-related particles.

Materials and Methods

Overview

Capture efficiencies (CE) were determined for four under-cabinet exhaust hoods under carefully controlled conditions in an experimental room. CE for burner pollutants was determined directly by comparing the CO₂ mass flow through the exhaust hood to the CO₂ produced at the burner. CE for cooking particles was determined indirectly by comparing particle concentrations in the room when a hood was in use to concentrations measured during the same cooking activity with no hood installed. The indirect approach was required because particle losses in the hood and ductwork would bias the concentrations seen in the hood exhaust stream and consequently bias the calculated particle CE. The room was supplied with particle free air through HEPA filters and the room was maintained at a positive pressure of 1 Pa relative to the outdoors. The flow rate of the main exhaust air pathway – through a blower door – was modulated to maintain a constant total exhaust flow as airflow through the cooking exhaust hoods was varied.

Range Hoods

Particle CEs were determined for four hoods previously investigated by Delp and Singer (2012). The tested hoods included a low cost model (L1), an Energy Star qualified model (E2), a premium hood (P1), and a combined microwave exhaust hood (M1) that represent common geometries and ranges in airflow rates. The microwave was mounted at the same height as the other hoods but the bottom of the unit was closer to the stovetop, as occurs in typical installations. The microwave drew air from both the bottom and top front of the unit.

Experimental Setup

A schematic of the laboratory layout is shown in Figures 1a and 1b. The volume of the room was 121 m³ (5.8 m by 7.2 m by 2.9 m high). A simulated residential cooking area was affixed to a 2.4 m by 2.4 m section of wall located approximately 1/3 of the length of the room closest to the supply air. Each range hood was mounted on this wall with the top of the hood positioned 76 cm above the cooktop of a 76 cm wide cooking range (Delp and Singer, 2012). The hoods were mounted between drywall boxes installed to simulate a kitchen with wall cabinets adjoining the hood. The cooking range was installed between drywall boxes topped with steel sheeting to simulate side cabinets and countertops. The top of the room consisted of structural 22.9 cm I-beams and the bottom of the steel roof deck with fiberglass batt insulation. Semi-rigid plastic sheeting was attached across the bottoms of the I-beams over the cooking area to keep the rising

exhaust plume out of the shallow channels formed by the I-beams. Baseline experiments were conducted with no hood in place above the stove.

The cooktop had one nominal 12,000 BTU h⁻¹ (12.7 MJ h⁻¹) burner at the front right position and three nominal 9500 BTU h⁻¹ (10.0 MJ h⁻¹) burners. The range was supplied 99.97% methane from certified cylinders (Airgas). Fuel flow was measured using a mass flow meter (Alicat, Model MLD-20SLPM-D/5M), factory calibrated for methane with an accuracy of 1%. Flow was reported at a reference condition of 1 atm and 25 C and logged at 1 Hz. Fuel flow was controlled using the burner adjustment knobs on the appliance.

Upon installation, a range hood was connected to a 0.6 m long section of 15.2 cm smooth galvanized ducting followed by 6 m of 15.2 cm diameter aluminum flexible ducting to vent to the outside. An Energy Conservatory Minneapolis Duct Blaster flow measurement device comprising a calibrated fan and throttling ring was placed inline approximately 2.4 m downstream of the hood. The Duct Blaster quantifies airflow based on the pressure difference measured across the throttling ring; it reports flow at a reference air density of 1.2014 kg m⁻³. An Energy Conservatory Automated Performance Testing (APT) measurement and control unit measured and recorded airflows and the Teclog software provided with the APT maintained a constant airflow rate. The flow rate through the hood was provided using both the hood fan and the Duct Blaster. An additional inline fan (Soler & Palau, PM-150X) was installed in the ducting to boost airflow when the exhaust hood and Duct Blaster together were not able to achieve the nominal airflow rates of the exhaust hood. Pressures and airflows were logged at 2 s intervals using Teclog software. The APT also measured temperature and relative humidity in the duct.

The room was operated at the same overall ventilation airflow rate for all experiments. Particle-free air was supplied to the room through HEPA filters (Airhandler, Terminal module 3EJY1) connected to inline blowers (Dayton, model 5TCK9) using 30 cm diameter aluminum flexible ducting. Room air was exhausted using an Energy Conservatory Minneapolis Blower Door. The pressure difference across the blower door was monitored using an Energy Conservatory DG-700 pressure and flow gauge with Teclog software to control the fan speed. The combined airflow supplied to the room was 765 L s⁻¹ (1620 cfm) as measured by constant injection tracer gas and confirmed by the measured SF₆ tracer decay rate of 23 hr⁻¹. Two household axial fans were added to improve mixing and reduce directional airflows around the range (Figure 1). Estimated airflows induced by Fans A and B were 292 L s⁻¹ and 552 L s⁻¹. The pressure across the building shell was monitored and recorded. When a range hood was used, the flow out of the blower door was lowered by the amount of flow through the hood while maintaining a positive pressure of approximately 1 Pa in the room.

Preliminary analysis of experimental results raised concerns about the accuracy of the recorded hood flow rates when the inline fan was used. The exhaust airflow rate for each range hood that was operated with the inline fan was checked using a second Duct Blaster connected to the inlet of the hood with a custom-fabricated connector. This is a routine field method, often called powered capture hood, used to measure flows for non-standard air system registers as described in the Duct Blaster manual (Energy Conservatory, 2007). For two of the three hoods used with the inline fan, the actual flow rate was higher than the set point. Adjustment factors were used to obtain accurate airflows for the hoods operated with the inline fan.

Airflow and Mixing Verification Experiments

During the set-up phase, we conducted tracer release experiments to investigate mixing and airflow patterns in the room

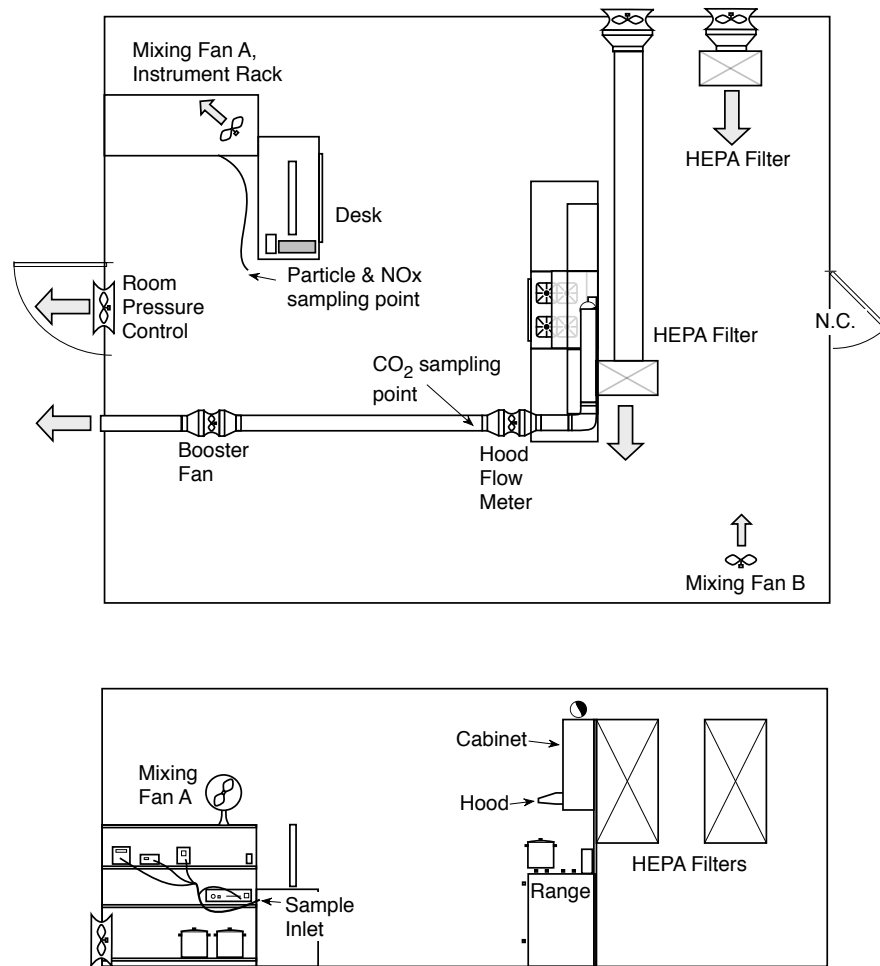


Figure 1. Experimental configuration of the room used to measure gas and particle phase capture efficiency.

The room is 5.8 m wide, 7.2 m in length, and 2.9 m high, and is drawn to scale.

In one experiment, SF₆ was released at the supply air inlet and concentrations were measured at the exit and at other locations within the room using an infrared gas analyzer (MIRAN SapphIRE Model 205B-XL, Thermo Scientific). The flow in the region in front of the stove was visualized using a smoke machine. The number, placement, and settings of mixing fans were adjusted to achieve generally consistent concentrations around the room and to minimize short-circuiting from the stove area or from the supply to the outlet.

The supplemental information provides details of experiments conducted to explore two key mixing questions: (1) whether there was any short-circuiting recirculation from the area above the hood – where pollutants would rise after not being captured on first pass – to the room air being drawn into the hood from the nearby surroundings, and (2) whether concentrations measured at the sampling location used throughout the CE tests accurately reflect concentrations in the air leaving the room through the blower door. Another experiment was conducted to compare CE values calculated using the direct method (based on mass flow of CO₂ through the exhaust hood) and the indirect method (based on particle flow out of the room). During a stir-fry cooking procedure, SF₆ was released into the wok through copper tubing formed into a Y and SF₆ concentrations were measured in both the hood (E2) and the room exhaust. Another

experiment examined the impact of ventilation and mixing fans on CE of burner pollutants: the blower door, supply and mixing fans were all turned off and CO₂ CEs were measured for hood E2. Results for these experiments are provided in Supplemental Figures S4 and S5.

Pollutant Measurements

Carbon dioxide concentrations in the range hood exhaust were measured each 2s using a PP Systems EGM-4 infrared analyzer. The flow in the exhaust was turbulent. The sampling location was 2 m downstream of the hood connection, corresponding to 12 duct diameters. Radial uniformity at this location was verified by moving the sampling probe through a full transverse during pilot experiments.

Particle number concentrations in room air were measured using two instruments. A condensation particle counter (CPC, Model 3781, TSI Incorporated) measured all particles ≥ 6 nm. An optical particle counter (OPC, Model BT-637S, MetOne Instruments) measured particles in 6 size bins: 0.3 to 0.5 μm , 0.5 to 0.7 μm , 0.7 to 1.0 μm , 1.0 to 2.0 μm , 2.0 to 5.0 μm , and above 5.0 μm . Measurements were recorded every 10 s.

Particle instruments sampled approximately 1.2 m away from the blower door fan 0.6 m off of the floor. This location was selected as the exhaust flow through the blower door ensured that all cooking emissions passed through this general location. The particles were sampled through a 1m length of 0.64 cm ID conductive tubing that was divided using flow splitters within a few centimeters of each instrument.

Cooking Procedures

Measuring CE for cooking-related particles requires cooking procedures with suitably repeatable particle generation rates; these depend on both the food being cooked and the cooking procedure. Carefully scripted cooking procedures were developed with the aim of repeatability.

We sought to develop at least two cooktop procedures and one oven procedure with distinct plume characteristics that vary in the challenge they present for capture. We developed a procedure for pan-frying a hamburger on medium heat on the back burner because the lower pan height, lower plume velocity, and the location on the back burner fully underneath all of the range hoods presents a geometry that facilitates high capture efficiency for exhaust gases. A stir-fry procedure using high heat with a wok on the front burner was developed as a more challenging, lower capture efficiency condition due to the wider and higher pan, more disruption of the plume by the activity of the cook (Huang et al., 2010), faster plume rise from higher energy input (Kosonen et al., 2006) and the location of the pan on the front burner. Efforts to develop an oven cooking activity are described in the Supporting Information.

Hamburgers were cooked on medium heat in vegetable oil in a nominal 11-inch (28 cm) stainless steel frying pan (Winco SSFT-11 Master Cook). The hamburgers were 85% lean / 15% fat, pre-formed, pure ground beef patties purchased at a local store of a nationwide specialty grocer. Individual patties were separated, wrapped in foil, and stored in a freezer. Patties were fully thawed and weighed before cooking. The pan was weighed and 3.5 \pm 0.05 g of canola oil was added. The burner was lit and adjusted to a gas flow rate of 1.7 \pm 0.1 lpm using the appliance burner control. The pan with oil was placed on the burner and the hamburger was added after 2 min. The burger was lightly pressed with a spatula for 5 s at each 1 min interval, flipped at 3 min, then pressed again at 1 min intervals until the burner was turned off after 6 min. The pan was allowed to cool for 30 s, after which it was covered, weighed, and removed from the room.

Green beans were selected for the stir-fry because they maintained structural integrity for the desired duration of cooking. Green beans were stir-fried using peanut oil in a nominal 15-inch (38 cm) carbon steel wok (Thunder Group Inc.). Green beans were purchased frozen in 680 g bags at the same store as the burgers. Twenty bags were purchased together and mixed to produce a homogeneous supply for experiments. Beans were measured into 150 ± 0.5 g portions, sealed in new plastic bags, and returned to the freezer. For each experiment, the wok was weighed and 10 ± 0.1 g of peanut oil added. The burner was lit and adjusted to a fuel flow rate of 4.4 ± 0.1 lpm. The wok was placed on the burner, and the beans added after 90 s. The beans were stirred continuously using a silicone spatula. After 3 min of cooking the burner was turned off and the wok was allowed to cool for 30 s; it then was covered, weighed, and removed from the room. Stir-fry experiments were conducted on the front burner for all hoods. The stir-fry procedure was conducted on the back burners to evaluate the effect of cooking burner position, using Hood E2 operating on low and high. A nominal 12-inch (30 cm) wok was used for these experiments because the 38 cm wok did not fit over the middle of the back burner.

CO₂-Based Capture Efficiency

Capture efficiency for burner combustion products was measured using the CO₂-based method outlined in Delp and Singer (2012). Two burner configurations were used: 1) both back burners and 2) both front burners. Covered 5L stainless steel pots filled with approximately 3L of water were placed on the cooktop burners to simulate use. The pots were placed on the stovetop, the burners were ignited and operated for 3 min, then turned off. The researcher moved away from the range after placing the pots of water to minimize activity-based air currents that can affect CE. This approach will be referred to as the POW (pots of water) CE test. Fuel flow rates were 8.5 ± 0.3 lpm for the two front burners and 7.6 ± 0.6 lpm for the two back burners.

The CO₂-based method was also used to calculate burner combustion product CE during the cooking activities; results of these calculations are identified in Figures 4–6 as “Cook”.

There were four important differences between the POW procedure and the scripted cooking activities: (1) the POW procedure used two burners whereas the cooking activities each used a single burner, resulting in different fuel flows and heat generation rates, (2) the water in the POW procedure provides a heat sink that can impact the burner plume; (3) the pans used in the cooking protocols have a different shape than those used in the POW procedure; and (4) a technician stood in front of the range to execute each cooking activity but avoided this area during the POW protocol. All four are expected to affect CE. Differences in vessel geometry, heat generation and removal rates, and the use of two vs. one burner all should impact both the geometry and fluid dynamic properties of the plume rising from the cooking burner(s). The activity of the cooking technician may intermittently disrupt the plume.

To explore the extent to which these factors affect CO₂-based CE, the CE of the frying pan and wok each were measured using a modified version of the POW test. The wok or pan was half-filled with water and covered with foil. Fuel flow rates and burner position were the same during the pan tests as during the cooking activities and CE was quantified similarly as the POW test.

Experimental Schedule

One of the supply fans providing HEPA filtered air operated continuously to maintain room air particle concentrations below ambient levels. The second supply fan and the exhaust fan(s) were

started at the beginning of each experimental day. Cooking experiments did not begin until the total particle concentrations in the room were stable and low, typically around 500 cm^{-3} .

Experiments were conducted June through October 2013. Five experiments each were conducted for most combinations of range hood, fan speed, and cooking procedure. Four experiments each were conducted for the hamburger and green beans on hood L1 at low fan speed and six were conducted with the hamburger on hood L1 at high speed. Experiments without a hood were conducted between the series of tests on the first and second hoods and toward the end of the experiments for a total of 18 experiments for both the pan and stir-frying. The range top was cleaned between experiments.

Capture Efficiency Calculations

As noted in the Introduction, *total* capture efficiency (CE) or pollutant removal effectiveness by a range hood is simply the mass exhausted through the hood divided by the mass emitted from the source:

$$CE = \frac{M_{\text{captured}}}{M_{\text{emitted}}} \quad 1$$

Total CE includes pollutants captured by the hood before they mix into the room as well as those that escape into the room and are then removed with the room air that is exhausted from the hood,

$$M_{\text{captured}} = M_{\text{first-pass}} + M_{\text{room-exhaust}} \quad 2$$

The mass that is captured directly from cooking and does not escape into the room can be used to calculate a “First Pass” capture efficiency CE_{FP} ,

$$CE_{FP} = \frac{M_{\text{first-pass}}}{M_{\text{emitted}}} \quad 3$$

In theory, the CE_{FP} offers a more useful measure of the performance of the hood as it can be combined with whatever general exhaust benefit provided by the extant space and ventilation conditions. In practice, the airflow dynamics of the room can impact first pass capture efficiency, so neither metric is uniformly applicable across installations.

CE for the exhaust of a combustion-based cooking burner can be determined by relating the mass flow of exhaust gases through the hood to the generation rate at the cooking surface. Carbon dioxide (CO_2) can be used as a surrogate for the exhaust gas mixture. For the typical case of complete (or nearly complete) combustion, the mass generation rate of CO_2 , S , can be calculated (estimated) from the fuel rate of the burner and knowledge of the carbon content of the fuel. The total mass flow of CO_2 through the hood can be calculated from the measured concentration of CO_2 in the exhaust air stream and an independent measurement of the exhaust airflow rate. To focus on the direct capture of CO_2 from the burner, the concentration of CO_2 from the room, C_{rooms} , is subtracted, as shown in Equation 4:

$$CE_{FP} = \frac{Q_{\text{hood}}(C_{\text{hood}} - C_{\text{room@hood}})}{S} \quad 4$$

In calculating CE, we accounted for a density difference of 1.5% in the reference conditions used by the Duct Blaster compared to those of the Alicat fuel flow sensor.

If a person is present in the immediate vicinity of the cooking surface and range hood, the contribution of exhaled CO₂ must be considered in the analysis. Exhaled CO₂ from occupants of the room is included in the room air CO₂ measurement and requires no special attention when quantifying first-pass CE. For our calculations, we assumed a CO₂ exhalation rate of 0.33 ± 0.15 LPM (Emmerich and Persily, 2001). This value is based on the assumption of a single female cook of 163 cm height with a metabolic activity factor of 1.3 (ASHRAE, 2013). The ± 0.15 LPM incorporates uncertainty in the rate for an individual female, the potential contribution of a cooking assistant coming close enough to contribute to CO₂ seen in the hood and some fraction of the cook's exhaled CO₂ not being drawn directly into the hood.

Determining the CE – either total or first-pass – for pollutants generated by an actual cooking process is more challenging because the generation rate is typically not calculable. This challenge may be addressed by generating a reproducible quantity of pollutants. In principle, one could volatilize or release an inert tracer into a cooking vessel and release a suitable quantity of heat at the cooking surface to simulate the buoyant plume that is characteristic of the represented cooking activity. The inert tracer generation approach was deemed unsuitable for the current study, which had the objective of evaluating CE for particles relevant to actual cooking activities.

The approach employed in this study was to attempt to generate a reproducible aerosol through execution of the tightly controlled cooking protocols described above. Instead of tracking particle mass, we tracked particles by number concentration in specified size ranges. The number of particles generated from the cooking event was quantified by measuring the airflow rate and concentration of particles leaving the chamber through the blower door, which was the route of all air exiting the room when no range hood was used. Since particle loss in the room is expected to be low due to the low residence time (high air exchange rate), the number of particles being removed by ventilation when no hood was operating is a good estimate of the emission rate and thus a valid reference point for calculating CE when hoods were operating:

$$M_{emitted} \cong M_{no-hood} = Q_{total} (C_{room@exh,no-hood} - C_{bkg}) \quad 5$$

This equation uses the symbol M for consistency with prior equations even though we have switched from talking about mass to number concentration. The equations could be used for either quantity. Similar to the CO₂-based calculation above, there is a need to account for particles in the room air that are not associated with the cooking activity, C_{bkg} .

The total CE associated with range hood use is calculated as the difference in the number of particles exhausted through the blower door when no hood was used relative to the number exhausted through the blower door when a hood was used:

$$M_{captured} = M_{no-hood} - M_{not-captured} \quad 6$$

The number of cooking-associated particles not captured by a range hood – i.e. those exiting through the blower door when a hood was used – is calculated as shown in Equation 7:

$$M_{not-captured} = (Q_{total} - Q_{hood})(C_{room@exh,with-hood} - C_{bkg}) \quad 7$$

The particle concentration in the room in Equation 7 ($C_{room@exh,with-hood}$) reflects the effects of particles being captured directly from cooking as well as some particles being removed with the room air exhausted through the hood during cooking. To calculate CE_{FP} , the room air particles removed by the hood must be added to the count of particles not captured on the first pass:

$$M_{not-captured,FP} = Q_{total} (C_{room@exh,with-hood} - C_{bkg}) \quad 8$$

Substitution of Equations 5 and 8 into Equation 6 results in the first pass capture by the hood

$$M_{captured,FP} = Q_{total} (C_{room@exh,no-hood} - C_{bkg}) - Q_{total} (C_{room@exh,with-hood} - C_{bkg}) \quad 9$$

The resulting equation for CE_{FP} for particles is

$$CE_{FP} = 1 - \frac{(C_{room@exh,with-hood} - C_{bkg})}{(C_{room@exh,no-hood} - C_{bkg})} = 1 - \frac{\Delta C_{tot,with-hood}}{\Delta C_{tot,no-hood}} \quad 10$$

The difference in particle concentrations in the numerator and denominator of Equation 10 are calculated by integrating the particle concentration measured from the time when cooking begins, t_0 , to when the particle concentration returns to background, t_b ,

$$\Delta C_{tot,i} = \int_{t_0}^{t_b} (C_{i,room@exh} - C_{i,bkg}) dt \quad 11$$

$C_{i,room@exh}$ is the particle concentration measured at the room exhaust for particle size bin i and $C_{i,bkg}$ is the background when no cooking is occurring. Particle concentrations vary between individual cooking events. As a result, the CE_{FP} is calculated using the average emissions over multiple cooking events

$$CE_{FP} = 1 - \frac{\overline{\Delta C_{tot,i;with-hood}}}{\overline{\Delta C_{tot,i;no-hood}}} \quad 12$$

The calculated CE represents the average CE over the measurement period.

The formulas for first-pass capture efficiency for the direct and indirect methods use the concentrations measured in the room, but in two different places: near the hood and near the exhaust. The two values may not be equivalent depending on the mixing conditions in the room. For a well-mixed room, the two concentrations will be equal. Any difference between these two values will be important when comparing resulting CEs.

All CEs reported in the Results section of this paper are first-pass CEs.

Uncertainty in Calculated Capture Efficiencies

Uncertainty in the calculated CE for burner pollutants is a function of uncertainties in (a) the measured hood airflow rate, (b) the measured CO_2 concentrations in the hood exhaust and background room air, and (c) the calculated mass emission rate of CO_2 . Uncertainty in the hood airflow rate is estimated to be 5% based on verification tests with a second duct blaster. The uncertainty in CO_2 concentration measured in the hood exhaust was calculated to be 3% based

on the standard deviation of the EGM4 calibrations; uncertainty in the background concentration was estimated as 2%. The mass emission rate of CO₂ depends on both gas flow and breathing rate. Uncertainty in fuel flow rate was 1%. Uncertainty in the breathing rate is estimated to be 45%, as noted earlier. Because these uncertainties are combined in quadrature, the fractional uncertainty of the breathing rate increases as the gas flow rate to the burner decreases and the contribution of breathing to the emitted CO₂ becomes greater. Total uncertainty in the CO₂-based CE ranged from 6.6% to 14.4%.

Uncertainty in particle CE was estimated using the standard error of CEs from replicate experiments combined in quadrature with the instrument measurement uncertainty. We estimate day-to-day instrument repeatability to be 3%. In general, the standard error across replicate experiments was larger than instrument accuracy and dominated uncertainty in particle CE.

Results and Discussion

Measured Concentrations

Figure 2 shows typical experimental results for pan-frying and stir-frying. Each figure shows time resolved measurements of CO₂ (ppm) in the hood exhaust, fuel flow (lpm), and size-resolved number concentrations of particles measured in the room: ≥ 6 nm (# cm⁻³) as measured by the CPC and 5 of 6 particle ranges measured by the OPC (# L⁻¹). There was no substantial response for the largest particle size (>5 μ m). Grey vertical lines on the figures mark the following experimental events: pan with oil placed on the stovetop, food added to the pan, fuel turned off, and pan covered and removed from the room. The top two plots show CO₂ in the hood and fuel flow increasing sharply just after the burners are ignited and remaining roughly constant throughout the experiment.

Stir-frying emitted more particles than pan-frying, and the difference was more pronounced for particles larger than 0.5 μ m. Particle emissions from pan-frying were predominately in the 0.3 to 0.5 μ m size range and below, as indicated by the OPC and CPC responses. The stir-fry plot shows particle concentrations (≥ 6 nm) starting to increase after the pan and oil were added and before the beans were added, whereas the other particle size channels increased sharply only after the beans were added. Adding the pan and oil to the medium flame did not produce such a clear increase in particles as adding the wok and oil to the larger flame did. This reflects a more rapid heating of the oil in the 1 mm steel wok over high heat compared to the pan with 5 mm aluminum bottom over medium heat. For the stir-fry, the OPC response shows that after the quick initial increase in all particle sizes when beans were added, particles larger than 0.3 μ m increased only gradually through the remainder of the cooking event. The continuing, steep increase in total particle concentration (CPC) throughout the experiment indicates ongoing emissions of particles smaller than 0.3 μ m, including ultrafine particles. Concentrations of all particle sizes followed an exponential decay (at the room AER) after the fuel was turned off and the pan or wok was covered and removed from the room.

An example of the variability in measured particle concentrations across replicate cooking experiments is displayed in Figure 3, which shows concentrations of 6 nm and larger particles for pan-frying hamburgers without a hood and for E2 operating on low and high speed. These data demonstrate a core challenge in conducting performance assessments using cooking-generated particles: despite precisely defined cooking protocols there was substantial variability in particle concentrations across replicate implementations for many of the conditions.

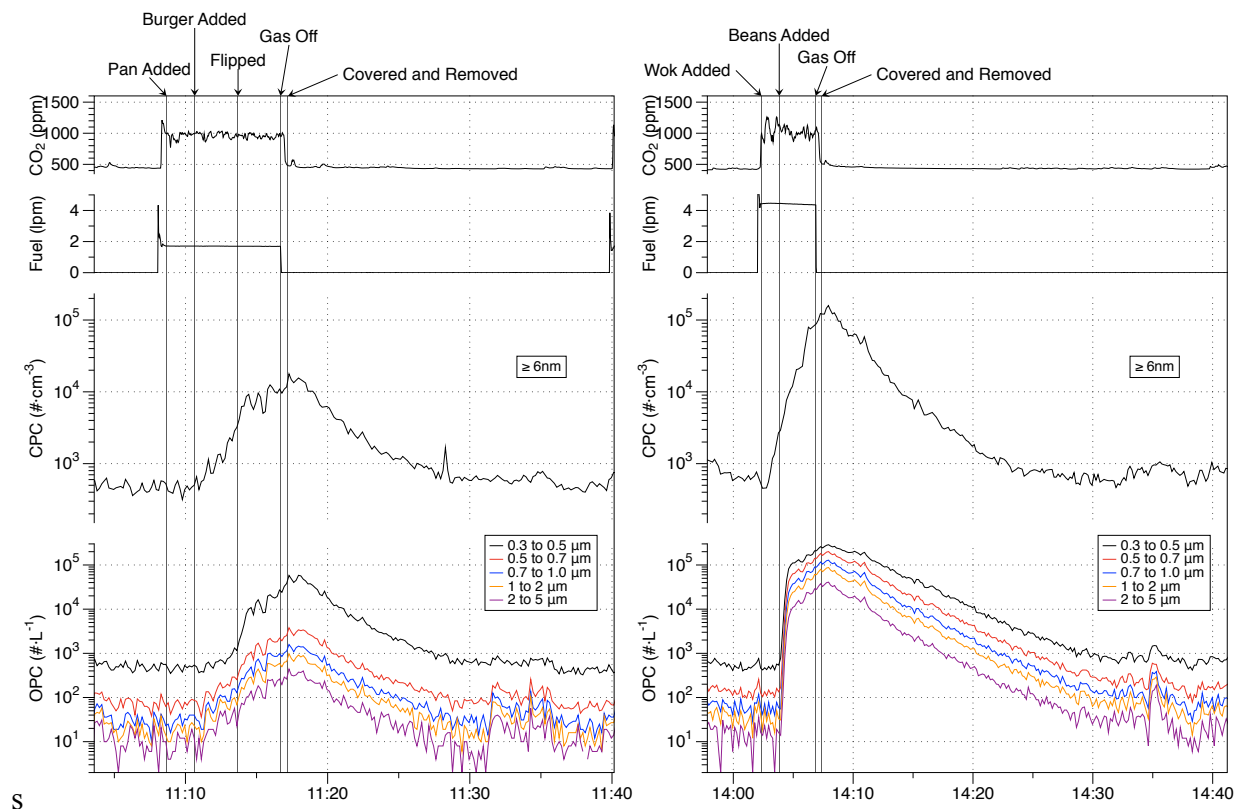


Figure 2. Concentrations of CO₂ in the hood exhaust and particles in room measured by the CPC and OPC resulting from (a) pan-fry and (b) stir-fry cooking activities.

Note that particle concentrations are shown on a log scale.

The relative standard deviation (RSD) of the time-integrated concentration for the no-hood condition was 23%, while those measured with the hood were 10% and 50% for the low and high fan speeds. Particle concentrations returned to the same range of background concentrations for both hood and no hood conditions. Plots analogous to Figure 3 are shown for each hood and cooking condition in Supplemental Figures S6 and S7.

The calculated total number of particles leaving the room through the blower door and RSDs for each hood and flow condition are provided in **Error! Reference source not found.** for pan-frying and **Error! Reference source not found.** for stir-frying. RSDs for specific combinations of hood and airflow rates ranged from approximately 10% to 90%. The mean RSD for the CPC and the five OPC channels with no hood operating was 48% for stir-frying and 35% for pan-frying. The mean RSDs across all combinations of hood and fan speed were 36% for stir-frying and 36% for pan-frying. Variability in emissions reflected by the RSDs is similar for the two cooking activities both with and without hood use, indicating that the variability in emissions is primarily from the cooking rather than airflow. A previous study that used a scripted procedure for pan-frying of steak (Sjaastad and Svendsen, 2010) reported similar variability in particle emissions in the 0.3 to 0.5 μm size range: RSDs ranged from 12% to 62% with an average value of 37%.

Table 1. Summary results for hamburger pan-frying experiments

Mean total number of particles removed through the blower door and relative standard deviation (RSD) of measurements by the condensation particle counter (CPC) and optical particle counter (OPC).

Setup	Hood flow ¹	# of expts	CPC		OPC									
			Total Particles		0.3 – 0.5 μm Particles		0.5 – 0.7 μm Particles		0.7 – 1.0 μm Particles		1.0 – 2.0 μm Particles		2.0- 5.0 μm Particles	
	lps		Mean (x10 ¹²)	RSD (%)	Mean (x10 ⁹)	RSD (%)	Mean (x10 ⁸)	RSD (%)	Mean (x10 ⁷)	RSD (%)	Mean (x10 ⁷)	RSD (%)	Mean (x10 ⁷)	RSD (%)
No Hood		18	36.1	23	31.1	91	29.7	33	124	22	76.4	22	32.4	21
L1	51	4	3.94	21	1.79	39	3.73	31	18.7	29	11.5	28	4.93	29
	81	5	0.94	42	0.36	21	0.89	27	4.35	30	2.72	36	1.15	36
E2	52	5	3.22	10	6.28	55	5.40	24	23.9	20	14.5	19	6.06	18
	109	5	0.21	50	0.88	55	0.83	34	.33	24	1.20	18	0.42	21
M1	68	5	0.74	25	1.18	80	0.90	27	3.48	18	1.95	20	0.68	18
	137	5	1.83	30	1.54	19	1.67	17	7.57	25	4.62	24	1.65	30
P1	138	5	0.30	73	0.14	69	0.34	87	1.24	70	0.70	67	0.23	87

¹Measured values

Table 2. Summary results for green bean stir-frying experiments

Mean total number of particles removed through the blower door and relative standard deviation (RSD) of measurements by the condensation particle counter (CPC) and optical particle counter (OPC).

Setup	Hood flow ¹	# of expts	CPC		OPC									
			Total Particles		0.3 – 0.5 μm Particles		0.5 – 0.7 μm Particles		0.7 – 1.0 μm Particles		1.0 – 2.0 μm Particles		2.0- 5.0 μm Particles	
	lps		Mean (x10 ¹³)	RSD (%)	Mean (x10 ¹⁰)	RSD (%)	Mean (x10 ¹⁰)	RSD (%)	Mean (x10 ¹⁰)	RSD (%)	Mean (x10 ¹⁰)	RSD (%)	Mean (x10 ⁹)	RSD (%)
No Hood		18	4.84	26	8.89	37	4.64	54	2.70	57	1.78	58	8.05	56
L1	51	4	4.25	35	8.59	45	4.44	57	2.49	59	1.59	59	6.78	58
	81	6	3.12	40	7.43	25	3.88	35	2.20	35	1.43	35	6.12	33
E2	52	5	2.94	33	8.39	12	4.46	18	2.56	21	1.63	22	7.12	24
	109	5	3.02	70	7.53	18	3.80	23	2.07	25	1.27	26	5.35	25
M1	68	5	3.18	24	8.22	30	4.39	39	2.54	41	1.63	42	7.28	42
	137	5	1.68	52	3.69	29	1.53	37	0.82	38	0.53	37	2.27	36
P1	138	5	2.11	54	3.77	34	1.65	45	0.89	46	0.57	47	2.46	47

¹Measured value

Capture Efficiency Results

Figure 4 shows the burner pollutant (CO₂) CEs calculated for pots of water (POW), pan with water (Pan), and cooking (Cook), along with cooking particle CEs calculated for hamburger pan-frying on a back burner. These CEs and all others presented in this section are first-pass CEs. CEs are shown for particles ≥ 6 nm (CPC) and for five size ranges measured by the OPC. CEs for pan-frying on the back burner were mostly above 90% for high fan speeds and mostly above 80% for low fan speeds. CO₂-based CEs measured during the cooking events were slightly lower than those measured by POW and pan with water for most combinations of hood and fan speed. Possible contributions to this result are the cook disrupting flow near the burners and the POW and pan with water drawing more heat than the pan with burger, producing less energetic

plumes. With the exception of the POW test for E2 on low speed (62% CE), CEs were 75% or better for both CO₂ and particles for all the hoods and fan settings.

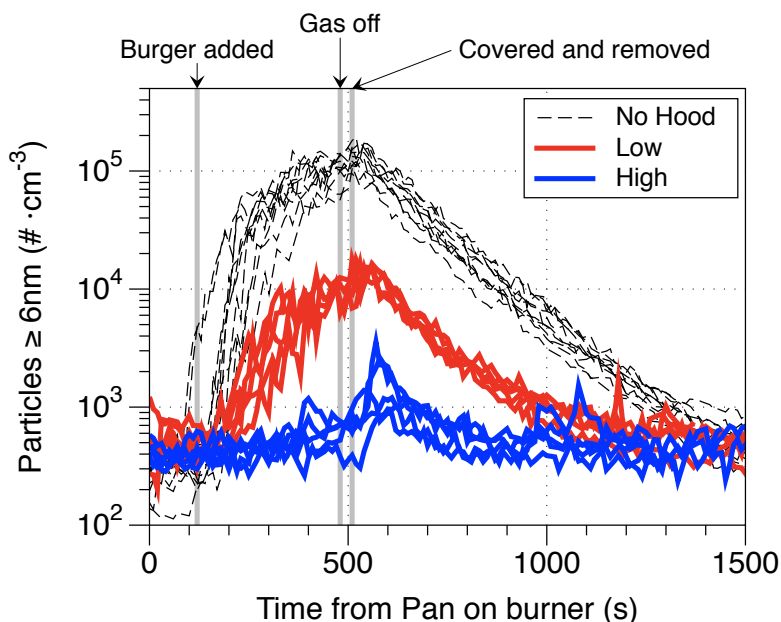


Figure 3. Concentration of particles ≥ 6 nm as measured by the CPC from a sampling point near the exhaust outlet of room. Data shown for pan-frying experiments with no hood present (black dashed line) and with hood E2 operating on low (red) and high (blue) fan speeds.

Note that particle concentrations are graphed using a log scale. Relative standard deviations are provided in Table 2. The time scale denotes the seconds since the pan was put on the burner.

Figure 5 displays CO₂-based CEs calculated for pots of water (POW), wok with water, and cooking, as well as particle CEs for stir-frying of green beans on front burner(s). CO₂-based CEs were similar for POW (2 pots on 2 burners) and wok with water (1 burner), suggesting that neither cooking vessel shape nor the number of burners had a large effect (unless the effects happened to balance).

CO₂-based CEs measured during cooking were substantially lower than those measured during POW and wok with water experiments for most combinations of hood and fan setting.

In stir-frying experiments, CEs for particles >0.3 μm were lower than CEs determined for CO₂ for all but one combination of hood and setting (M1 on high). The difference between particle CE and CO₂ CE during cooking varied across hoods. For example, P1 (only one fan speed) had particle CEs of 56–69% across the particle size bins and a cooking CO₂ CE of 72%. By contrast, Hood E2 on high speed had size-resolved particle CEs of 15–38% and a CO₂ CE of 54% during cooking. When hoods L1, E2 and M1 were operated at low speed, particle CE values for the stir-fry were extremely low for the particles in the OPC size range: CEs for 0.3 μm and larger particles were 3–16%. CEs for all particles ≥ 6 nm were 34% for M1 on low, 39% for E2 and 12% for L1 on low fan speed. CO₂-based CEs measured during the stir-fry experiments with hoods on low speed were all in the range of 35–38%

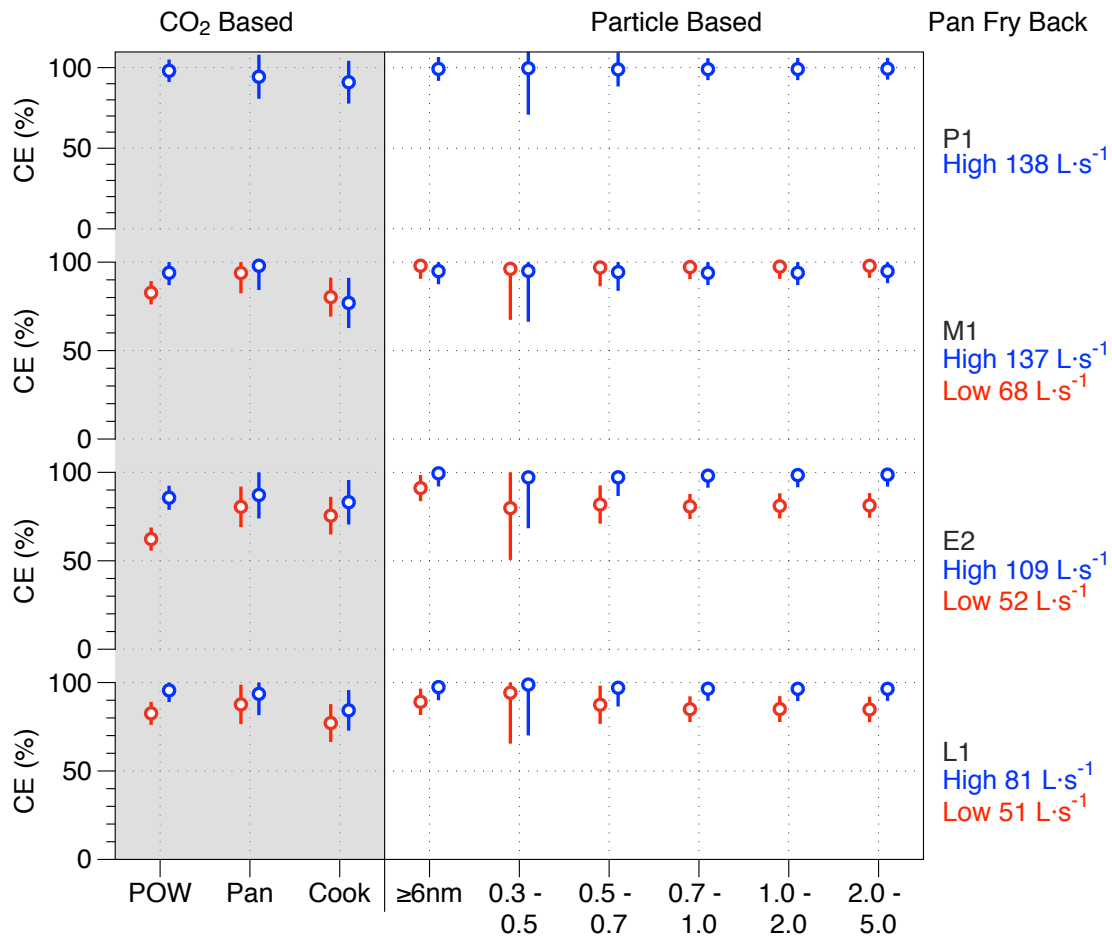


Figure 4. Capture efficiencies (CE) calculated using CO₂ measured in hood exhaust and particles measured in room for pan-frying hamburger.

CEs calculated using CO₂ in the shaded, left side of the graph show results for two pots of water on rear burners operating on highest setting (POW) using the method described in Delp and Singer (2012); for a single frying pan half-filled with water, covered with foil, and placed on a single back burner operating on medium heat (Pan); and during the cooking experiments (Cook). CE calculated using particle concentrations measured in the room are shown on the right side of the graph. Values for CE are shown for all particles ≥ 6 nm, as measured by the CPC, and for five size bins measured by the OPC

Figure 6 compares capture efficiencies for stir-frying on either the front or back burners with hood E2. This plot further illustrates the sharp contrast between particle CEs at the two locations. While the particle capture efficiencies measured on the front burner are low – varying between 4% and 39% by hood, fan setting and particle size – those on the back burner were much higher, varying between 70% and 99%. The results for cooking on the back burner are similar to those measured during pan-frying for the same hood. In addition, like the pan-frying results, CEs for the different particle size bins were similar to the CO₂ CE measured using POW. At the high flow rate, CEs for both cooking activities on the back burner for hood E2 are close to 100%. At the low fan setting, particle CEs averaged 83% for pan-frying and 78% for stir-frying. It is clear that the burner location has a much more significant effect on capture efficiency than the cooking activity. Cooking on the rear burner means that the hood fully covers the area over which the emissions occur, resulting in higher capture efficiency.

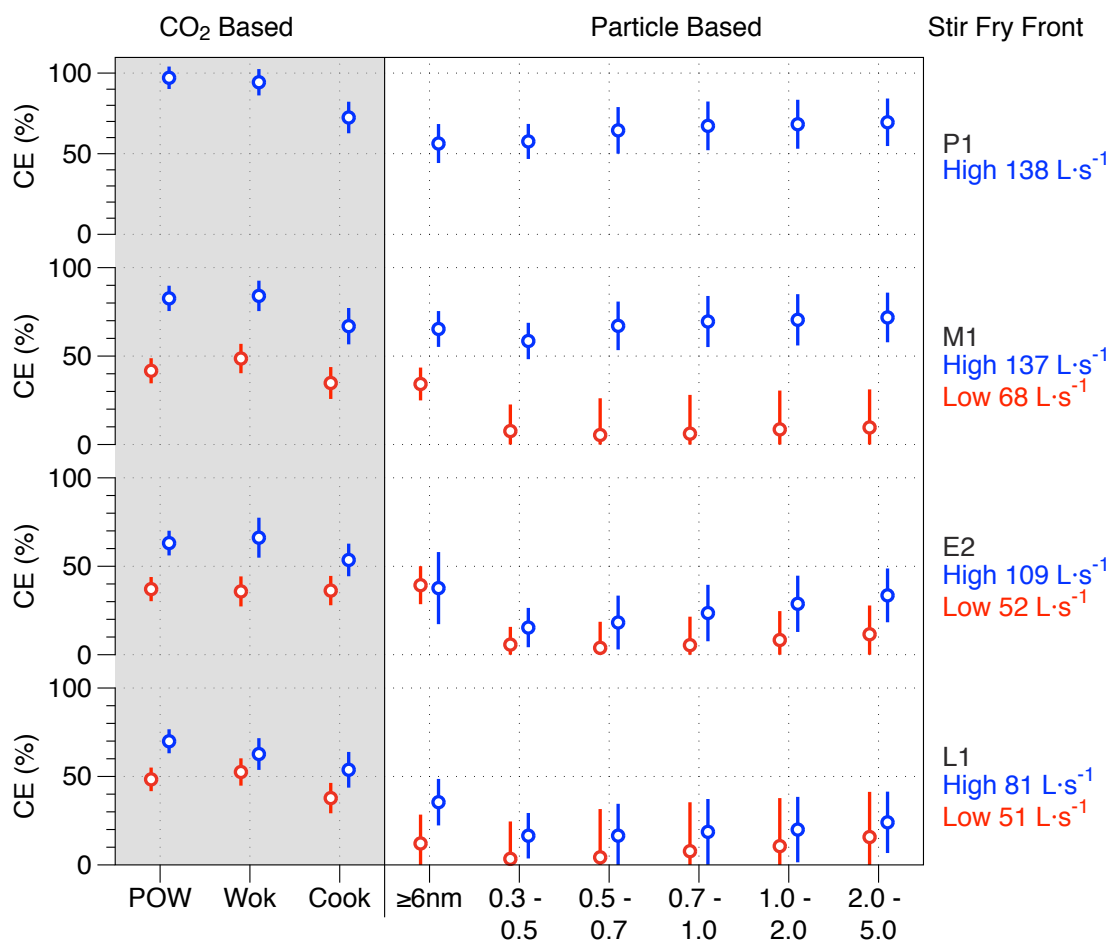


Figure 5. Capture efficiencies (CE) calculated using CO₂ measured in hood exhaust and particles measured in room for stir-frying green beans.

CEs calculated using CO₂ in the shaded, left side of the graph show results for two pots of water on front burners operating on highest setting (POW) using the method described in Delp and Singer (2012); for a single wok half-filled with water, covered with foil, and placed on a single front burner operating on high heat (Wok); and during the cooking experiments (Cook). CE calculated using particle concentrations measured in the room are shown on the right side of the graph. Values for CE are shown for all particles ≥ 6 nm, as measured by the CPC, and for five size bins measured by the OPC.

Airflow and Mixing Verification Experiments

Results of the airflow and mixing experiments are presented in the supplemental information; here we note only the summary findings. One set of experiments indicated a short-circuit loop that increased the apparent first-pass capture efficiency relative to the ideal pattern of pollutants mixing evenly throughout the room if they are not captured on the first pass. The same experiments found variations of roughly 15% in SF₆ concentration in the vicinity of the blower door during an experiment. These variations are much smaller than the variance in room air particle concentrations across replicate experiments. These two features are displayed in Supplemental Figures S2 and S3.

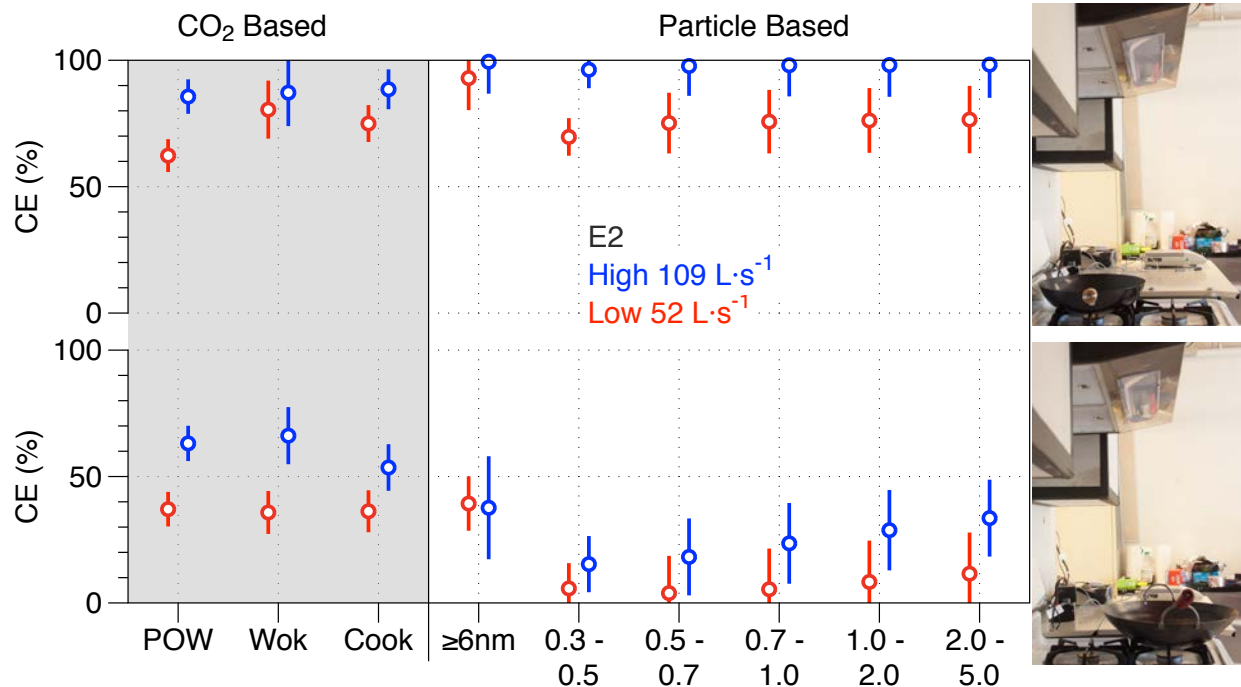


Figure 6. Capture efficiencies (CE) calculated using CO₂ and particle measurements for stir frying on the front or back burners.

CEs calculated using CO₂ in the shaded, left side of the graph show results for two pots of water on rear or front burners operating on highest setting (POW) using the method described in Delp and Singer (2012); for a single wok half-filled with water, covered with foil, and placed on a single front or back burner operating on high heat (Wok); and during cooking experiments (Cook) on front or back burners. CE calculated using particle concentrations in the room are shown on the right side of the graph. Values for CE are shown for all particles ≥ 6 nm, as measured by the CPC, and for five size bins measured by the OPC.

In a set of experiments in which SF₆ was released into the wok during stir-fry procedures, capture efficiencies calculated based on SF₆ measurements in the hood exhaust were roughly 5% higher than CEs calculated from measurements in the room. This result, displayed in Supplemental Figure S4, is consistent with short-circuiting causing a bias in the apparent first-pass CE.

Supplemental Figure S5 shows that CO₂-based CEs measured with the blower door, supply and room air mixing fans off were indistinguishable from CEs measured under the standard mixing conditions that applied through the experiments measuring CE.

Comparisons to Published Studies on Cooking Hood Effectiveness

The new results for burner exhaust pollutants, obtained using the CO₂-based POW, pan with water, and cooking tests, in some cases indicate higher CEs than previously reported for the same hoods executing the same POW procedures in a different laboratory (Delp and Singer, 2012). At this time, we cannot explain the differences. Experiments exploring the potential effects of airflow patterns were conducted with the configuration reported in this new study but not in the earlier study.

The particle CEs presented in Figures 4-6 expand on the published record of range hood effectiveness for particles. Rim et al. (2012) quantified exhaust hood effectiveness for ultrafine particle concentrations measured in the bedroom of a test house, examining burner-generated particles in the size range of 2-20 nm. That study found a strong size dependence on effectiveness over the range studied with higher effectiveness for higher hood airflow rates and back burners compared with oven or front burners. Yet even for the lowest airflow hood with oven or front burner use, effectiveness exceeded 70% for the largest particles (14-20 nm) observed. Sjaastad and Svendsen (2010) measured concentrations of 0.3–0.5 μm particles 1.3 m to the side of the burner during and just after pan-frying a beefsteak in a 56- m^3 chamber. The scripted cooking procedure was repeated for 9–13 replicates of each condition, examining cooking area location (wall, corner, or middle of room), variations in exhaust airflow, and two installation heights for three hoods. The study did not report effectiveness per se and hood airflow variations had a large effect on overall chamber air exchange. These factors and the single measurement location to the source limit the generalizability of the reported results.

Conclusions

Capture efficiencies (CE) were measured for cooking-generated particles during scripted cooking procedures and for burner produced CO_2 during the same cooking activities and separately for pots and pans containing water. CEs were determined for four exhaust hoods including a basic low-volume hood, an energy-efficient device with a flat bottom, a microwave exhaust hood and a high performance hood with large capture volume. For pan-frying a hamburger over medium heat on the back burner, CEs for particles were similar to those for burner combustion products, as indicated by CO_2 , and mostly above 80%. For stir-frying green beans in a wok on the front burner over high heat, CEs for burner produced CO_2 during cooking varied by hood and airflow: CEs were 34–38% for low (51–68 L s^{-1}) and 54–72% for high (109–138 L s^{-1}) settings. CEs for 0.3–2.0 μm particles during front burner stir-frying were 3–11% on low and 16–70% on high settings. High CE was obtained when stir-frying on a back burner. Results indicate that CO_2 -based CEs measured for combustion pollutants are not predictive of CEs for cooking-generated particles under all conditions; but they may be suitable to identify devices with CEs above 80% for both burner exhaust gases and cooking-related particles.

Acknowledgements

Funding was provided by the California Energy Commission PIER-Environmental Program via Contract 500-09-024; the U.S. Dept. of Energy Building America Program via Contract DE-AC02-05CH11231; the U.S. Dept. of Housing and Urban Development, Office of Healthy Homes and Lead Hazard Control via Agreement I-PHI-01070; and the U.S. Environmental Protection Agency Indoor Environments Division via Agreement DW-89-92322201-0. We thank Tosh Hotchi and Doug Sullivan for chamber set-up and Marcella Barrios and Omsri Bharat for carefully conducting the cooking experiment

Literature Cited

- Abdullahi, K.L., Delgado-Saborit, J.M. and Harrison, R.M. (2013) Emissions and indoor concentrations of particulate matter and its specific chemical components from cooking: A review, *Atmos. Environ.*, **71**, 260-294.
- Afshari, A., Matson, U. and Ekberg, L.E. (2005) Characterization of indoor sources of fine and ultrafine particles: A study conducted in a full-scale chamber, *Indoor Air*, **15**, 141-150.
- ASHRAE (2013) Chapter 9. Thermal Comfort, *ASHRAE Handbook: Fundamentals*, Atlanta GA, ASHRAE, 9.6.
- Buonanno, G., Morawska, L. and Stabile, L. (2009) Particle emission factors during cooking activities, *Atmos. Environ.*, **43**, 3235-3242.
- Delp, W.W. and Singer, B.C. (2012) Performance assessment of U.S. residential cooking exhaust hoods, *Environ. Sci. Technol.*, **46**, 6167-6173.
- Dennekamp, M., Howarth, S., Dick, C.a.J., Cherrie, J.W., Donaldson, K. and Seaton, A. (2001) Ultrafine particles and nitrogen oxides generated by gas and electric cooking, *Occupational and Environmental Medicine*, **58**, 511-516.
- Emmerich, S.J. and Persily, A.K. (2001) State-of-the-Art Review of CO2 Demand Controlled Ventilation Technology and Application, Springfield VA, National Institute of Standards and Technology.
- Energy Conservatory (2007) Minneapolis Duct Blaster Operation Manual (Series B Systems), Minneapolis MN, The Energy Conservatory.
- Farnsworth, C., Waters, A., Kelso, R.M. and Fritsche, D. (1989) Development of a fully vented gas range, *ASHRAE Trans.*, **95**, 759-768.
- Fortmann, R., Kariher, P. and Clayton, R. (2001) Indoor air quality: Residential cooking exposures, Sacramento, CA, Prepared for California Air Resources Board.
- Fullana, A., Carbonell-Barrachina, A.A. and Sidhu, S. (2004) Volatile aldehyde emissions from heated cooking oils, *J. Sci. Food Agric.*, **84**, 2015-2021.
- He, C.R., Morawska, L.D., Hitchins, J. and Gilbert, D. (2004) Contribution from indoor sources to particle number and mass concentrations in residential houses, *Atmos. Environ.*, **38**, 3405-3415.
- Huang, R.F., Dai, G.Z. and Chen, J.K. (2010) Effects of mannequin and walk-by motion on flow and spillage characteristics of wall-mounted and jet-isolated range hoods, *Ann. Occup. Hyg.*, **54**, 625-639.
- HVI (2013a) HVI Airflow Test Procedure, Wauconda, IL, Home Ventilating Institute.
- HVI (2013b) HVI Loudness Testing and Rating Procedure, Wauconda IL, Home Ventilating Institute.
- IEC (2005) Household range hoods - Methods for measuring performance, Standard IEC 61591, Ed. 1.1, International Electrotechnical Commission.
- Kosonen, R., Koskela, H. and Saarinen, P. (2006) Thermal plumes of kitchen appliances: Cooking mode, *Energy Build.*, **38**, 1141-1148.
- Li, Y., Delsante, A. and Symons, J. (1997) Residential kitchen range hoods - Buoyancy-capture principle and capture efficiency revisited, *Indoor Air*, **7**, 151-157.
- Li, Y.G. and Delsante, A. (1996) Derivation of capture efficiency of kitchen range hoods in a confined space, *Build. Environ.*, **31**, 461-468.
- Logue, J.M., Klepeis, N.E., Lobscheid, A.B. and Singer, B.C. (2013) Pollutant exposures from unvented gas cooking burners: A simulation-based assessment for Southern California, *Environ. Health Perspect.*, **122**, 43-50.

- Moschandreas, D.J. and Relwani, S.M. (1989) Field-measurements of NO₂ gas range-top burner emission rates, *Environ. Int.*, **15**, 489-492.
- Parrott, K., Emmel, J. and Beamish, J. (2003) Use of kitchen ventilation: Impact on indoor air quality, *The Forum for Family and Consumer Issues*, **8**.
- Rim, D., Wallace, L., Nabinger, S. and Persily, A. (2012) Reduction of exposure to ultrafine particles by kitchen exhaust hoods: The effects of exhaust flow rates, particle size, and burner position, *Sci. Total Environ.*, **432**, 350-356.
- Seaman, V.Y., Bennett, D.H. and Cahill, T.M. (2009) Indoor acrolein emission and decay rates resulting from domestic cooking events, *Atmos. Environ.*, **43**, 6199-6204.
- Singer, B.C., et al. (2010) Natural Gas Variability in California: Environmental Impacts and Device Performance: Experimental Evaluation of Pollutant Emissions from Residential Appliances, Sacramento CA, California Energy Commission.
- Singer, B.C., Delp, W.W., Price, P.N. and Apte, M.G. (2012) Performance of installed cooking exhaust devices, *Indoor Air*, **22**, 222-234.
- Sjaastad, A.K. and Svendsen, K. (2010) Different types and settings of kitchen canopy hoods and particulate exposure conditions during pan-frying of beefsteak, *Indoor and Built Environment*, **19**, 267-274.
- Wallace, L.A., Emmerich, S.J. and Howard-Reed, C. (2004) Source strengths of ultrafine and fine particles due to cooking with a gas stove, *Environ. Sci. Technol.*, **38**, 2304-2311.
- Zhang, Q.F., Gangupomu, R.H., Ramirez, D. and Zhu, Y.F. (2010) Measurement of ultrafine particles and other air pollutants emitted by cooking activities, *International Journal of Environmental Research and Public Health*, **7**, 1744-1759.

Appendix A: Supporting Information

Efforts to Develop Oven Cooking Activity

Identifying an acceptable oven cooking activity proved to be extremely challenging. We conducted pilot experiments with several typical oven-cooked foods, including frozen pizza and chocolate chip cookies, but found that none produced substantial and consistent quantities of particles. These experiments indicated that particles were emitted only when part of the cooked food either dropped to the hot oven bottom or on the hot pan surface when using the broiler. A procedure that simulated a spill of a small amount of pie filling onto the oven floor proved to be the most promising source of particle emissions. Particle generation rates during repeated implementation of this procedure were more variable than those from either the pan or stir-fry. The large number of replicates required to discern differences between hood and no hood conditions given the variability of emissions within each condition made the cost of including an oven condition prohibitive.

Airflow and Mixing Experiments

This section provides additional details about experiments conducted to explore the potential impacts of imperfect room air mixing on the measurement of capture efficiency. Figure S1 shows the locations of the SF₆ release point and SF₆ measurement locations for experiments exploring two questions: (1) whether there was any short-circuiting recirculation from the area above the hood – where pollutants would rise after not being captured on first pass – to the room air being drawn into the hood from the nearby surroundings, and (2) whether concentrations measured at the sampling location used throughout the CE tests accurately reflect concentrations in the air leaving the room through the blower door. In these experiments, applied for hoods L1 and E2, a dilute mixture of SF₆ was released approximately 60 cm above the hood and concentrations were measured in the hood exhaust, just in front of the room exhaust, and for hood E2 also just above and in front of the hood. The dilute SF₆ mixture was released for 15 minutes while a pot of water was heated on a front burner operating with a fuel flow rate of 4.2 lpm. SF₆ concentrations were measured from 30 to 45 min with 30 s resolution in the two or three locations noted.

Regarding the first question, results in Figures S2 and S3 indicate that there was short-circuiting from above the hood, as indicated by higher SF₆ concentrations in the hood exhaust compared to those measured nearby to the room air exhaust. Comparing concentrations measured at A and in the hood exhaust stream (C) suggests an airflow pattern in which air from above the hood is drawn back down toward the hood; the result is that some of the burner exhaust that misses the hood on first pass is drawn back toward the hood before fully mixing throughout the room. This type of short-circuiting improves capture, and is credited as first-pass capture efficiency using the calculation procedures described above. To further investigate this possible recirculation, a measurement location directly in front of the hood was added to the experiments conducted using hood L1. The concentration at this location (D in Figures S3) showed a higher concentration of SF₆ than at the hood exhaust. In addition, sonic anemometer measurements of the airflow direction in front of the hood indicated a small but measureable net downward flow. These

results indicate the presence of a recirculation/short-circuiting of exhaust from above the hood back into the hood.

Regarding the second question, results in Figures S2 and S3 indicate that the air leaving the room through the blower door could for any individual condition, have had particle concentrations that differed by roughly 15% from the concentrations measured at location A during the CE tests. For hood E2, the SF₆ concentrations measured at A was 14% higher than at location B just in front of the blower door. For hood L1, SF₆ measured at A was 13% lower than at B. An important caveat to these results is that sampling point B may not precisely reflect the concentration of SF₆ in all air leaving through the blower door. To the extent that an experimental variable would be causing changes to room airflow, mixing and concentration patterns, we would expect that variable to be the airflow through the blower door, which varies with hood airflow rate. Changes in flow through the blower door could change air velocities and circulation patterns in the room in the vicinity of the blower door. The caveat here is that the blower door airflows with hoods operating were 84-94% of the flows that occurred during no hood conditions. For the two hoods shown in Figures S2 and S3, airflows through the blower door were very similar for the low-speed operation and also for the high-speed operation and the biggest difference was between low-speed and high-speed operation. Yet these figures show consistent trend in A vs. B for the low-speed and high-speed of E2 and again for the low-speed and high-speed of L1. Perhaps most important is the fact that the magnitude of the variation between A and B is much smaller than the variance of room air concentrations extant across replicate experiments. And since the uncertainty in the calculated CE values reflects this variance the effect of uncertainty in the particle concentrations of air leaving the chamber is incorporated.

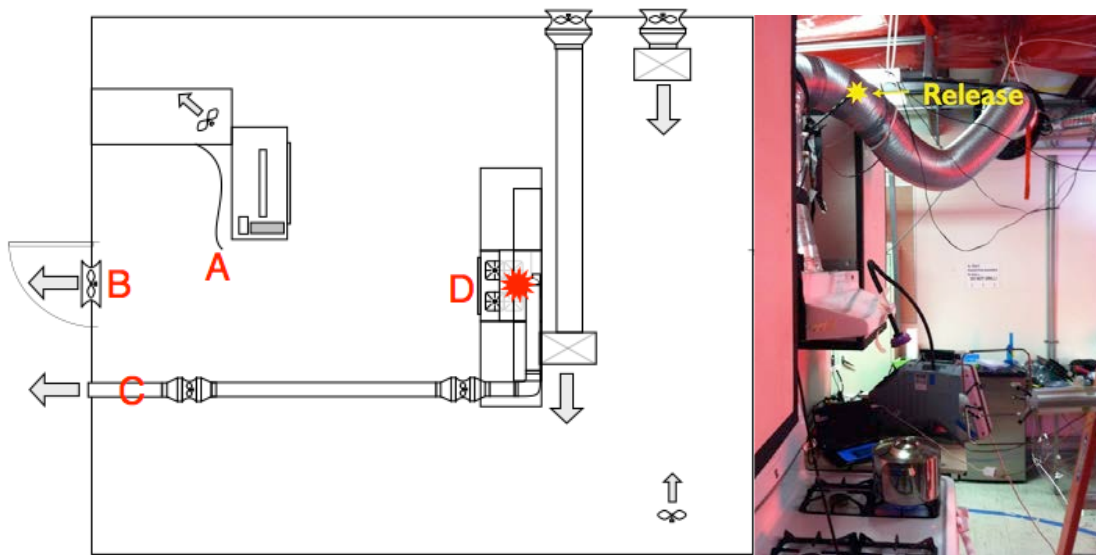


Figure A1. Release and measurement locations for the mixing experiments in which SF₆ was released above the hood.

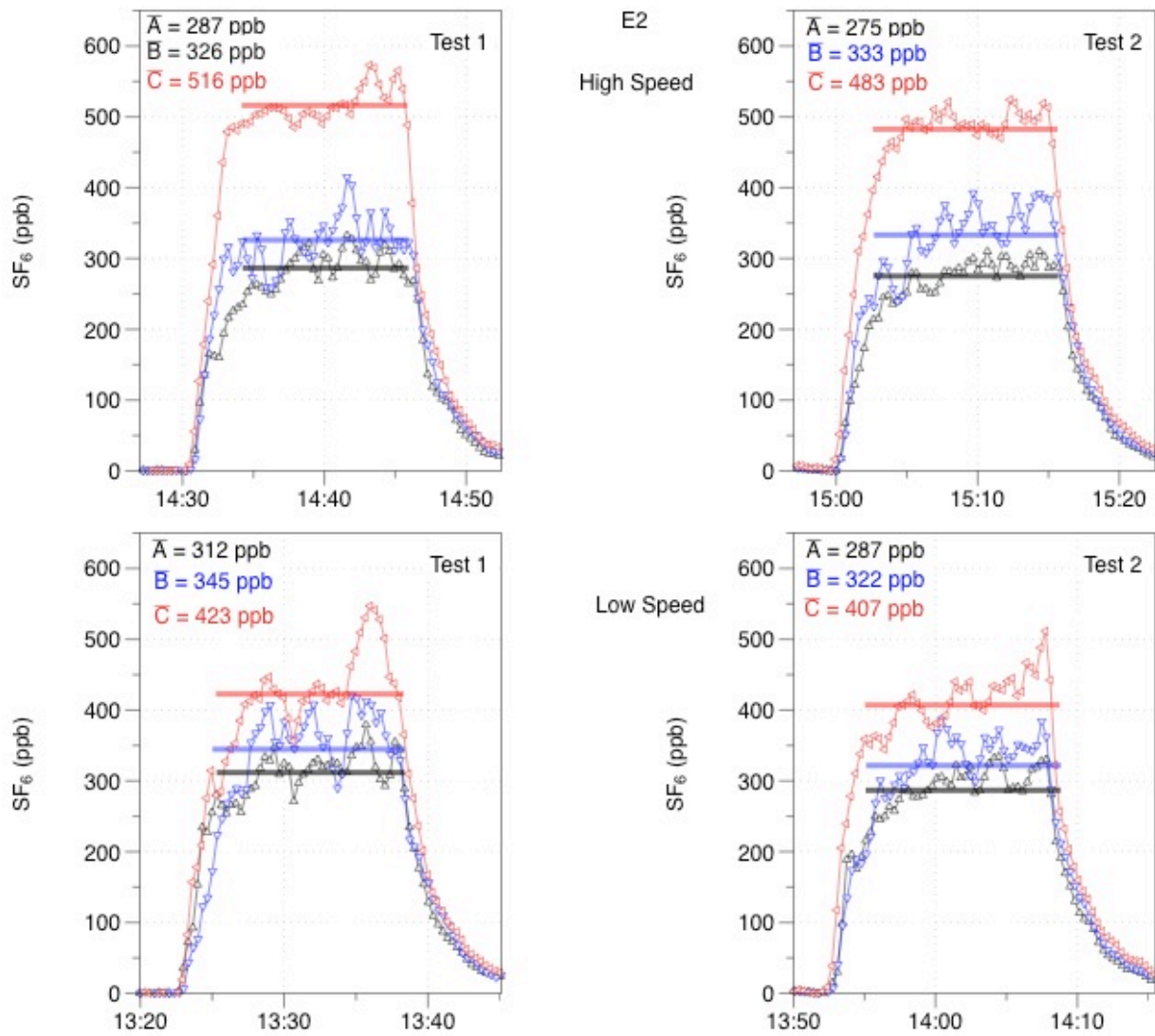


Figure A 2. SF₆ concentrations measured at the experimental sampling location (A), the blower door exit (B), and in the hood exhaust (C) for SF₆ released above hood E2 operating at high speed (top panels) and low speed (bottom panels).

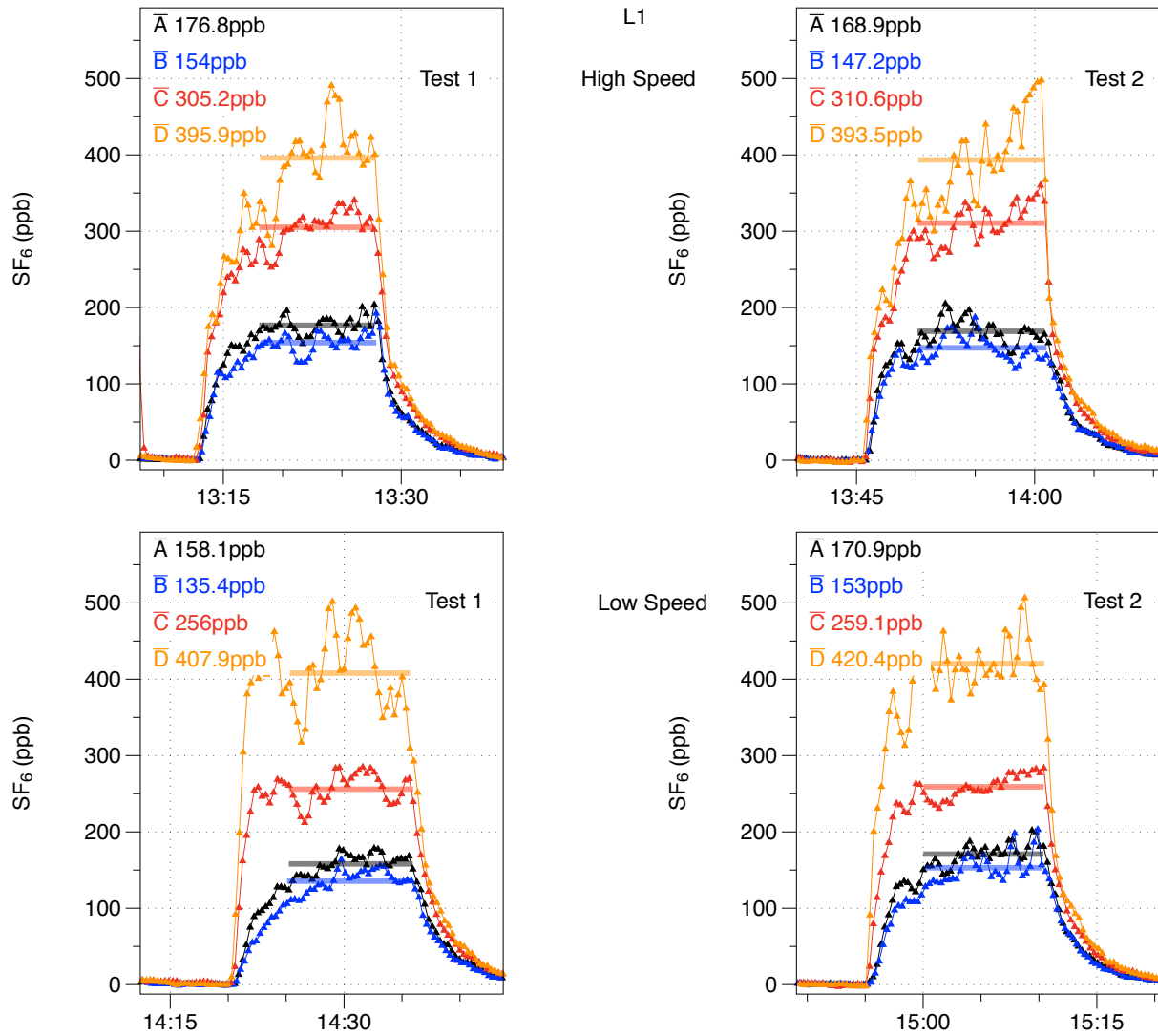


Figure A 3. SF₆ concentrations measured at the experimental sampling location (A), the blower door exit (B), in the hood exhaust (C), and just in front of the hood (D) for hood L1 operating at high speed (top panels) and at low speed (bottom panels).

In another experiment, SF₆ was released into the wok through copper tubing formed into a Y with two gas outlets during a stir-fry procedure. SF₆ concentrations were measured in both the hood (E2) and the room exhaust, allowing calculation of CE using both the direct (based on mass flow through the exhaust hood) and indirect (based on mass flow out of the room) methods.

CEs calculated from SF₆ measurements in both the hood and room for the experiment in which SF₆ was released in this experiment are shown below in Figure S5. Results show that CEs calculated by both methods are highly correlated, with CEs calculated from the hood exhaust consistently higher than those calculated from measurements in the room. This result is consistent with the previously discussed recirculation / short-circuit loop from above the hood causing an increase in the first pass CE calculated using the hood exhaust measurements

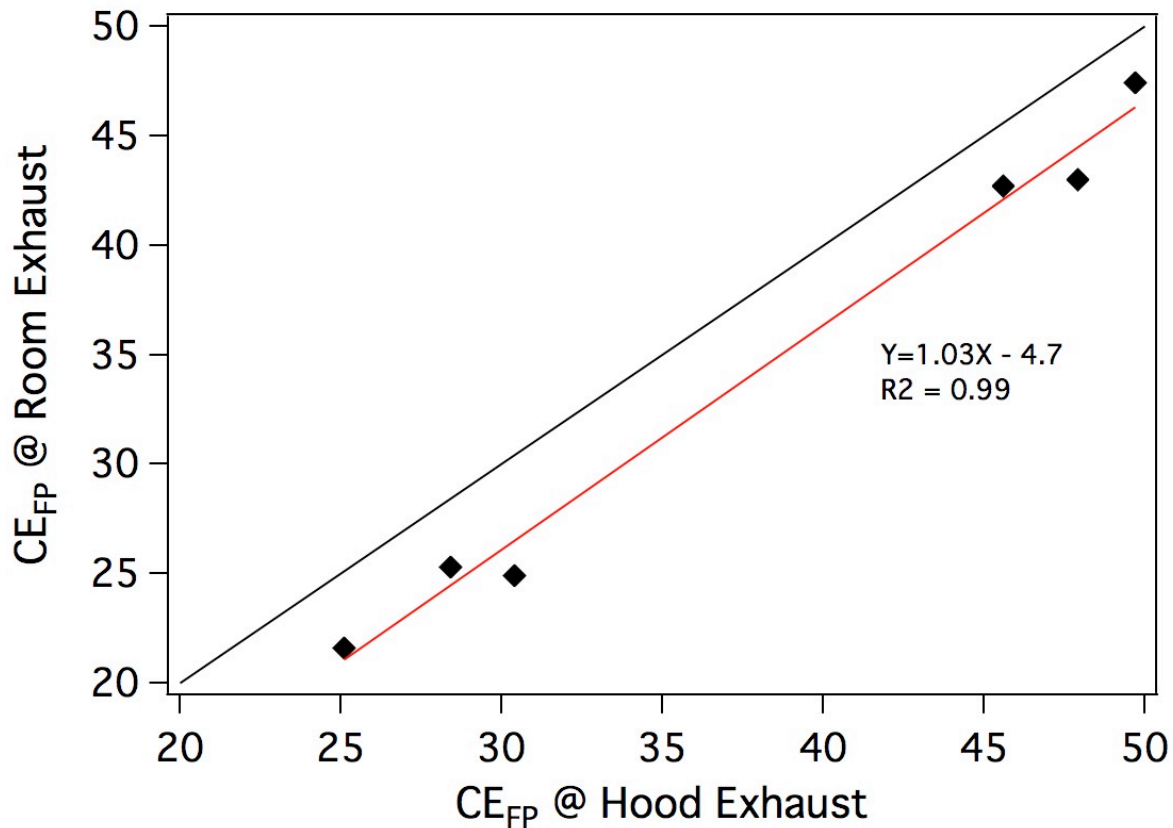


Figure A 4. First-pass capture efficiencies calculated based on SF₆ concentrations measured near the room exhaust, i.e. analogous to CEs calculated for cooking particles, and in the hood exhaust for experiments in which SF₆ was released into the wok while conducting green bean stir fry procedure with hood E2 on low speed and high speed settings.

Figure S5 below presents capture efficiencies determined using CO₂ measurements in the hood exhaust for the pot-of-water (POW) procedure under quiescent conditions with blower door, supply fans and mixing fans off. These are compared to the CEs determined using the same methods with all fans operating as described in the Methods section of the paper. Figure S5 shows that CO₂-based CEs measured with the blower door, supply and room air mixing fans off were indistinguishable from CEs measured under the standard mixing conditions that applied through the experiments measuring CE.

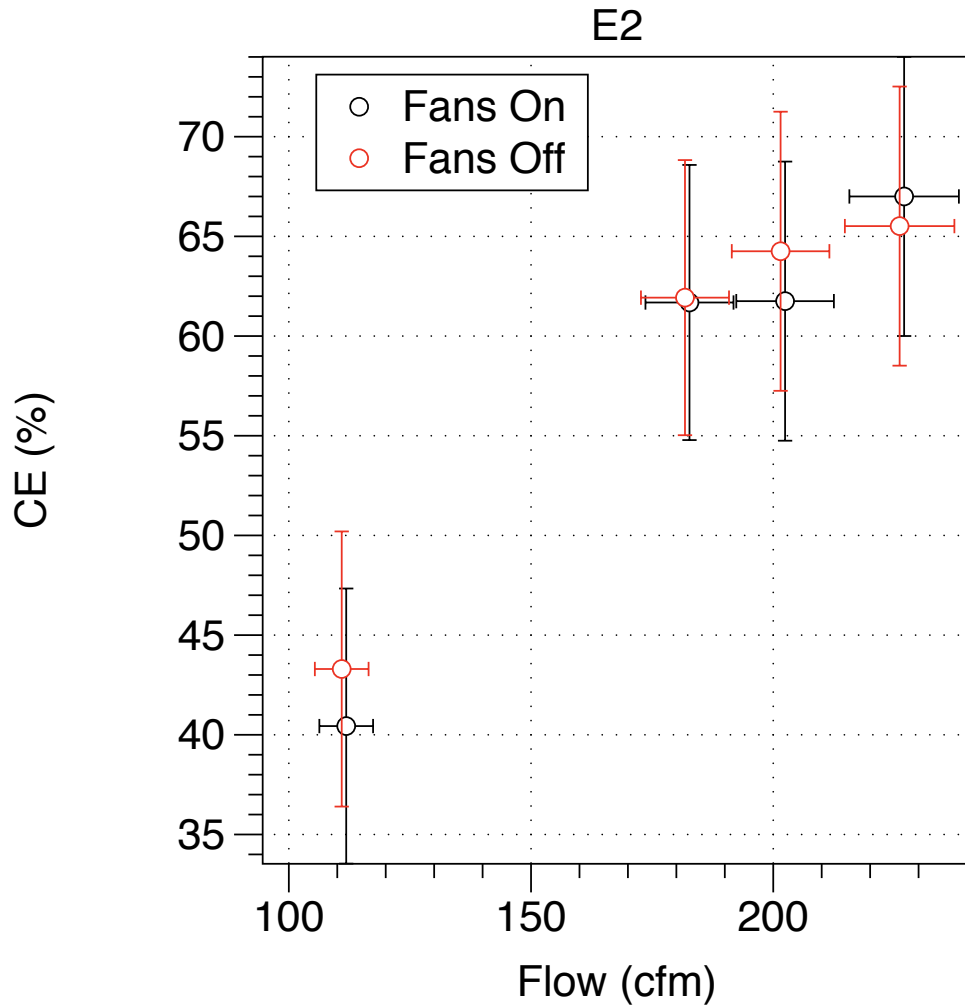


Figure A 5. Capture efficiencies determined by CO₂ measurements in the hood exhaust for the pot of water procedure under conditions of all fans other than the range hood being off and for typical conditions with ventilation and mixing fans on.

Total Particle Concentrations in Room During Hamburger Pan-Fry Experiments

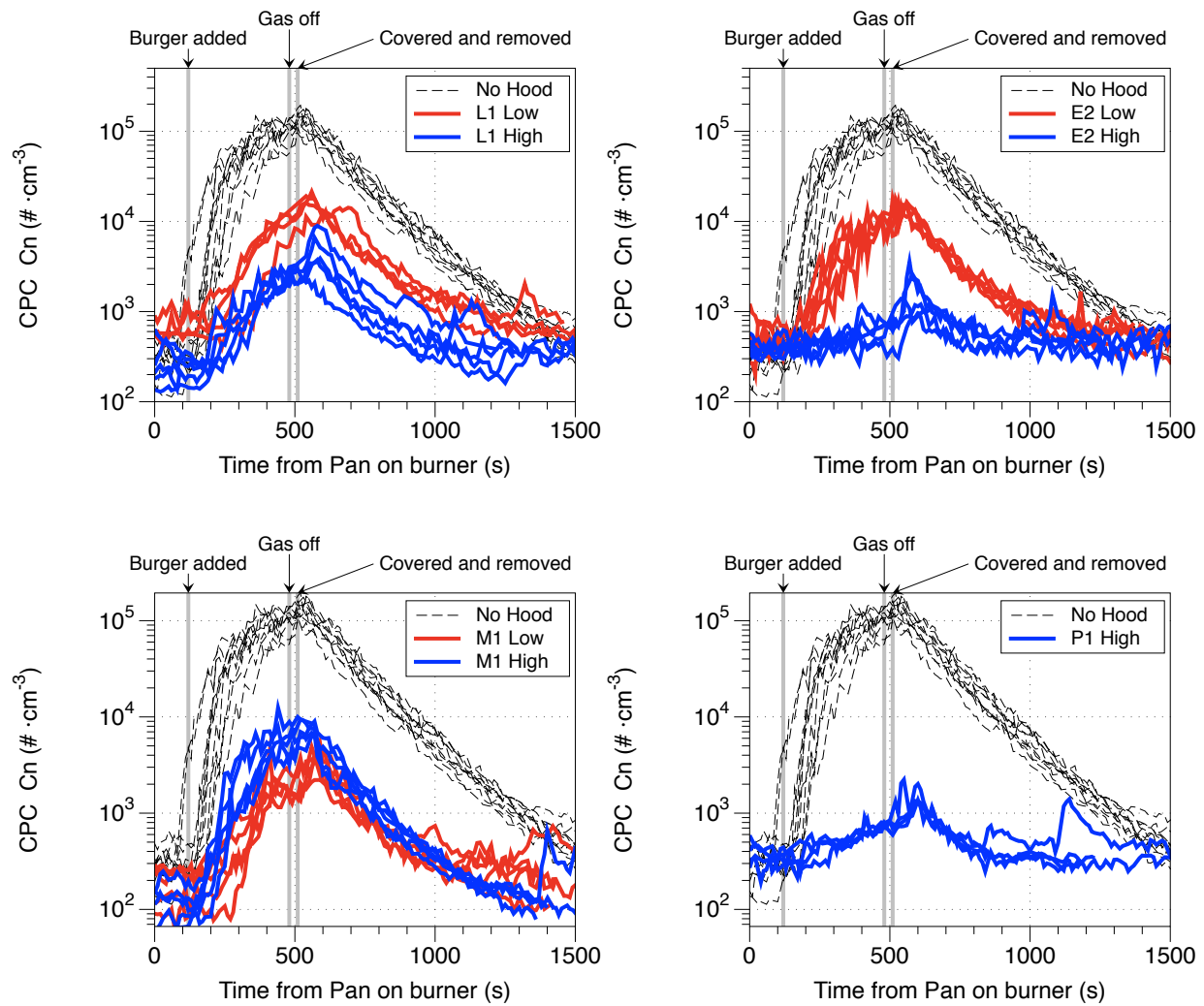


Figure A 6. Total particle concentration measured near the exhaust outlet of room during pan-frying experiments on back burner with no hood present (black dashed line) and with range hoods operating on low (red) and high (blue) fan speeds. Note that particle concentrations are graphed using a log scale. The time scale denotes the seconds since the pan was put on the burner.

Total Particle Concentrations in Room During Green Bean Stir-Fry Experiments

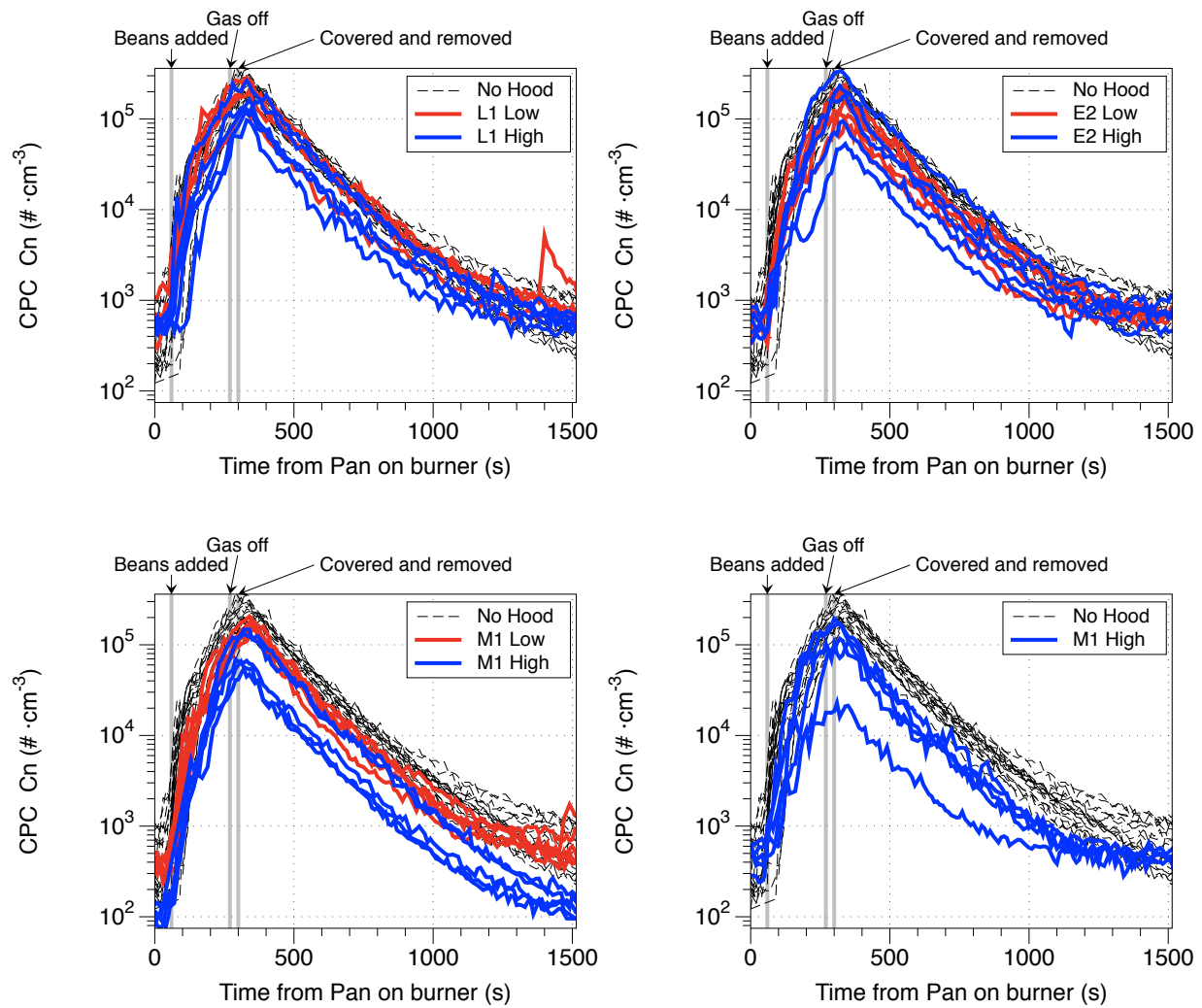


Figure A 7. Total particle concentration measured near the exhaust outlet of room during stir-frying experiments on front burner with no hood present (black dashed line) and with range hoods operating on low (red) and high (blue) fan speeds. Note that particle concentrations are graphed using a log scale. The time scale denotes the seconds since the pan was put on the burner.

Appendix B: Detailed Cooking Protocols

Procedure for Stir-Frying Green Beans in Wok

Background: Twenty, one-pound bags of frozen green beans (Trader Joe's product), were emptied into a large ice chest containing bottles of frozen water, and mixed together (by hand) to produce a homogenous mixture of beans from the twenty individual bags. These mixed beans were then measured into 150g portions, sealed into quart-size Ziploc bags and returned to the freezer.

Note: Be sure to keep track of the windows for the data collection instruments. Re-open any windows that may close during the cooking and monitoring processes.

Procedure:

1. Take a bag of beans from freezer, and mark the bag with burn number
2. Tare scale
3. Weigh the sample (Bag with beans)
4. Return bag to the freezer
5. **Record** weight of sample on Bean Data Sheet
6. Cut a piece of foil that is large enough to use as a lid for the wok
7. Fold foil, and place on electronic scale
8. Rest the wok on the foil
9. Tare scale
10. Add 10.00 grams of peanut oil to the center of the wok
11. **Record** the weight of oil on the Bean Data Sheet
12. **Record** baseline range for MetOne on Bean Data Sheet (Typically between 400-600)
13. **Record** baseline range for CPC on Bean Data Sheet (Typically between 300-500)
14. Gently swirl oil to coat lower portion of wok wall
15. Wait for carbon dioxide monitoring line on Teclog to return to baseline (Approximately 400)
16. Turn gas on to 4.40 liters per minute (See the gas flow meter)
17. Center wok over the flame, and start stopwatch
18. **Record** time that the wok was placed on the flame on the Bean Data Sheet
19. **Record** gas flow rate on Bean Data Sheet (Record the gas flow rate at the time the wok was placed on the flame – See 'Alicat' monitor)
20. At 50 seconds, remove marked bag from freezer
21. At 60 seconds, dump contents of bag into heated peanut oil
22. Stir beans for 3 minutes and 30 seconds (Be sure to move beans around the lower wall of the wok in a 'stir fry' fashion ~ Do not let pieces of bean stick to the wok and burn)
23. Once a total of 4 minutes and 30 seconds have elapsed on the stopwatch, turn off flame and remove wok to a similarly located burner that is off (Either a rear burner if cooking has been conducted in the rear, or a front burner if the cooking has been conducted in the front)
24. Let the wok rest for 30 seconds (The elapsed time will read 5 minutes on the stopwatch)
25. Cover the wok with the foil lid, gently crimping down the edges of the foil around the lip of the wok
26. Place wok on the scale
27. **Record** the weight of the cooked beans on the Bean Data Sheet

28. Take the wok outside of the room and remove foil cover (Foil cover may be re-used)
29. Leave wok outside to cool
30. Tare scale
31. Weigh the Ziploc bag that the beans were in
32. **Record** the weight of the Ziploc bag on the Bean Data Sheet (This weight can be subtracted from 'sample weight' to verify starting bean weight)
33. **Record** Teclog Start and Stop times (Start is recorded just before CO₂ spike, and Stop is recorded when Teclog returns to baseline)
34. Allow monitoring instruments to return to baseline (Be sure to re-open any windows that may close/drop during the cooking and monitoring processes)
35. Discard beans and wash wok with warm water and soap
36. Thoroughly dry wok
37. Repeat steps 1-36 for all bean cooking events

Procedure for Pan-Frying Hamburger

Background: Quarter pound (approximately 110 grams) pre-formed burgers that were 85% lean and 15% fat (Trader Joe's product) were used in these cooking events. Burgers were separated and individually wrapped in foil and stored in the freezer.

Note: Be sure to keep track of the windows for the data collection instruments. Re-open any windows that may close during the cooking and monitoring processes.

Procedure:

1. Place foil wrapped burger on counter to defrost (Note that you might like to have 2-3 burgers out at a time)
2. Examine burger for signs of defrosting (The burger should be soft/flexible and free of ice crystals)
3. Place a piece of foil on top of the electronic scale
4. Tare scale
5. Place unwrapped burger patty on the foil
6. **Record** the weight of the burger on Burger Data Sheet
7. Move burger and foil to counter
8. Cut a piece of foil that is large enough to use as a lid for the pan
9. Fold foil, and place under pan on the electronic scale
10. Tare scale
11. Add 3.5 grams of canola oil to the center of the pan
12. **Record** the weight of oil on the Burger Data Sheet
13. **Record** baseline range for MetOne on Burger Data Sheet (Typically between 400-600)
14. **Record** baseline range for CPC on Burger Data Sheet (Typically between 300-500)
15. Gently swirl oil to coat center of pan
16. Wait for carbon dioxide monitoring line on Teclog to return to baseline (Approximately 400)
17. Turn gas on to 1.71 liters per minute (See the gas flow meter) [Use left rear burner unless instructed otherwise]
18. Center pan over the flame, and start stopwatch

19. **Record** time that the pan was placed on the flame on the Burger Data Sheet
20. **Record** gas flow rate on Burger Data Sheet (Record the gas flow rate at the time the pan was placed on the flame)
21. After the oil has heated for 2 minutes place the burger patty on the oil in the center of the pan
22. Allow burger to cook for one minute (Time will read 3:00 on stopwatch)
23. After one minute of cooking has elapsed, gently press down on patty with metal spatula for five seconds
24. When a second full minute of cooking time has elapsed (Time will read 4:00 on stopwatch), gently press down on patty with metal spatula for five seconds.
25. When a third full minute of cooking time has elapsed (Time will read 5:00 on stopwatch), slide metal spatula under the patty and gently flip it over into the cooking location at the center of the pan.
26. After one minute of cooking on the flipped side (Time will read 6:00 on the stopwatch), gently press down on the patty with the metal spatula for five seconds
27. When a second full minute of cooking has elapsed for the flipped side (Time will read 7:00 on the stopwatch), gently press down on the patty with the metal spatula for five seconds
28. When a third full minute of cooking has elapsed for the flipped side (Time will read 8:00 on the stopwatch), turn off the burner and move the pan to a similarly located burner that is off (Either a rear burner if cooking has been conducted in the rear, or a front burner if the cooking has been conducted in the front)
29. Allow the pan to rest for 30 seconds (Time elapsed will read 8:30 on the stopwatch)
30. Cover the pan with the foil lid, gently crimping down the edges of the foil around the lip of the pan
31. Place pan on the scale
32. **Record** the weight of the cooked burger on the Burger Data Sheet
33. Take the pan outside of the room and remove foil cover (Foil cover may be re-used)
34. Leave pan outside to cool
35. **Record** Teclog Start and Stop times ~ Start is recorded just before carbon dioxide spike, and Stop is recorded when Teclog returns to baseline (Approximately 400)
36. Allow monitoring instruments to return to baseline (Be sure to re-open any windows that may close/drop during the cooking and monitoring processes)
37. Discard burger and wash pan with warm water and soap
38. Thoroughly dry pan
39. Repeat steps 1-38 for all burger cooking events

Procedure for CO₂-Based Capture Efficiency with Pots used for Beans and Burgers

Background: The various cooking utensils used in preparing the beans and burgers were filled approximately halfway with water and tested on the stove at the appropriate cooking gas flow rates. This was done to better understand how the physical feature of the utensil influenced the flow of carbon dioxide into the range hood.

Note: Be sure to keep track of the windows for the data collection instruments. Re-open any windows that may close during the heating and monitoring processes. Label each water-heating event by using the “Event” button on the Teclog screen. Include the utensil location and ‘Burn Number’ in the event label (Ex: Rear 1).

Procedure when alternating pan and wok:

1. Fill the burger cooking pan approximately half-way with tap water
2. Cut a piece of foil that can be used as a lid for the pan
3. Cover the pan with the foil, gently crimping down the foil around the lip of the pan
4. Wait for carbon dioxide monitoring line on Teclog to return to baseline (Approximately 400)
5. Turn gas on to 1.71 liters per minute (See the gas flow meter) [Use left rear burner unless instructed otherwise]
6. Center pan over the flame, and start stopwatch
7. **Record** gas flow rate on the Pots of Water Data Sheet (Record the gas flow rate at the time the pan was placed on the flame)
8. Allow water to heat for 3 minutes
9. After the water has heated for 3 minutes, turn off the gas
10. Allow the pan to remain on the stove until the carbon dioxide reading returns to baseline (Approximately 400)
11. **Record** Teclog Start and Stop times ~ Start is recorded just before carbon dioxide spike, and Stop is recorded when Teclog returns to baseline (Approximately 400)
12. Place pan on the floor
13. Fill the stir fry wok approximately half-way with tap water
14. Cut a piece of foil that can be used as a lid for the wok
15. Cover the wok with the foil, gently crimping down the foil around the lip of the wok
16. Wait for carbon dioxide monitoring line on Teclog to return to baseline (Approximately 400)
17. Turn gas on to 4.40 liters per minute (See the gas flow meter) [Use right front burner unless instructed otherwise]
18. Center wok over the flame, and start stopwatch
19. **Record** gas flow rate on the Pots of Water Data Sheet (Record the gas flow rate at the time the pan was placed on the flame)
20. Allow water to heat for 3 minutes
21. After the water has heated for 3 minutes, turn off the gas
22. Allow the wok to remain on the stove until the carbon dioxide reading returns to baseline (Approximately 400)
23. **Record** Teclog Start and Stop times ~ Start is recorded just before carbon dioxide spike, and Stop is recorded when Teclog returns to baseline (Approximately 400)
24. Place wok on the floor
25. Repeat steps 4-12, 16-24 as directed

Water Heating Procedure - Pots:

Background: Pots approximately half-filled water were tested on the stove to better understand how the physical feature of the pot influenced the flow of carbon dioxide into the range hood

Note: Be sure to keep track of the windows for the data collection instruments. Re-open any windows that may close during the heating and monitoring processes. Label each water-heating event by using the “Event” button on the Teclog screen. Include the utensil location and ‘Burn Number’ in the event label (Ex: Rear 1).

Procedure when alternating sets of pots:

1. Fill four pots approximately half-way with tap water
2. Place a lid on each of the pots
3. Wait for carbon dioxide monitoring line on Teclog to return to baseline (Approximately 400)
4. Turn on flame between high and medium with the line on the knob more towards the high (Use two front burners)
5. Center each of two pots over the burners, and start stopwatch - You will be alternating heating events between the two sets of pots
6. Allow water to heat for 3 minutes
7. After the water has heated for 3 minutes, turn off the gas
8. Allow the pots to remain on the stove until the carbon dioxide reading returns to baseline (Approximately 400)
9. **Record** Teclog Start and Stop times ~ Start is recorded just before carbon dioxide spike, and Stop is recorded when Teclog returns to baseline (Approximately 400)
10. Place pots on the floor
11. Wait for carbon dioxide monitoring (Teclog) to return to baseline (Approximately 400) - Your breathing may have caused a small spike
12. Turn on flame between high and medium with the line on the knob more towards the black dot (Use two rear burners)
13. Center each of two pots over the burners, and start stopwatch - You should use the second set of pots
14. Allow water to heat for 3 minutes
15. After the water has heated for 3 minutes, turn off the gas
16. Allow the pots to remain on the stove until the carbon dioxide reading returns to baseline (Approximately 400)
17. **Record** Teclog Start and Stop times ~ Start is recorded just before carbon dioxide spike, and Stop is recorded when Teclog returns to baseline (Approximately 400)
18. Place pots on the floor
19. Repeat steps 3-18 as necessary

Water Heating Procedure - Wok and Pot:

Background: Woks and pots were tested on the front right burner, to better understand how the physical feature of the utensil influenced the flow of carbon dioxide into the range hood.

Note: Be sure to keep track of the windows for the data collection instruments. Re-open any windows that may close during the heating and monitoring processes. Label each water-heating event by using the “Event” button on the Teclog screen. Include the utensil location and ‘Burn Number’ in the event label (Ex: Rear 1).

Procedure when using woks and pots on front right burner:

Wok at High

1. Fill two woks approximately half-way with tap water
2. Cut two pieces of foil that can be used as lids for the woks

3. Cover the woks with the foil, gently crimping down the foil around the lip of the wok
4. Wait for carbon dioxide monitoring line on Teclog to return to baseline (Approximately 400)
5. Turn flame on to high (Use the front right burner)
6. Center one wok over the flame, and start stopwatch - Leave other wok on the ground
7. Allow water to heat for 3 minutes
8. After the water has heated for 3 minutes, turn off the gas
9. Allow the wok to remain on the stove until the carbon dioxide reading returns to baseline (Approximately 400)
10. **Record** Teclog Start and Stop times ~ Start is recorded just before carbon dioxide spike, and Stop is recorded when Teclog returns to baseline (Approximately 400)
11. Place the wok on the floor
12. Wait for carbon dioxide monitoring (Teclog) to return to baseline (Approximately 400) - Your breathing may have caused a small spike
13. Turn flame on to high (Use the front right burner)
14. Center the second wok over the flame, and start stopwatch - Leave other wok on the ground to cool
15. Allow water to heat for 3 minutes
16. After the water has heated for 3 minutes, turn off the gas
17. Allow the wok to remain on the stove until the carbon dioxide reading returns to baseline (Approximately 400)
18. **Record** Teclog Start and Stop times ~ Start is recorded just before carbon dioxide spike, and Stop is recorded when Teclog returns to baseline (Approximately 400)
19. Place the wok on the floor
20. Repeat steps 4-19 as directed

Wok at 4.40 lpm of gas flow

1. Fill two woks approximately half-way with tap water (You may use the woks used in the previous “high’ burn events)
2. Cut two pieces of foil that can be used as lids for the woks
3. Cover the woks with the foil, gently crimping down the foil around the lip of the wok
4. Wait for carbon dioxide monitoring line on Teclog to return to baseline (Approximately 400)
5. Turn gas on to 4.40 liters per minute (Use the front right burner)
6. Center one wok over the flame, and start stopwatch - Leave other wok on the ground
7. Allow water to heat for 3 minutes
8. After the water has heated for 3 minutes, turn off the gas
9. Allow the wok to remain on the stove until the carbon dioxide reading returns to baseline (Approximately 400)
10. **Record** Teclog Start and Stop times ~ Start is recorded just before carbon dioxide spike, and Stop is recorded when Teclog returns to baseline (Approximately 400)
11. Place the wok on the floor
12. Wait for carbon dioxide monitoring (Teclog) to return to baseline (Approximately 400) - Your breathing may have caused a small spike
13. Turn gas on to 4.40 liters per minute (Use the front right burner)
14. Center the second wok over the flame, and start stopwatch - Leave other wok on the ground to cool

15. Allow water to heat for 3 minutes
16. After the water has heated for 3 minutes, turn off the gas
17. Allow the wok to remain on the stove until the carbon dioxide reading returns to baseline (Approximately 400)
18. **Record** Teclog Start and Stop times ~ Start is recorded just before carbon dioxide spike, and Stop is recorded when Teclog returns to baseline (Approximately 400)
19. Place the wok on the floor
20. Repeat steps 4-19 as directed

Pot at 4.40 lpm gas flow

1. Fill two pots approximately half-way with tap water
2. Cut two pieces of foil that can be used as lids for the pots
3. Cover the pots with the foil, gently crimping down the foil around the lip of the pots
4. Wait for carbon dioxide monitoring line on Teclog to return to baseline (Approximately 400)
5. Turn gas on to 4.40 liters per minute (Use the front right burner)
6. Center one pot over the flame, and start stopwatch - Leave other pot on the ground
7. Allow water to heat for 3 minutes
8. After the water has heated for 3 minutes, turn off the gas
9. Allow the pot to remain on the stove until the carbon dioxide reading returns to baseline (Approximately 400)
10. **Record** Teclog Start and Stop times ~ Start is recorded just before carbon dioxide spike, and Stop is recorded when Teclog returns to baseline (Approximately 400)
11. Place the pot on the floor
12. Wait for carbon dioxide monitoring (Teclog) to return to baseline (Approximately 400) - Your breathing may have caused a small spike
13. Turn gas on to 4.40 liters per minute (Use the front right burner)
14. Center the second pot over the flame, and start stopwatch - Leave other pot on the ground to cool
15. Allow water to heat for 3 minutes
16. After the water has heated for 3 minutes, turn off the gas
17. Allow the pot to remain on the stove until the carbon dioxide reading returns to baseline (Approximately 400)
18. **Record** Teclog Start and Stop times ~ Start is recorded just before carbon dioxide spike, and Stop is recorded when Teclog returns to baseline (Approximately 400)
19. Place the pot on the floor
20. Repeat steps 4-19 as directed

Water Heating Procedure - Pan and Pot:

Background: Pans and pots were tested on the left rear burner, to better understand how the physical feature of the utensil influenced the flow of carbon dioxide into the range hood. (Note that only 2 pot events were completed and no pans were done)

Note: Be sure to keep track of the windows for the data collection instruments. Re-open any windows that may close during the heating and monitoring processes. Label each water-heating

event by using the “Event” button on the Teclog screen. Include the utensil location and ‘Burn Number’ in the event label (Ex: Rear 1).

Procedure when using pans and pots on left rear burner:

Pan at High

1. Fill two pans approximately half-way with tap water
2. Cut two pieces of foil that can be used as lids for the pans
3. Cover the pans with the foil, gently crimping down the foil around the lip of the pans
4. Wait for carbon dioxide monitoring line on Teclog to return to baseline (Approximately 400)
5. Turn flame on to high (Use the left rear burner)
6. Center pan over the flame, and start stopwatch - Leave other pan on the ground
7. Allow water to heat for 3 minutes
8. After the water has heated for 3 minutes, turn off the gas
9. Allow the pan to remain on the stove until the carbon dioxide reading returns to baseline (Approximately 400)
10. **Record** Teclog Start and Stop times ~ Start is recorded just before carbon dioxide spike, and Stop is recorded when Teclog returns to baseline (Approximately 400)
11. Place the pan on the floor
12. Wait for carbon dioxide monitoring (Teclog) to return to baseline (Approximately 400) - Your breathing may have caused a small spike
13. Turn flame on to high (Use the left rear burner)
14. Center the second pan over the flame, and start stopwatch - Leave other pan on the ground to cool
15. Allow water to heat for 3 minutes
16. After the water has heated for 3 minutes, turn off the gas
17. Allow the pan to remain on the stove until the carbon dioxide reading returns to baseline (Approximately 400)
18. **Record** Teclog Start and Stop times ~ Start is recorded just before carbon dioxide spike, and Stop is recorded when Teclog returns to baseline (Approximately 400)
19. Place the pan on the floor
20. Repeat steps 4-19 as directed

Pan at 1.71 lpm of gas flow

1. Fill two pans approximately half-way with tap water (You may use the pans used in the previous “high” burn events)
2. Cut two pieces of foil that can be used as lids for the pans
3. Cover the pans with the foil, gently crimping down the foil around the lip of the pans
4. Wait for carbon dioxide monitoring line on Teclog to return to baseline (Approximately 400)
5. Turn gas on to 1.71 liters per minute (Use the left rear burner)
6. Center pan over the flame, and start stopwatch - Leave other pan on the ground
7. Allow water to heat for 3 minutes
8. After the water has heated for 3 minutes, turn off the gas
9. Allow the pan to remain on the stove until the carbon dioxide reading returns to baseline (Approximately 400)

10. **Record** Teclog Start and Stop times ~ Start is recorded just before carbon dioxide spike, and Stop is recorded when Teclog returns to baseline (Approximately 400)
11. Place the pan on the floor
12. Wait for carbon dioxide monitoring (Teclog) to return to baseline (Approximately 400) - Your breathing may have caused a small spike
13. Turn gas on to 1.71 liters per minute (Use the left rear burner)
14. Center the second pan over the flame, and start stopwatch - Leave other pan on the ground to cool
15. Allow water to heat for 3 minutes
16. After the water has heated for 3 minutes, turn off the gas
17. Allow the pan to remain on the stove until the carbon dioxide reading returns to baseline (Approximately 400)
18. **Record** Teclog Start and Stop times ~ Start is recorded just before carbon dioxide spike, and Stop is recorded when Teclog returns to baseline (Approximately 400)
19. Place the pan on the floor
20. Repeat steps 4-19 as directed

Pot at 1.71 lpm gas flow

1. Fill two pots approximately half-way with tap water
2. Cut two pieces of foil that can be used as lids for the pots
3. Cover the pots with the foil, gently crimping down the foil around the lip of the pots
4. Wait for carbon dioxide monitoring line on Teclog to return to baseline (Approximately 400)
5. Turn gas on to 1.71 liters per minute (Use the left rear burner)
6. Center one pot over the flame, and start stopwatch - Leave other pot on the ground
7. Allow water to heat for 3 minutes
8. After the water has heated for 3 minutes, turn off the gas
9. Allow the pot to remain on the stove until the carbon dioxide reading returns to baseline (Approximately 400)
10. **Record** Teclog Start and Stop times ~ Start is recorded just before carbon dioxide spike, and Stop is recorded when Teclog returns to baseline (Approximately 400)
11. Place the pot on the floor
12. Wait for carbon dioxide monitoring (Teclog) to return to baseline (Approximately 400) - Your breathing may have caused a small spike
13. Turn gas on to 1.71 liters per minute (Use the left rear burner)
14. Center the second pan over the flame, and start stopwatch - Leave other pot on the ground to cool
15. Allow water to heat for 3 minutes
16. After the water has heated for 3 minutes, turn off the gas
17. Allow the pot to remain on the stove until the carbon dioxide reading returns to baseline (Approximately 400)
18. **Record** Teclog Start and Stop times ~ Start is recorded just before carbon dioxide spike, and Stop is recorded when Teclog returns to baseline (Approximately 400)
19. Place the pot on the floor
20. Repeat steps 4-19 as directed

Appendix C: Summary of Experiments

Table C- 1. Summary information about Burger Pan-Frying Experiments.

Experiment	Date	Pan	Gas Flow (lpm)	Pre Cooking Mass (g)		Post Cook (g)	Mass Loss	
				Oil	Beans		(g)	(%)
L1-L-BU-B-01	6/17/13	1	1.73	3.47	106.8	80.6	29.7	26.9
L1-L-BU-B-02	6/17/13	2	1.76	3.49	106.2	83.7	26.0	23.7
L1-L-BU-B-03	6/17/13	1	1.76	3.52	107.1	83.5	27.1	24.5
L1-L-BU-B-04	6/17/13	2	1.70	3.50	106.7	81.0	29.2	26.5
L1-H-BU-B-01	6/18/13	1	1.76	3.50	109.1	87.0	25.6	22.7
L1-H-BU-B-02	6/18/13	2	1.71	3.49	108.4	87.1	24.7	22.1
L1-H-BU-B-03	6/18/13	1	1.71	3.50	108.7	86.5	25.7	22.9
L1-H-BU-B-04	6/18/13	2	1.69	3.51	108.3	85.9	25.8	23.1
L1-H-BU-B-05	6/18/13	1	1.70	3.49	101.5	81.3	23.7	22.6
E2-L-BU-B-01	6/27/13	1	1.72	3.50	108.2	84.5	27.3	24.4
E2-L-BU-B-02	6/27/13	1	1.71	3.51	107.3	83.1	27.7	25.0
E2-L-BU-B-03	6/27/13	1	1.71	3.51	108.4	83.6	28.3	25.3
E2-L-BU-B-04	6/27/13	1	1.71	3.50	107.4	81.6	29.3	26.4
E2-L-BU-B-05	6/27/13	1	1.71	3.51	110.2	85.1	28.6	25.1
E2-H-BU-B-01	7/1/13	1	1.71	3.51	105.8	83.4	25.8	23.6
E2-H-BU-B-02	7/1/13	1	1.72	3.51	102.7	77.5	28.8	27.1
E2-H-BU-B-03	7/1/13	1	1.71	3.50	101.0	76.9	27.7	26.4
E2-H-BU-B-04	7/1/13	1	1.71	3.51	102.5	75.5	30.4	28.7
E2-H-BU-B-05	7/1/13	1	1.72	3.50	109.5	81.4	31.6	27.9
M1-L-BU-B-01	7/3/13	1	1.70	3.51	108.3	84.2	27.6	24.7
M1-L-BU-B-02	7/3/13	1	1.71	3.50	107.2	84.0	26.7	24.1
M1-L-BU-B-03	7/3/13	1	1.72	3.51	106.1	80.2	29.5	26.9
M1-L-BU-B-04	7/3/13	1	1.71	3.50	109.2	82.7	30.0	26.6
M1-L-BU-B-05	7/3/13	1	1.71	3.51	101.7	77.4	27.9	26.5
M1-H-BU-B-01	7/5/13	1	1.71	3.50	104.5	87.2	20.7	19.2
M1-H-BU-B-02	7/5/13	1	1.70	3.51	105.6	84.8	24.3	22.3
M1-H-BU-B-03	7/5/13	1	1.71	3.51	104.1	83.8	23.9	22.2
M1-H-BU-B-04	7/5/13	1	1.70	3.51	107.4	84.9	26.1	23.5
M1-H-BU-B-05	7/5/13	1	1.71	3.51	107.5	84.9	26.1	23.5
P1-H-BU-B-01	6/25/13	1	1.71	3.50	109.7	86.3	27.0	23.8
P1-H-BU-B-02	6/25/13	1	1.70	3.51	110.5	85.7	28.3	24.8
P1-H-BU-B-03	6/25/13	1	1.72	3.50	110.6	84.7	29.4	25.8
P1-H-BU-B-04	6/25/13	1	1.71	3.51	110.2	86.2	27.6	24.2
P1-H-BU-B-05	6/25/13	1	1.69	3.51	109.8	85.6	27.7	24.4

Table C- 2. Summary information about green bean stir-fry experiments on front burner.

Experiment	Date	Pan	Gas Flow (lpm)	Pre Cooking Mass (g)		Post Cook (g)	Mass Loss	
				Oil	Beans		(g)	(%)
L1-L-SF-F-01	6/19/13	2	4.44	10.03	91.7	46.1	45.6	-
L1-L-SF-F-02	6/19/13	1	4.41	10.02	150.1	122.1	38.0	23.8
L1-L-SF-F-03	6/19/13	2	4.46	10.06	150.4	144.7	5.6	-
L1-L-SF-F-04	6/19/13	1	4.38	10.02	150.3	128.9	21.4	13.4
L1-L-SF-F-05	6/19/13	2	4.39	10.04	150.9	121.4	29.5	18.3
L1-L-SF-F-06	6/19/13	1	4.37	10.06	150.4	134.1	16.3	10.2
L1-H-SF-F-01	6/20/13	1	4.40	10.03	150.3	131.4	18.9	11.8
L1-H-SF-F-02	6/20/13	2	4.37	10.01	150.3	124.8	25.5	15.9
L1-H-SF-F-03	6/20/13	1	4.42	10.02	150.2	129.7	20.5	12.8
L1-H-SF-F-04	6/20/13	2	4.37	10.03	150.3	131.9	18.4	11.5
L1-H-SF-F-05	6/20/13	1	4.40	10.08	150.2	125.4	24.8	15.5
E2-L-SF-F-01	6/27/13	2	4.40	10.02	150.1	127.5	22.6	14.1
E2-L-SF-F-02	6/27/13	2	4.43	10.03	149.7	125.9	23.9	14.9
E2-L-SF-F-03	6/27/13	2	4.40	10.02	149.8	125.3	24.5	15.4
E2-L-SF-F-04	6/28/13	2	4.41	10.00	149.7	123.2	26.4	16.5
E2-L-SF-F-05	6/28/13	2	4.42	10.01	149.7	124.7	25.0	15.6
E2-H-SF-F-01	6/28/13	2	4.42	10.00	149.3	128.3	21.1	13.2
E2-H-SF-F-02	6/28/13	2	4.40	10.03	150.2	128.7	21.5	13.4
E2-H-SF-F-03	6/28/13	2	4.39	10.04	149.5	126.6	22.9	14.3
E2-H-SF-F-04	6/28/13	2	4.43	10.00	150.1	128.4	21.7	13.5
E2-H-SF-F-05	6/28/13	2	4.41	10.01	150.0	127.0	23.0	14.4
M1-L-SF-F-01	7/3/13	2	4.39	10.01	149.7	124.8	25.0	15.6
M1-L-SF-F-02	7/3/13	2	4.42	10.01	149.9	128.3	21.6	13.5
M1-L-SF-F-03	7/3/13	2	4.41	10.01	150.1	124.9	25.2	15.7
M1-L-SF-F-04	7/3/13	2	4.41	10.01	149.5	128.0	21.5	13.5
M1-L-SF-F-05	7/3/13	2	4.40	10.01	150.1	124.6	25.5	15.9
M1-H-SF-F-01	7/5/13	2	4.38	10.03	149.8	128.3	21.5	13.5
M1-H-SF-F-02	7/5/13	2	4.41	10.04	149.9	127.3	22.6	14.1
M1-H-SF-F-03	7/5/13	2	4.40	10.01	150.0	121.8	28.3	17.7
M1-H-SF-F-04	7/5/13	2	4.40	10.00	149.7	125.5	24.2	15.2
M1-H-SF-F-05	7/5/13	2	4.43	10.01	150.0	127.2	22.9	14.3
P1-H-SF-F-01	6/25/13	2	4.10	10.01	149.8	121.5	28.2	17.7
P1-H-SF-F-02	6/25/13	2	4.39	10.02	149.6	129.9	19.8	12.4
P1-H-SF-F-03	6/25/13	2	4.39	10.00	149.8	129.0	20.9	13.1
P1-H-SF-F-04	6/25/13	2	4.38	10.02	149.7	130.0	19.7	12.3
P1-H-SF-F-05	6/25/13	2	4.42	10.00	149.8	126.1	23.7	14.8

Table C- 3. Summary information about green bean stir-fry experiments on back burner.

Experiment	Date	Pan	Gas Flow (lpm)	Pre Cooking Mass (g)		Post Cook	Mass Loss	
				Oil	Beans	(g)	(g)	(%)
E2-H-SF-B-01	7/17/13	2	4.41	10.00	150.1	121.6	28.5	17.8
E2-H-SF-B-02	7/17/13	2	4.41	10.01	149.9	124.6	25.3	15.8
E2-H-SF-B-03	7/17/13	2	4.41	10.01	150.1	123.4	26.8	16.7
E2-H-SF-B-04	7/17/13	2	4.39	10.03	149.4	121.8	27.7	17.3
E2-H-SF-B-05	7/17/13	2	4.43	9.99	149.7	122.7	27.0	16.9
E2-L-SF-B-01	7/17/13	2	4.40	10.02	150.5	124.9	25.6	15.9
E2-L-SF-B-02	7/17/13	2	4.41	9.99	149.8	117.4	32.4	20.3
E2-L-SF-B-03	7/17/13	2	4.39	10.04	149.1	123.2	25.9	16.3
E2-L-SF-B-04	7/17/13	2	4.40	10.04	149.7	123.7	26.0	16.3
E2-L-SF-B-05	7/17/13	2	4.41	10.01	150.0	123.4	26.6	16.6

Appendix D: Results of Experiments Conducted without Exhaust

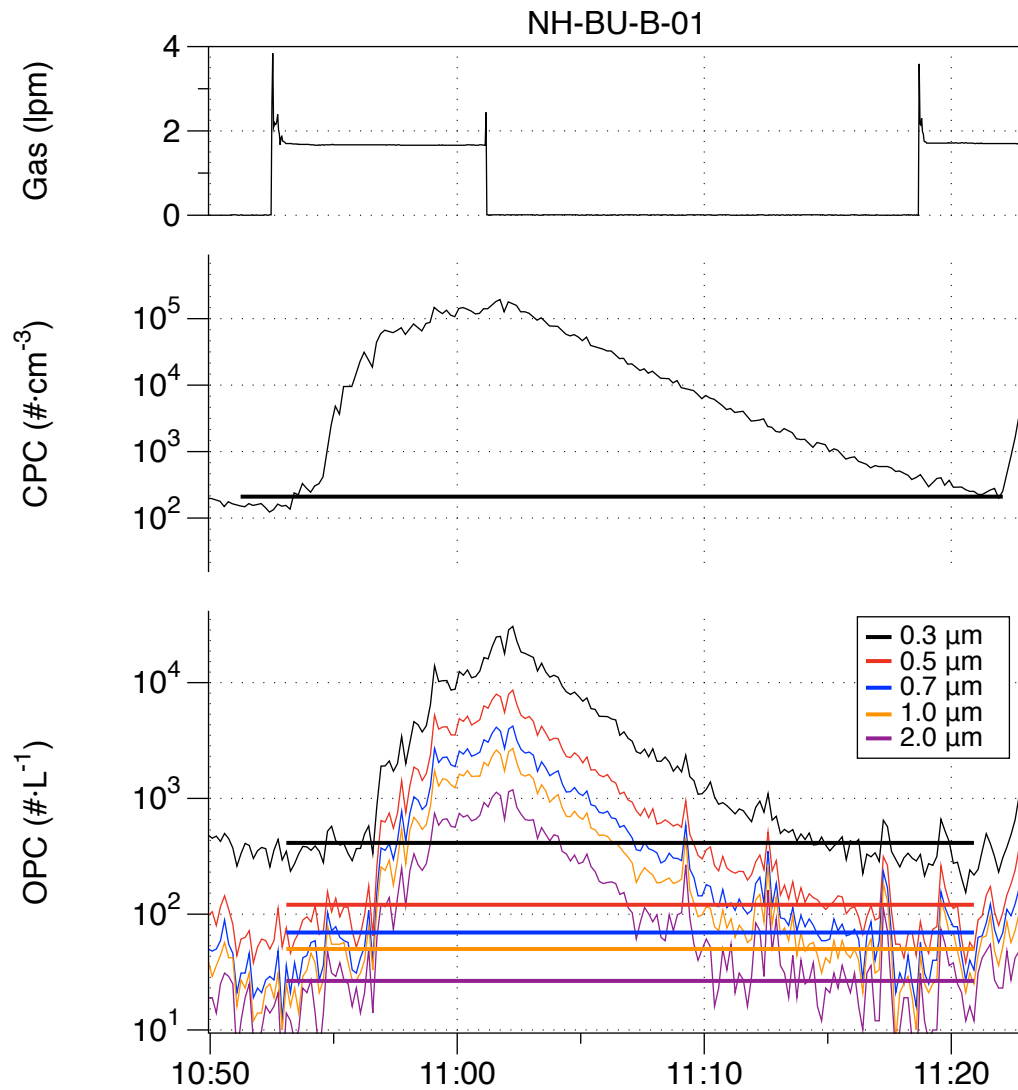


Figure D- 1. Results from experiment NH-BU-B-01 with burger on back burner and no hood.

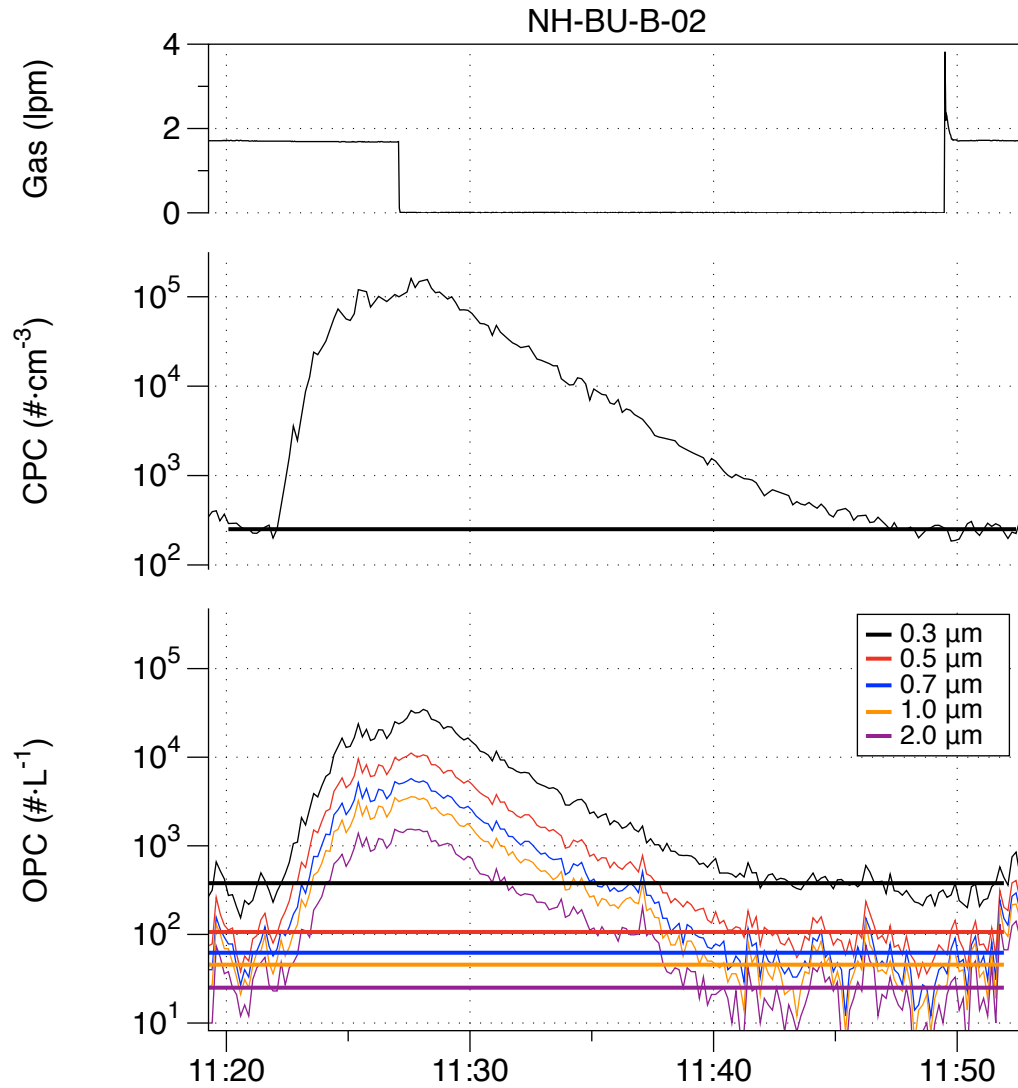


Figure D- 2. Results from experiment NH-BU-B-02 with burger on back burner and no hood.

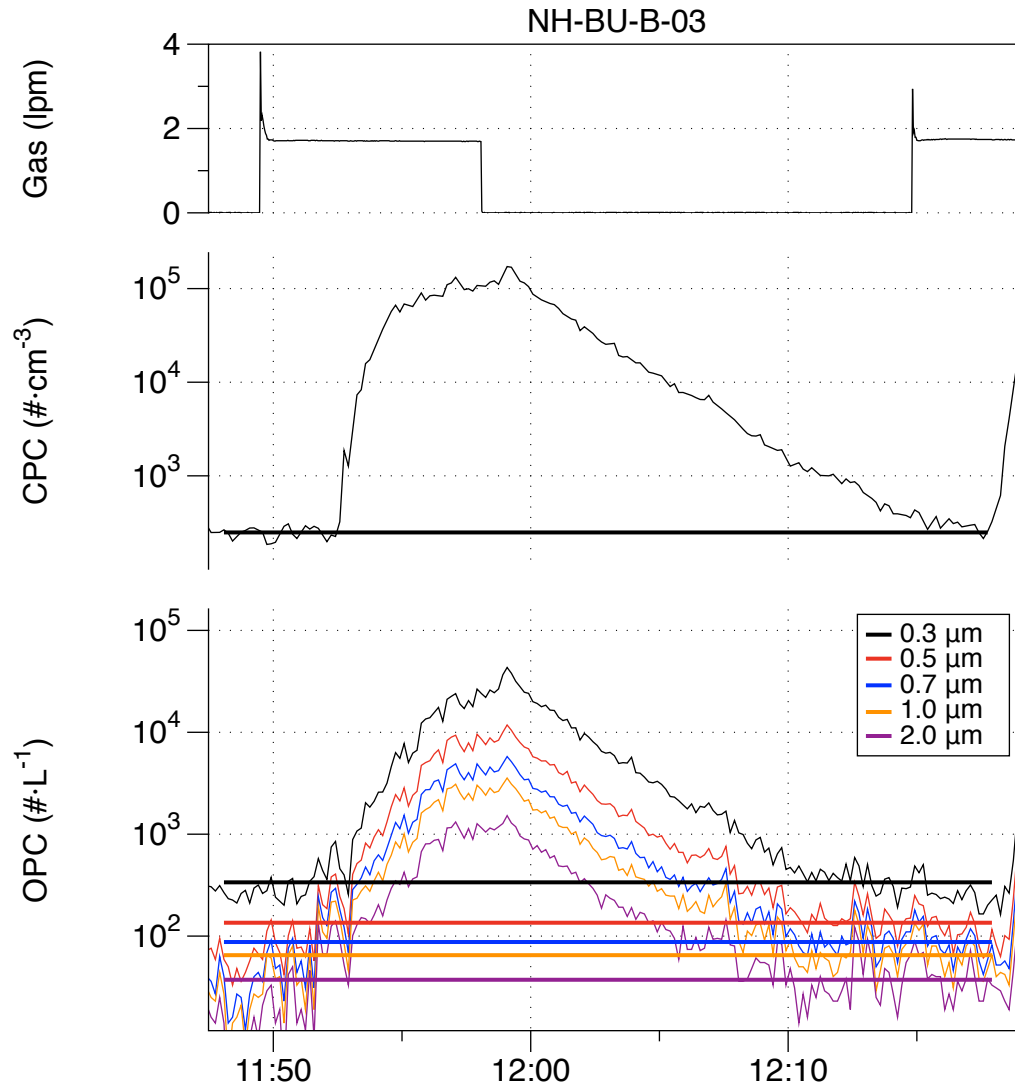


Figure D- 3. Results from experiment NH-BU-B-03 with burger on back burner and no hood.

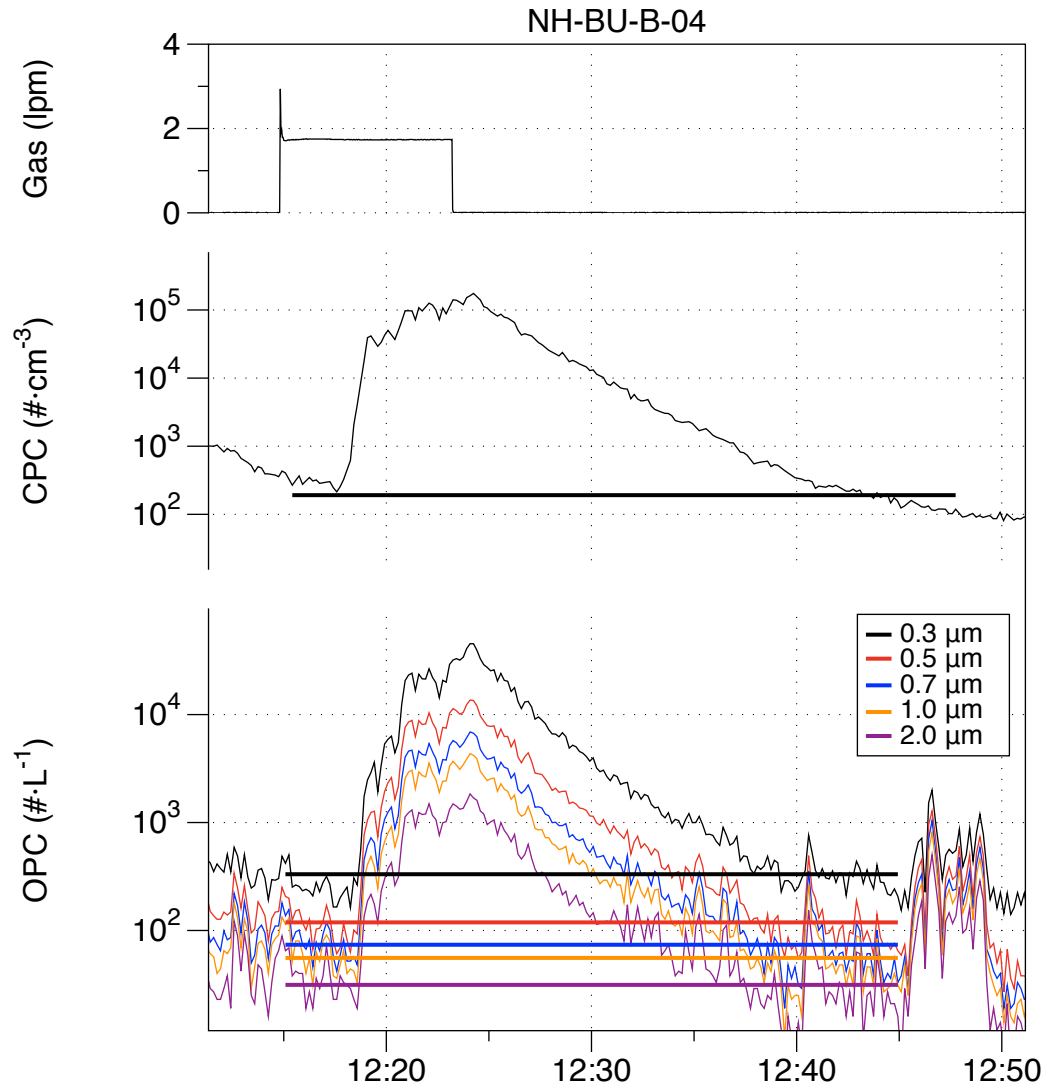


Figure D- 4. Results from experiment NH-BU-B-04 with burger on back burner and no hood.

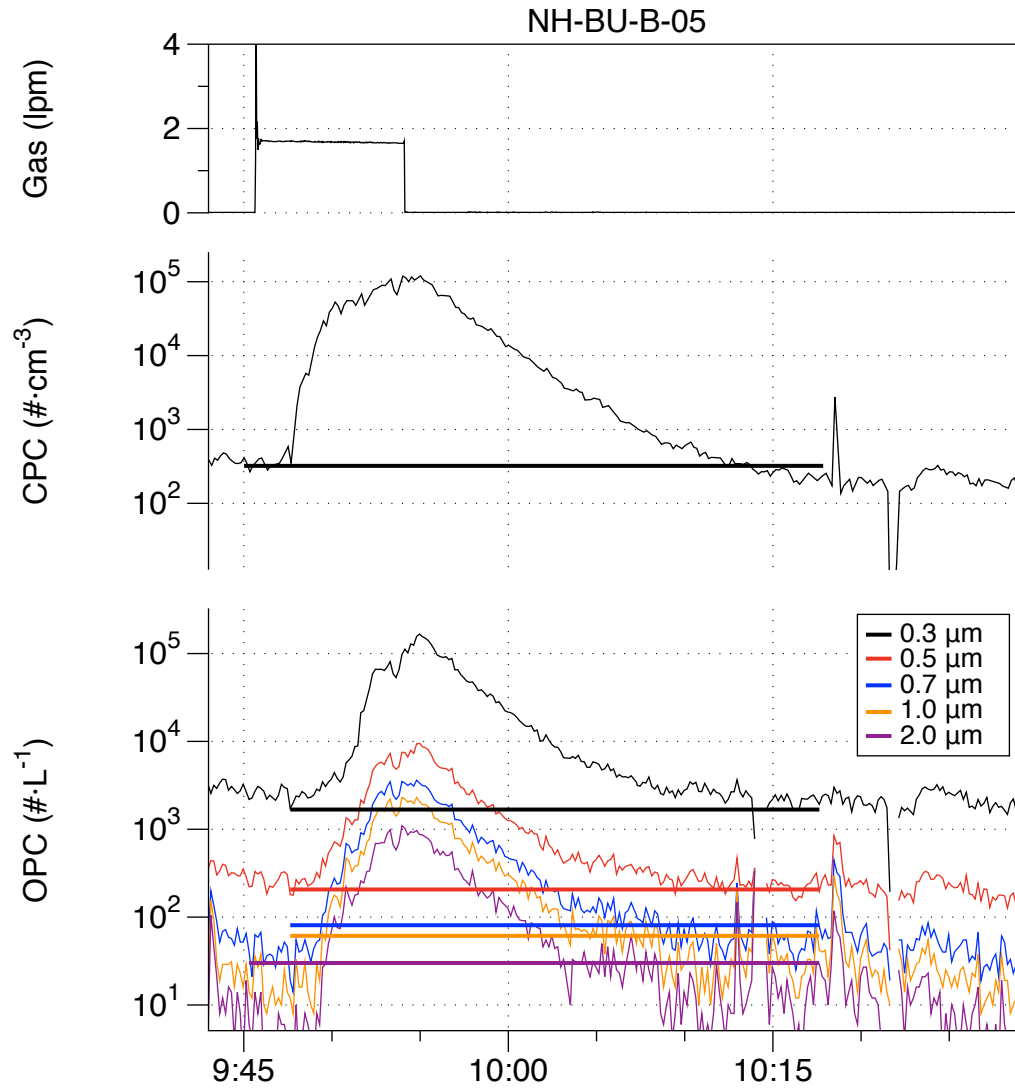


Figure D- 5. Results from experiment NH-BU-B-05 with burger on back burner and no hood.

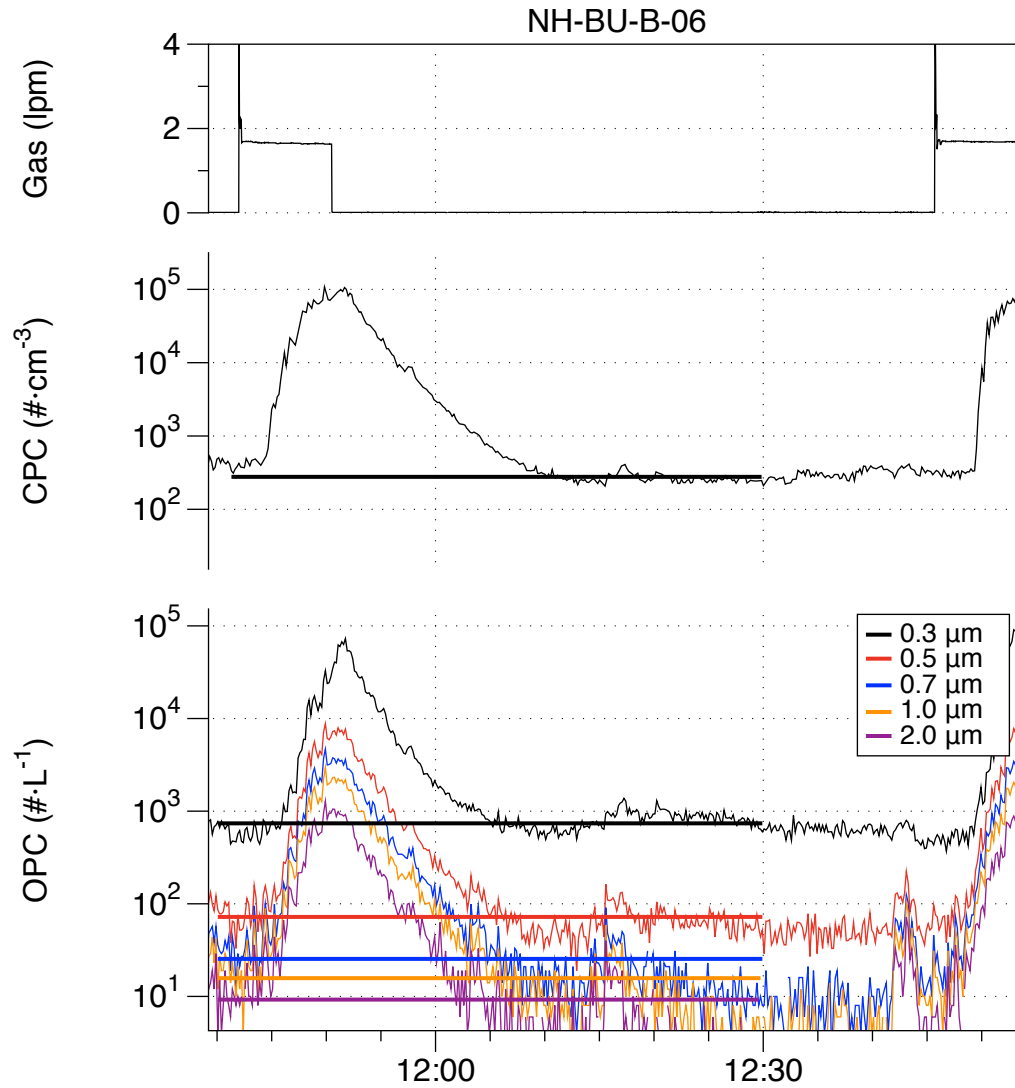


Figure D- 6. Results from experiment NH-BU-B-06 with burger on back burner and no hood..

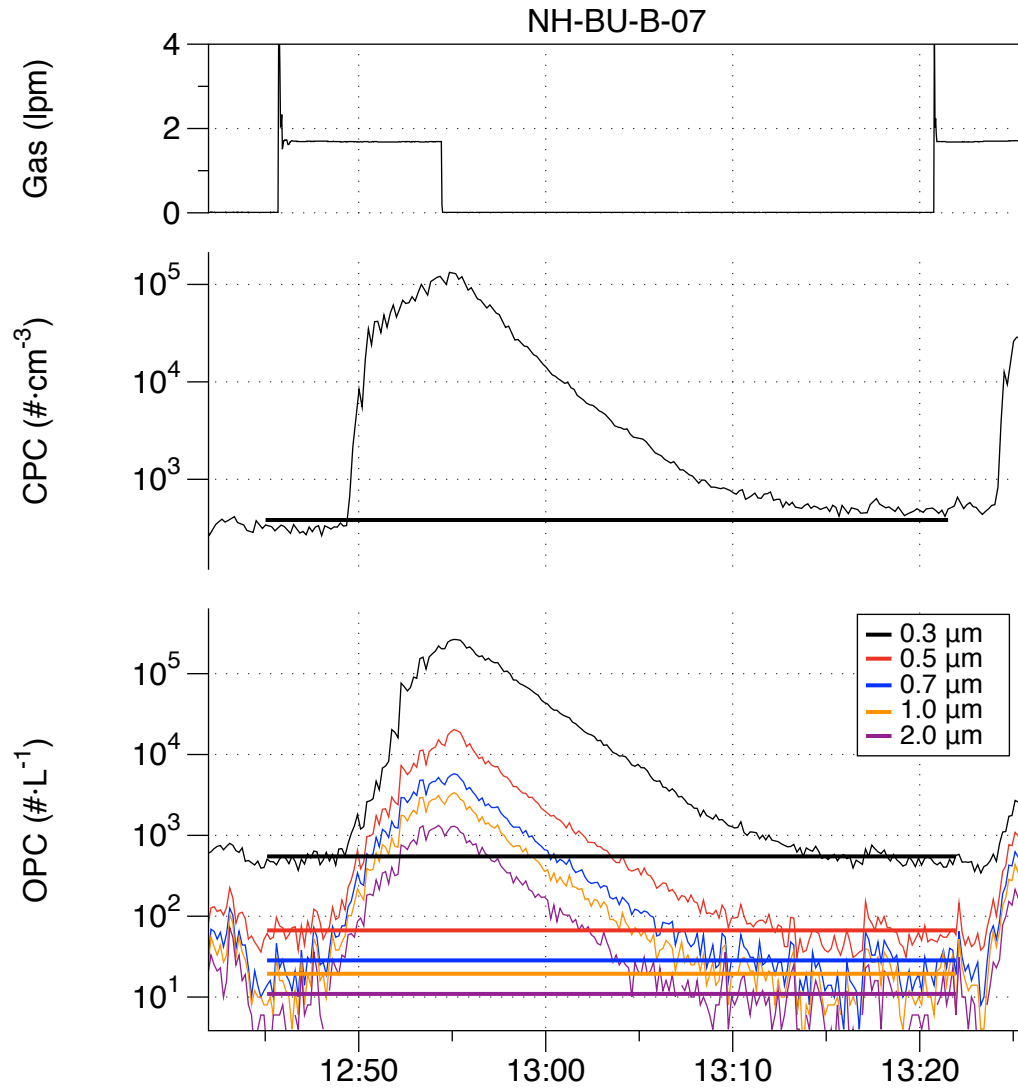


Figure D- 7. Results from experiment NH-BU-B-07 with burger on back burner and no hood.

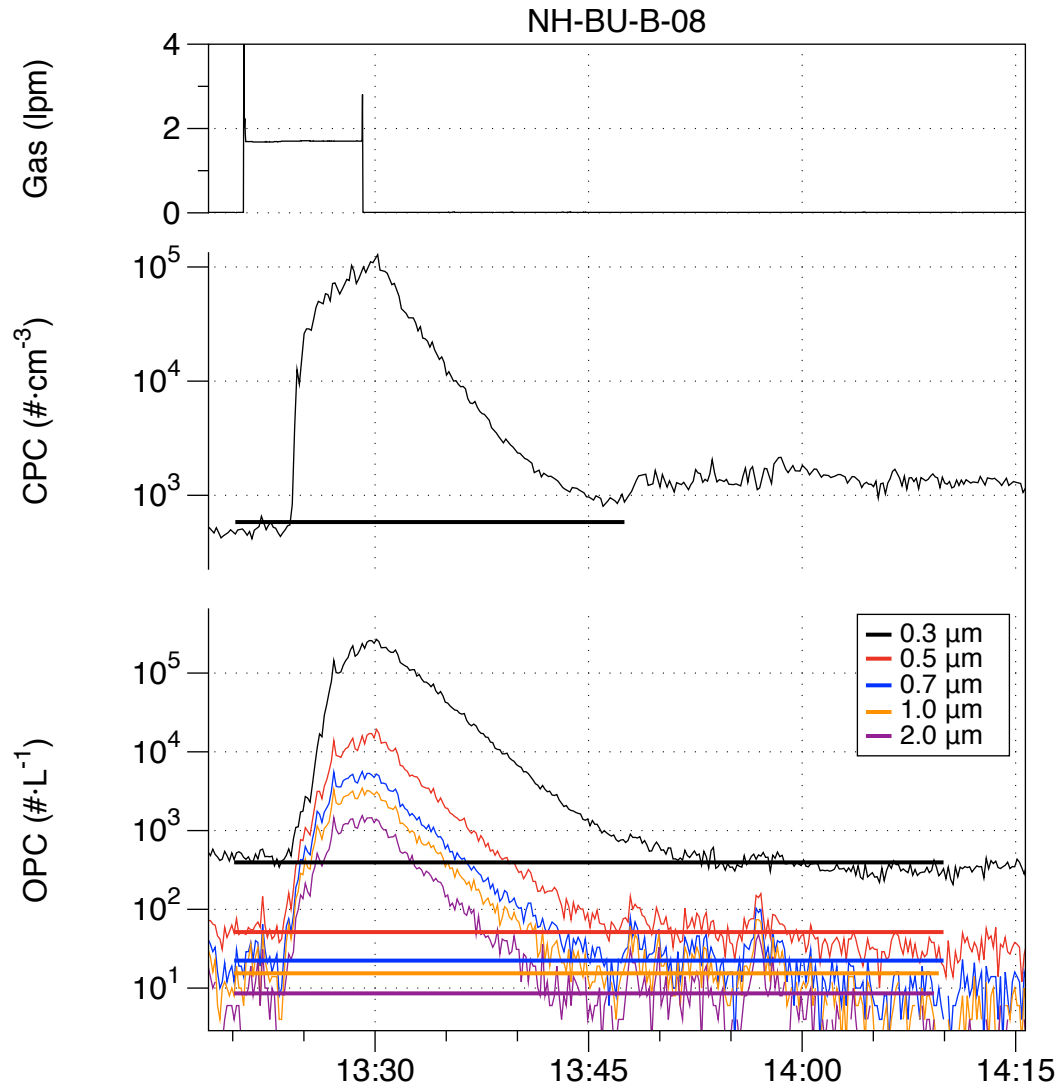


Figure D- 8. Results from experiment NH-BU-B-08 with burger on back burner and no hood.

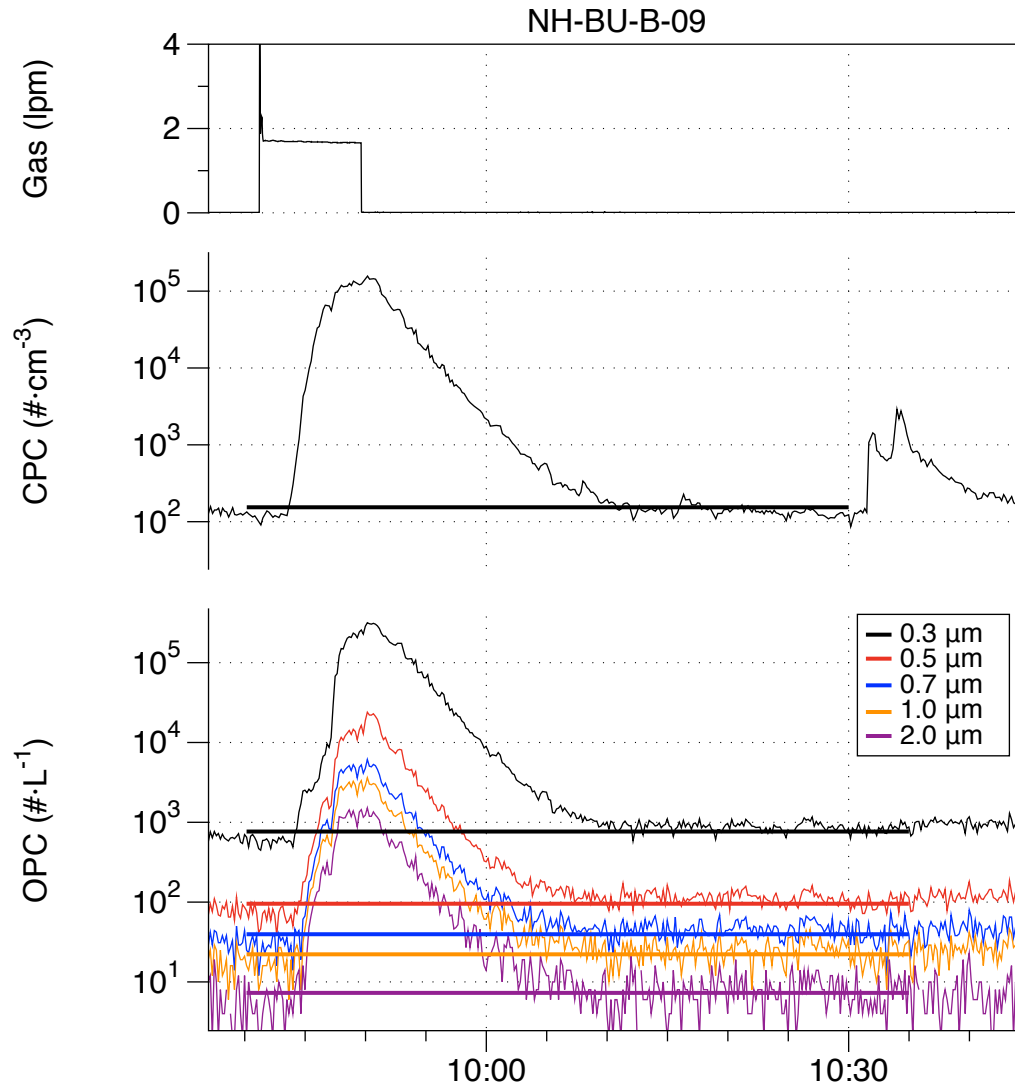


Figure D- 9. Results from experiment NH-BU-B-09 with burger on back burner and no hood.

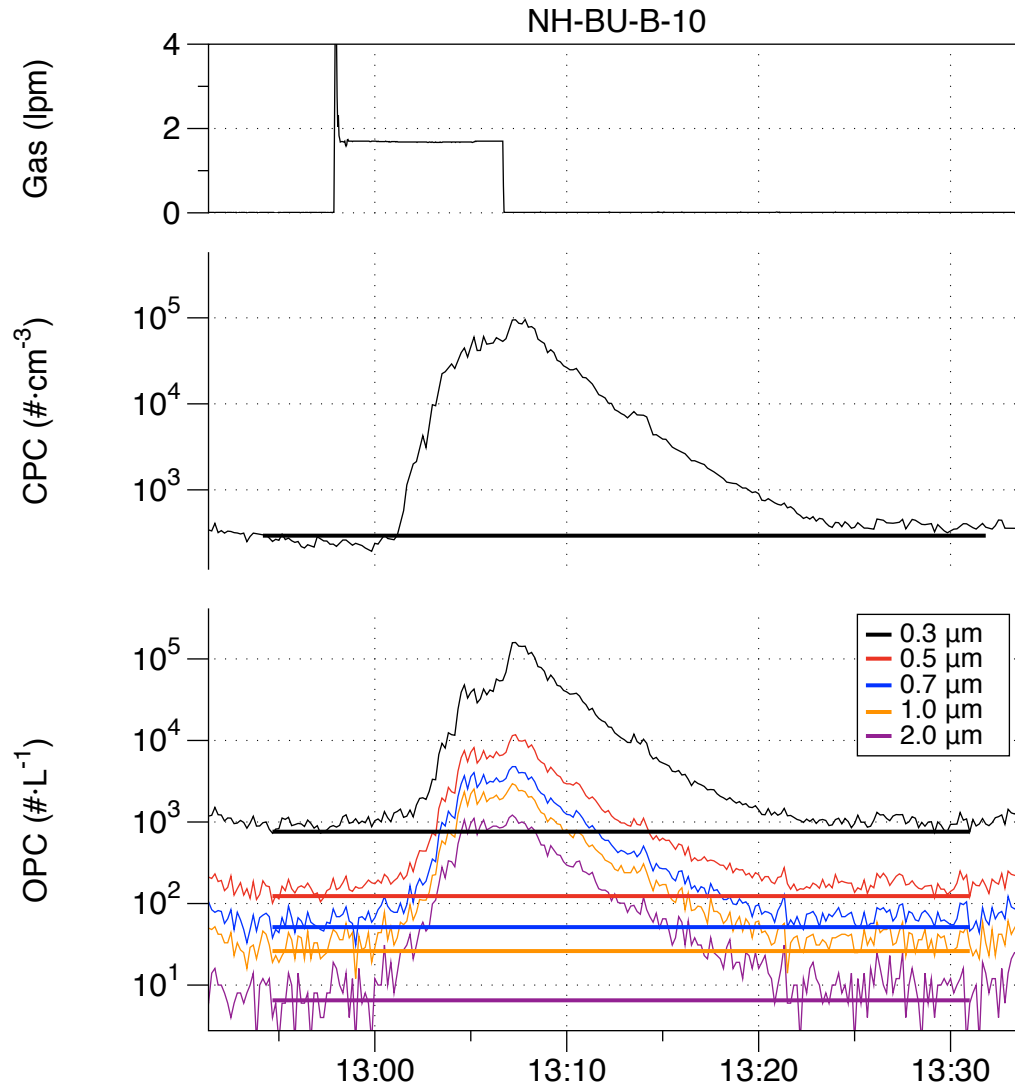


Figure D- 10. Results from experiment NH-BU-B-10 with burger on back burner and no hood.

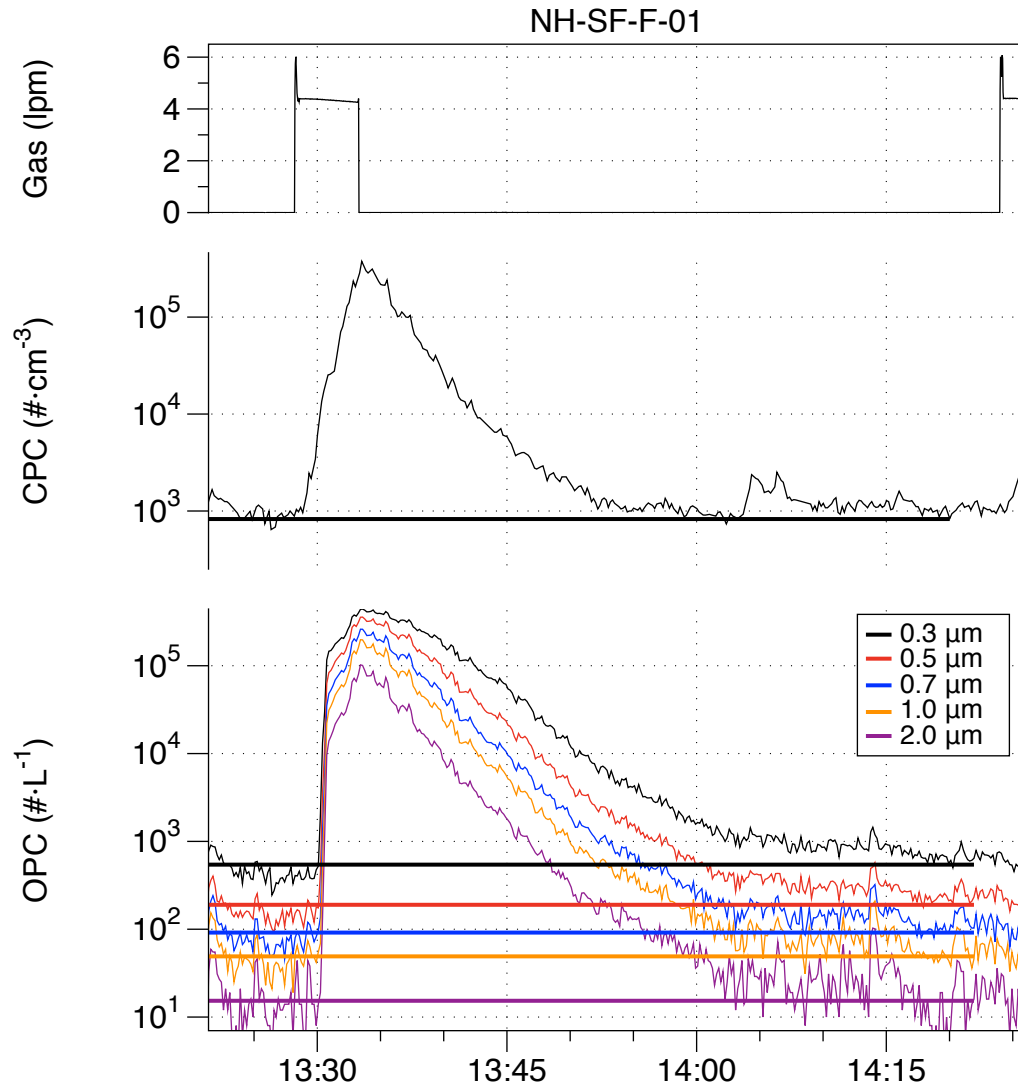


Figure D- 11. Results from experiment NH-SF-F-01 with stir-fry on back burner and no hood.

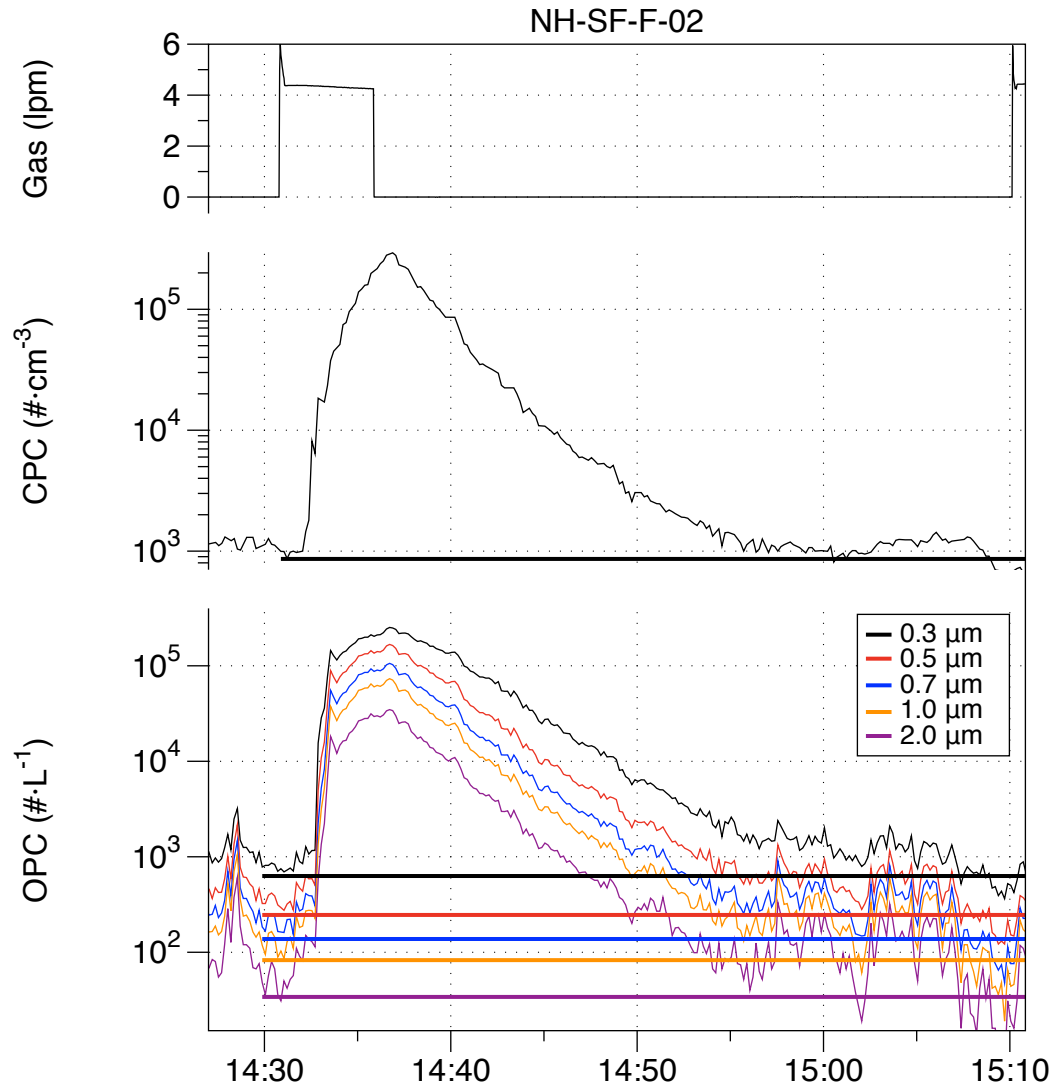


Figure D- 12. Results from experiment NH-SF-F-02 with stir-fry on back burner and no hood.

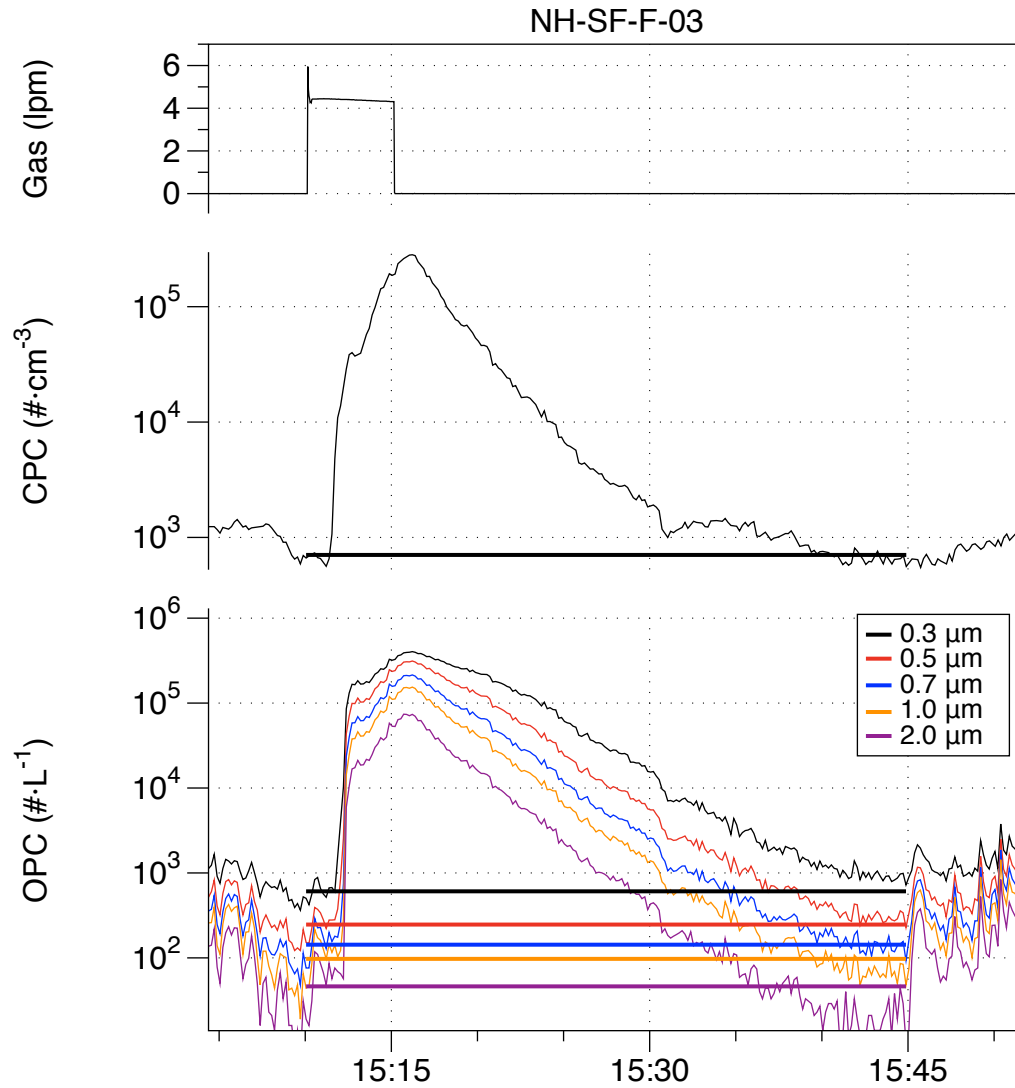


Figure D- 13. Results from experiment NH-SF-F-03 with stir-fry on back burner and no hood.

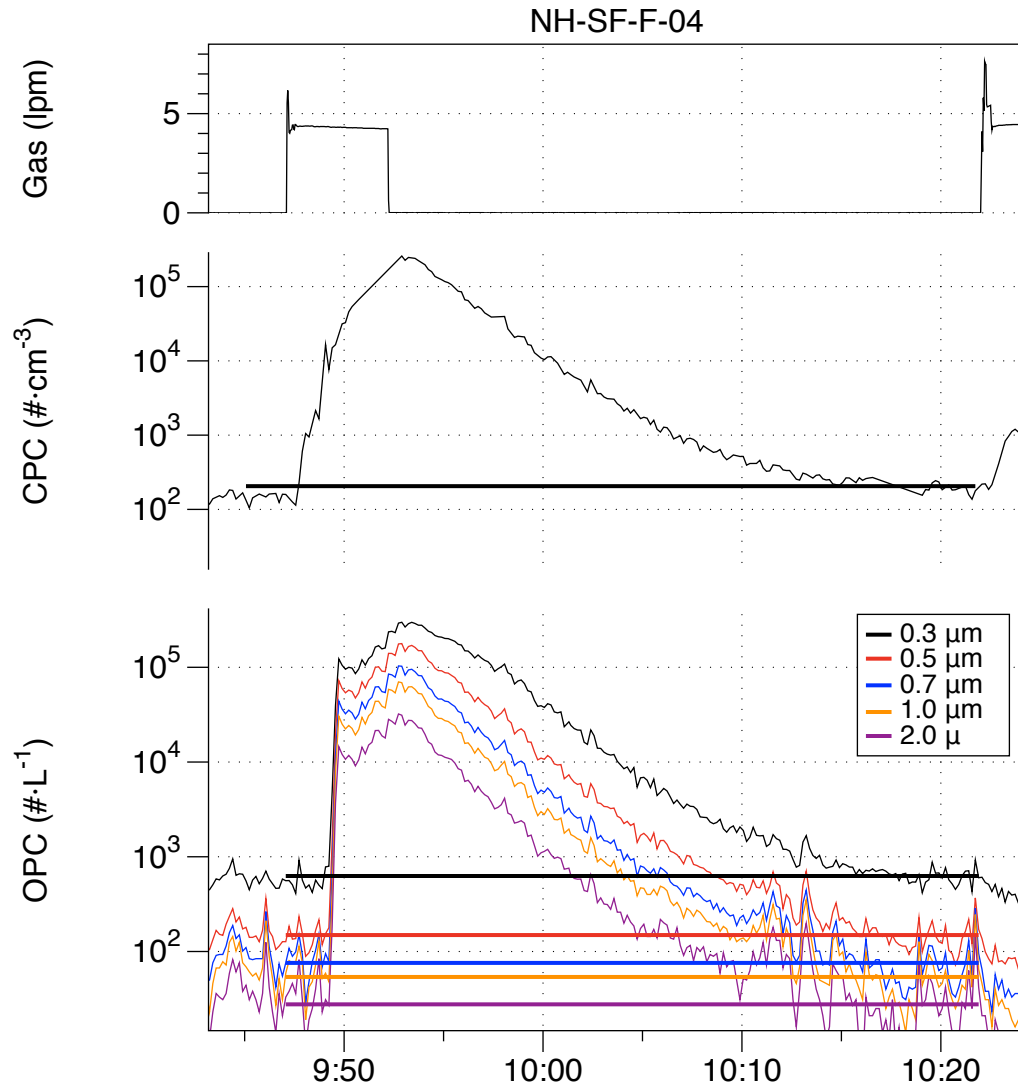


Figure D- 14. Results from experiment NH-SF-F-04 with stir-fry on front burner and no hood.

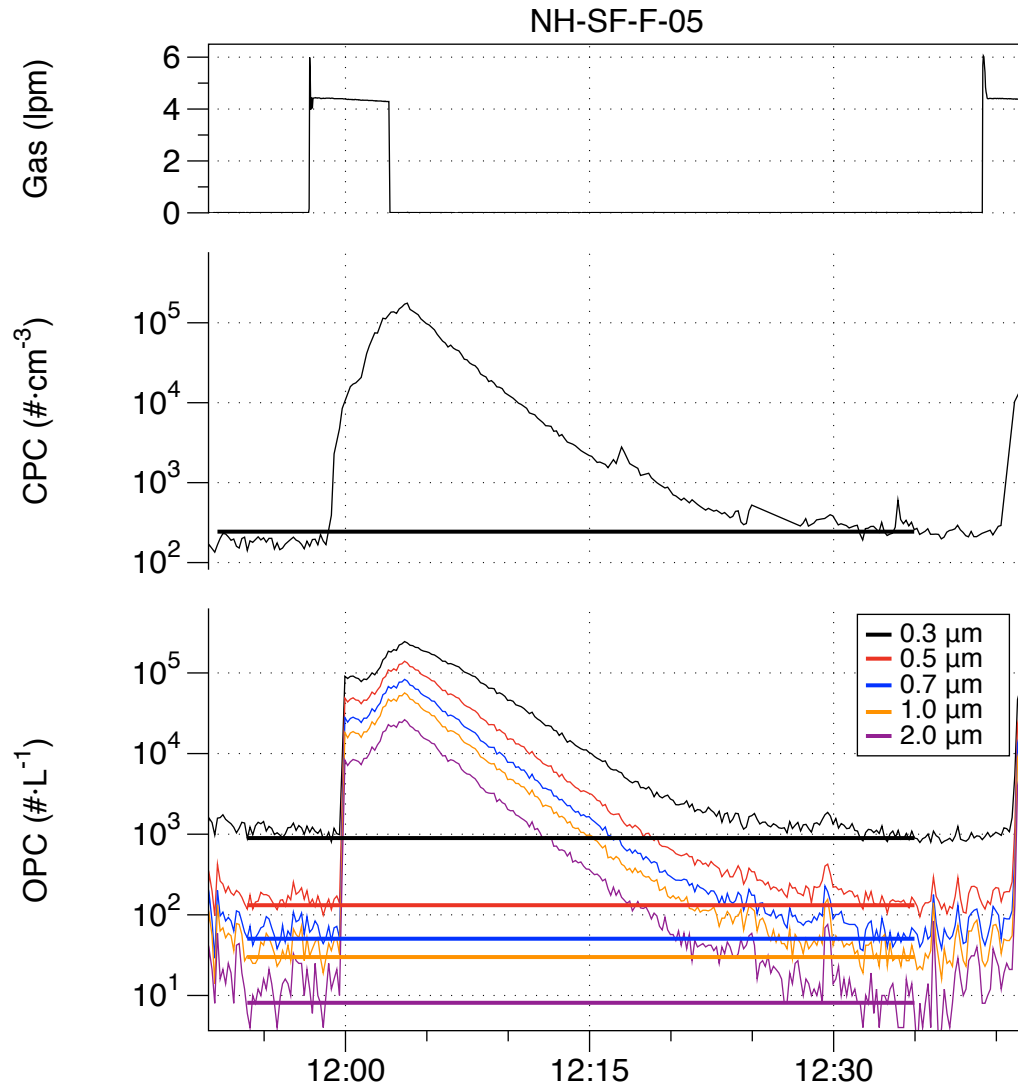


Figure D- 15. Results from experiment NH-SF-F-05 with stir-fry on front burner and no hood.

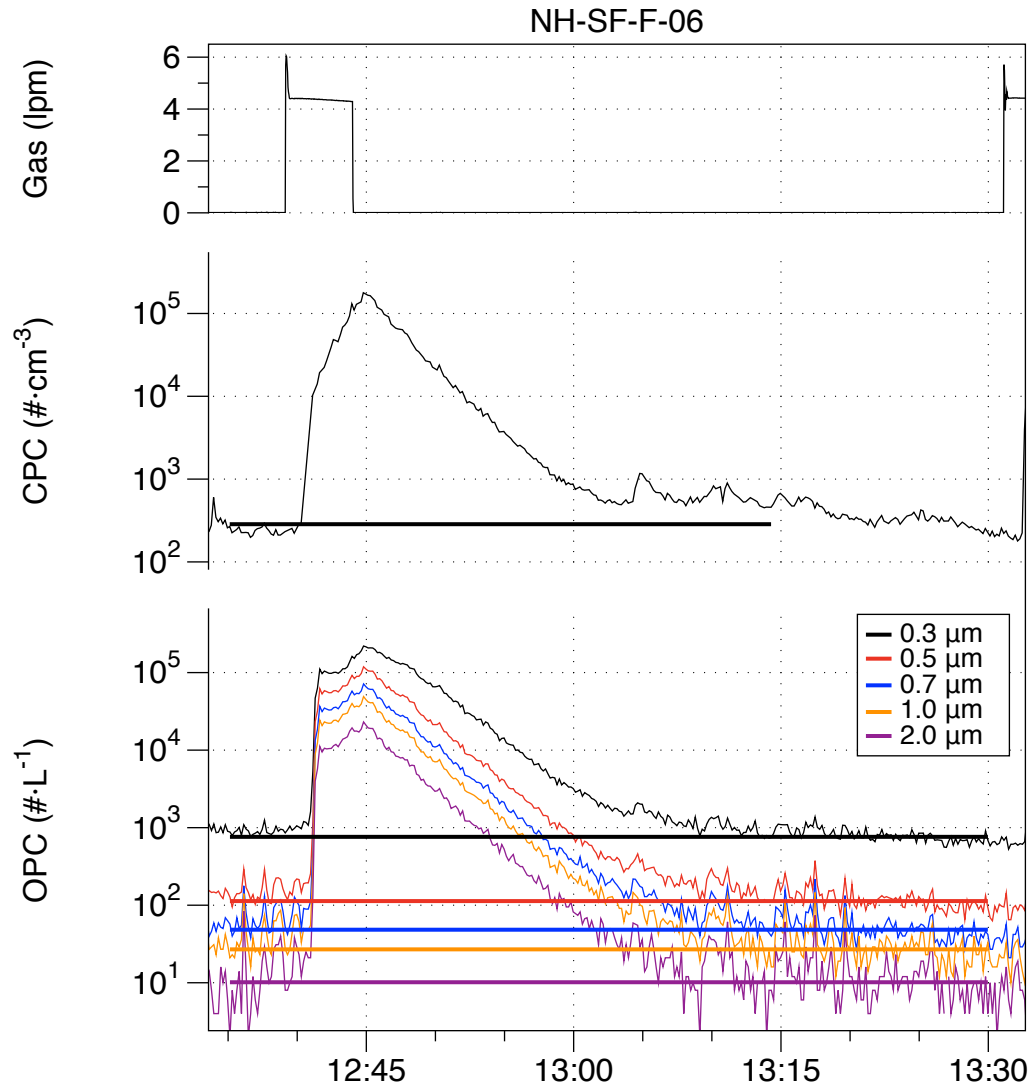


Figure D- 16. Results from experiment NH-SF-F-06 with stir-fry on front burner and no hood.

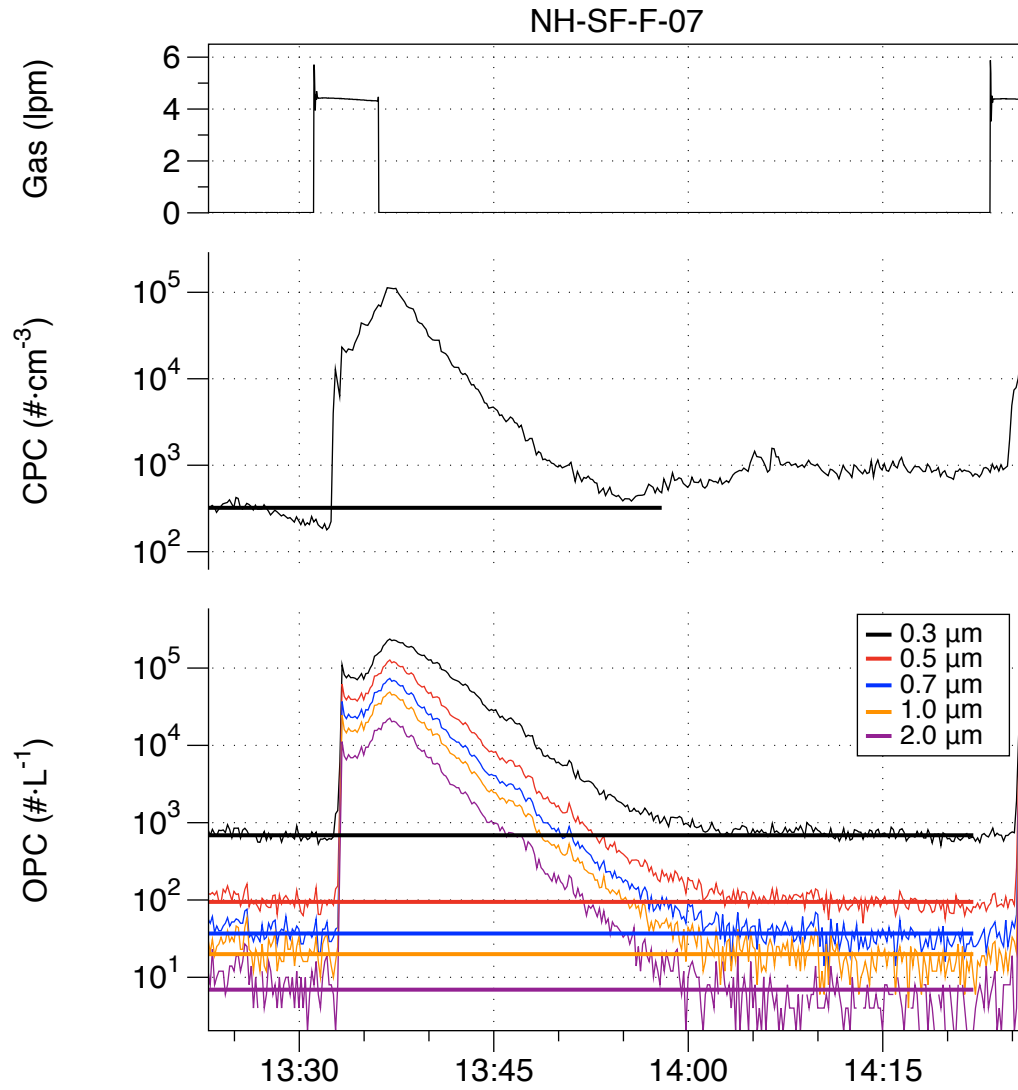


Figure D- 17. Results from experiment NH-SF-F-07 with stir-fry on front burner and no hood.

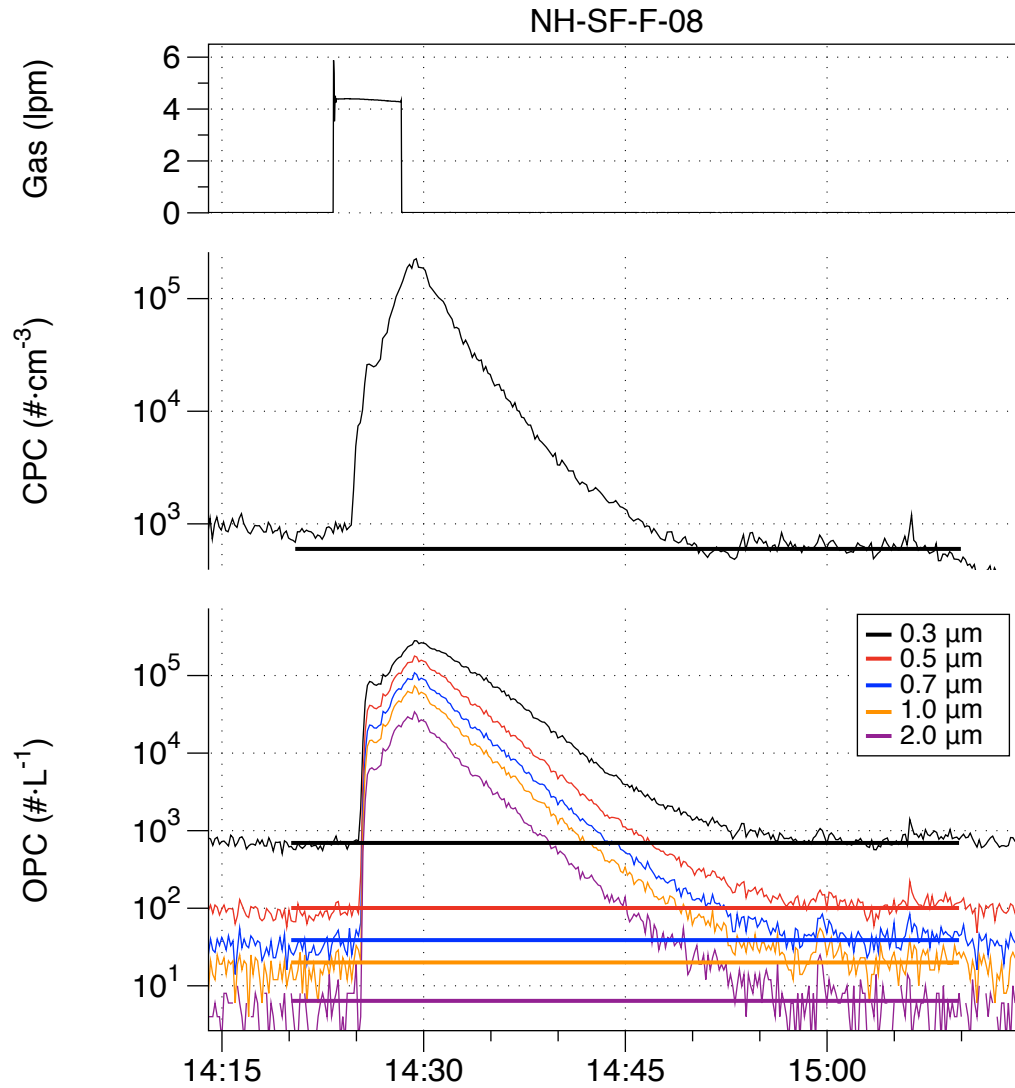


Figure D- 18. Results from experiment NH-SF-F-08 with stir-fry on front burner and no hood.

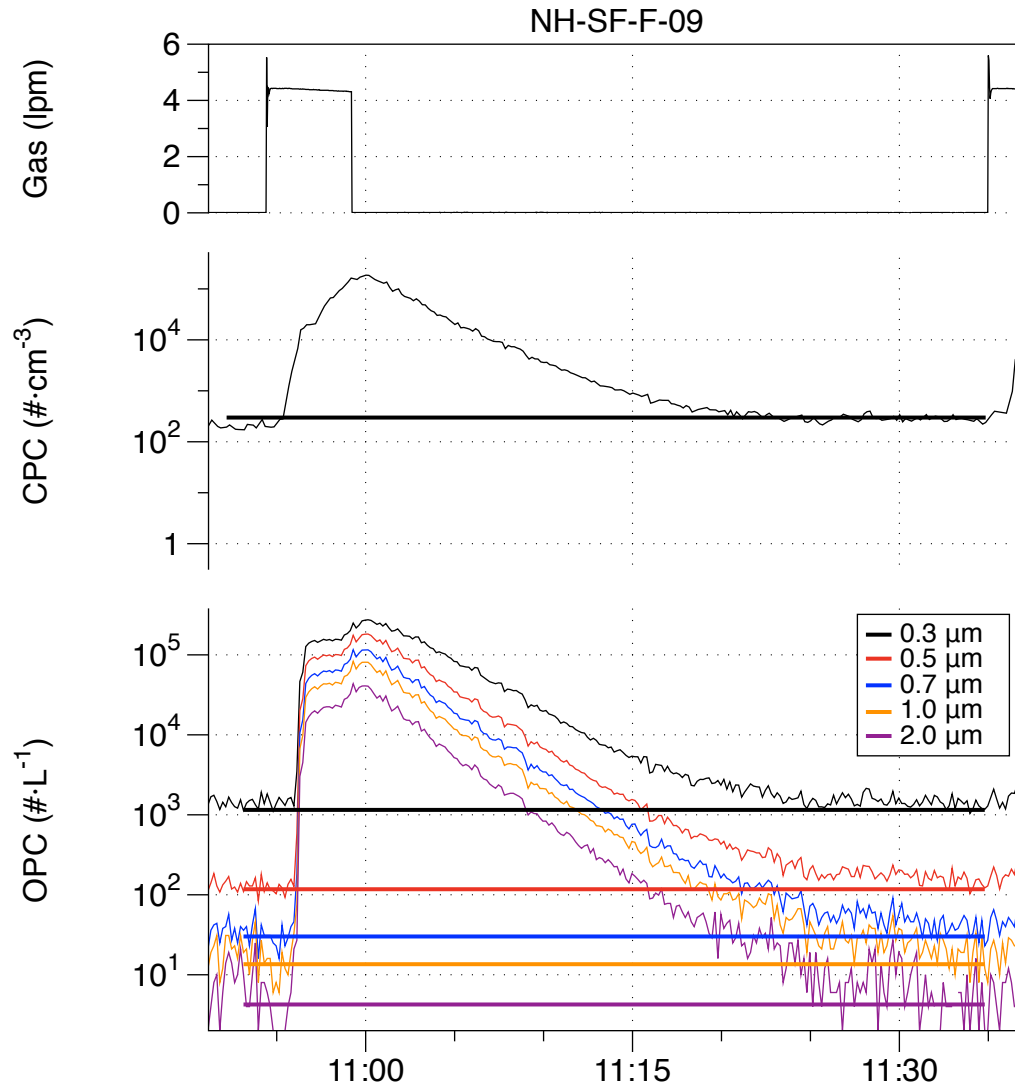


Figure D- 19. Results from experiment NH-SF-F-09 with stir-fry on front burner and no hood.

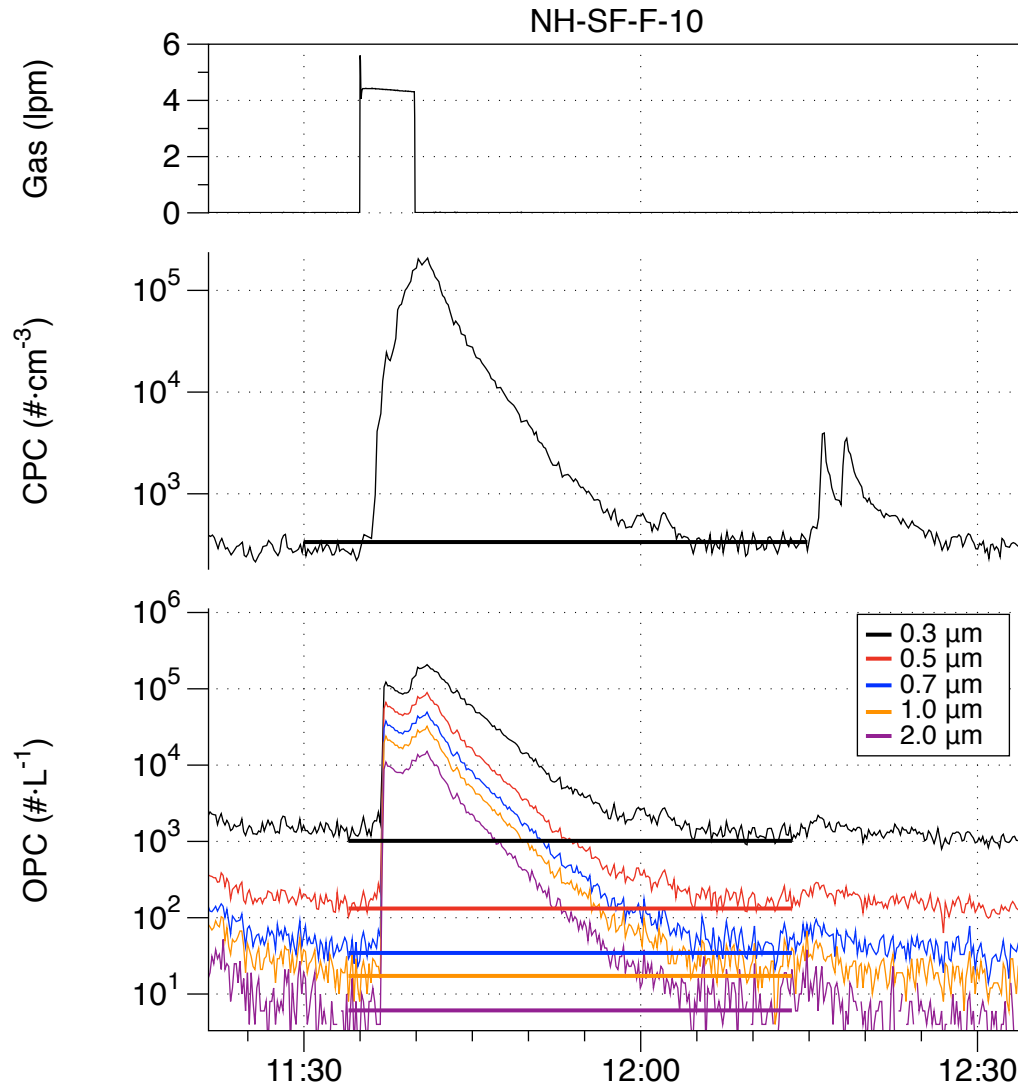


Figure D- 20. Results from experiment NH-SF-F-10 with stir-fry on front burner and no hood.

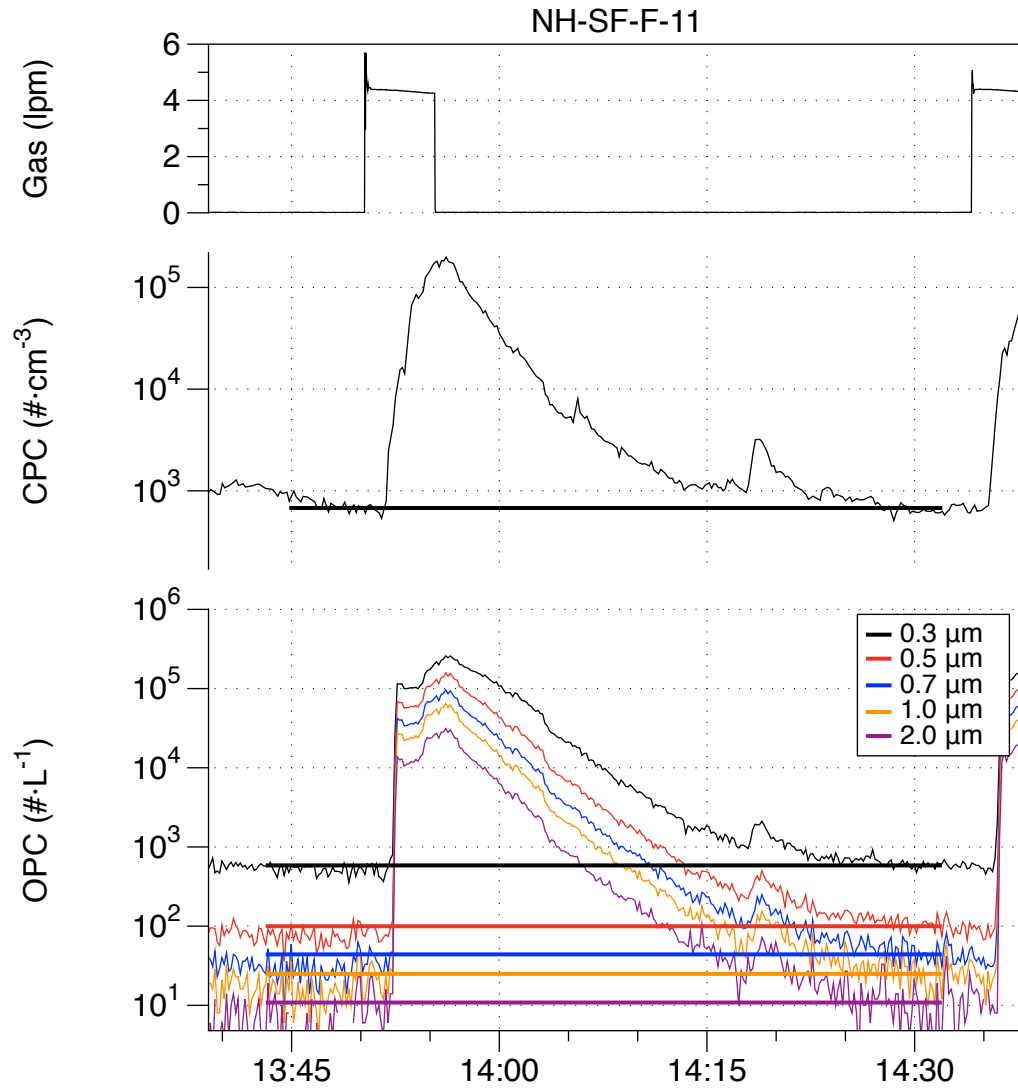


Figure D- 21. . Results from experiment NH-SF-F-11 with stir-fry on front burner and no hood.

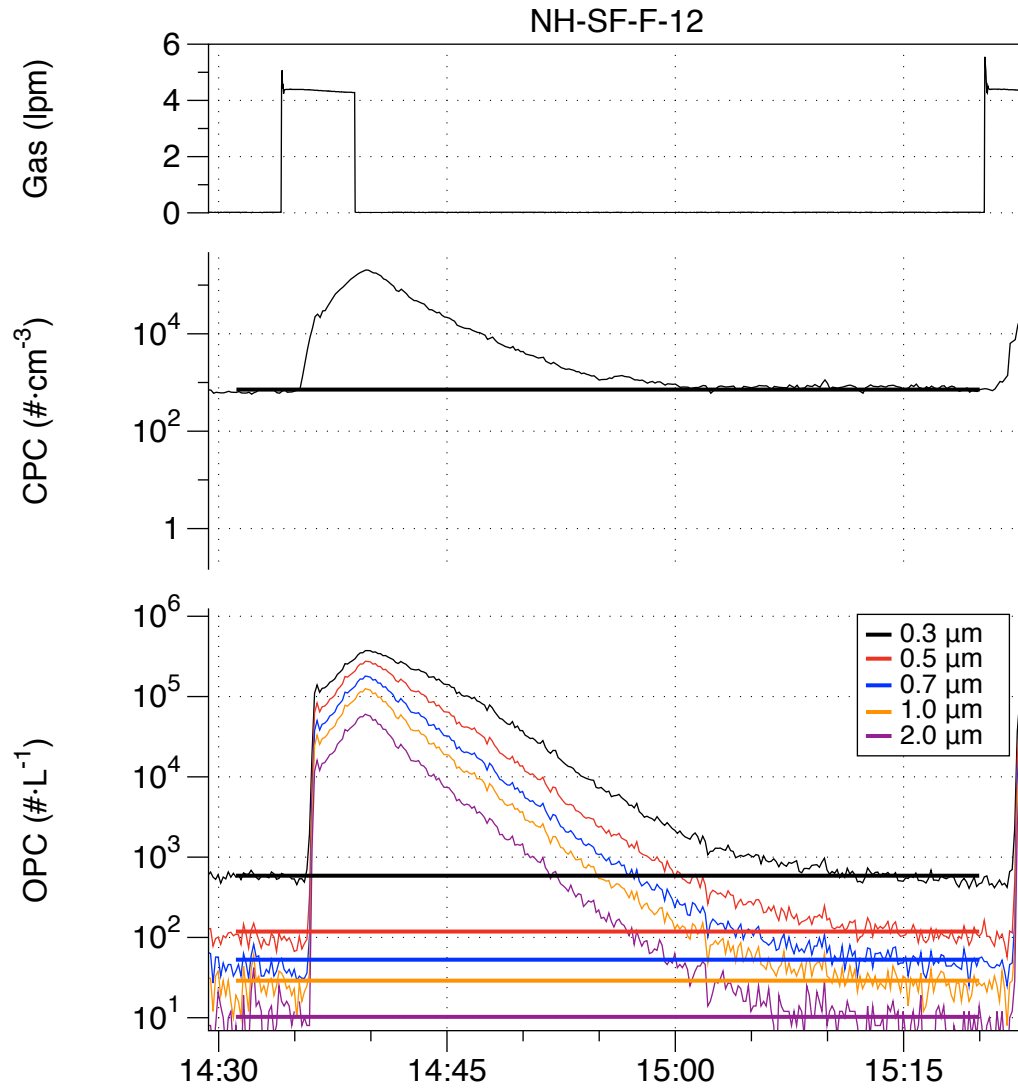


Figure D- 22. Results from experiment NH-SF-F-12 with stir-fry on front burner and no hood.

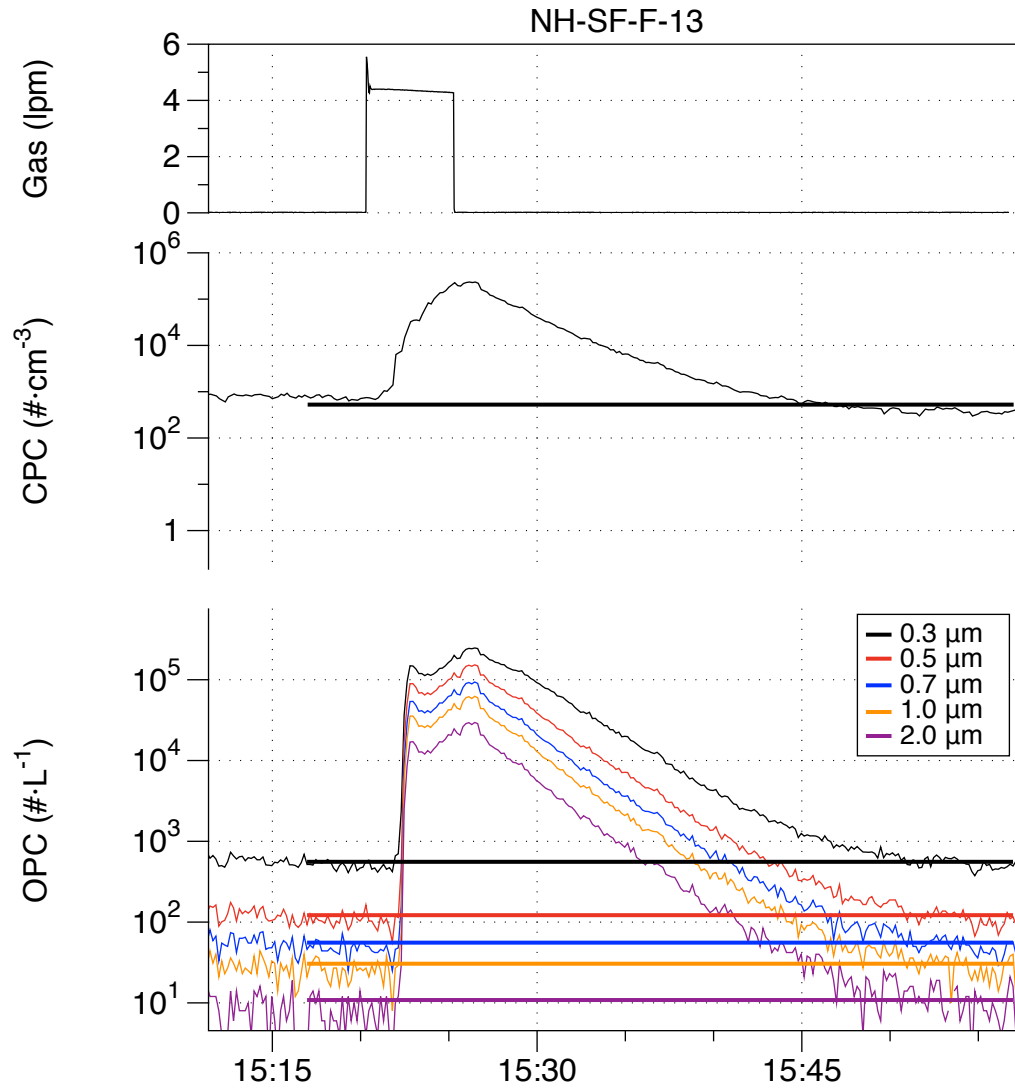


Figure D- 23. Results from experiment NH-SF-F-13 with stir-fry on front burner and no hood.

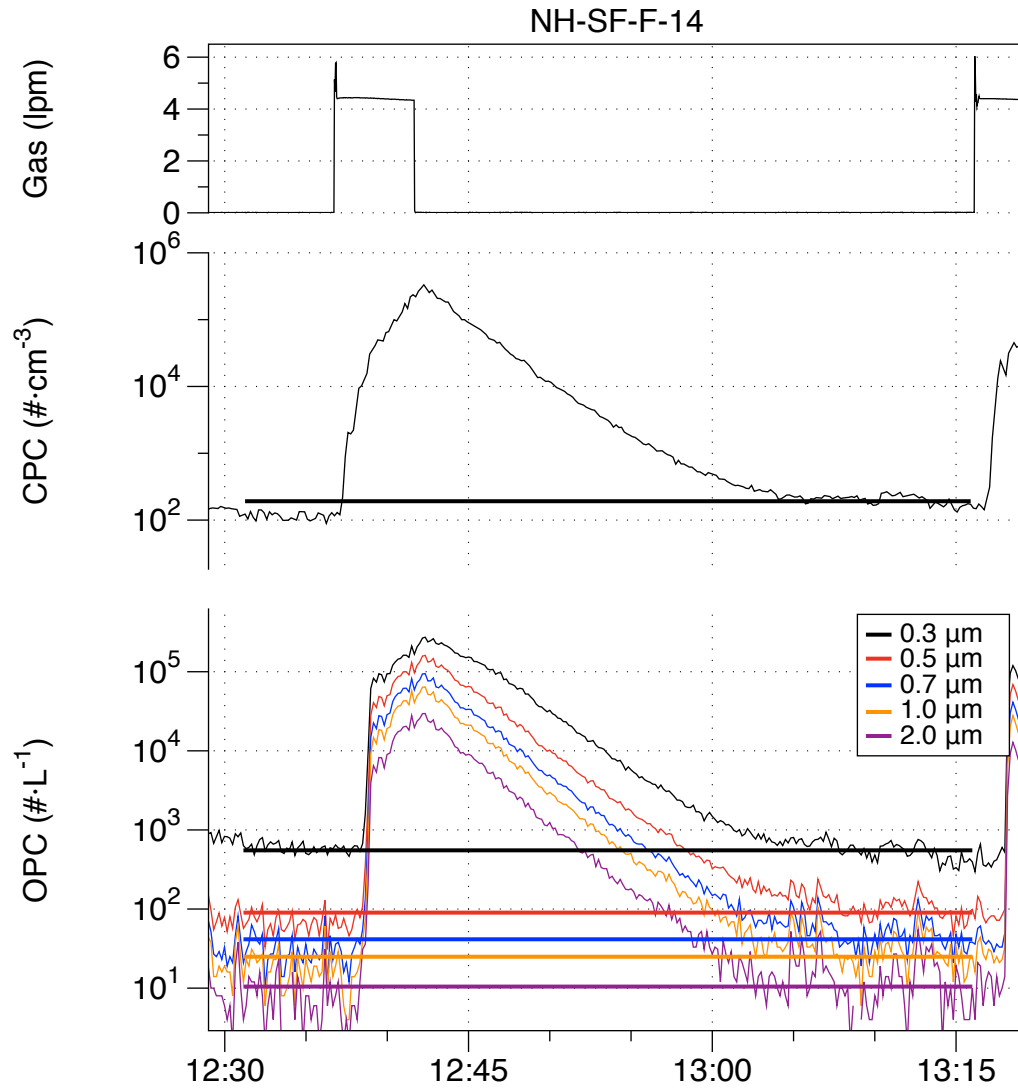


Figure D- 24. Results from experiment NH-SF-F-14 with stir-fry on front burner and no hood.

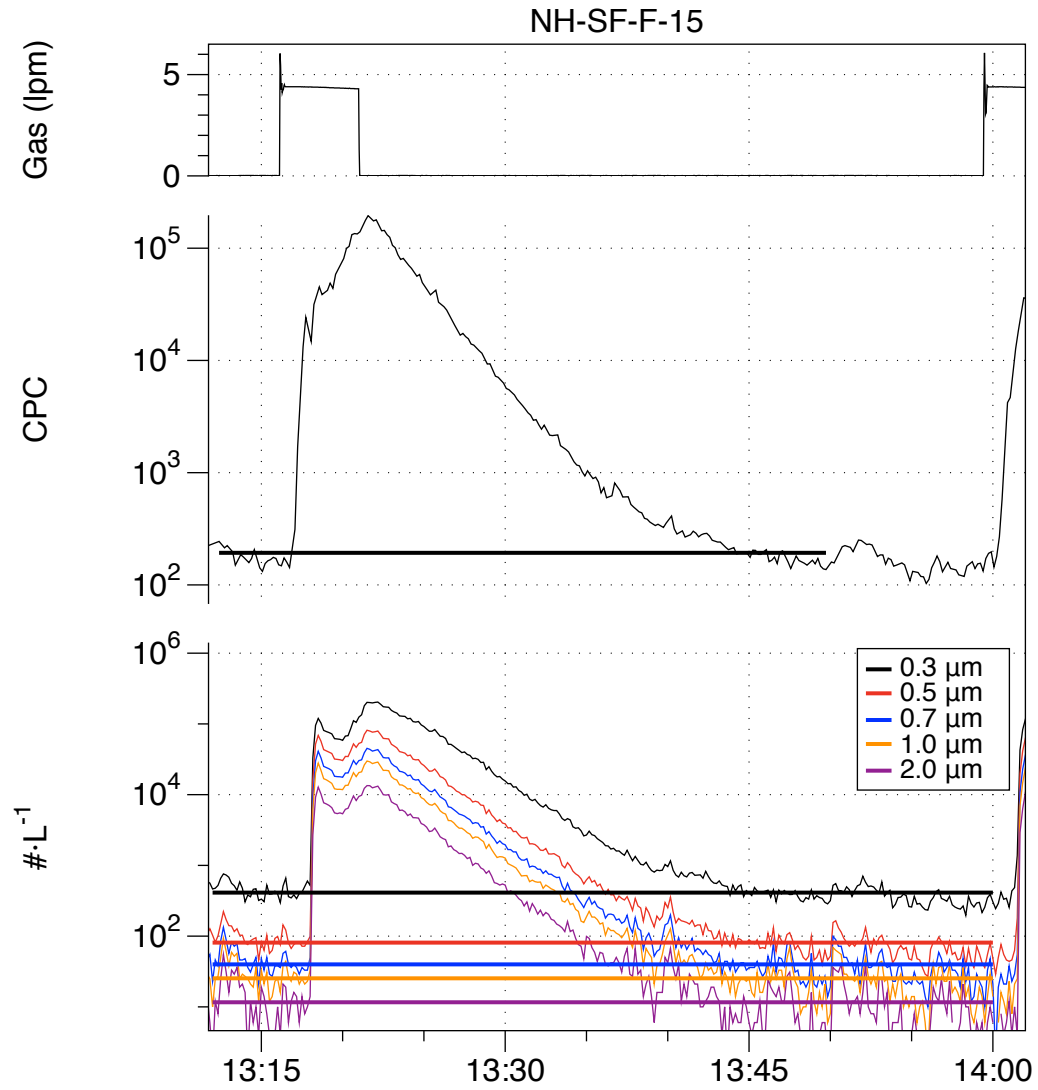


Figure D- 25. Results from experiment NH-SF-F-15 with stir-fry on front burner and no hood.

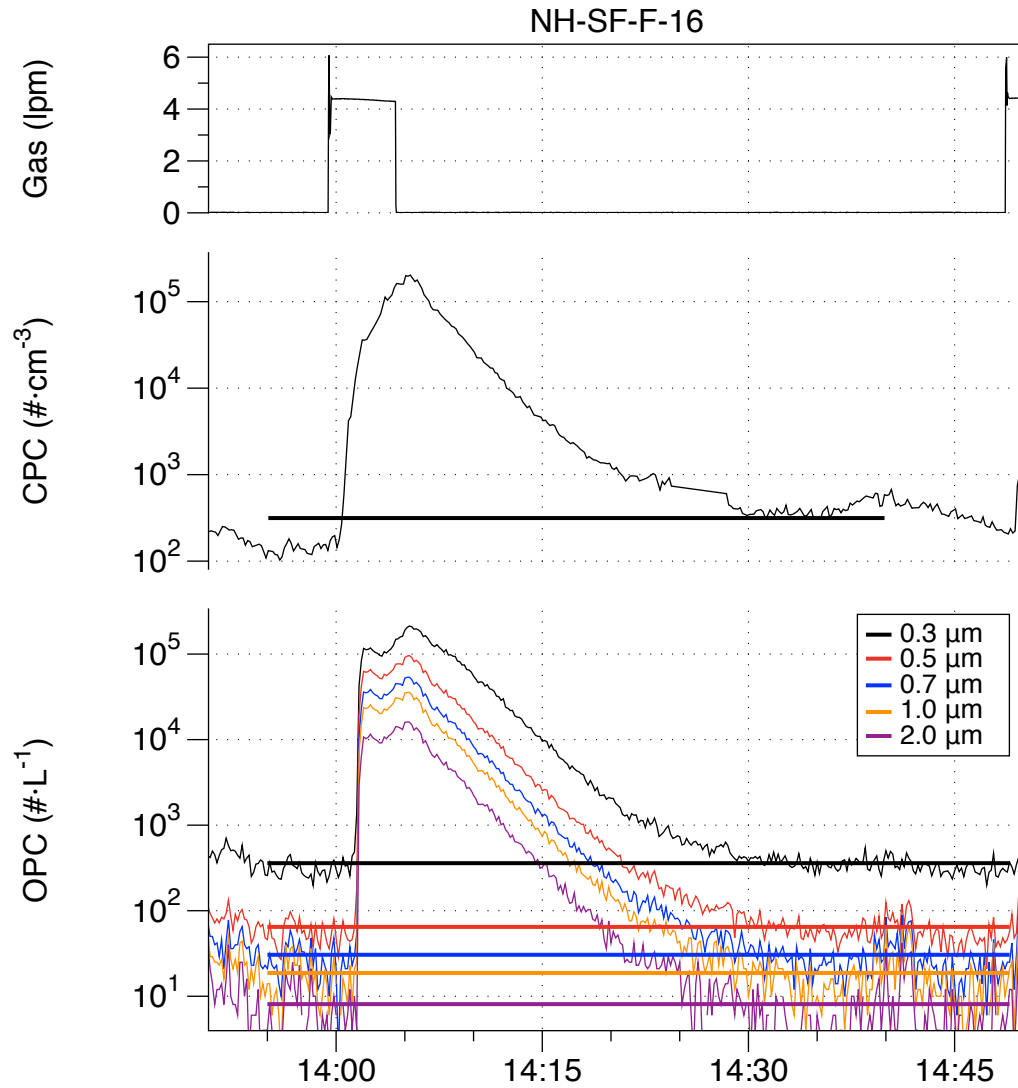


Figure D- 26. Results from experiment NH-SF-F-16 with stir-fry on front burner and no hood.

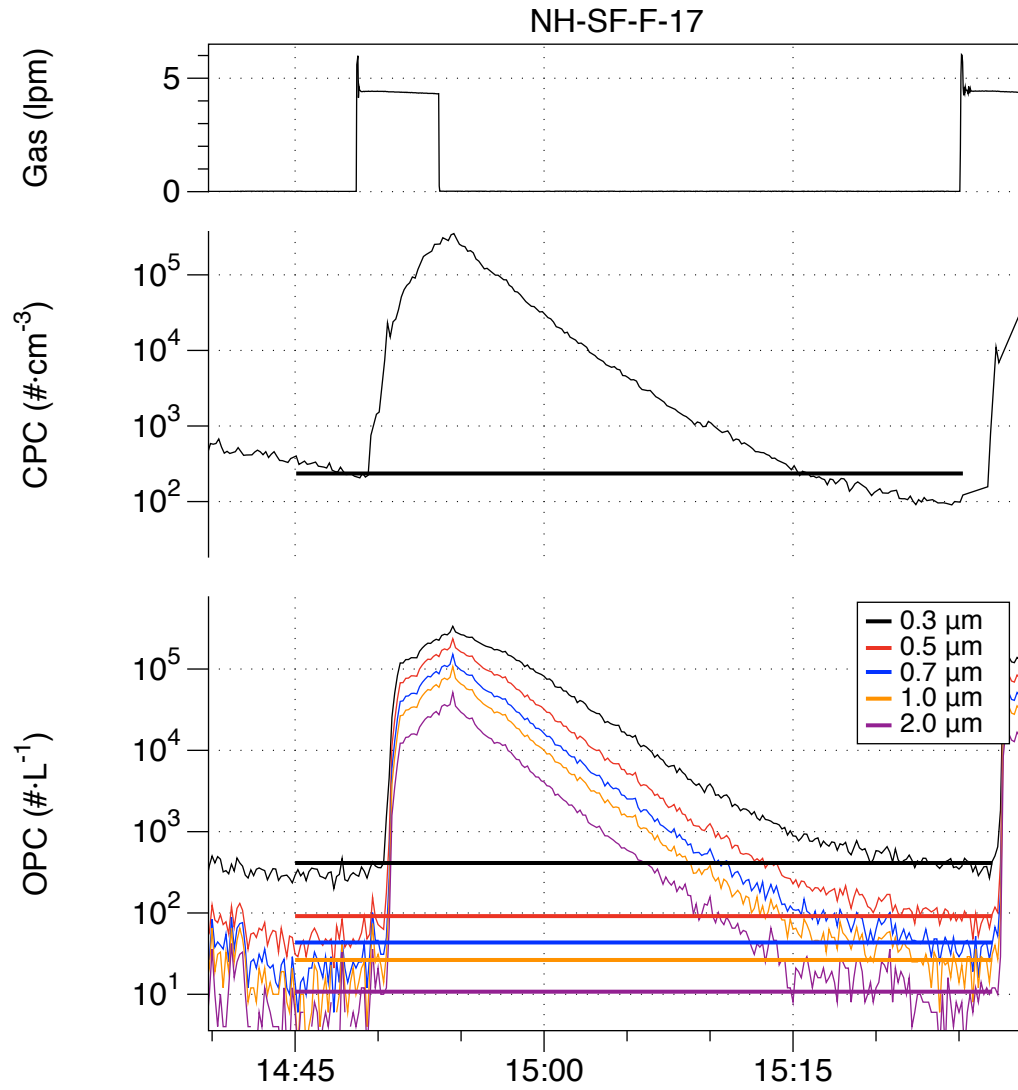


Figure D- 27. Results from experiment NH-SF-F-17 with stir-fry on front burner and no hood.

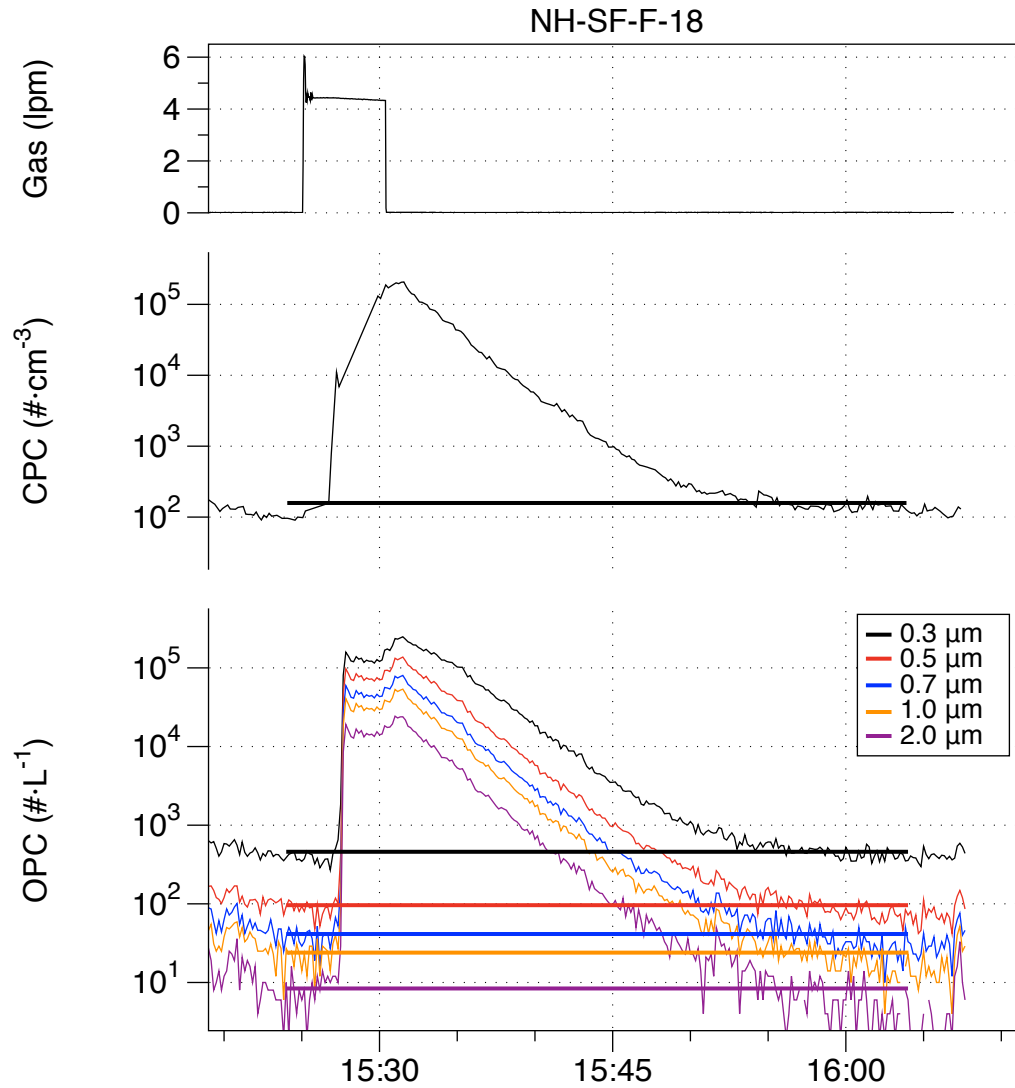


Figure D- 28. . Results from experiment NH-SF-F-18 with stir-fry on front burner and no hood.

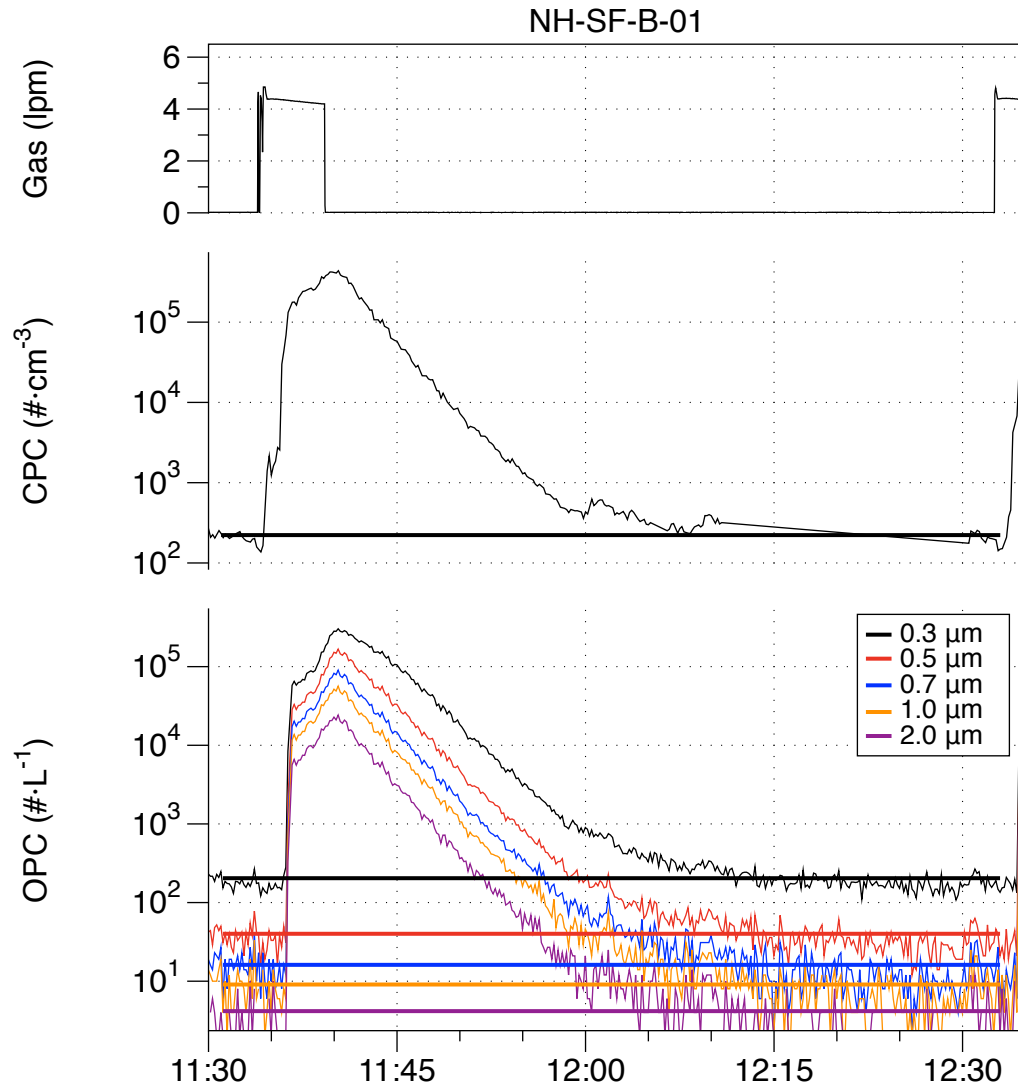


Figure D- 29. Results from experiment NH-SF-B-01 with stir-fry on back burner and no hood.

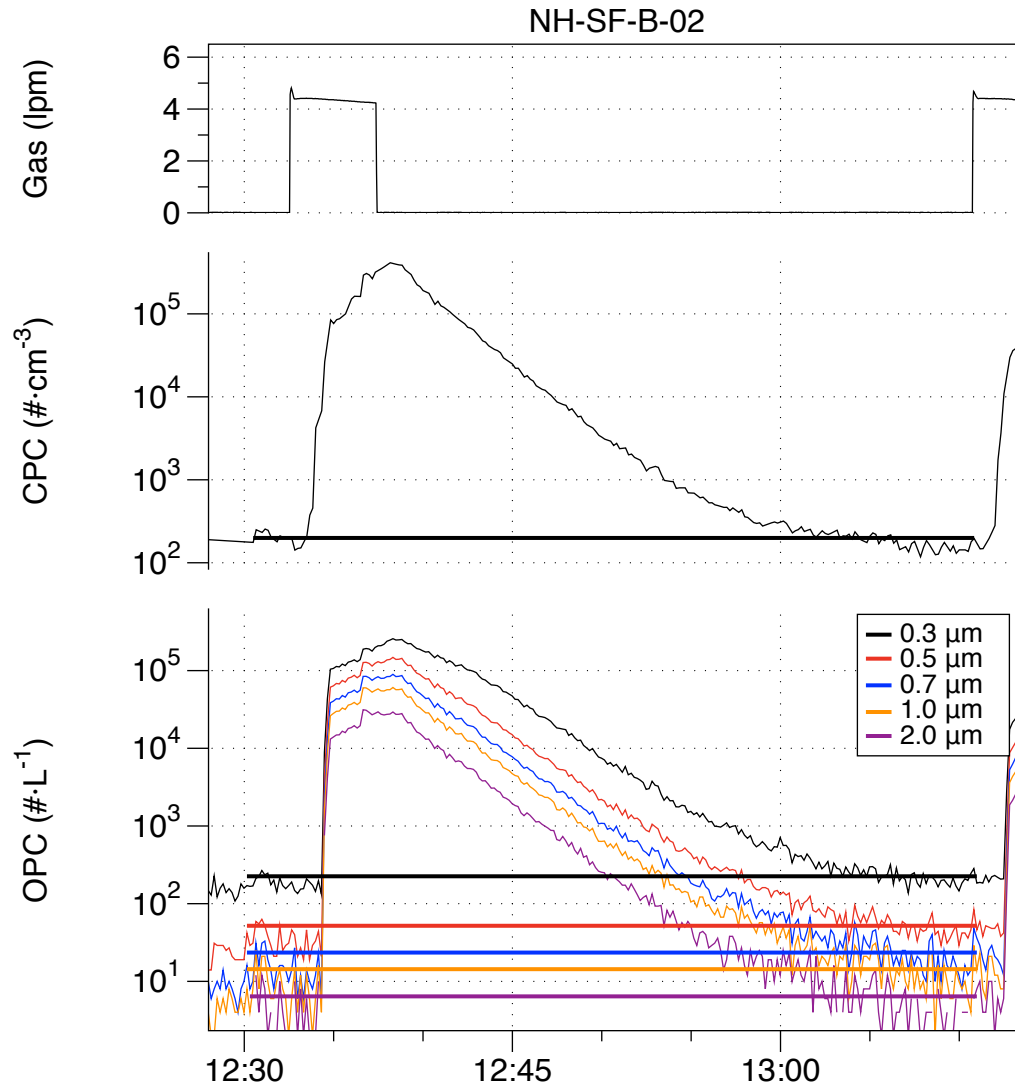


Figure D- 30. Results from experiment NH-SF-B-02 with stir-fry on back burner and no hood.

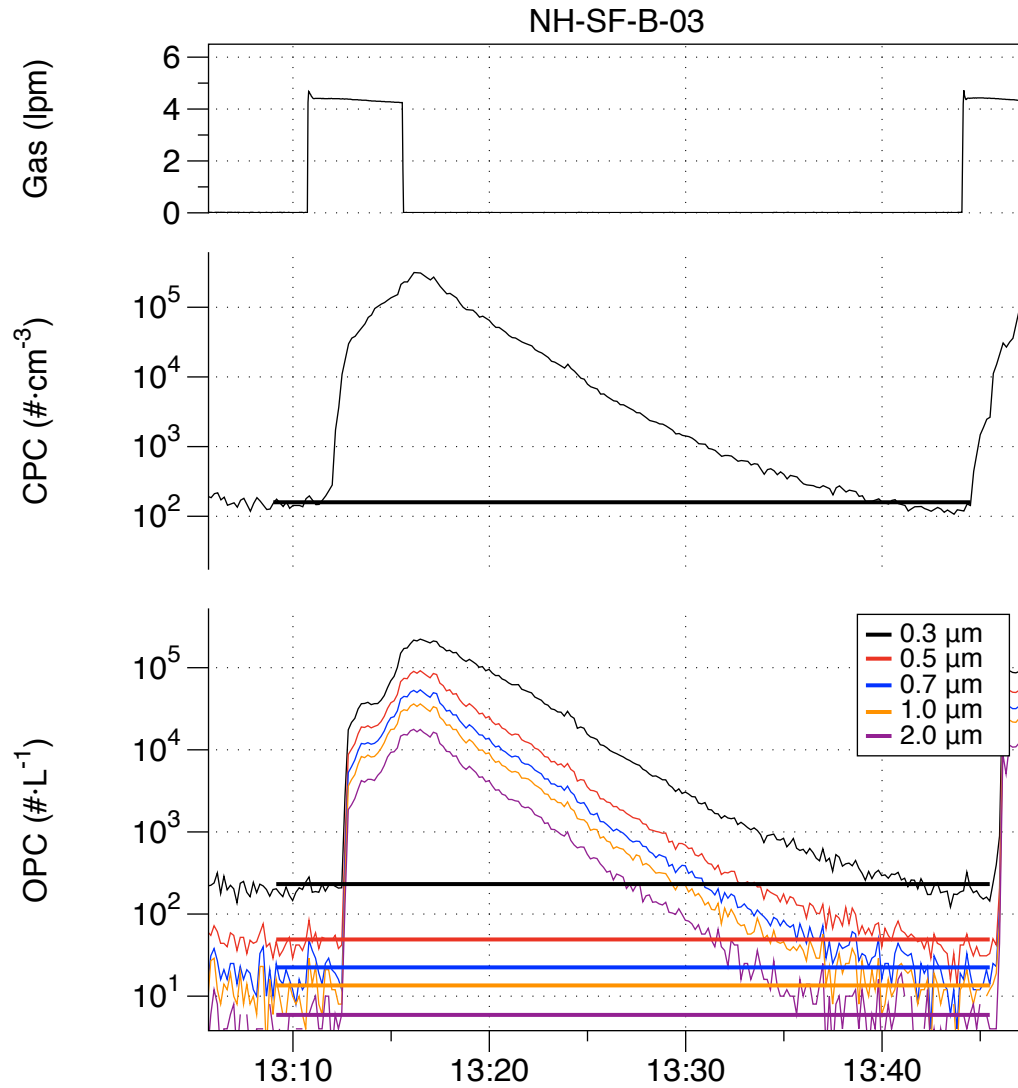


Figure D- 31. Results from experiment NH-SF-B-03 with stir-fry on back burner and no hood.

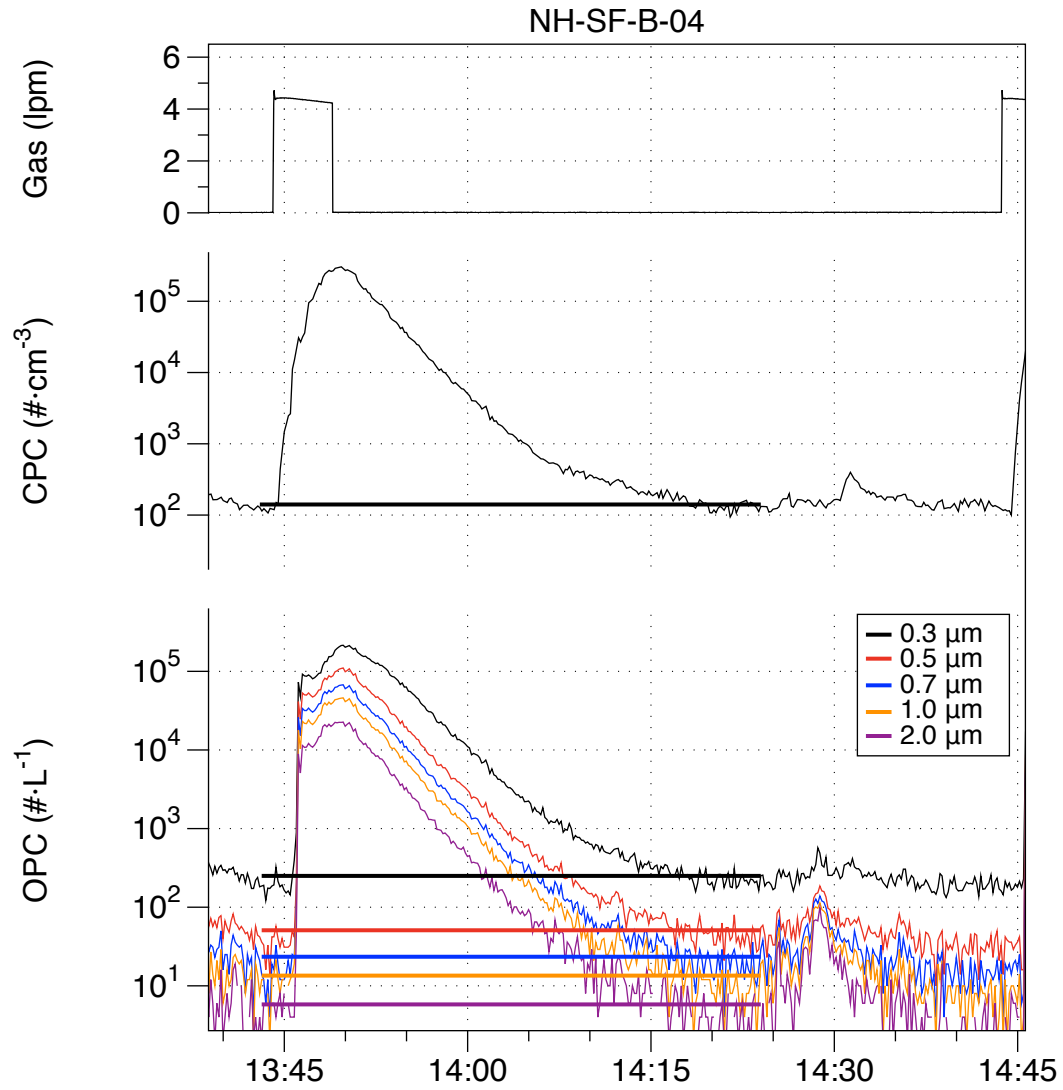


Figure D- 32. Results from experiment NH-SF-B-04 with stir-fry on back burner and no hood.

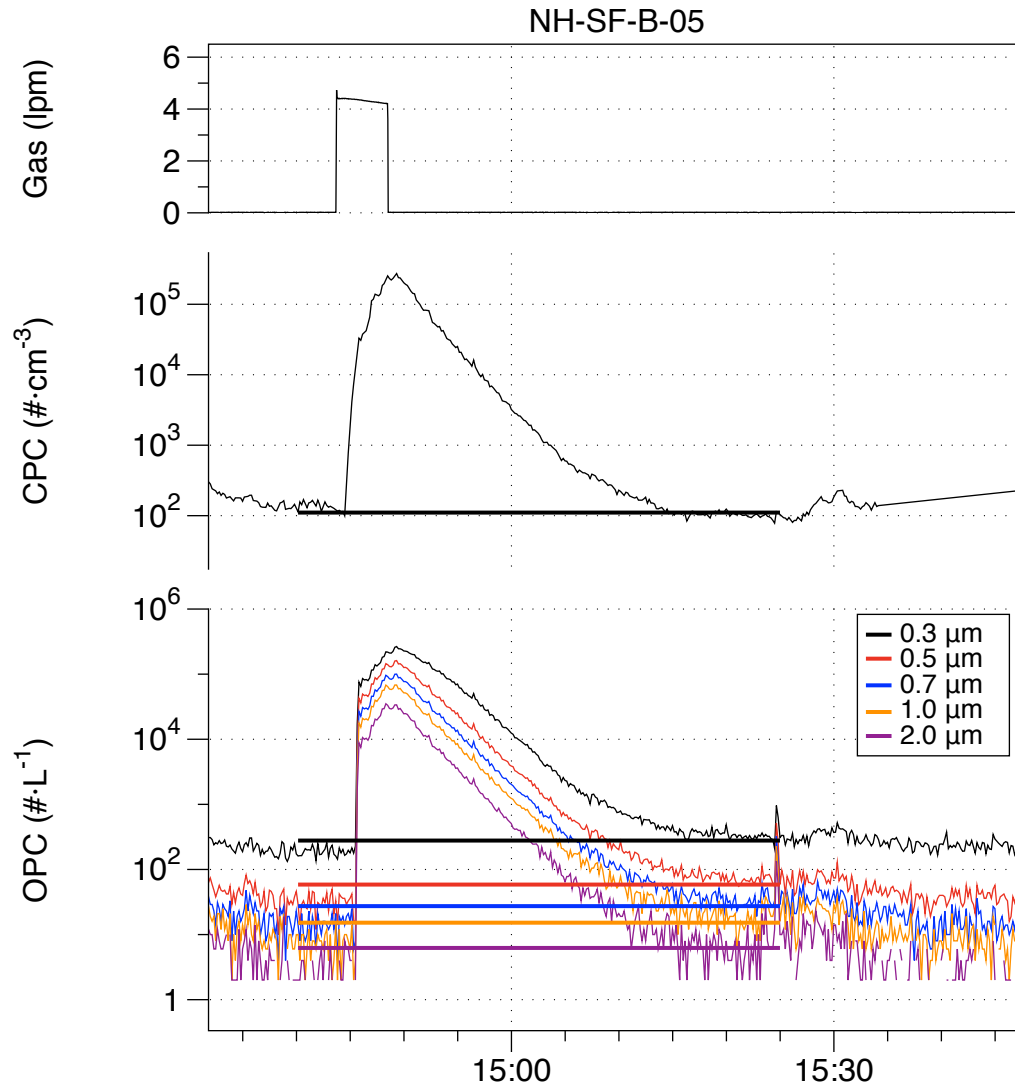


Figure D- 33. Results from experiment NH-SF-B-05 with stir-fry on back burner and no hood.

Appendix E: Results of Experiments Conducted with Hood L1

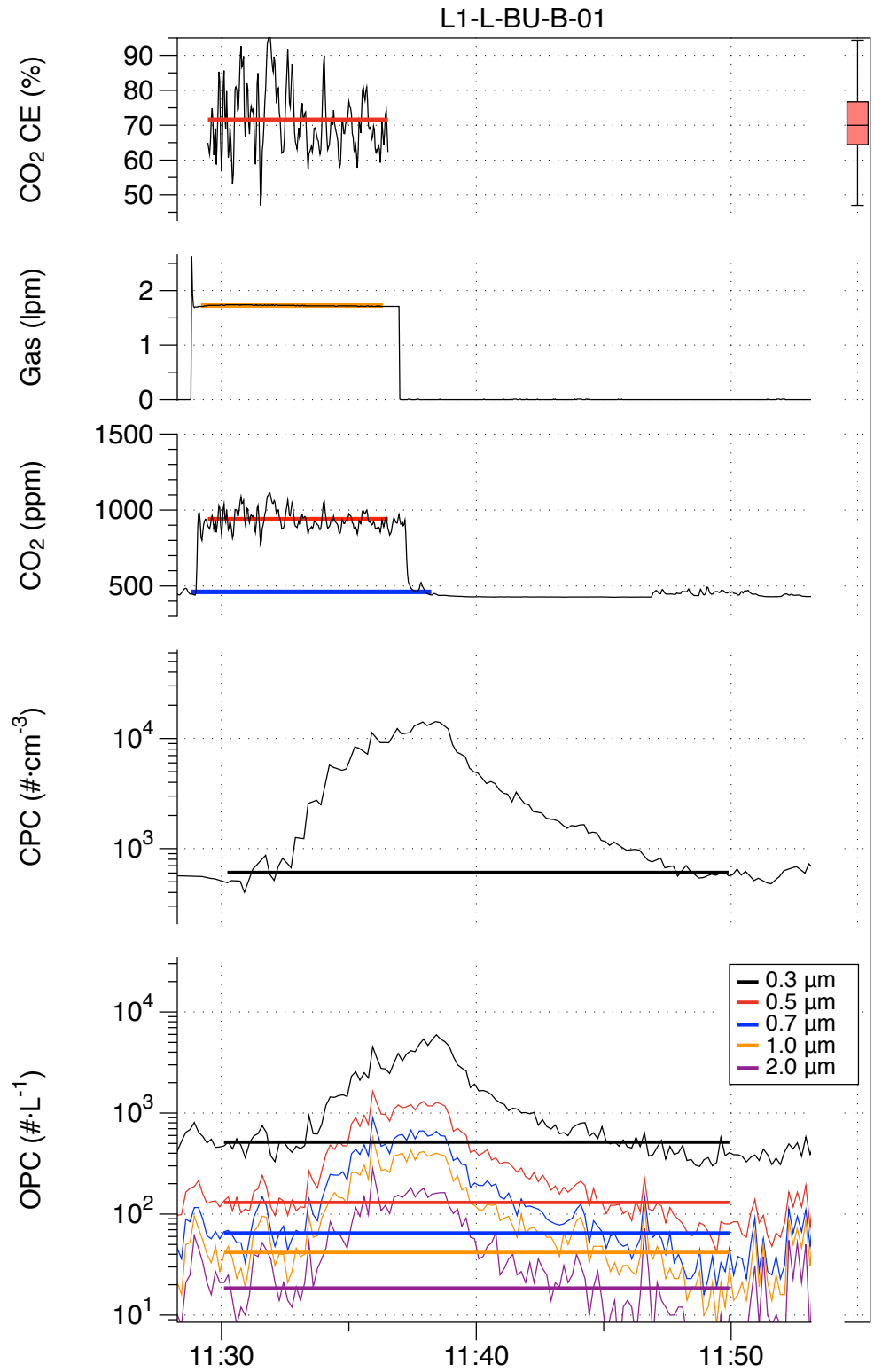


Figure E- 1. Results from experiment L1-L-BU-01: burger on back burner, Hood L1 on low speed.

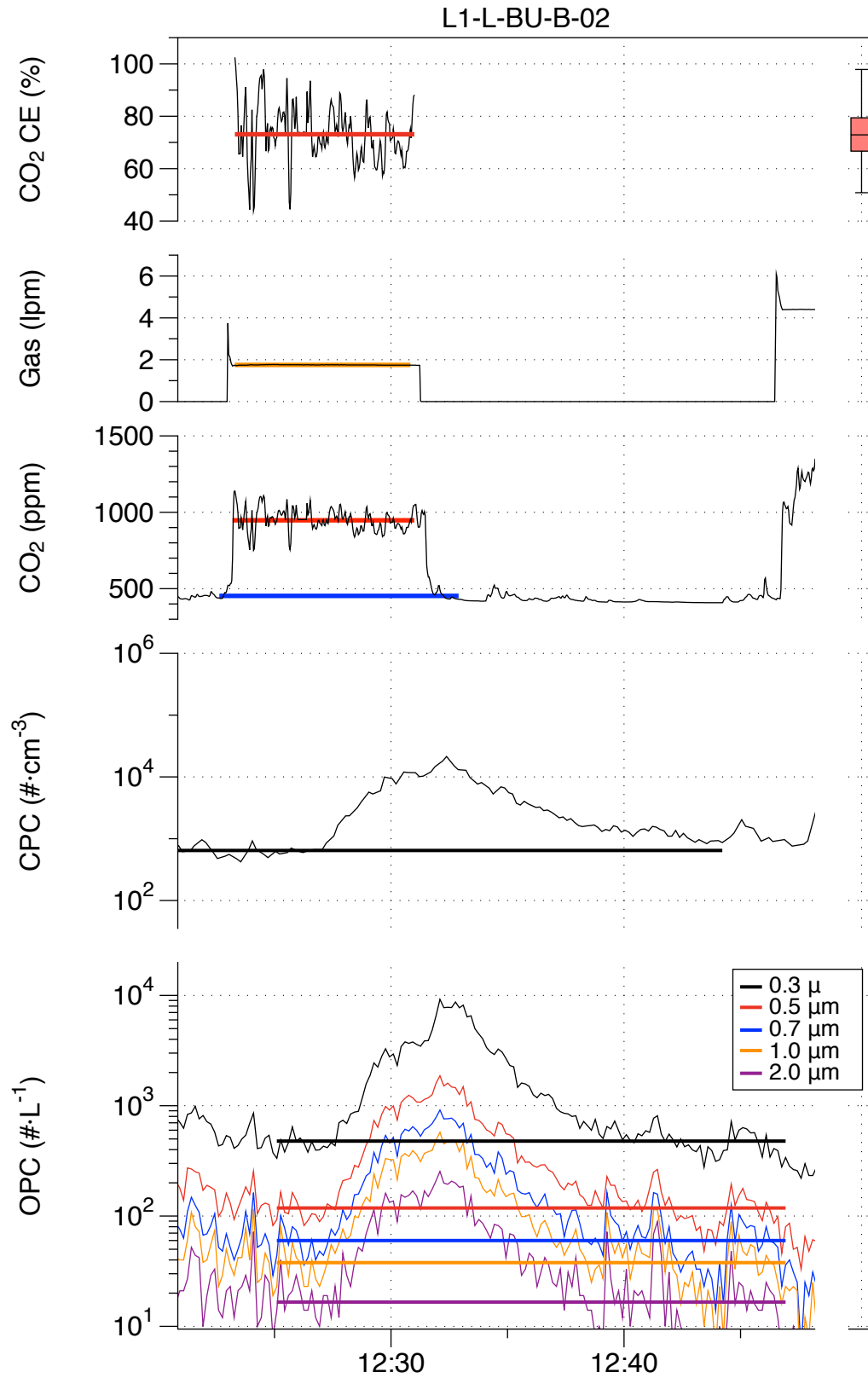


Figure E- 2. Results from experiment L1-L-BU-02: burger on back burner, Hood L1 on low speed.

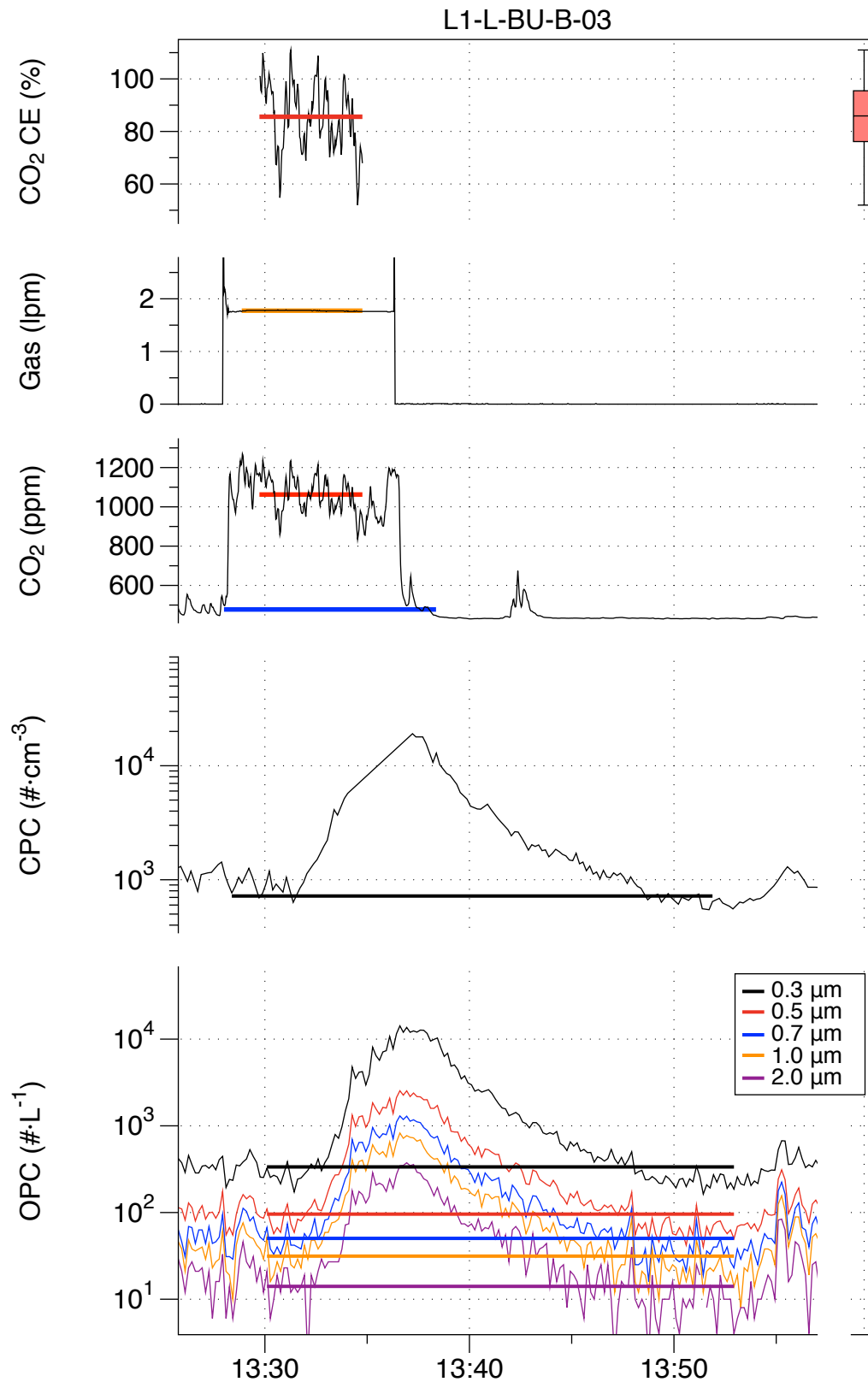


Figure E- 3. Results from experiment L1-L-BU-03: burger on back burner, Hood L1 on low speed.

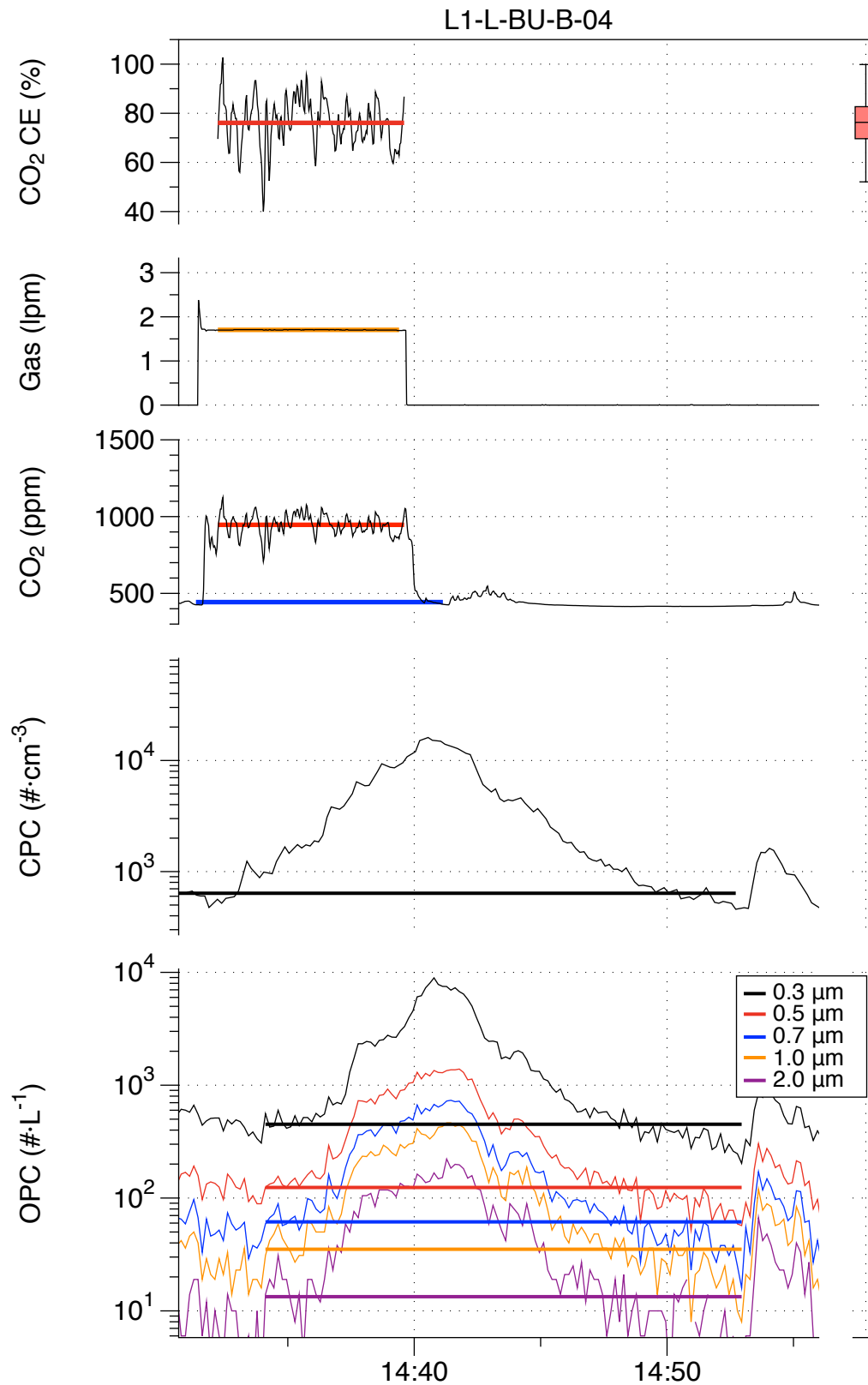


Figure E- 4. Results from experiment L1-L-BU-04: burger on back burner, Hood L1 on low speed.

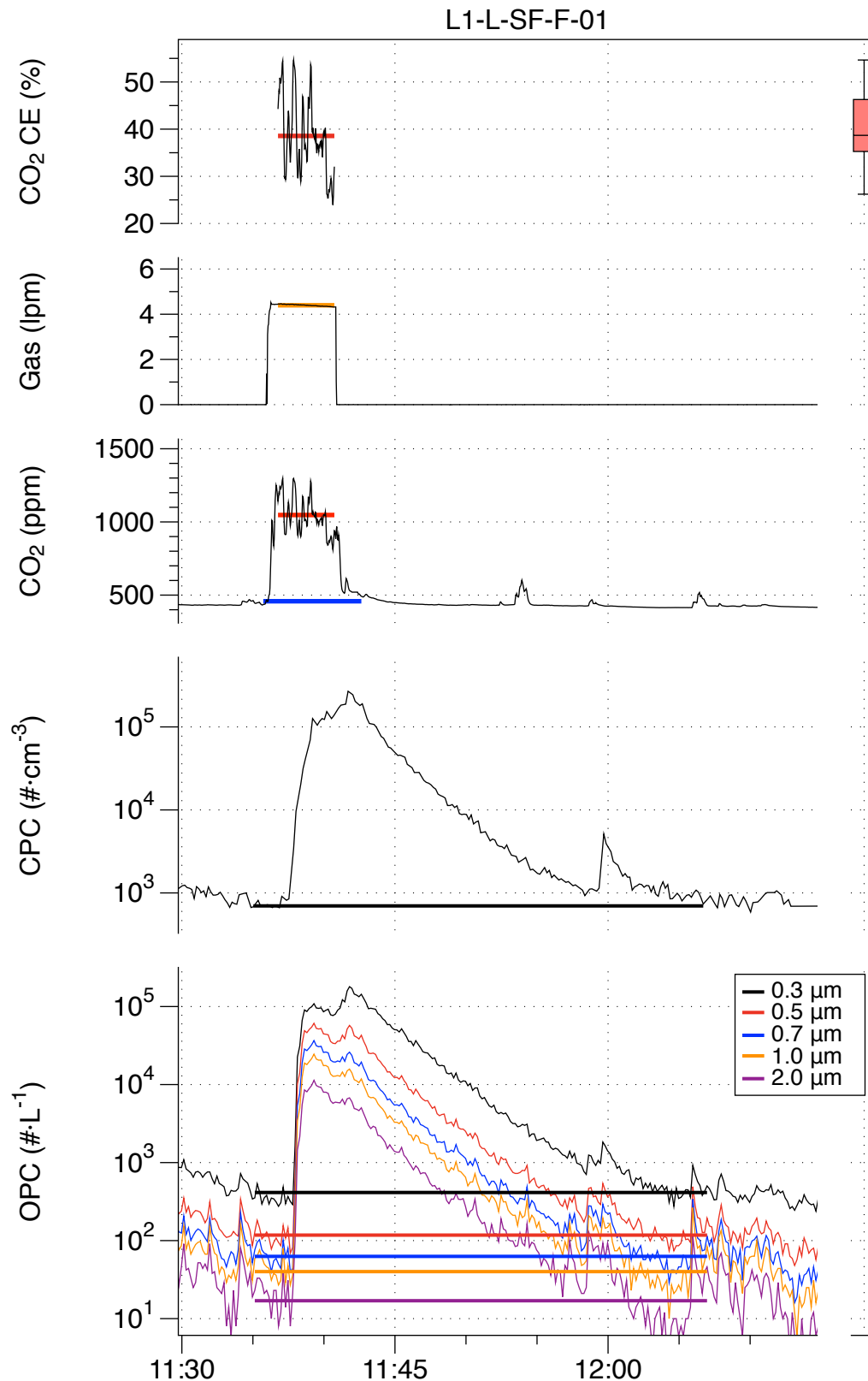


Figure E- 5. Results from experiment L1-L-SF-F-01: stir-fry on front burner, Hood L1 on low speed.

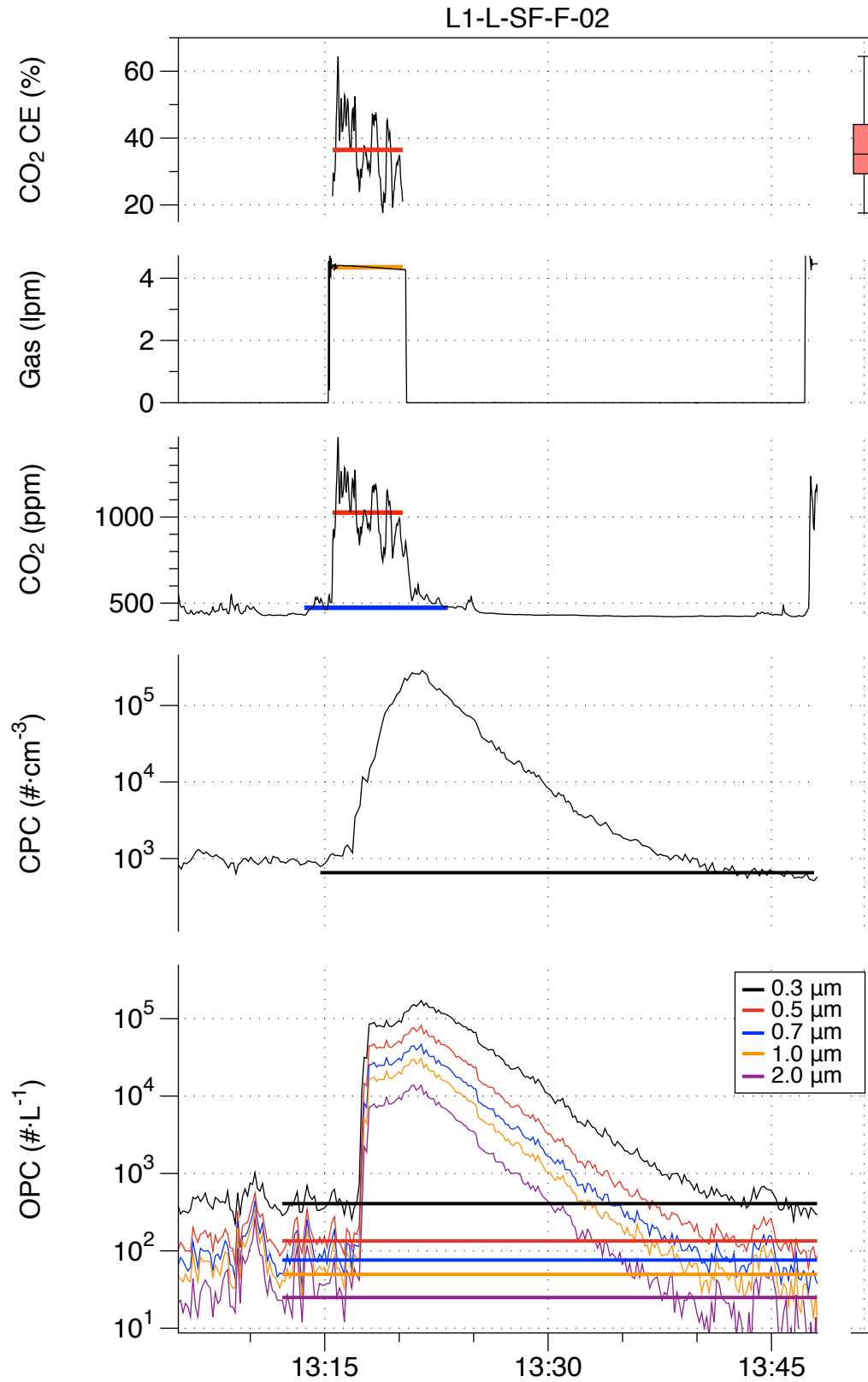


Figure E- 6. Results from experiment L1-L-SF-F-02: stir-fry on front burner, Hood L1 on low speed.

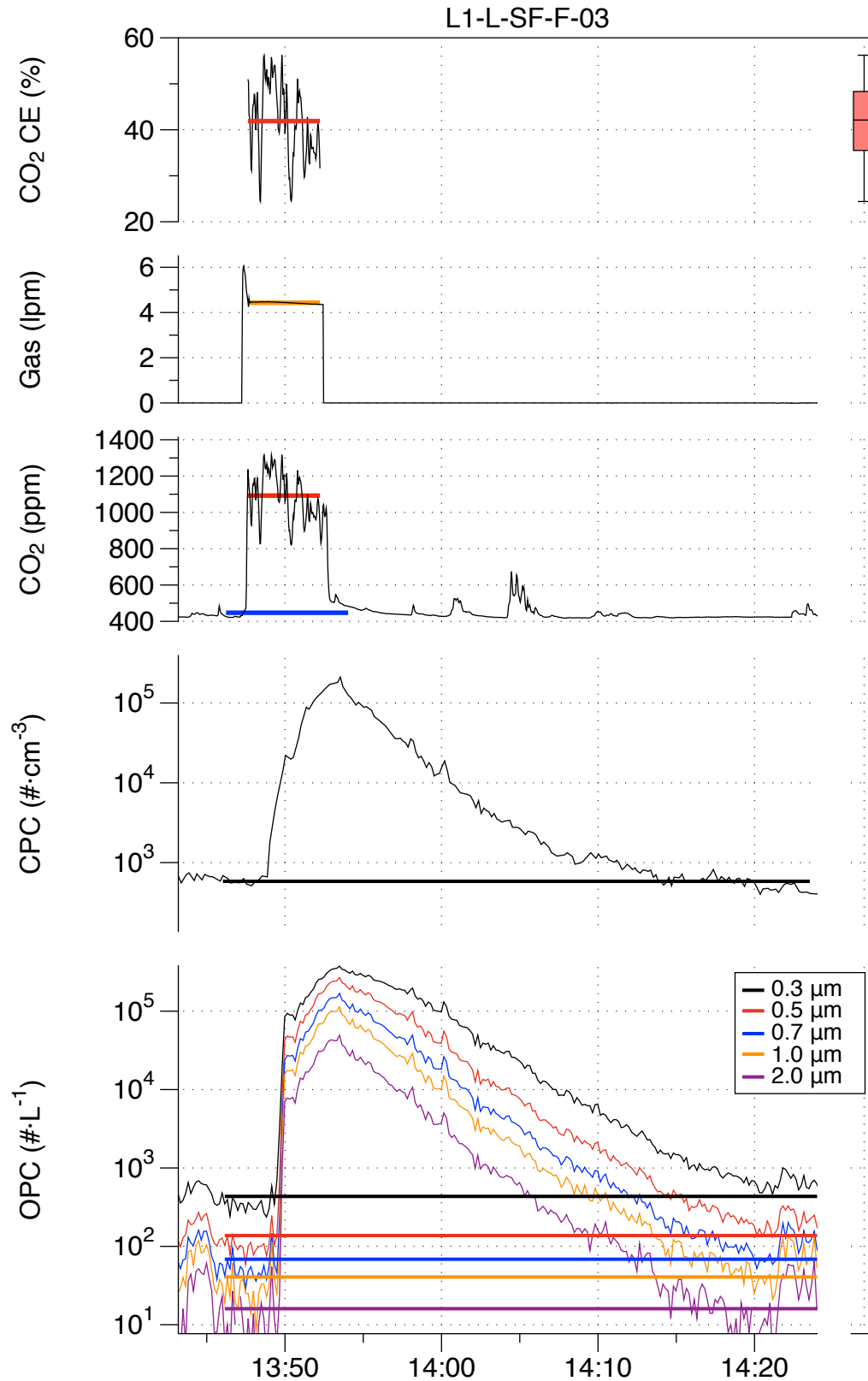


Figure E- 7. Results from experiment L1-L-SF-F-03: stir-fry on front burner, Hood L1 on low speed.

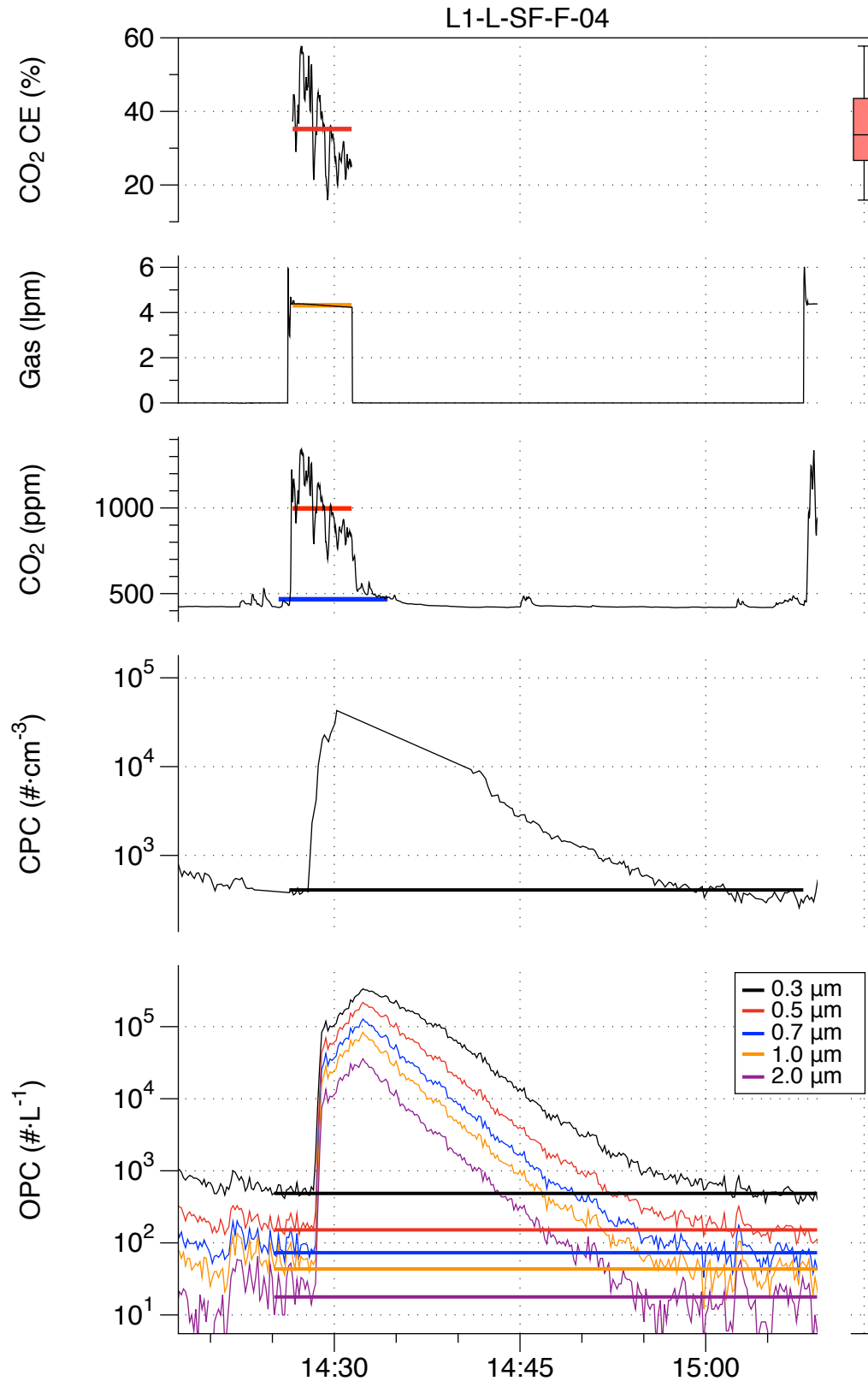


Figure E- 8. Results from experiment L1-L-SF-F-04: stir-fry on front burner, Hood L1 on low speed.

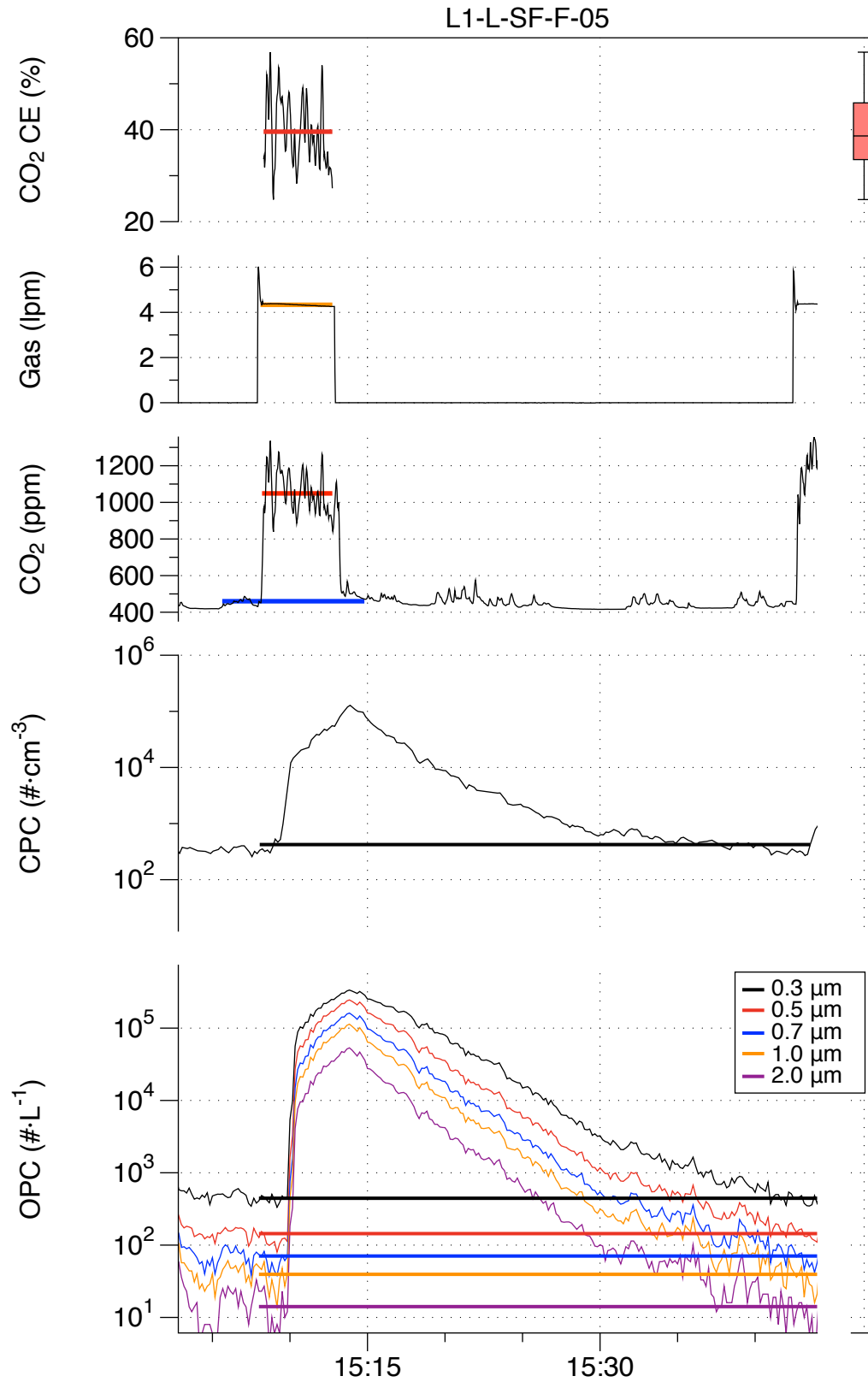


Figure E- 9. Results from experiment L1-L-SF-F-05: burger on back burner, Hood L1 on low speed.

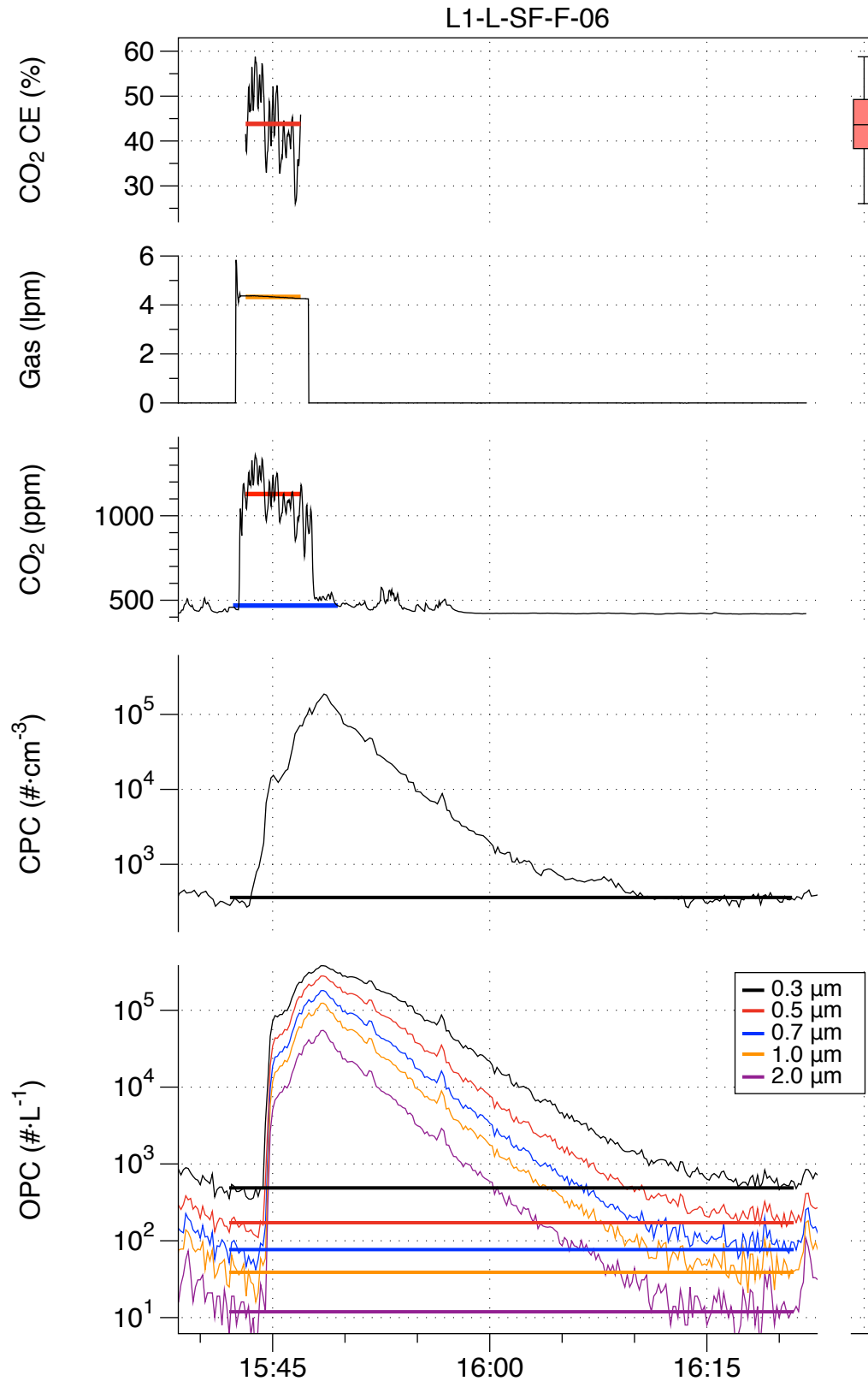


Figure E- 10. Results from experiment L1-L-SF-F-06: burger on back burner, Hood L1 on low speed.

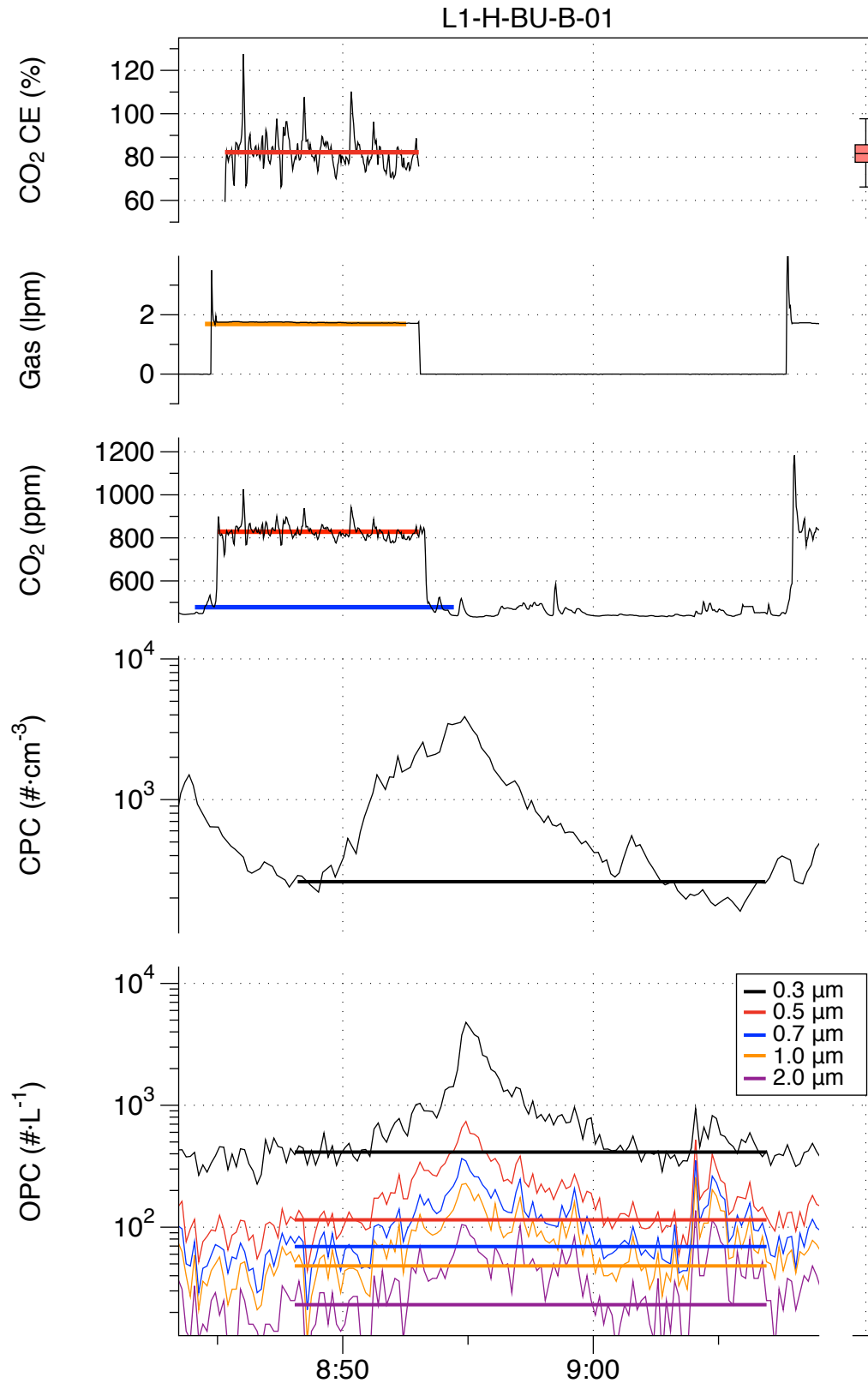


Figure E- 11. Results from experiment L1-H-BU-B-01: burger on back burner, Hood L1 on high speed.

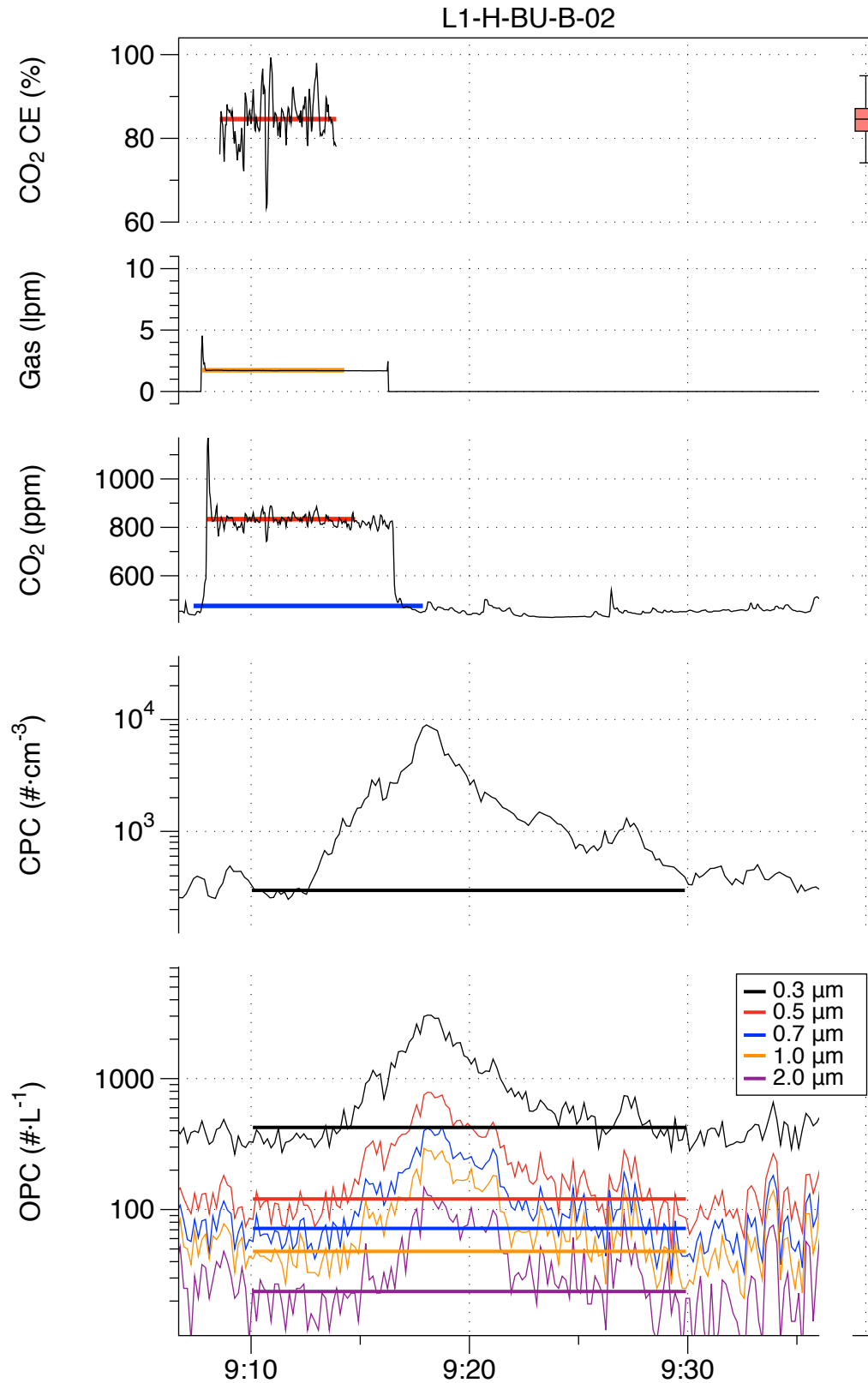


Figure E- 12. Results from experiment L1-H-BU-B-02: burger on back burner, Hood L1 on high speed.

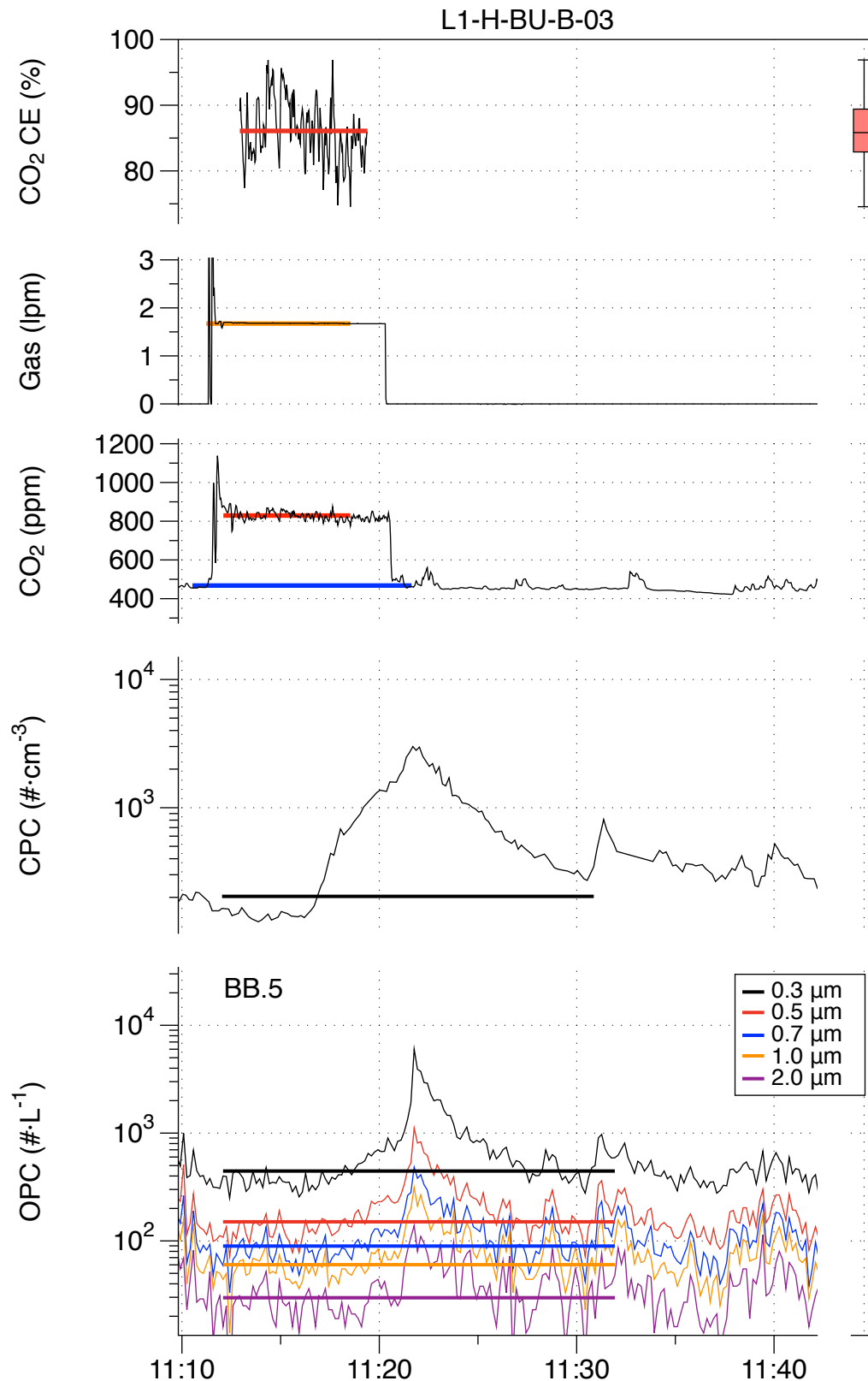


Figure E- 13. Results from experiment L1-H-BU-B-03: burger on back burner, Hood L1 on high speed.

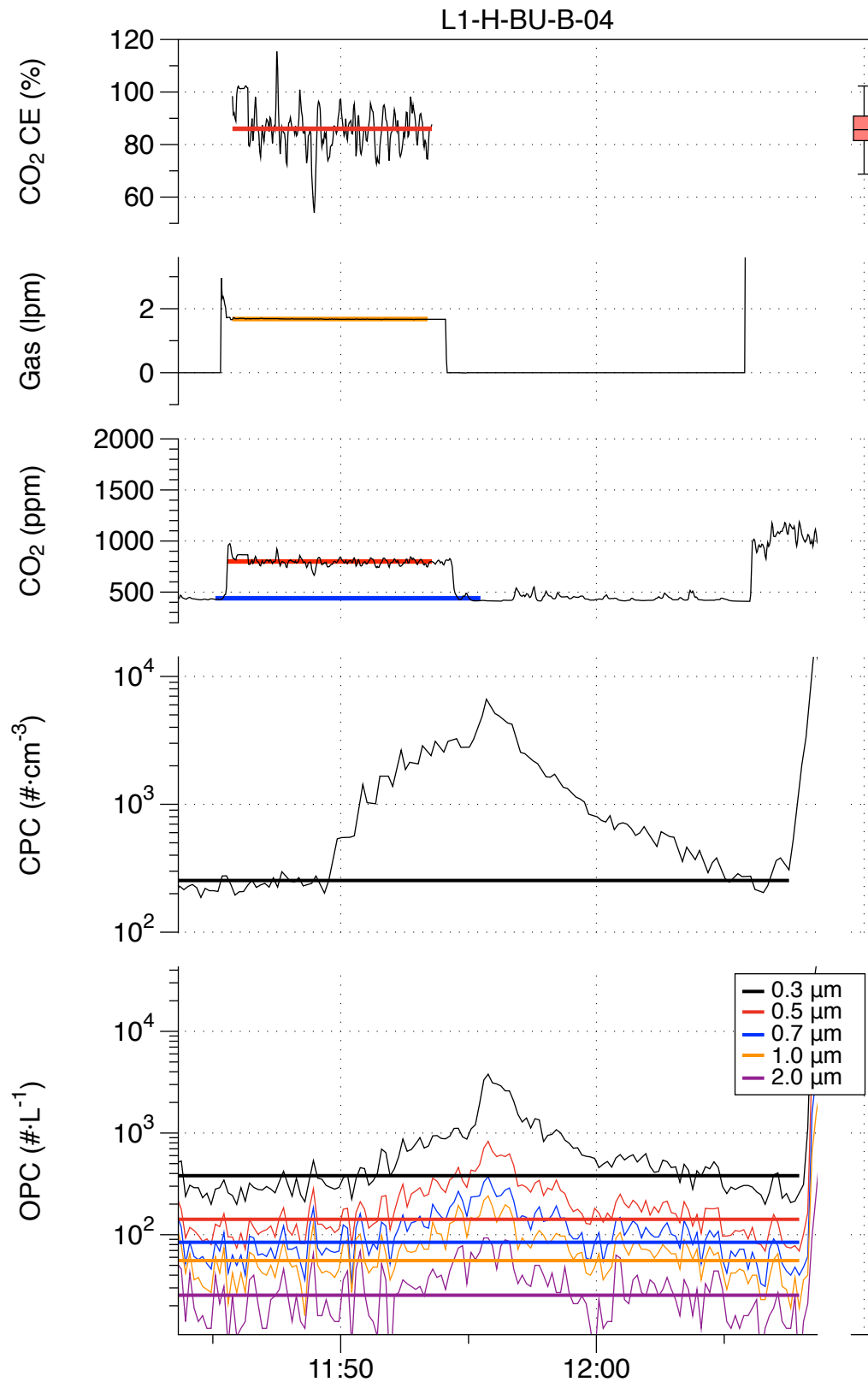


Figure E- 14. Results from experiment L1-H-BU-B-04: burger on back burner, Hood L1 on high speed.

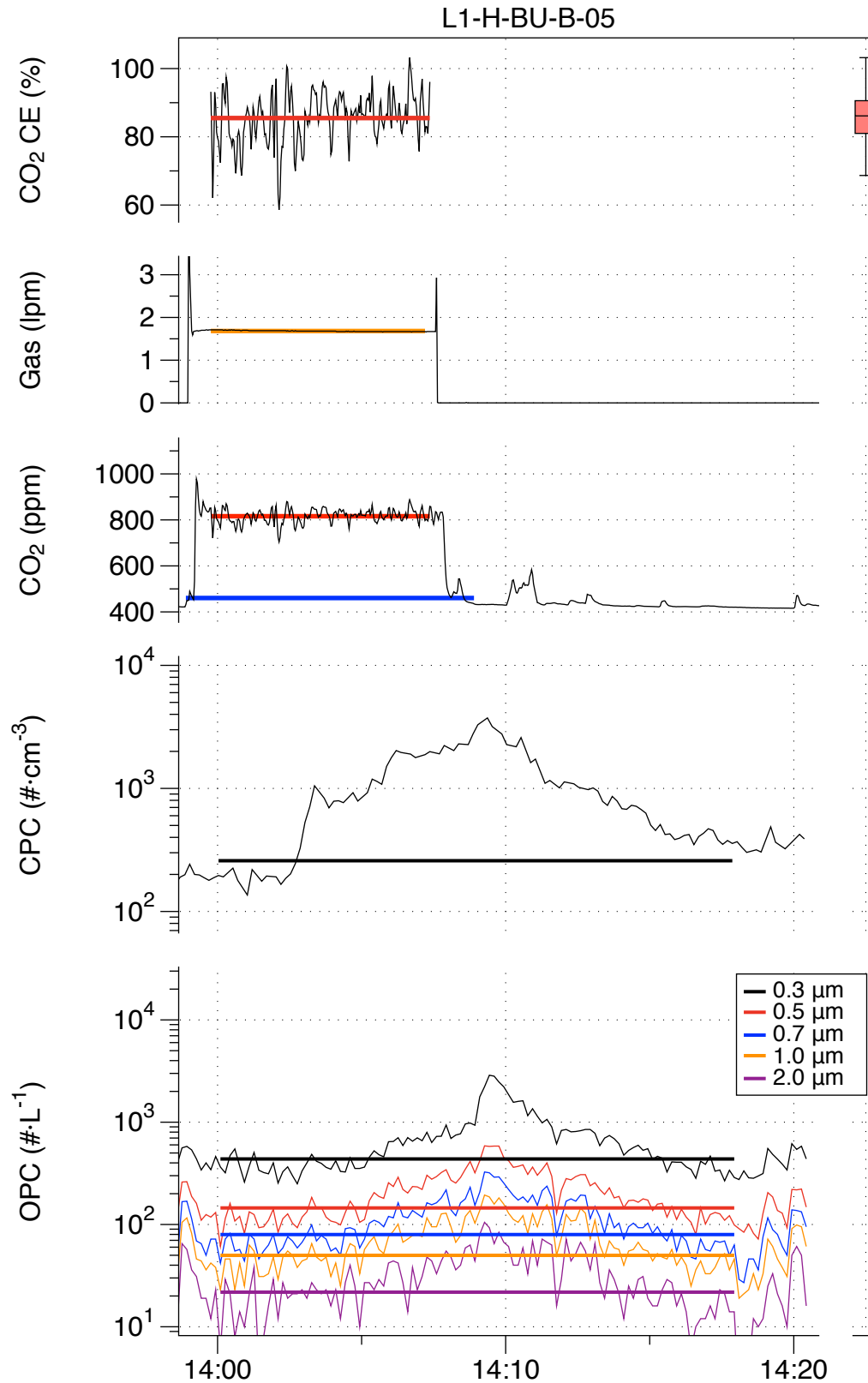


Figure E- 15. Results from experiment L1-H-BU-B-05: burger on back burner, Hood L1 on high speed.

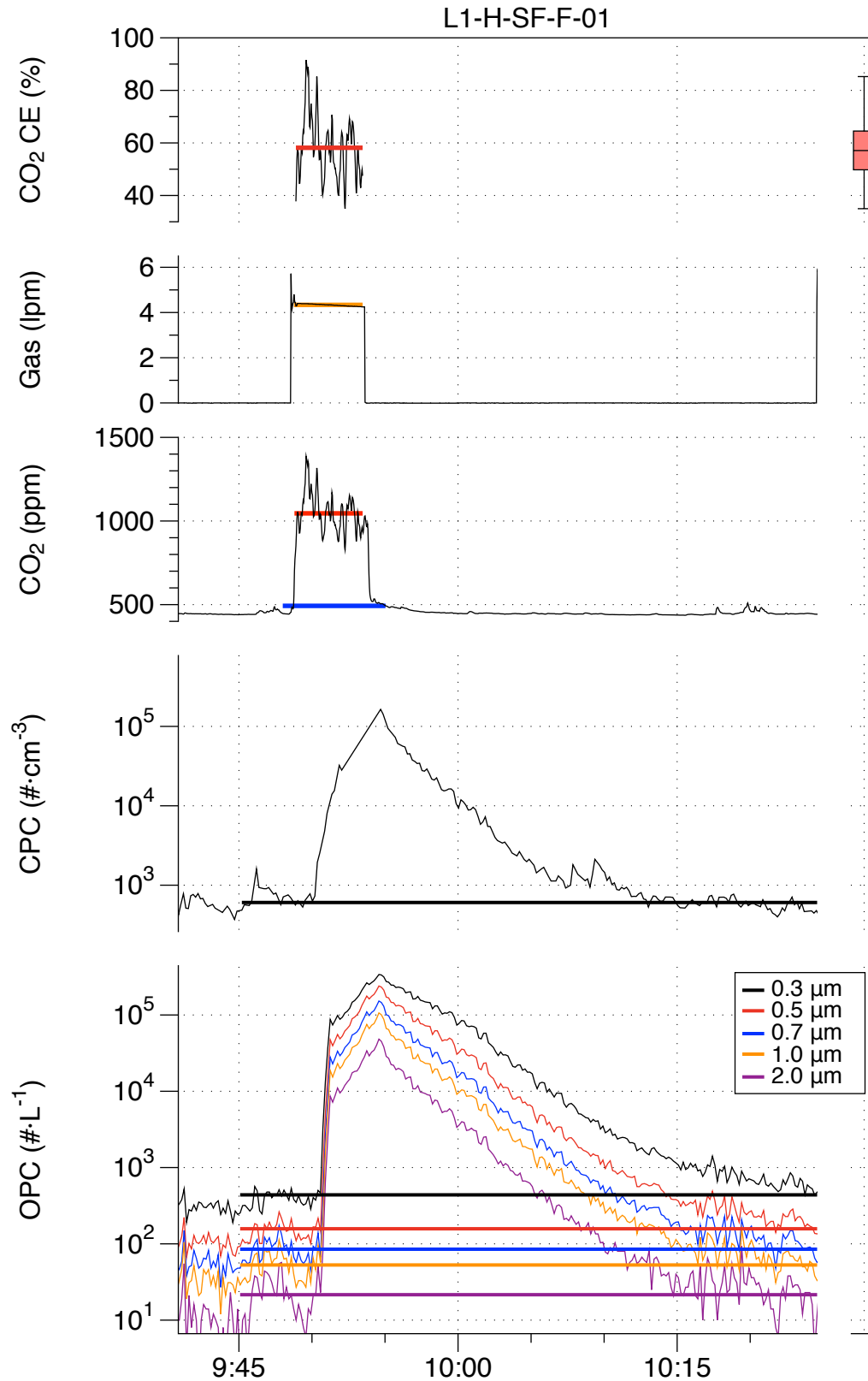


Figure E- 16. Results from experiment L1-H-SF-F-01: burger on back burner, Hood L1 on high speed.

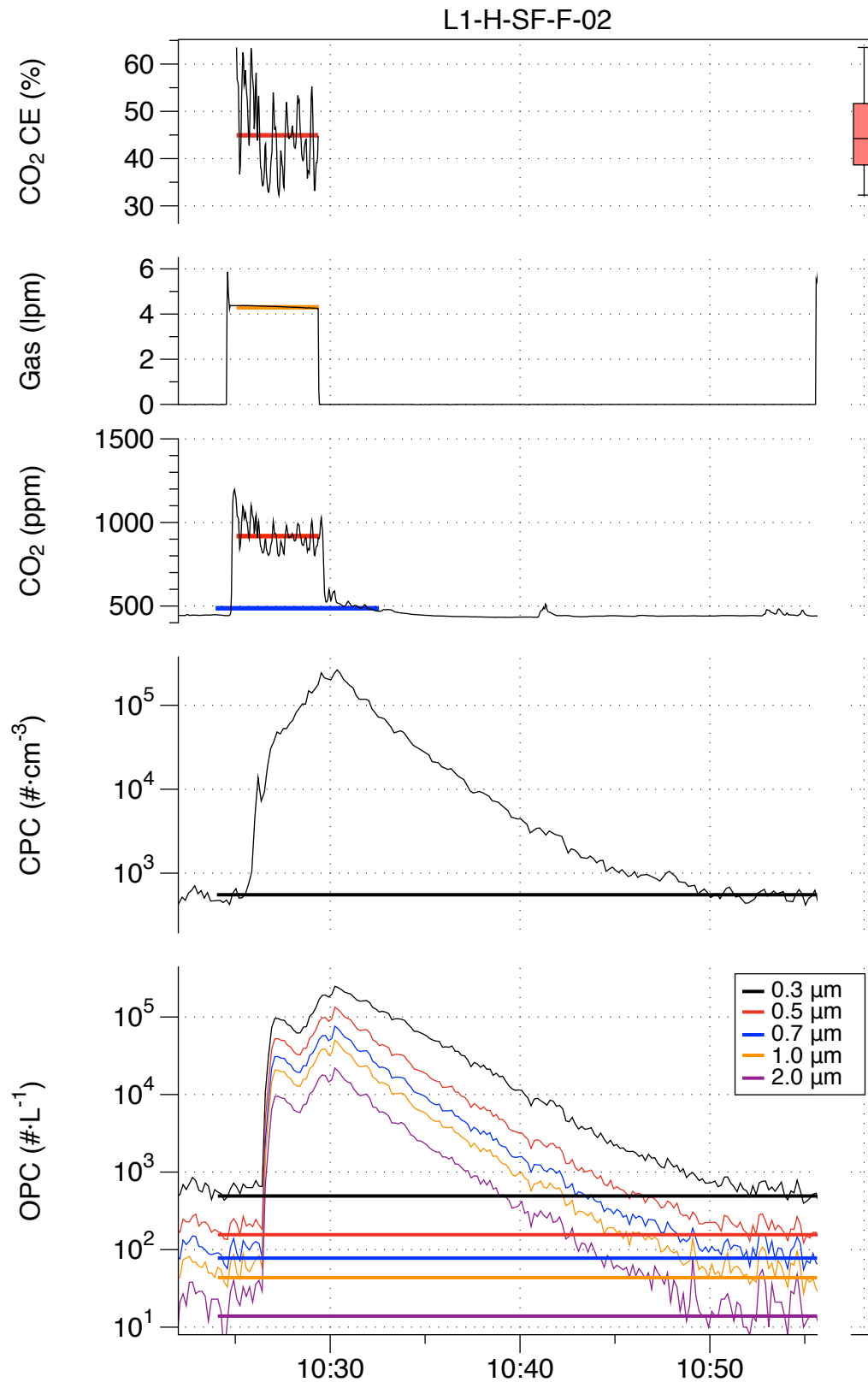


Figure E- 17. Results from experiment L1-H-SF-F-02: burger on back burner, Hood L1 on high speed.

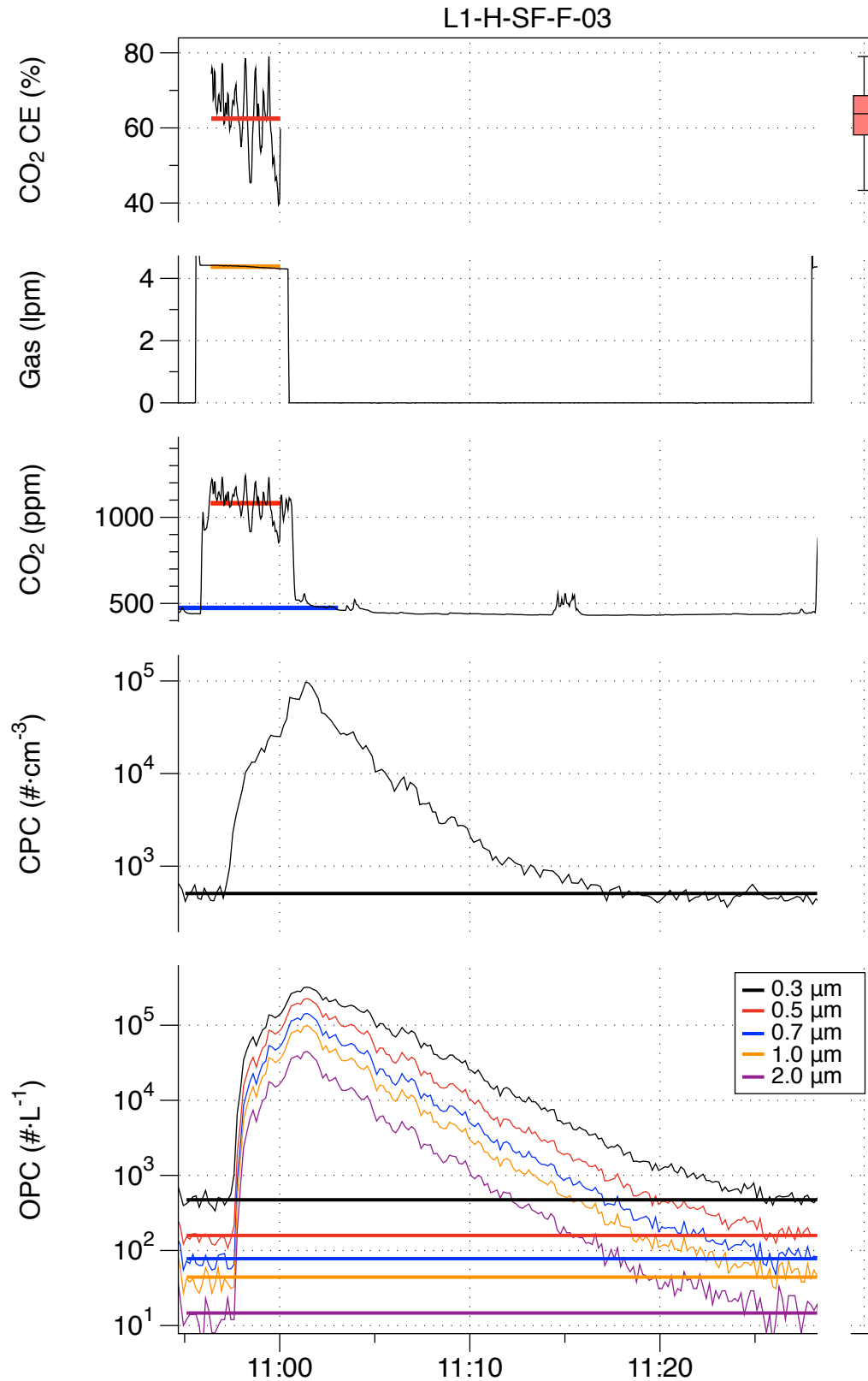


Figure E- 18. Results from experiment L1-H-SF-F-03: burger on back burner, Hood L1 on high speed.

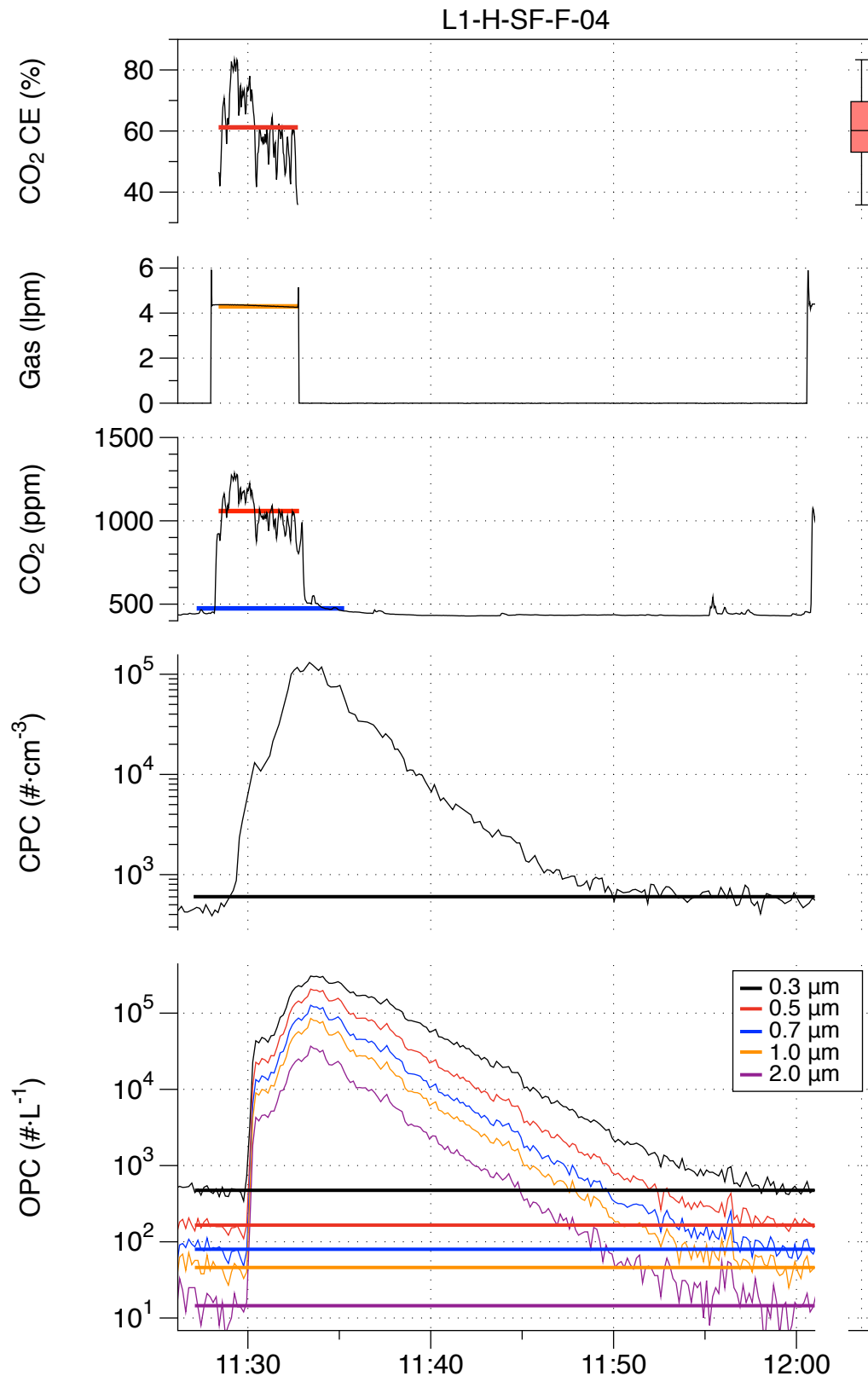


Figure E- 19. Results from experiment L1-H-SF-F-04: burger on back burner, Hood L1 on high speed.

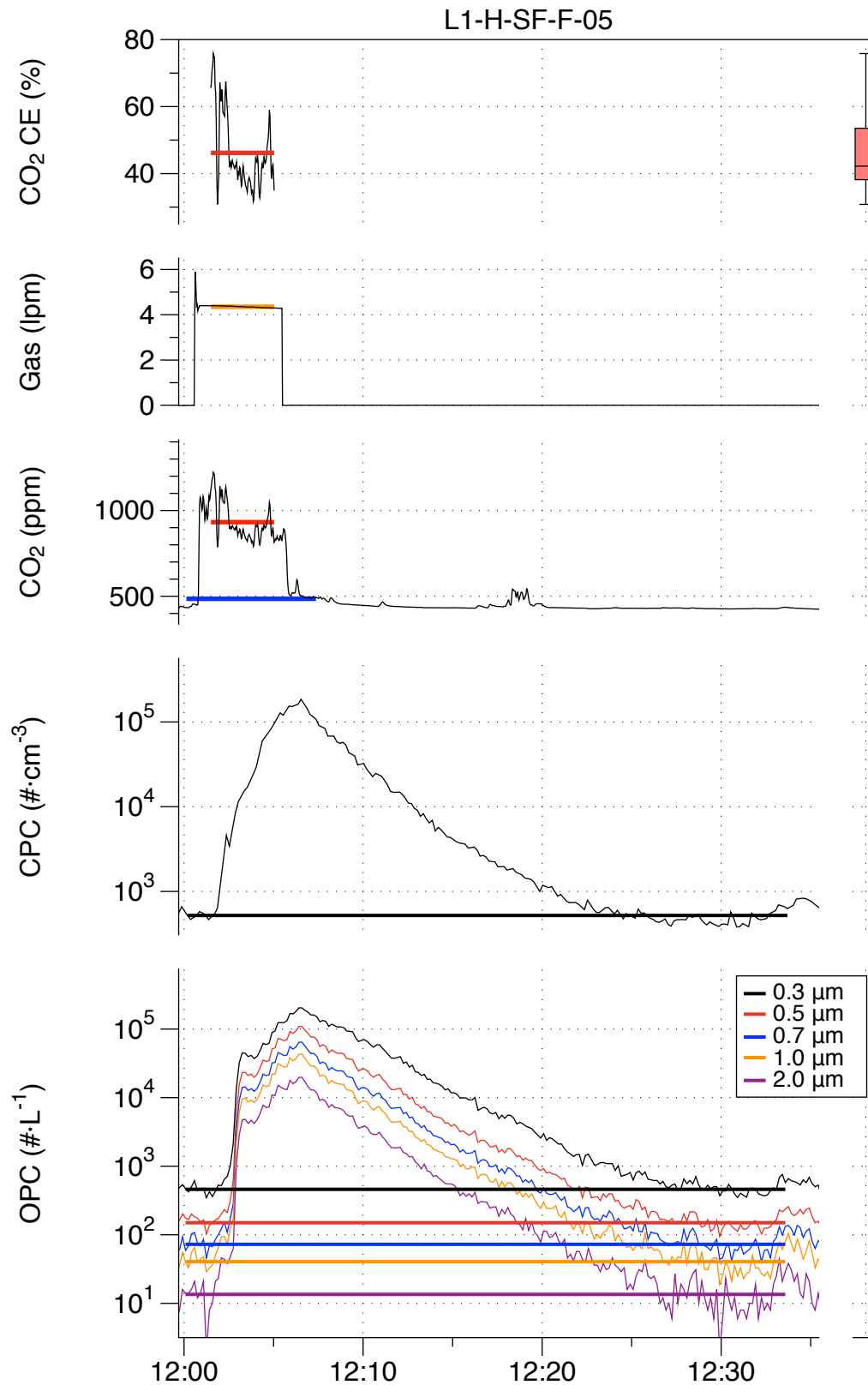


Figure E- 20. Results from experiment L1-H-SF-F-05: burger on back burner, Hood L1 on high speed.

Appendix F: Results of Experiments Conducted with Hood E2

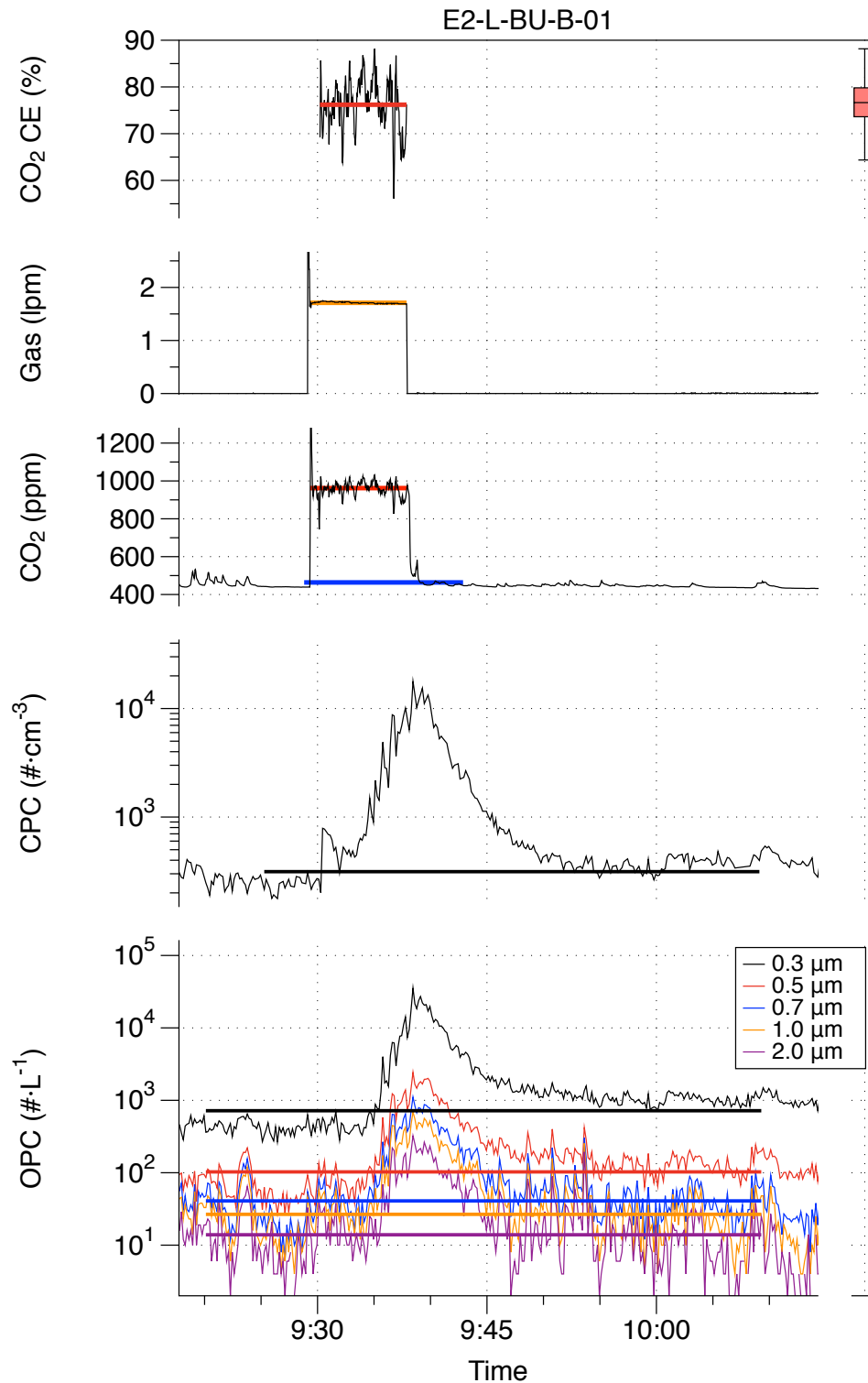


Figure F- 1. Results from experiment E2-L-BU-B-01: burger on back burner, Hood E2 on low speed.

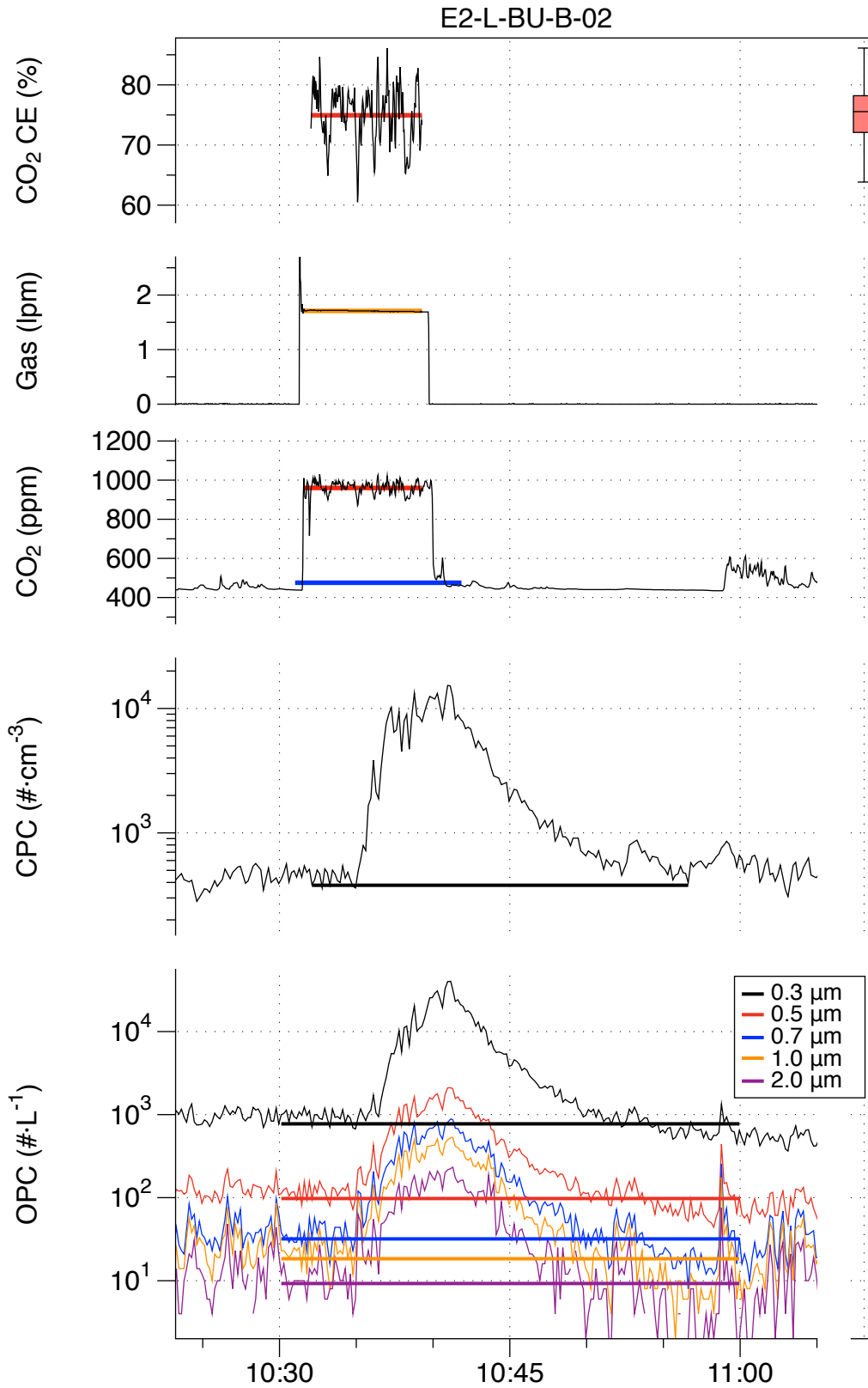


Figure F- 2. Results from experiment E2-L-BU-B-02: burger on back burner, Hood E2 on low speed.

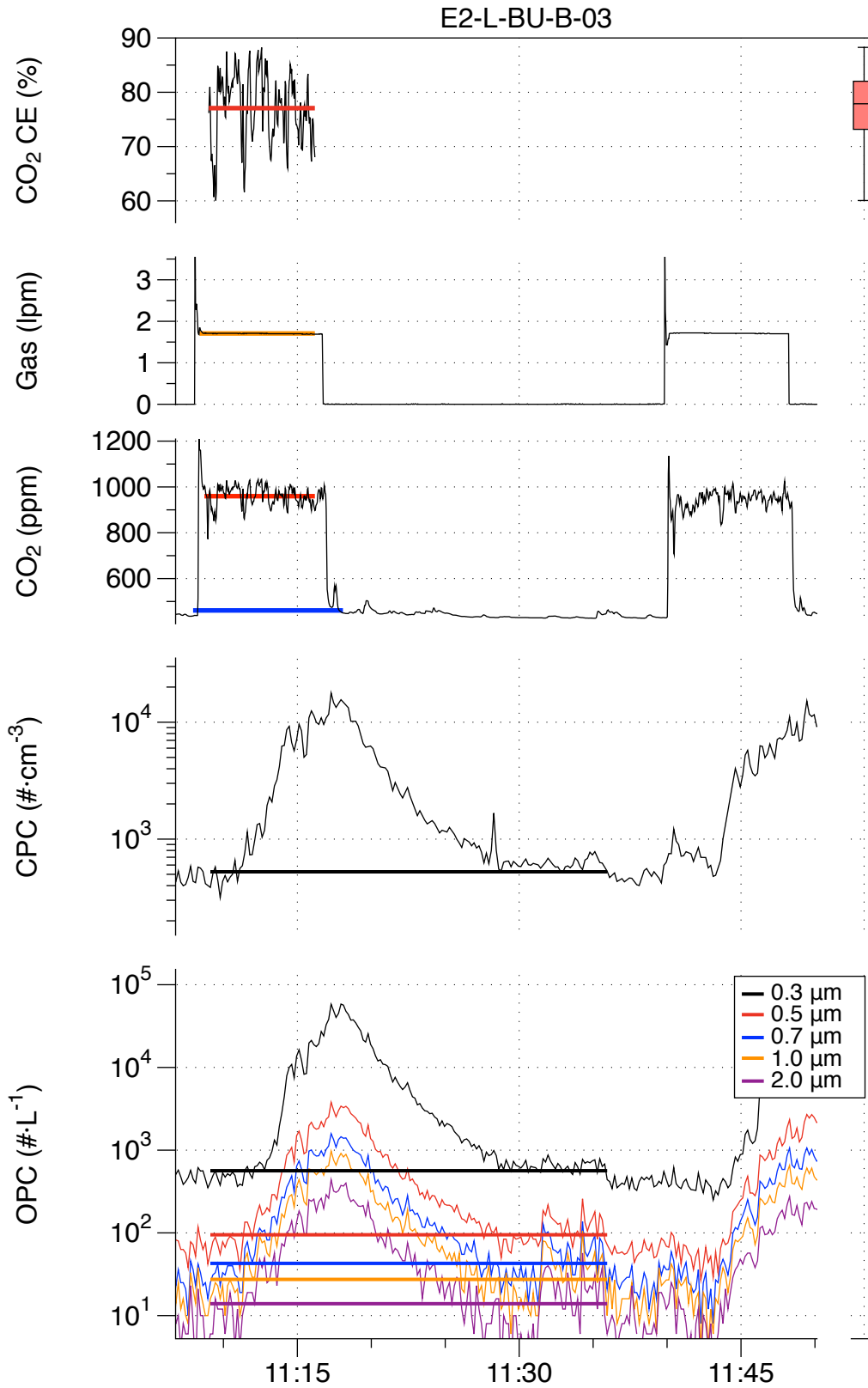


Figure F- 3. Results from experiment E2-L-BU-B-03: burger on back burner, Hood E2 on low speed.

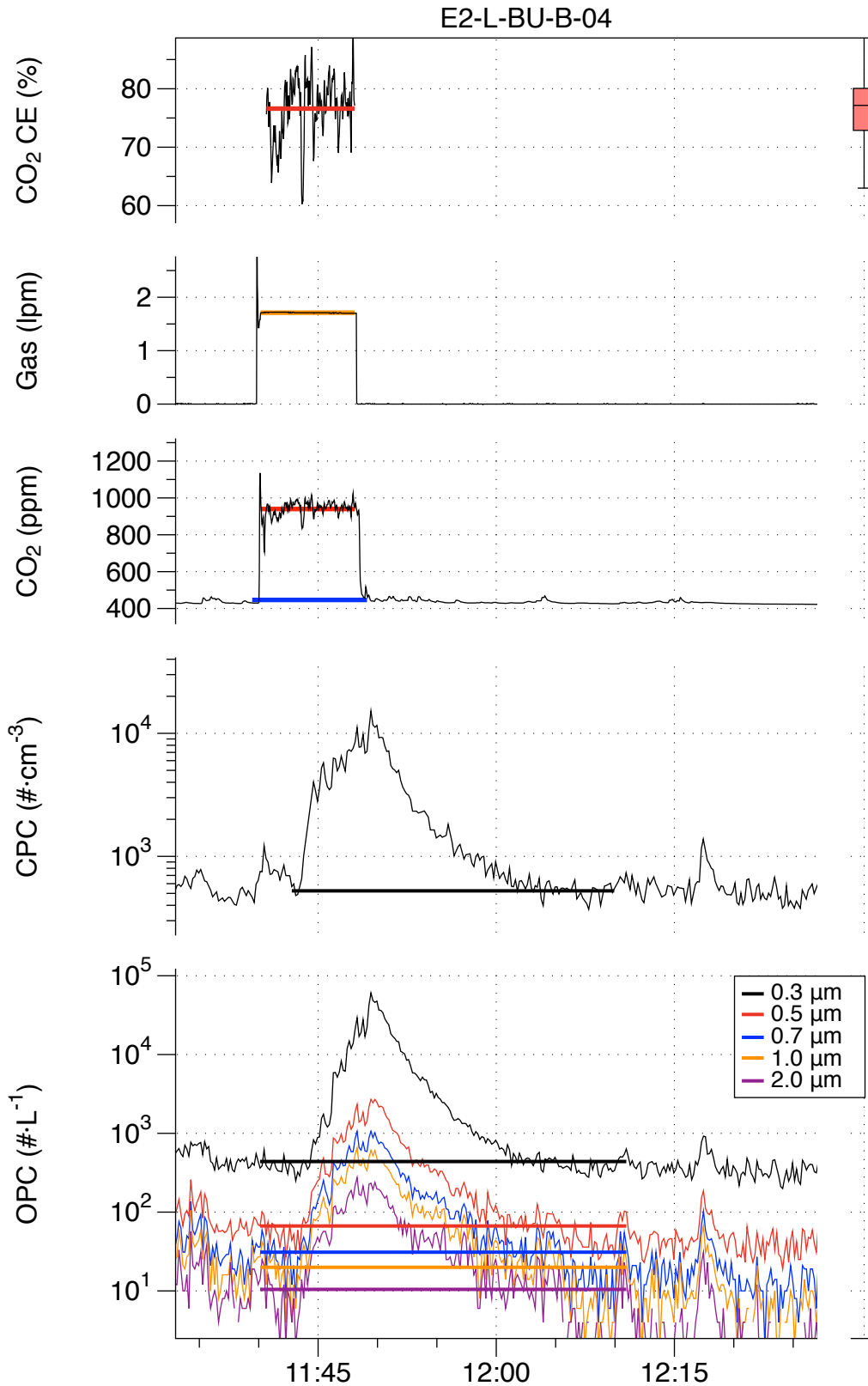


Figure F- 4. Results from experiment E2-L-BU-B-04: burger on back burner, Hood E2 on low speed.

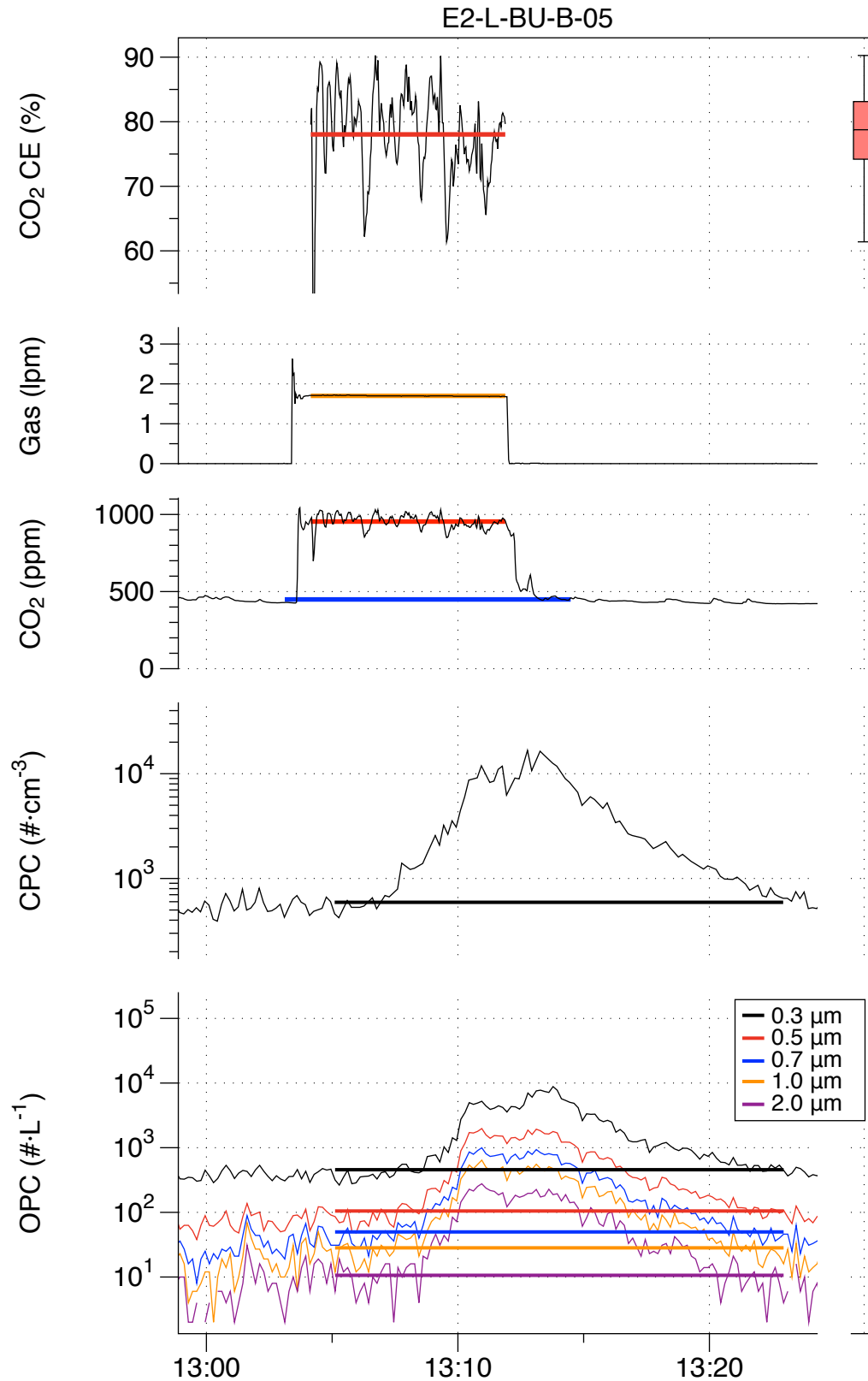


Figure F- 5. Results from experiment E2-L-BU-B-05: burger on back burner, Hood E2 on low speed.

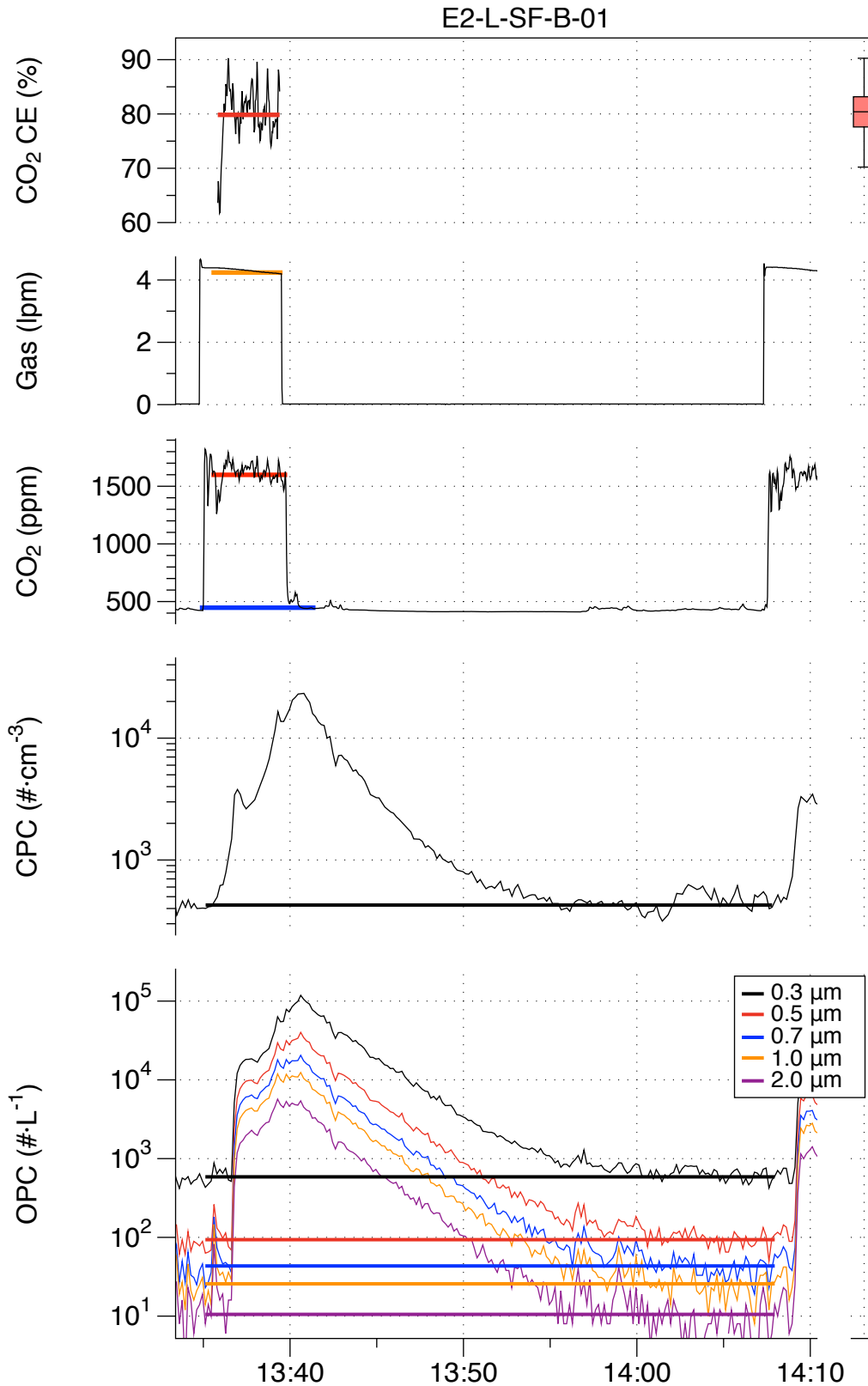


Figure F- 6. Results from experiment E2-L-SF-B-01: stir-fry on back burner, Hood E2 on low speed.

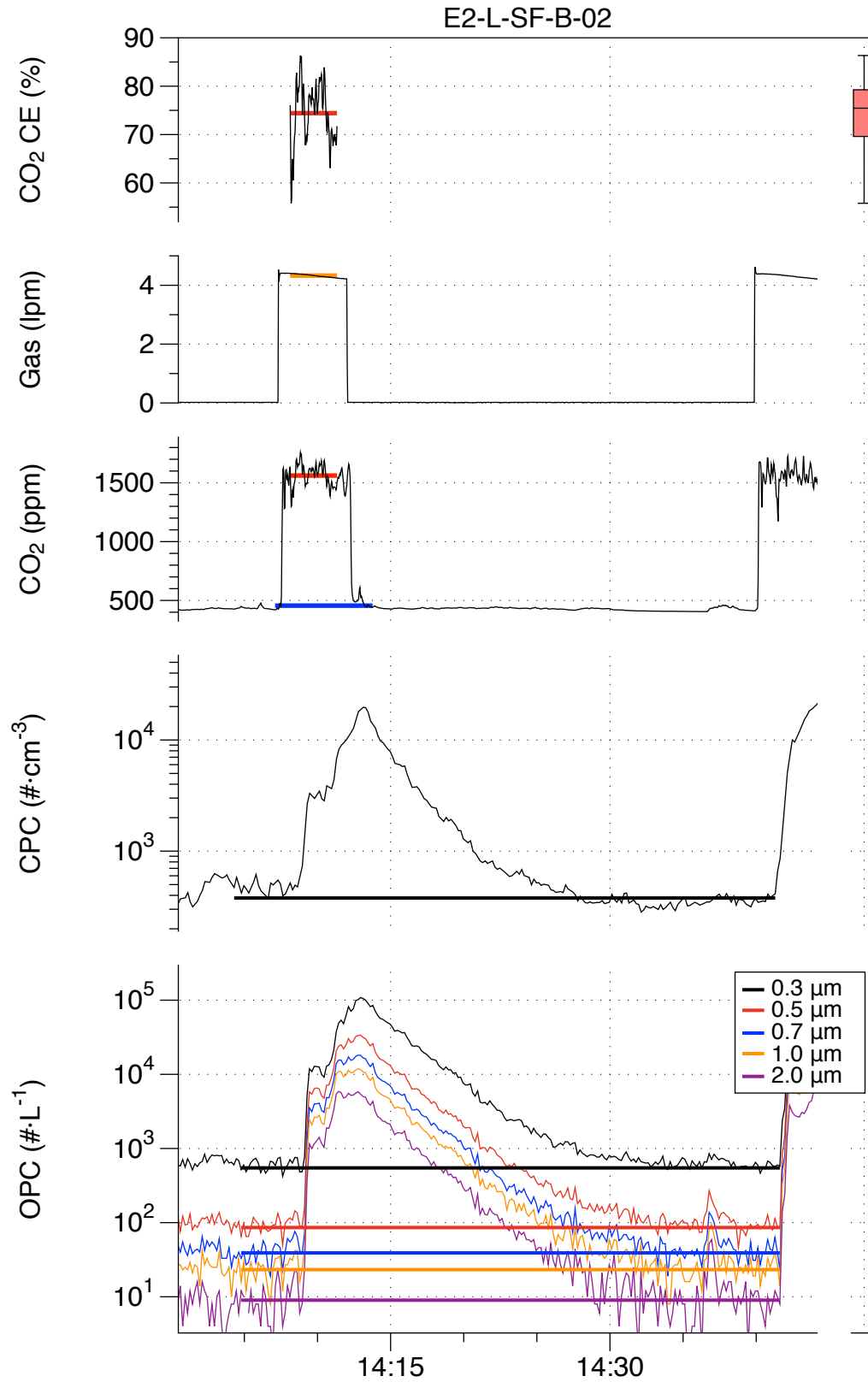


Figure F- 7. Results from experiment E2-L-SF-B-02: stir-fry on back burner, Hood E2 on low speed.

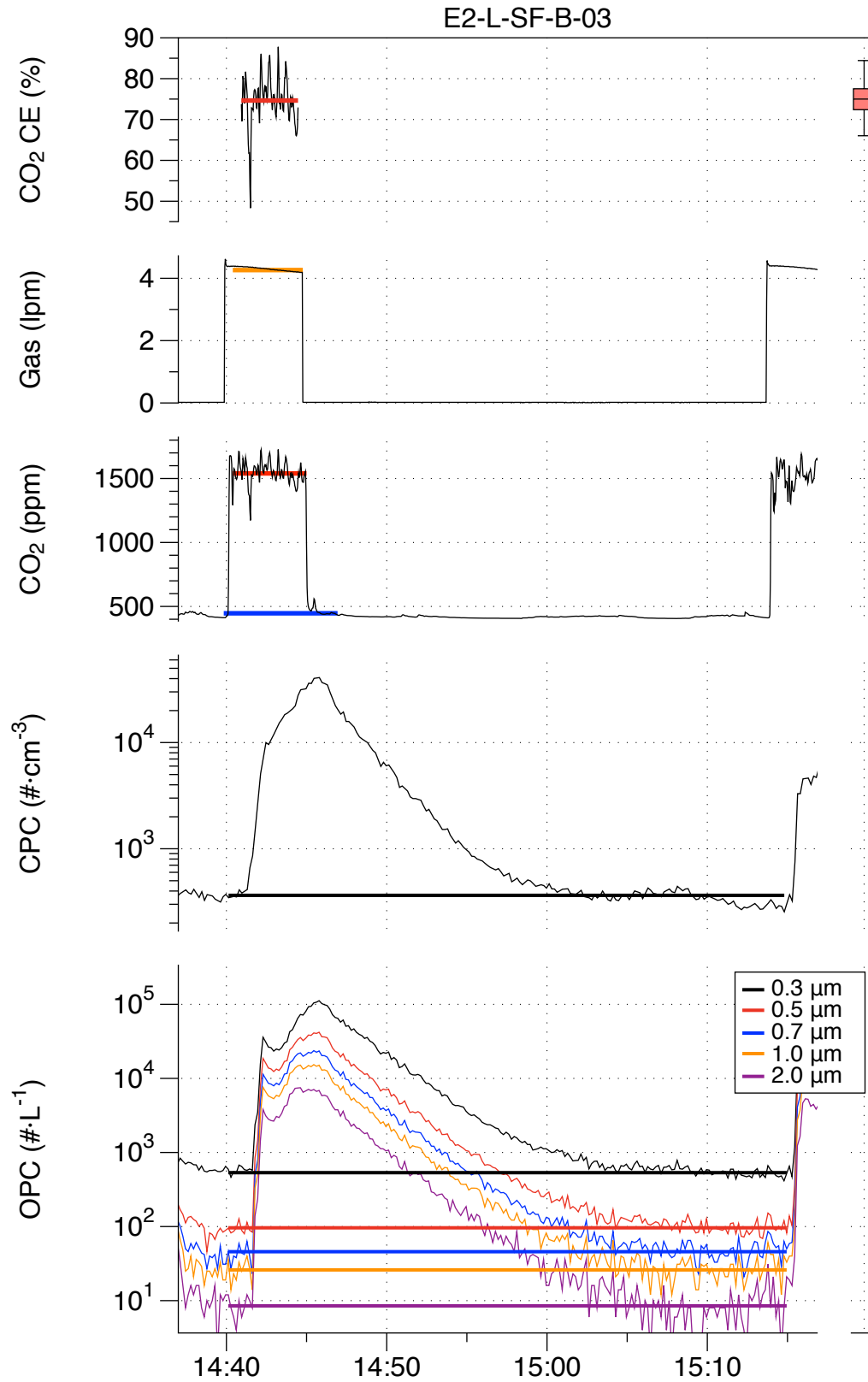


Figure F- 8. Results from experiment E2-L-SF-B-03: stir-fry on back burner, Hood E2 on low speed.

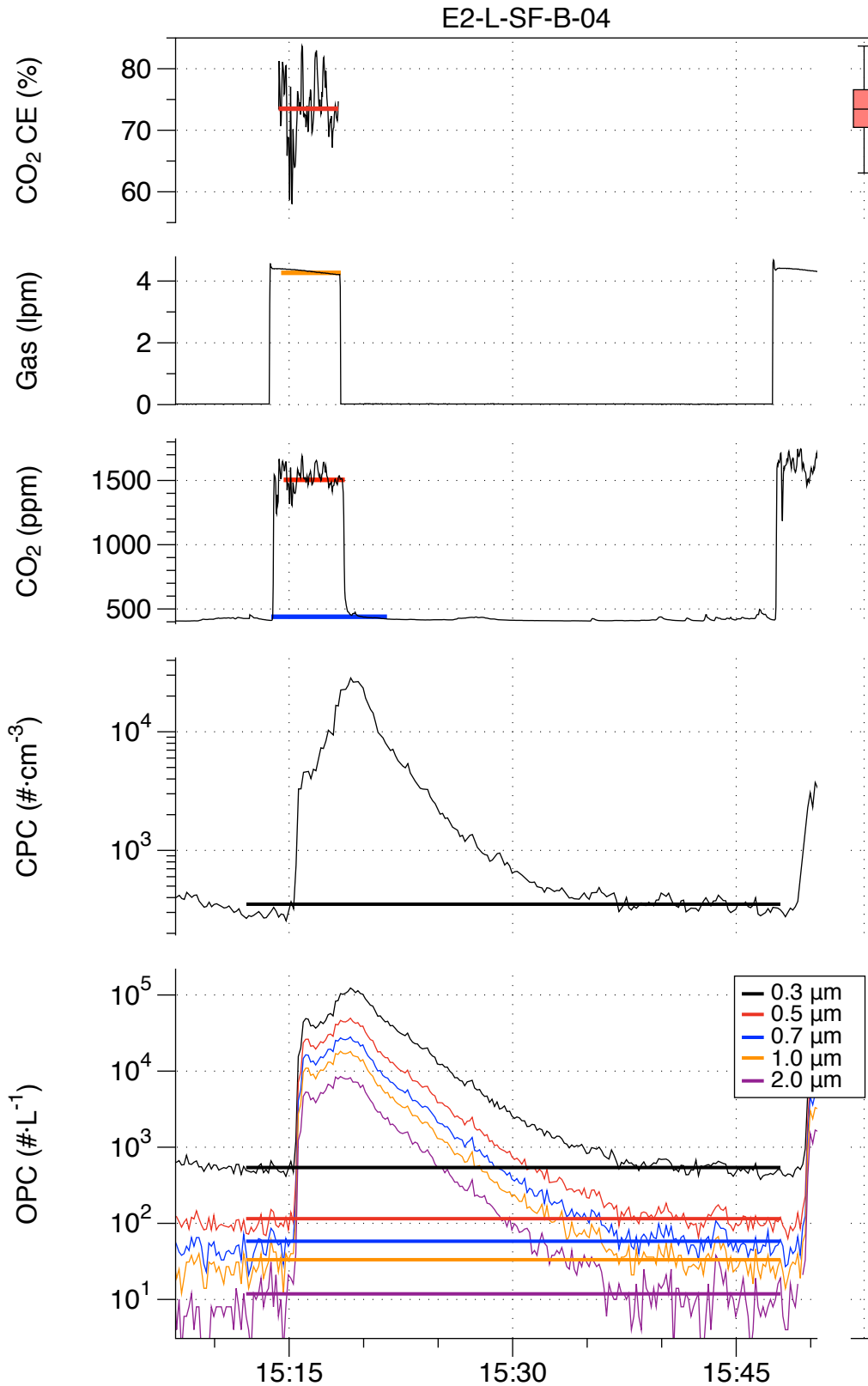


Figure F- 9. Results from experiment E2-L-SF-B-04: stir-fry on back burner, Hood E2 on low speed.

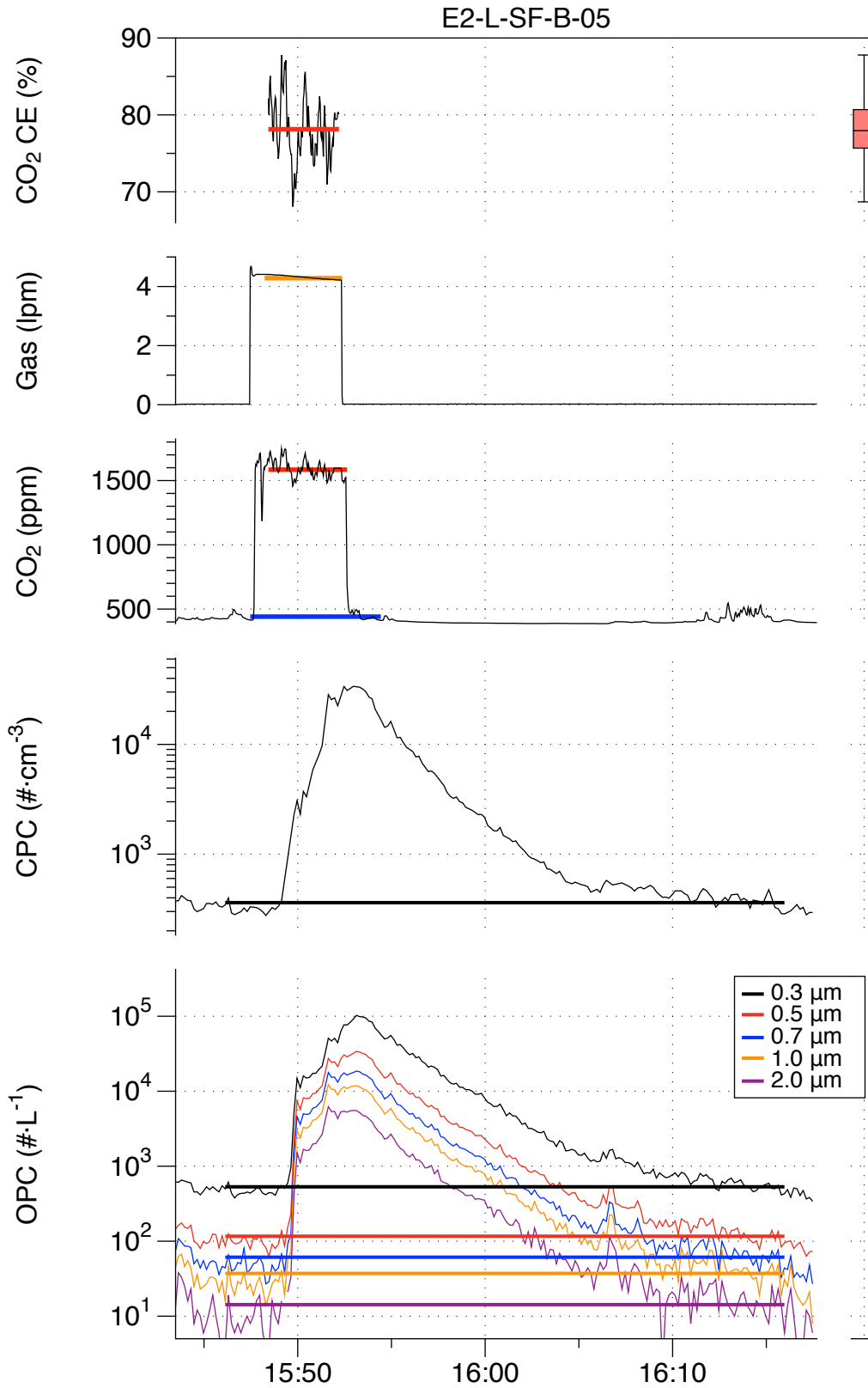


Figure F- 10. Results from experiment E2-L-SF-B-05: stir-fry on back burner, Hood E2 on low speed.

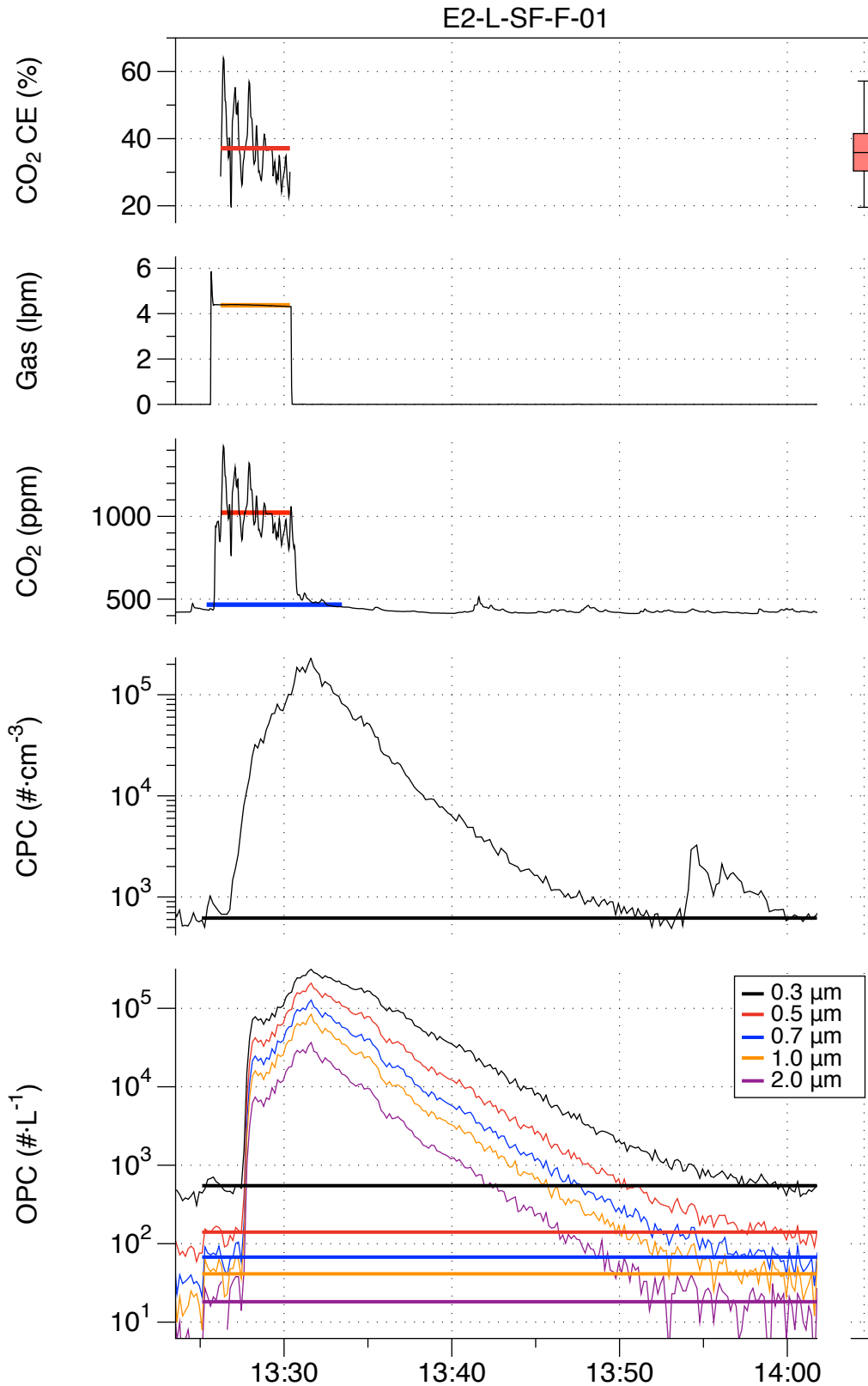


Figure F- 11. Results from experiment E2-L-SF-F-01: stir-fry on front burner, Hood E2 on low speed.

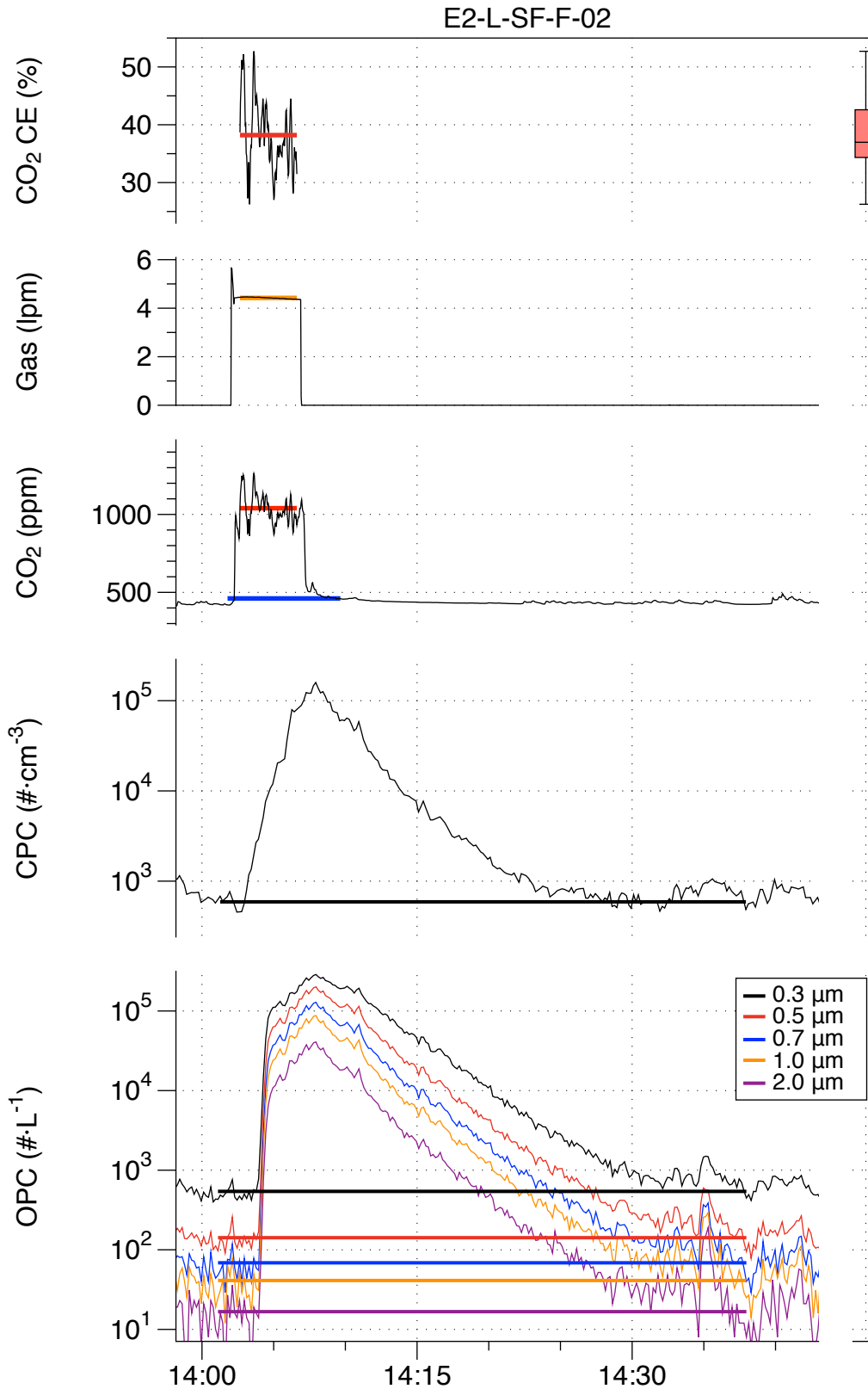


Figure F- 12. Results from experiment E2-L-SF-F-02: stir-fry on front burner, Hood E2 on low speed.

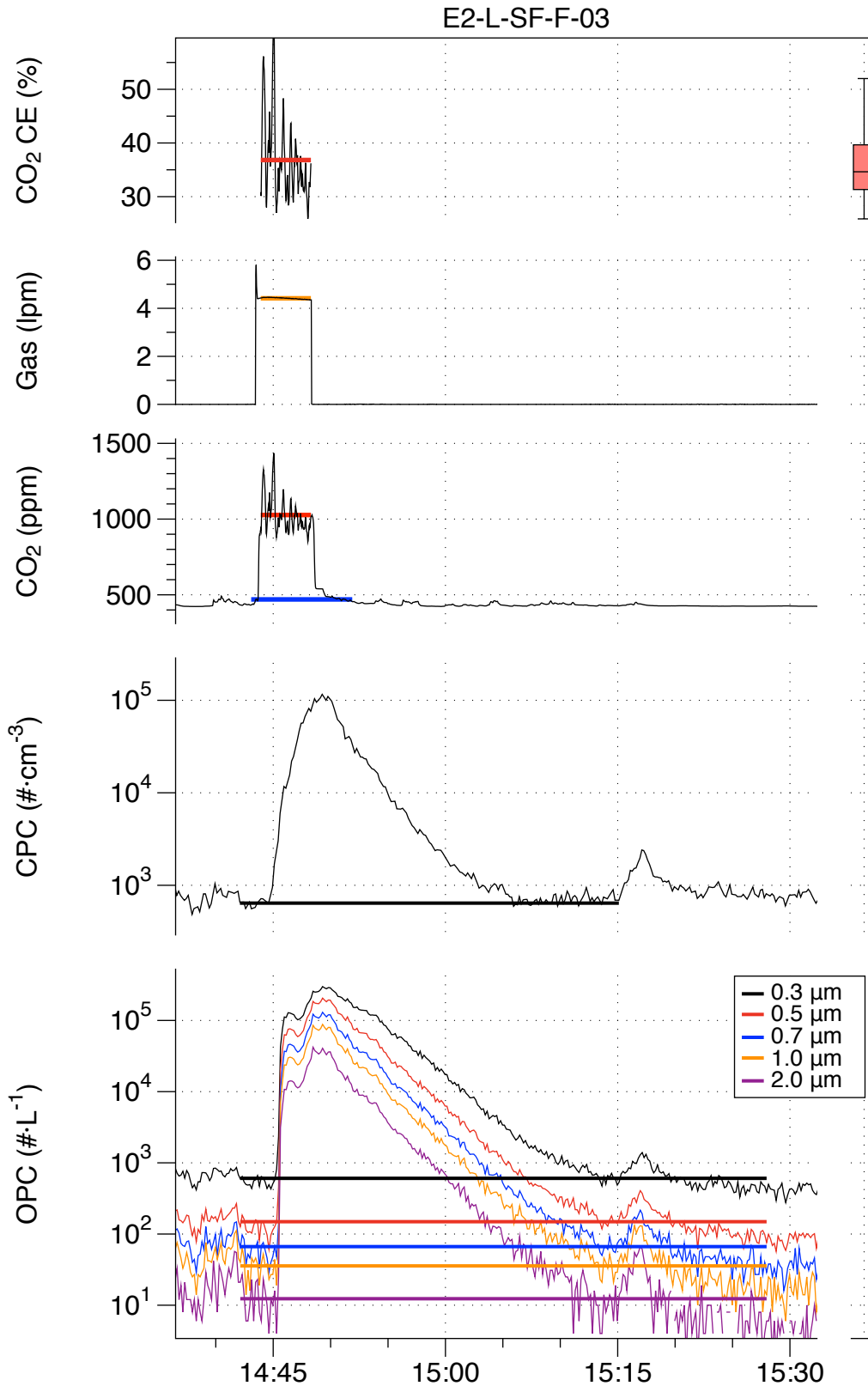


Figure F- 13. Results from experiment E2-L-SF-F-03: stir-fry on front burner, Hood E2 on low speed.

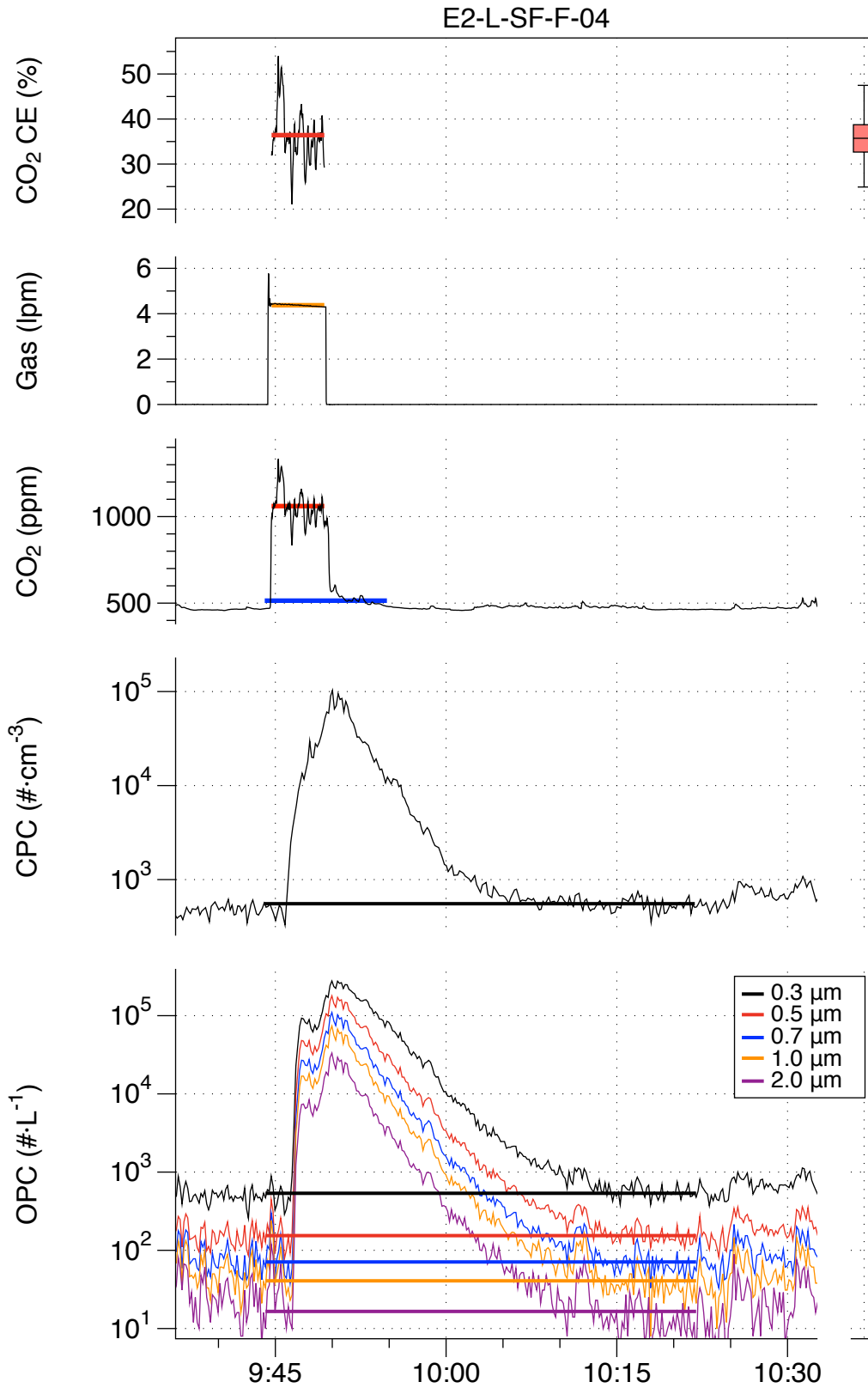


Figure F- 14. Results from experiment E2-L-SF-F-03: stir-fry on front burner, Hood E2 on low speed.

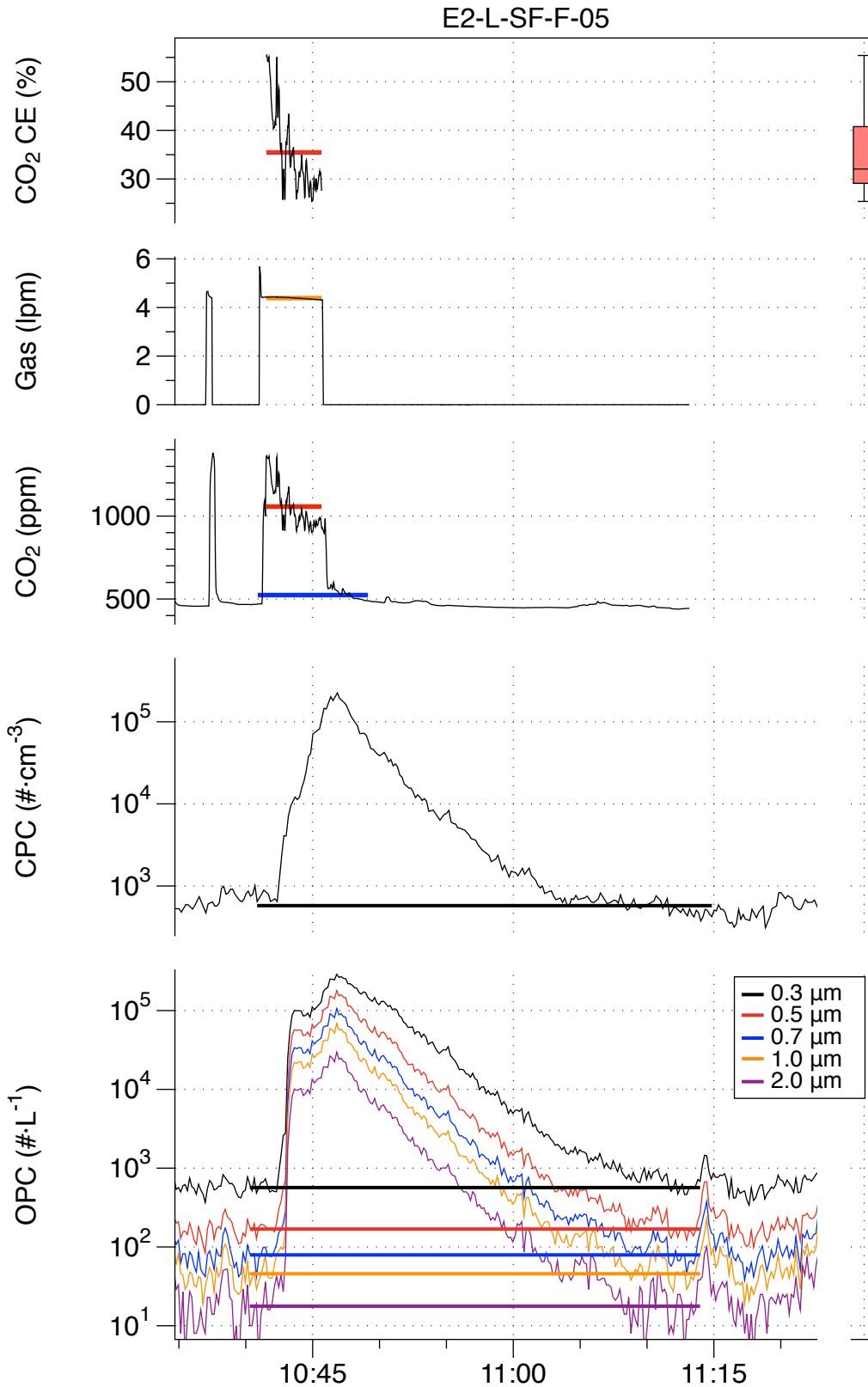


Figure F- 15. Results from experiment E2-L-SF-F-05: stir-fry on front burner, Hood E2 on low speed.

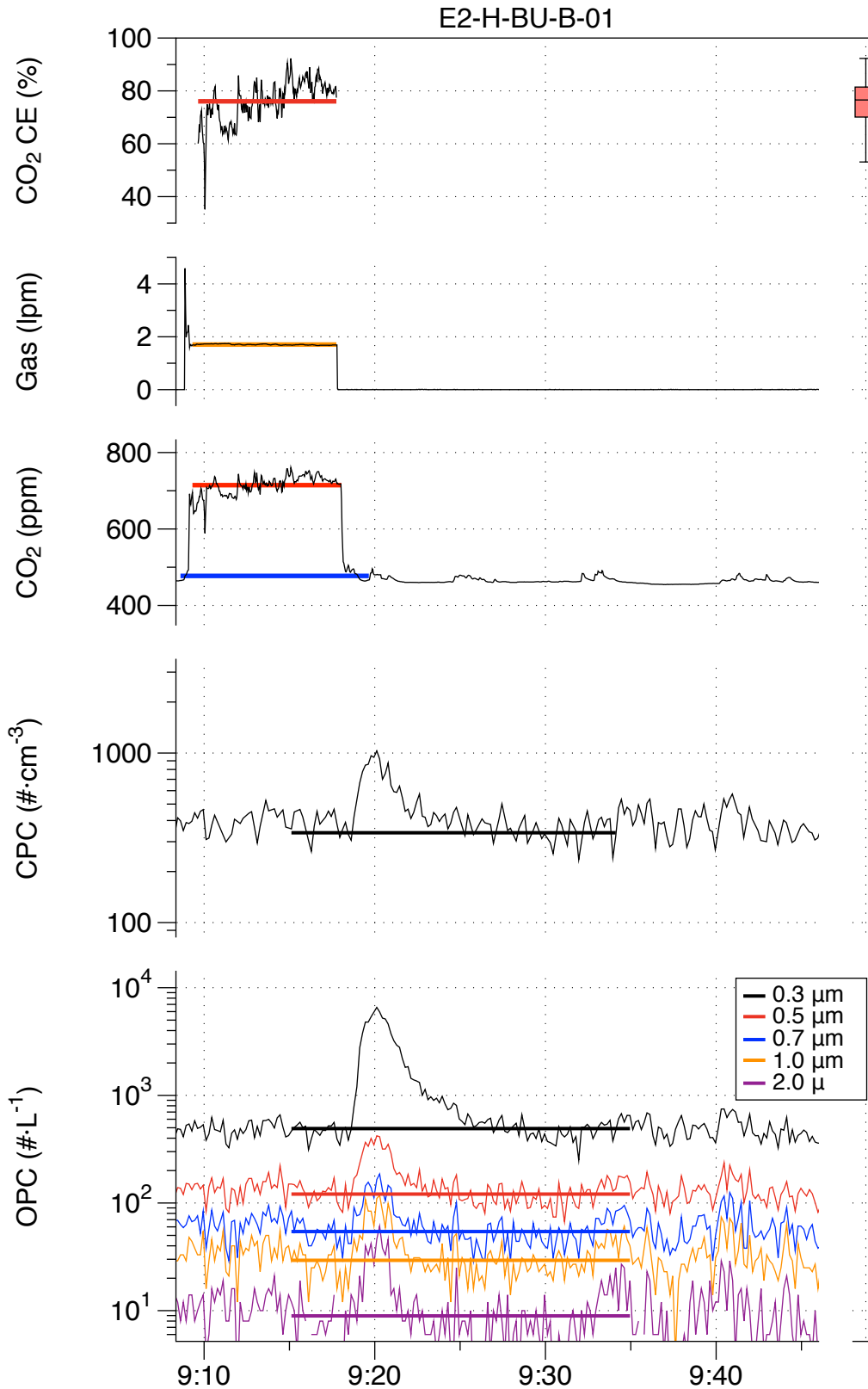


Figure F- 16. Results from experiment E2-H-BU-B-01: burger on back burner, Hood E2 on high speed.

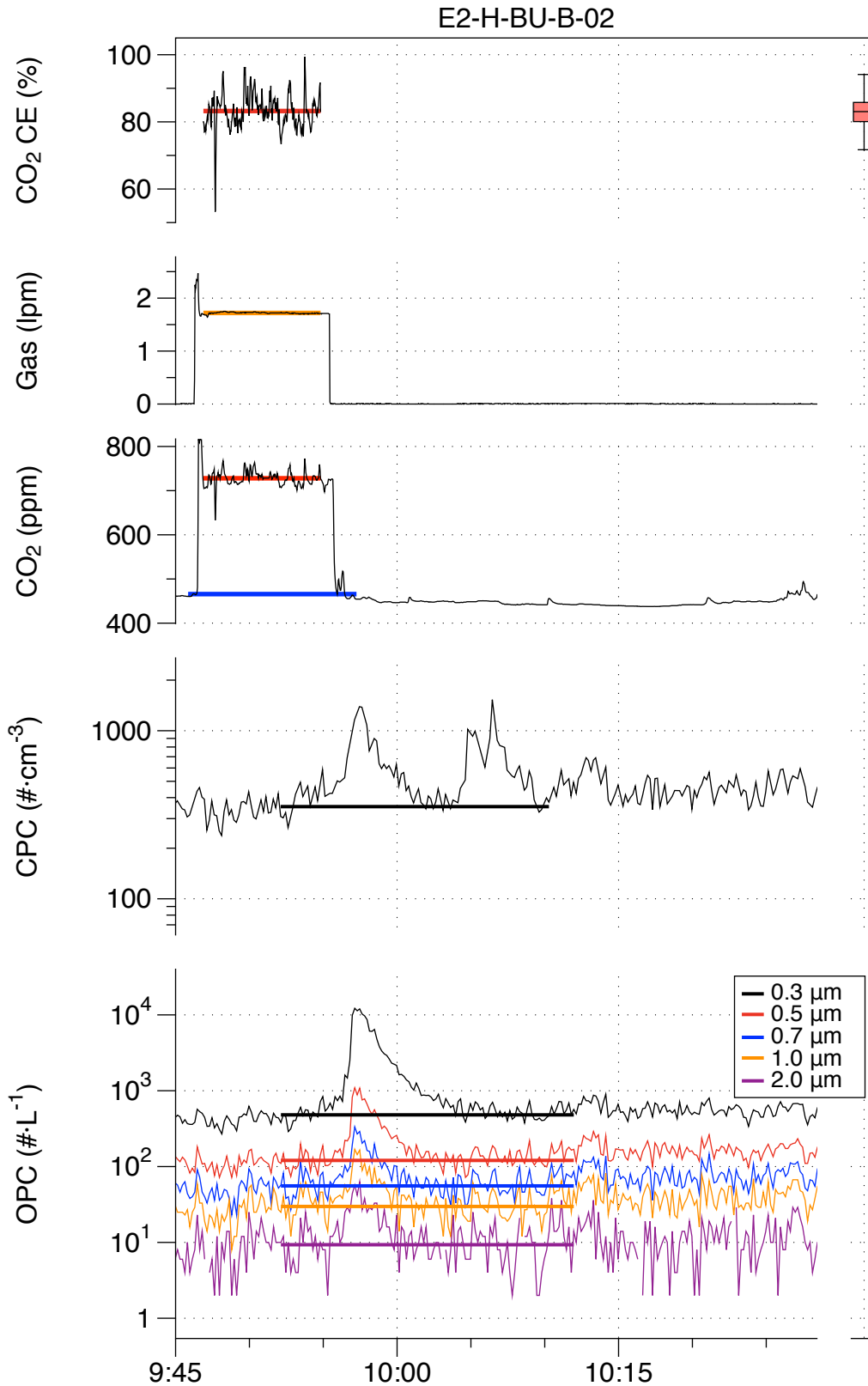


Figure F- 17. Results from experiment E2-H-BU-B-02: Burger on front burner, Hood E2 on high speed.

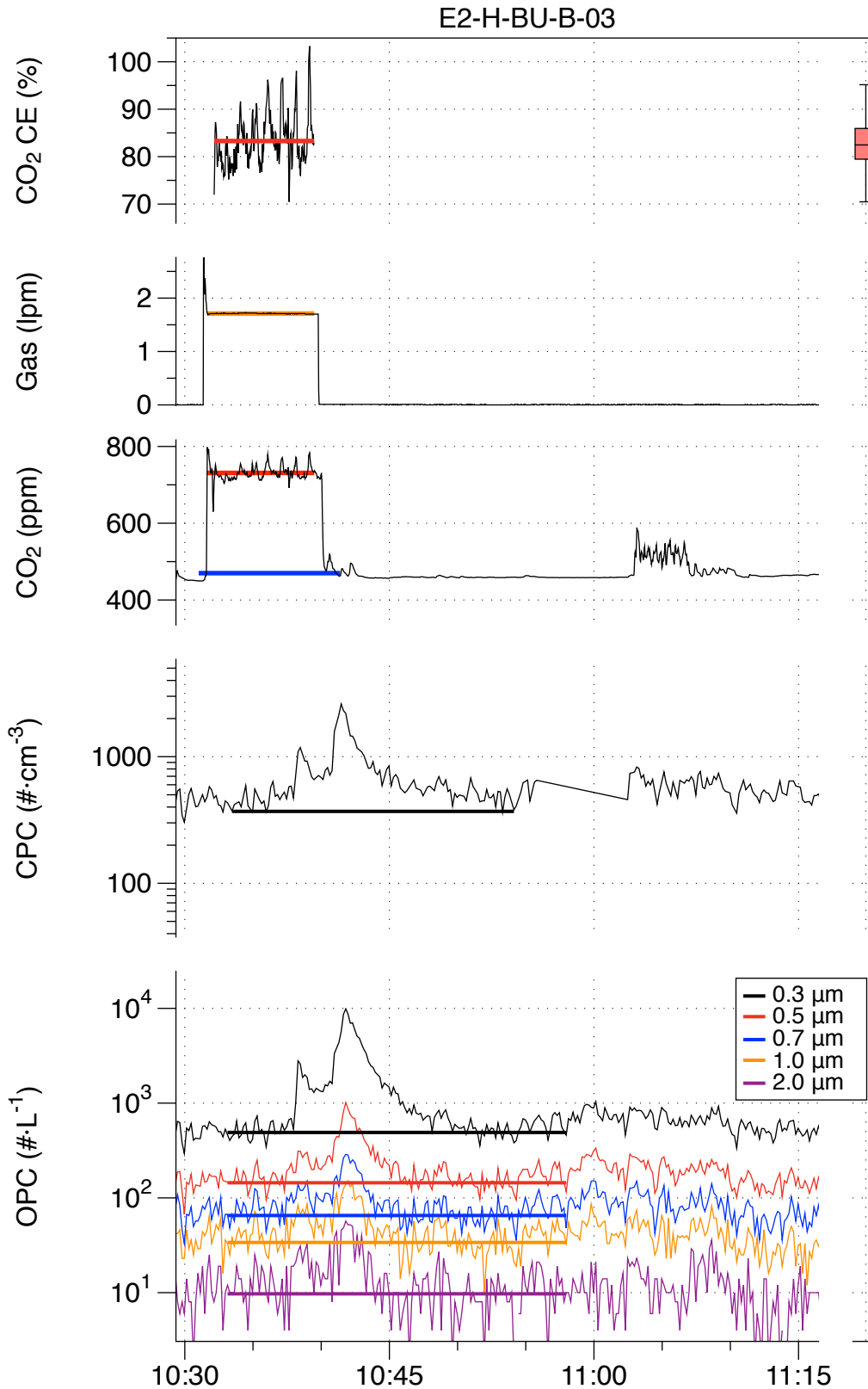


Figure F- 18. Results from experiment E2-H-BU-B-03: Burger on back burner, Hood E2 on high speed.

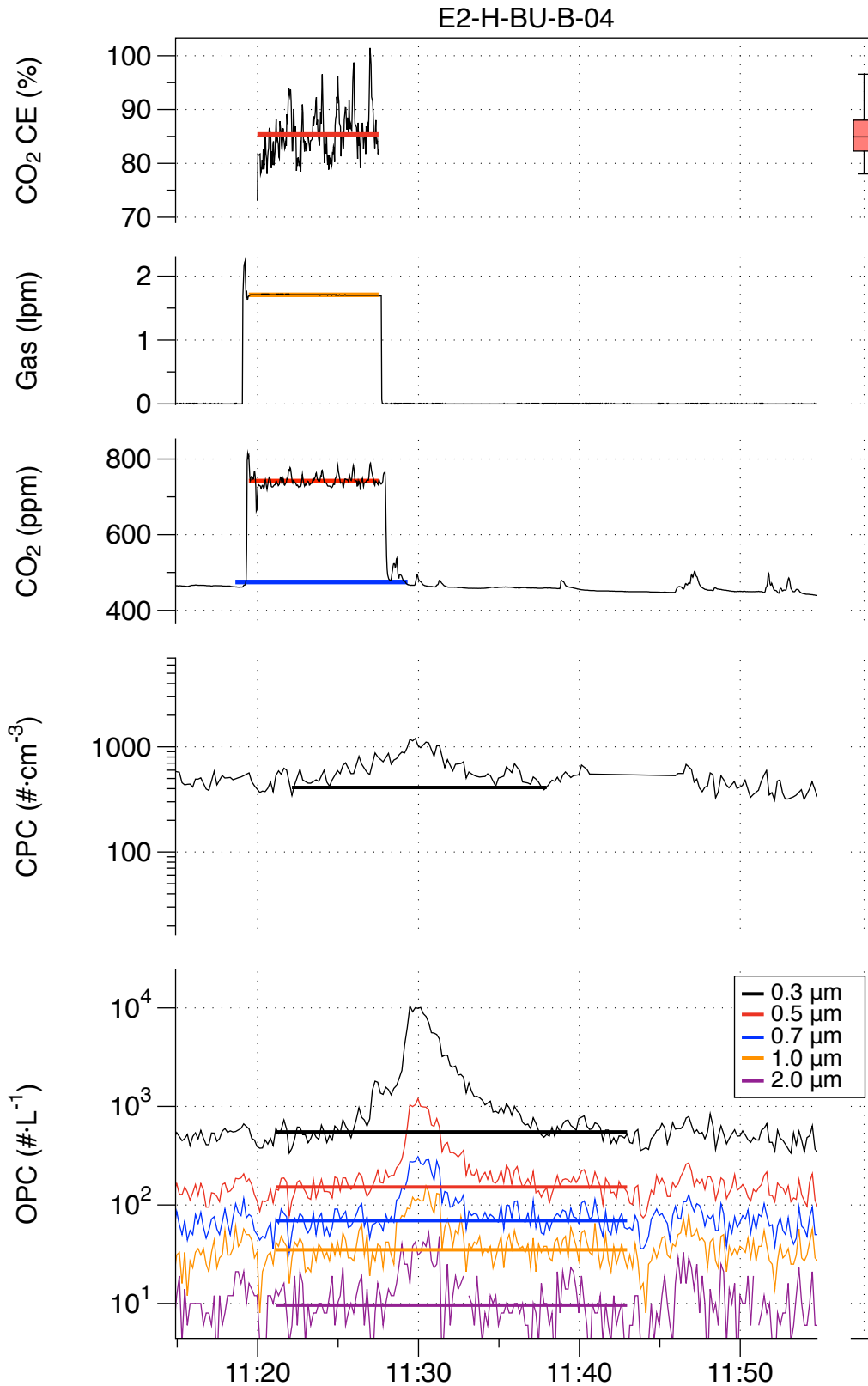


Figure F- 19. Results from experiment E2-H-BU-B-04: Burger on back burner, Hood E2 on high speed

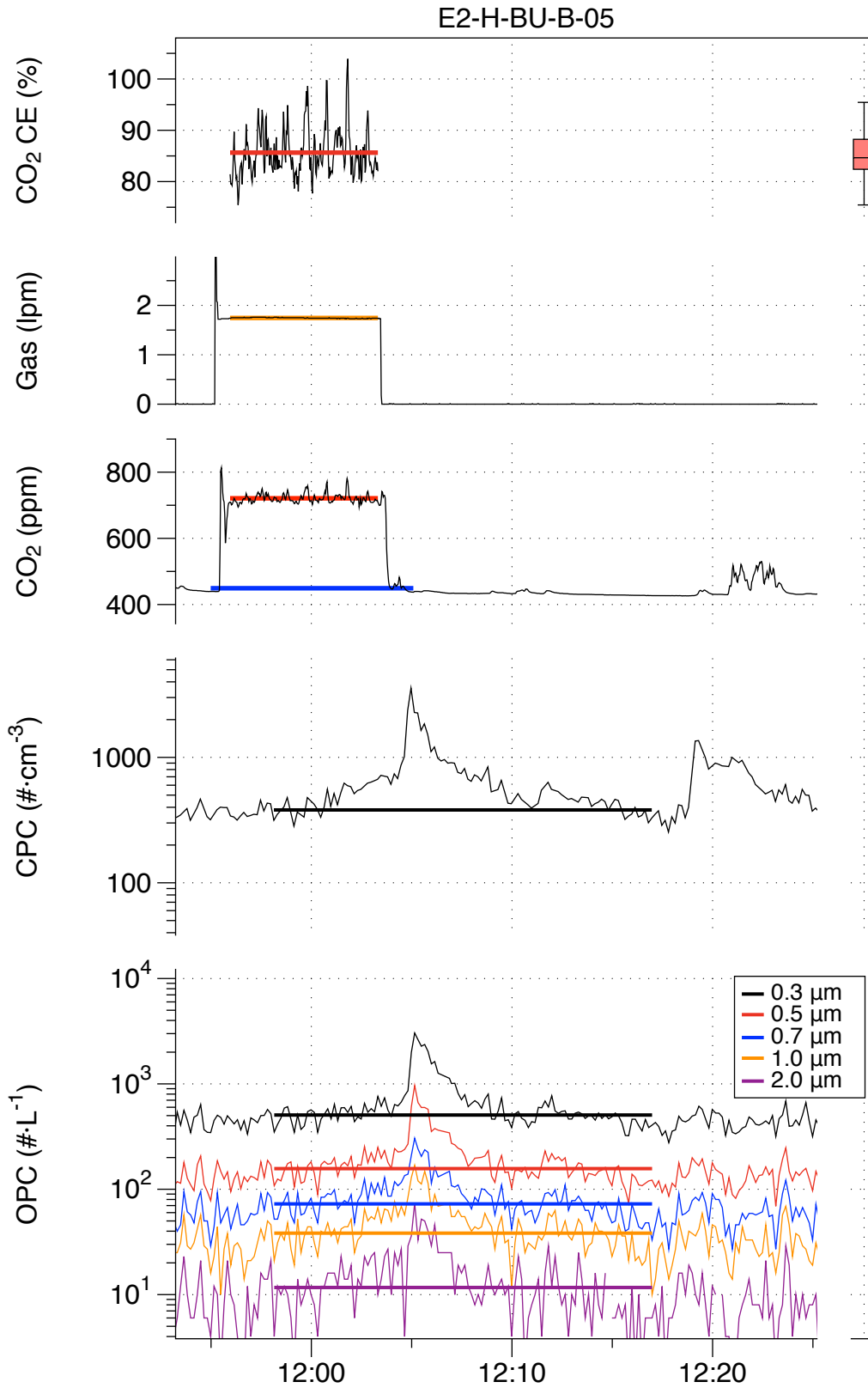


Figure F- 20. Results from experiment E2-H-BU-B-05: Burger on back burner, Hood E2 on high speed.

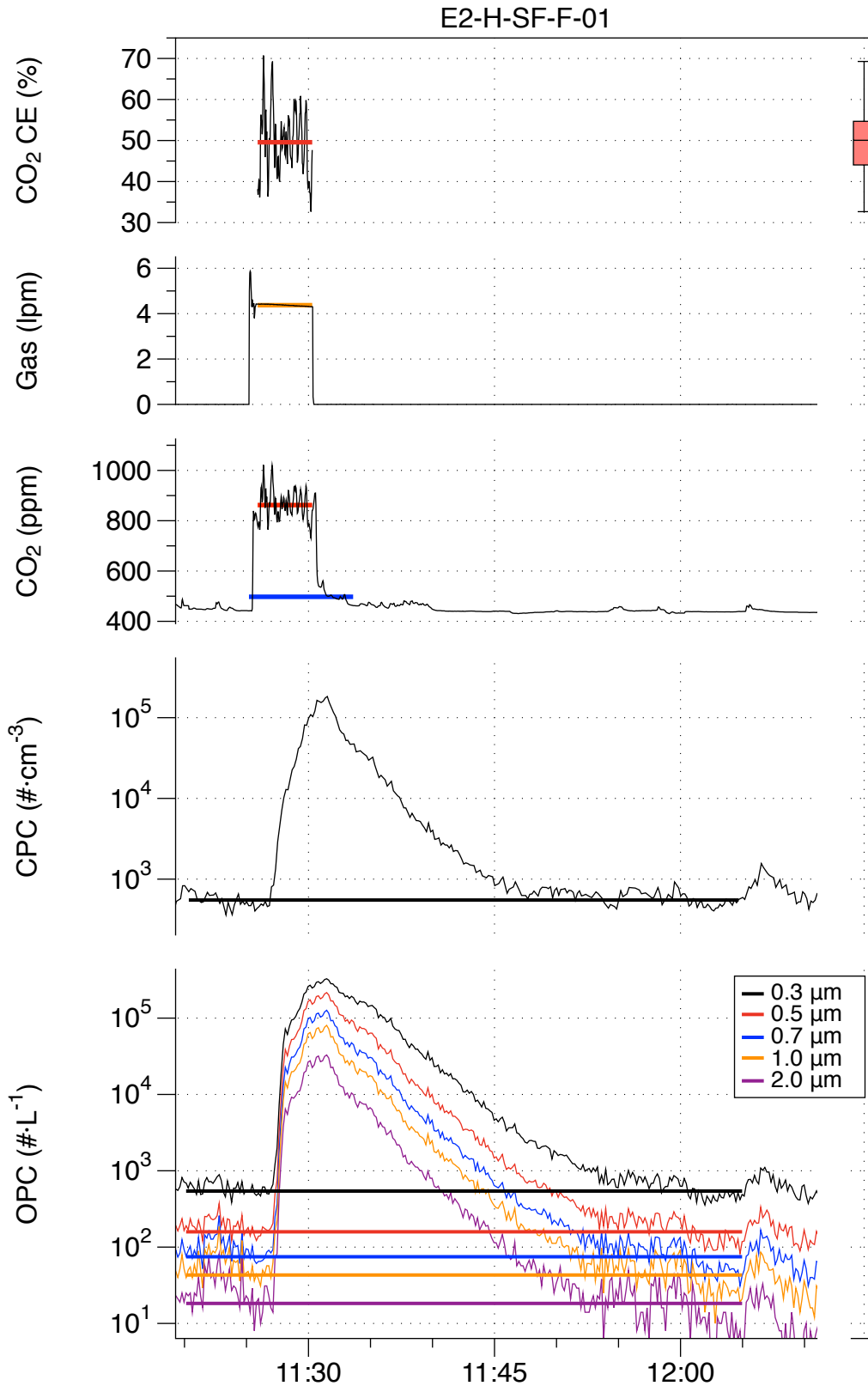


Figure F- 21. Results from experiment E2-H-SF-F-01: stir-fry on front burner, Hood E2 on high speed.

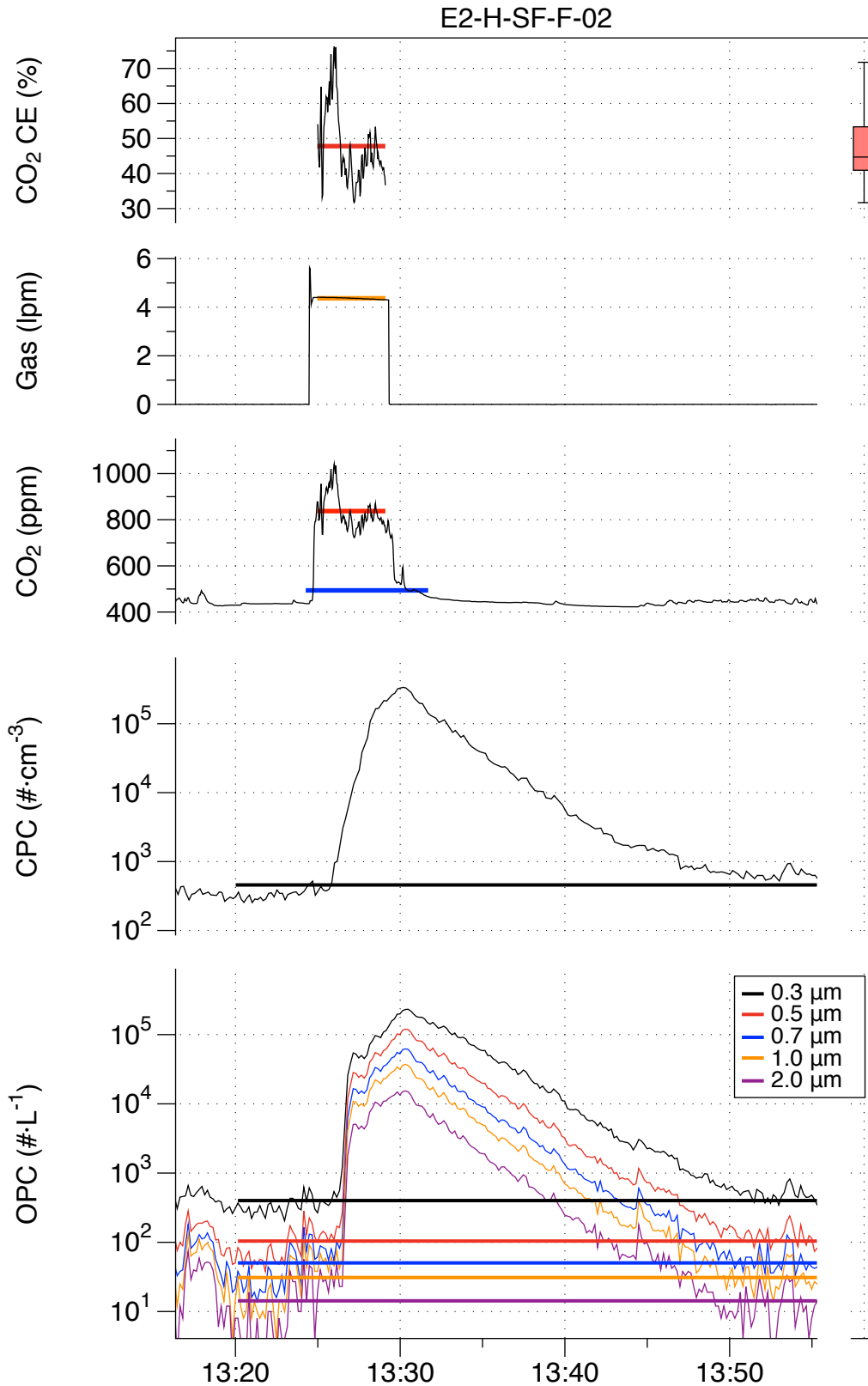


Figure F- 22. Results from experiment E2-H-SF-F-02: stir-fry on front burner, Hood E2 on high speed.

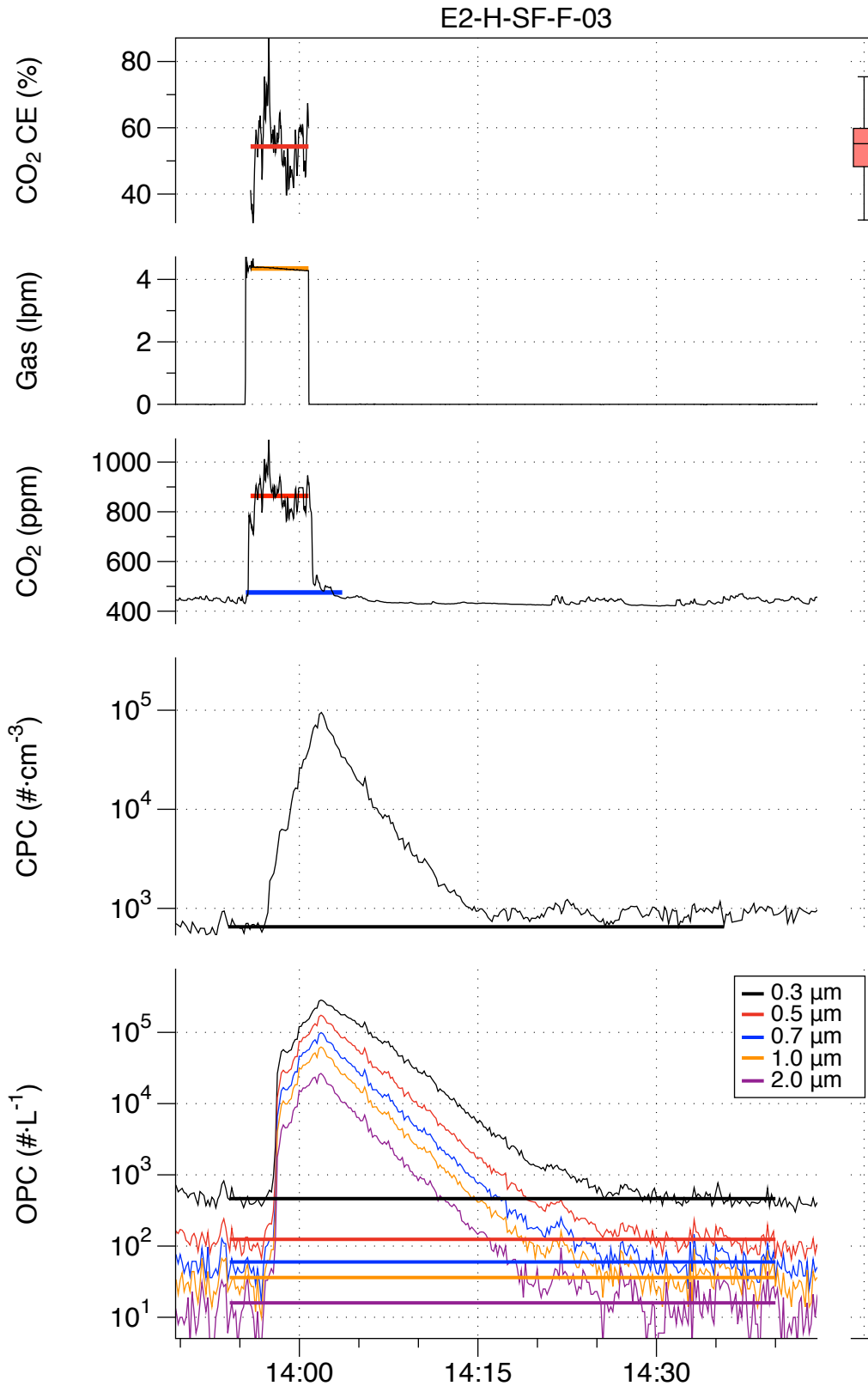


Figure F- 23. Results from experiment E2-H-SF-F-03: stir-fry on front burner, Hood E2 on high speed.

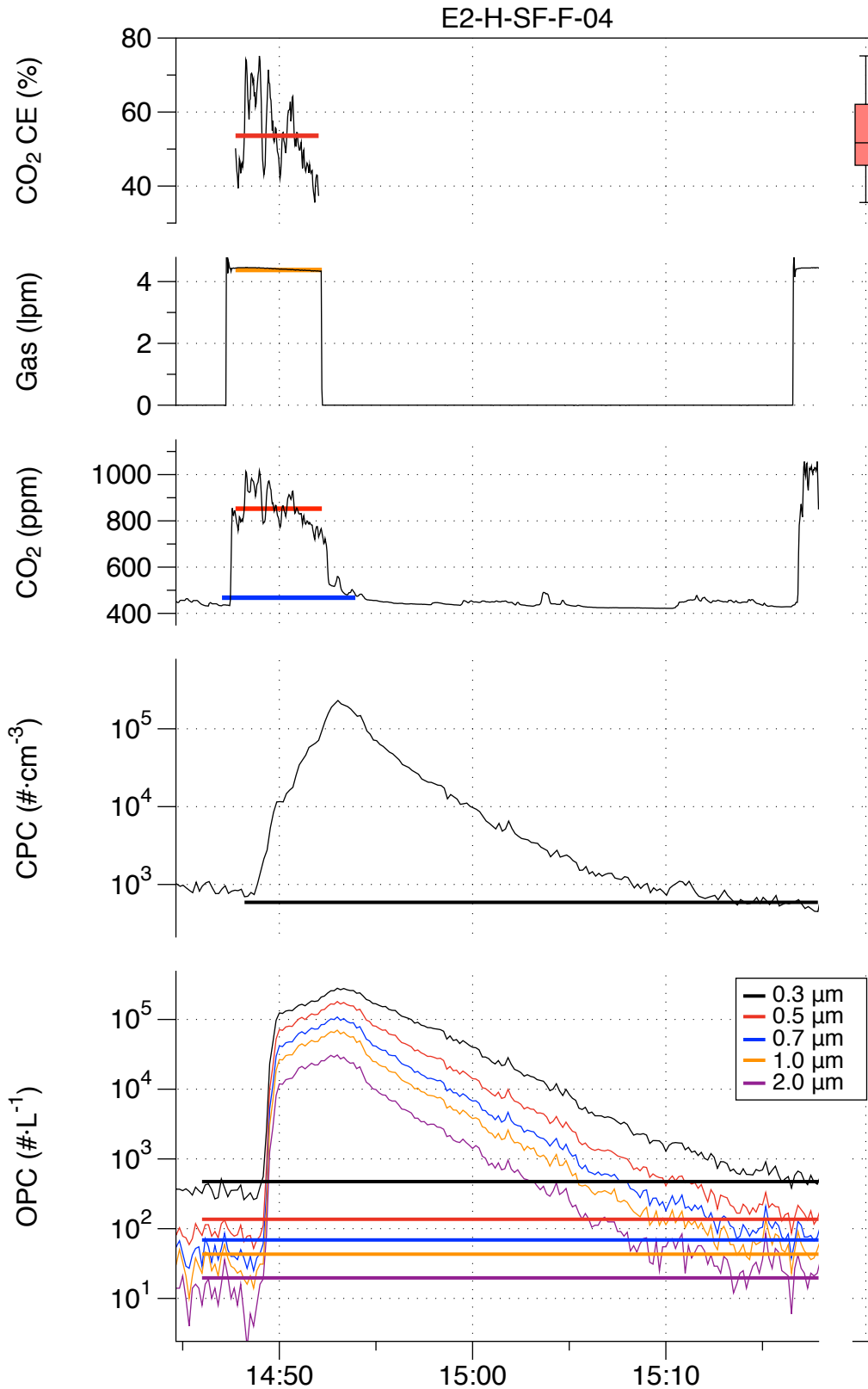


Figure F- 24. Results from experiment E2-H-SF-F-04: stir-fry on front burner, Hood E2 on high speed.

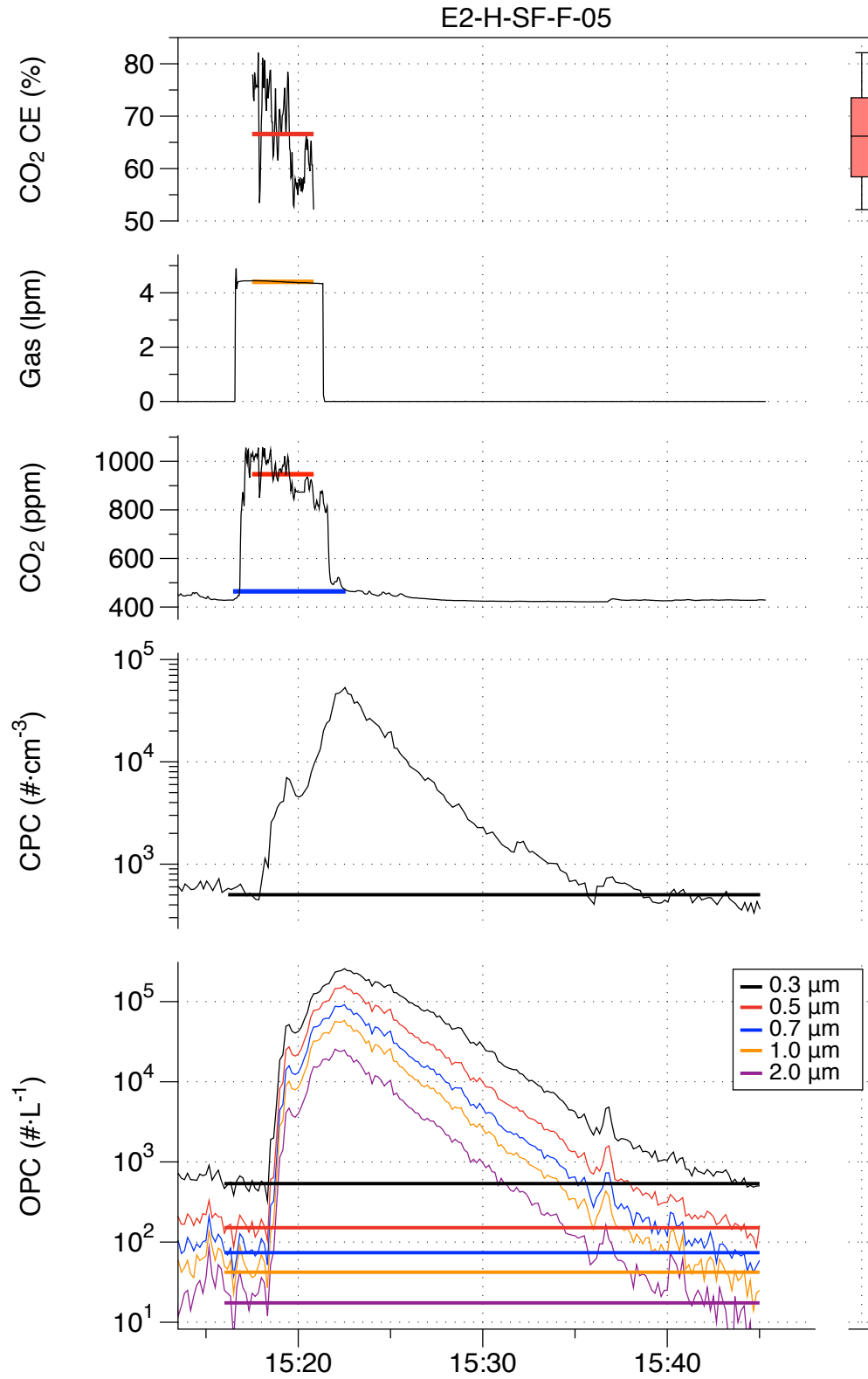


Figure F- 25. Results from experiment E2-H-SF-F-05: stir-fry on front burner, Hood E2 on high speed.

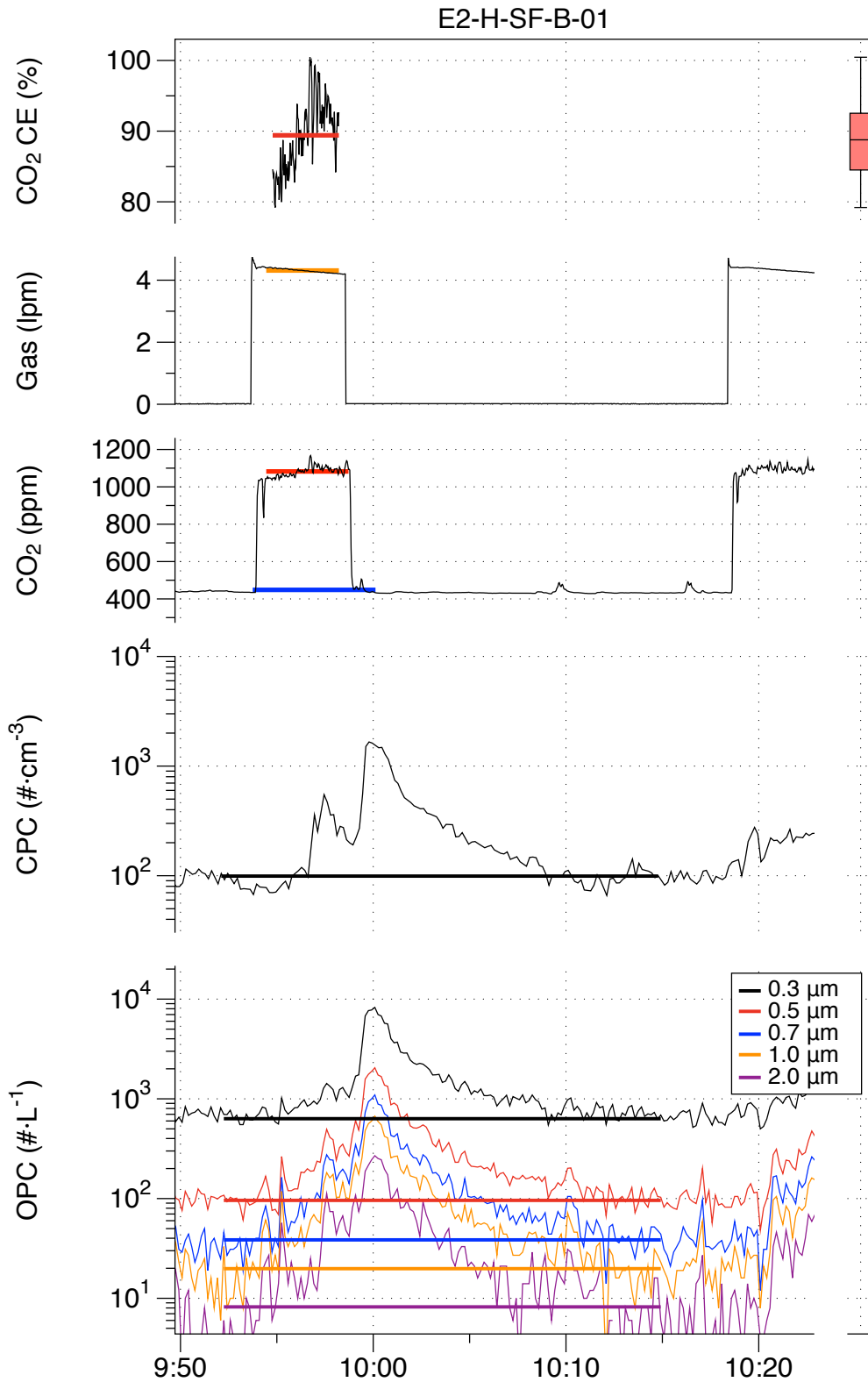


Figure F- 26. Results from experiment E2-H-SF-B-01: stir-fry on back burner, Hood E2 on high speed.

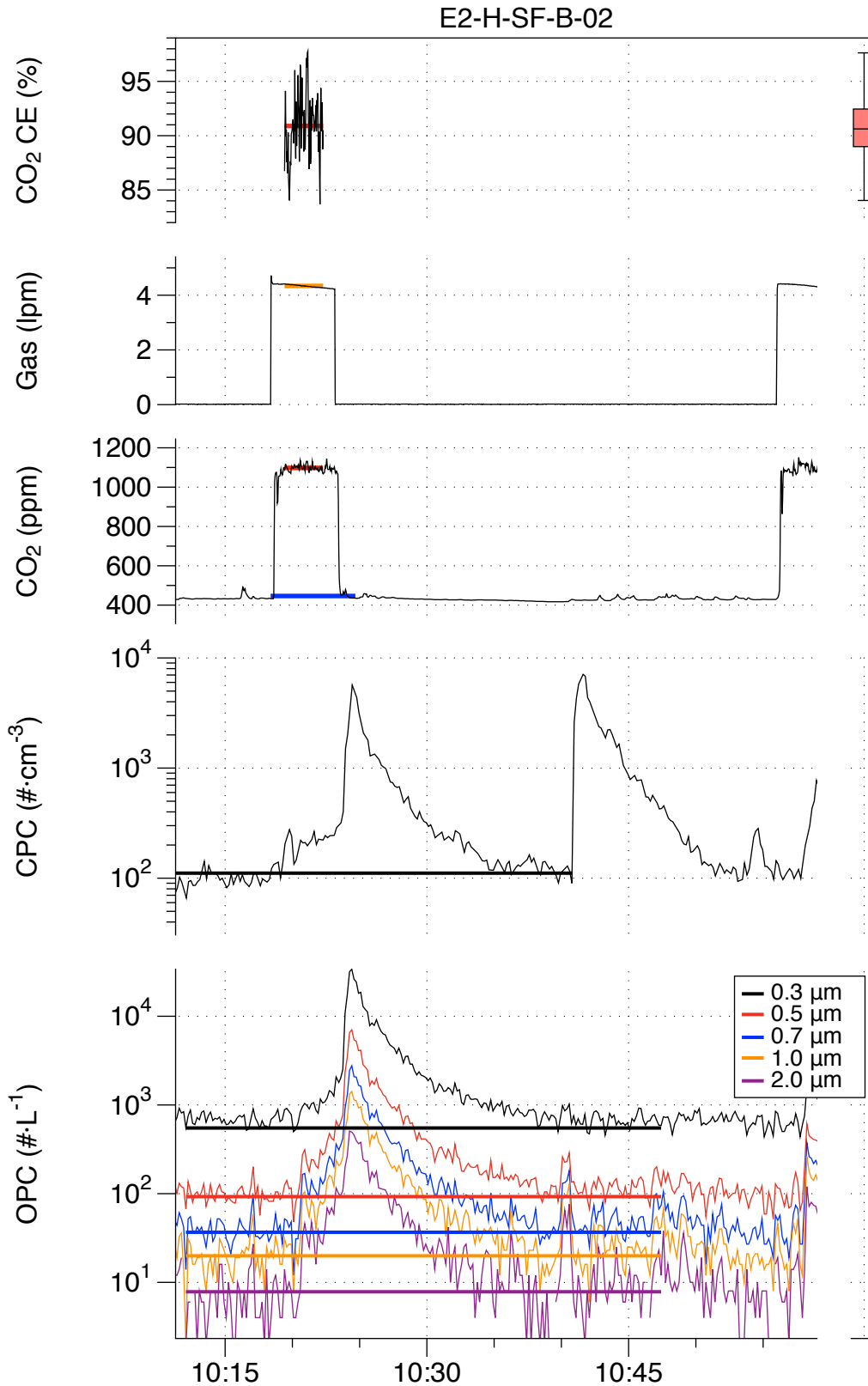


Figure F- 27. Results from experiment E2-H-SF-B-02: stir-fry on back burner, Hood E2 on high speed.

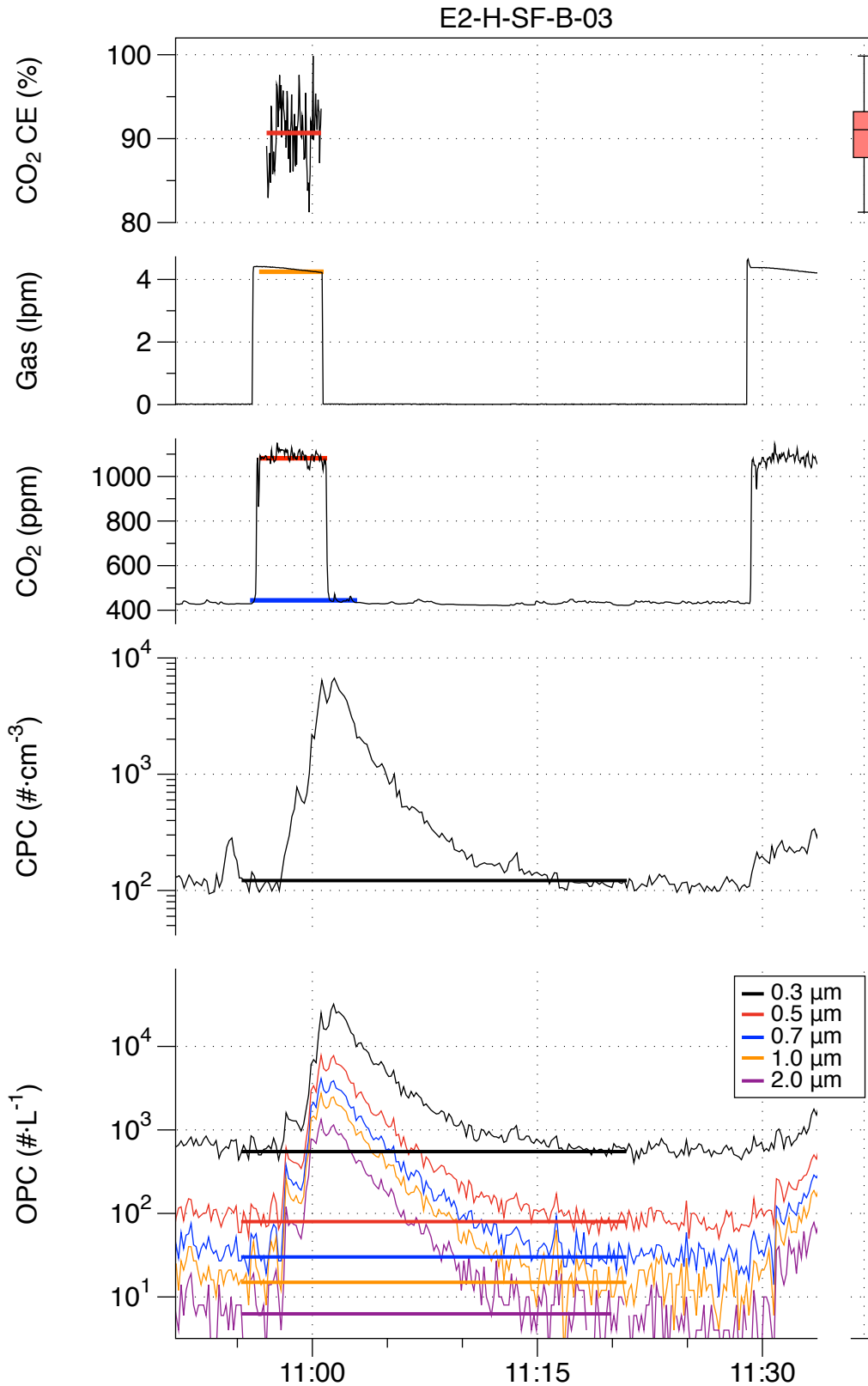


Figure F- 28. Results from experiment E2-H-SF-B-03: stir-fry on back burner, Hood E2 on high speed.

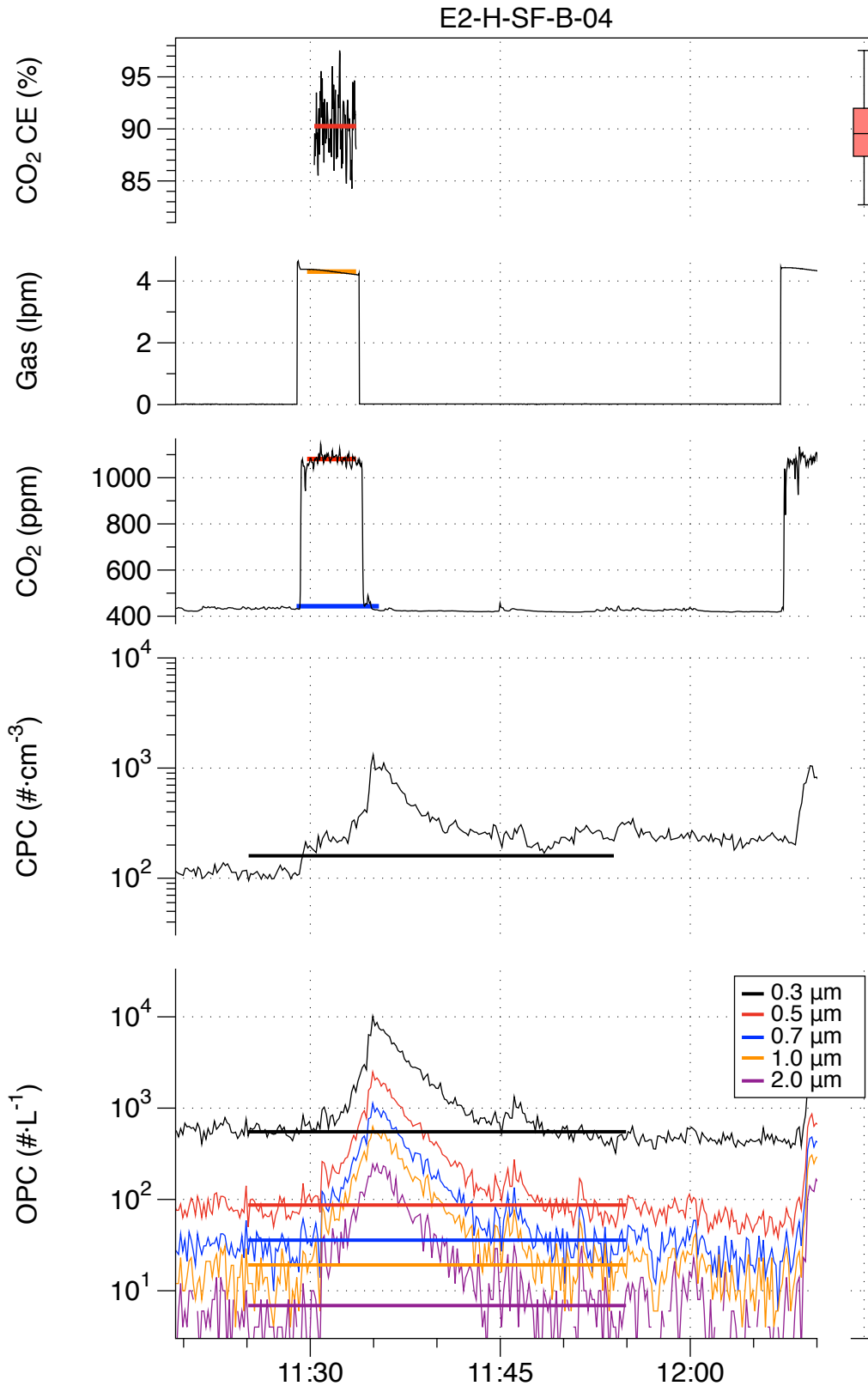
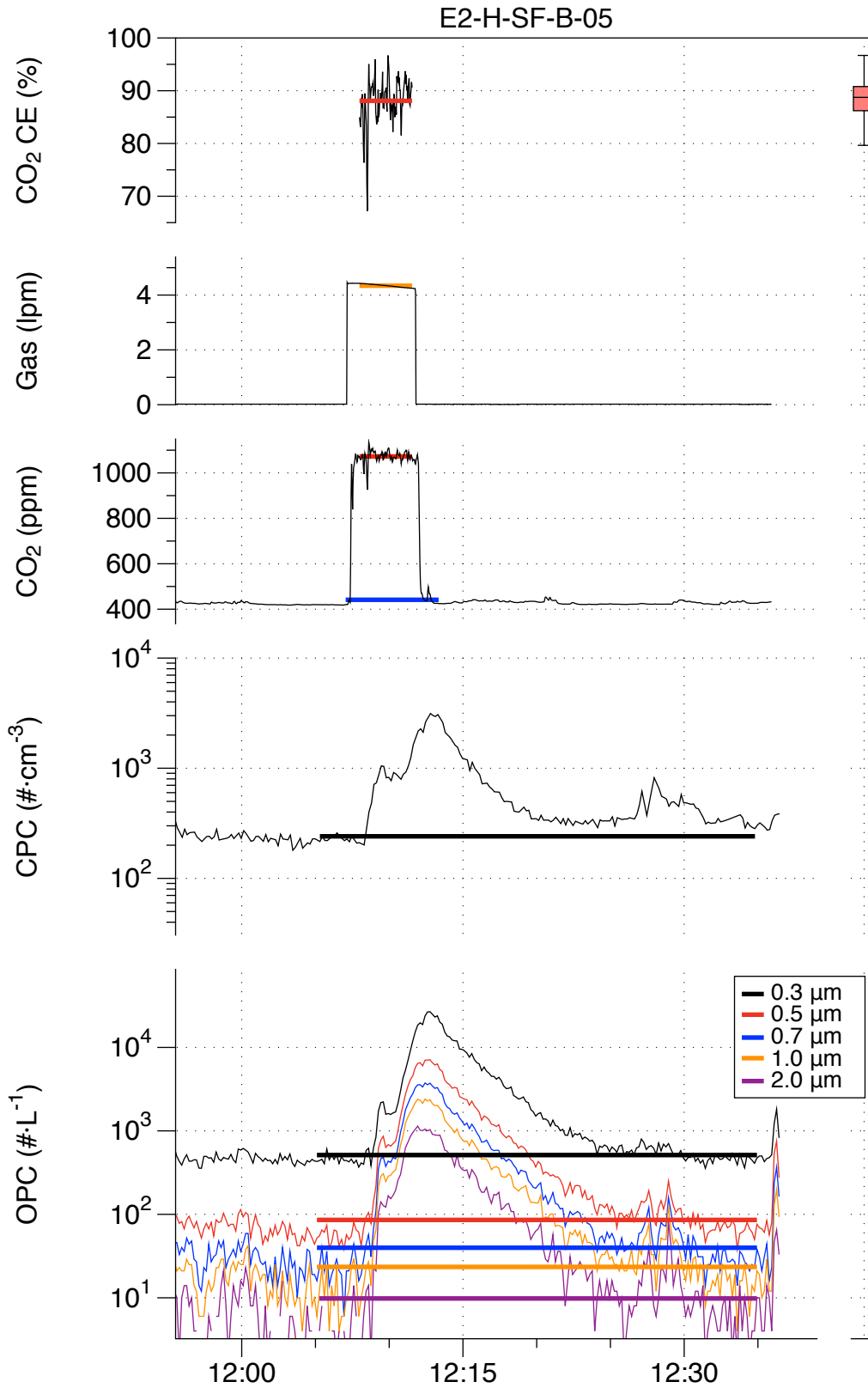


Figure F- 29. Results from experiment E2-H-SF-B-04: stir-fry on back burner, Hood E2 on high speed.



Appendix G: Results of Experiments Conducted with Hood M1

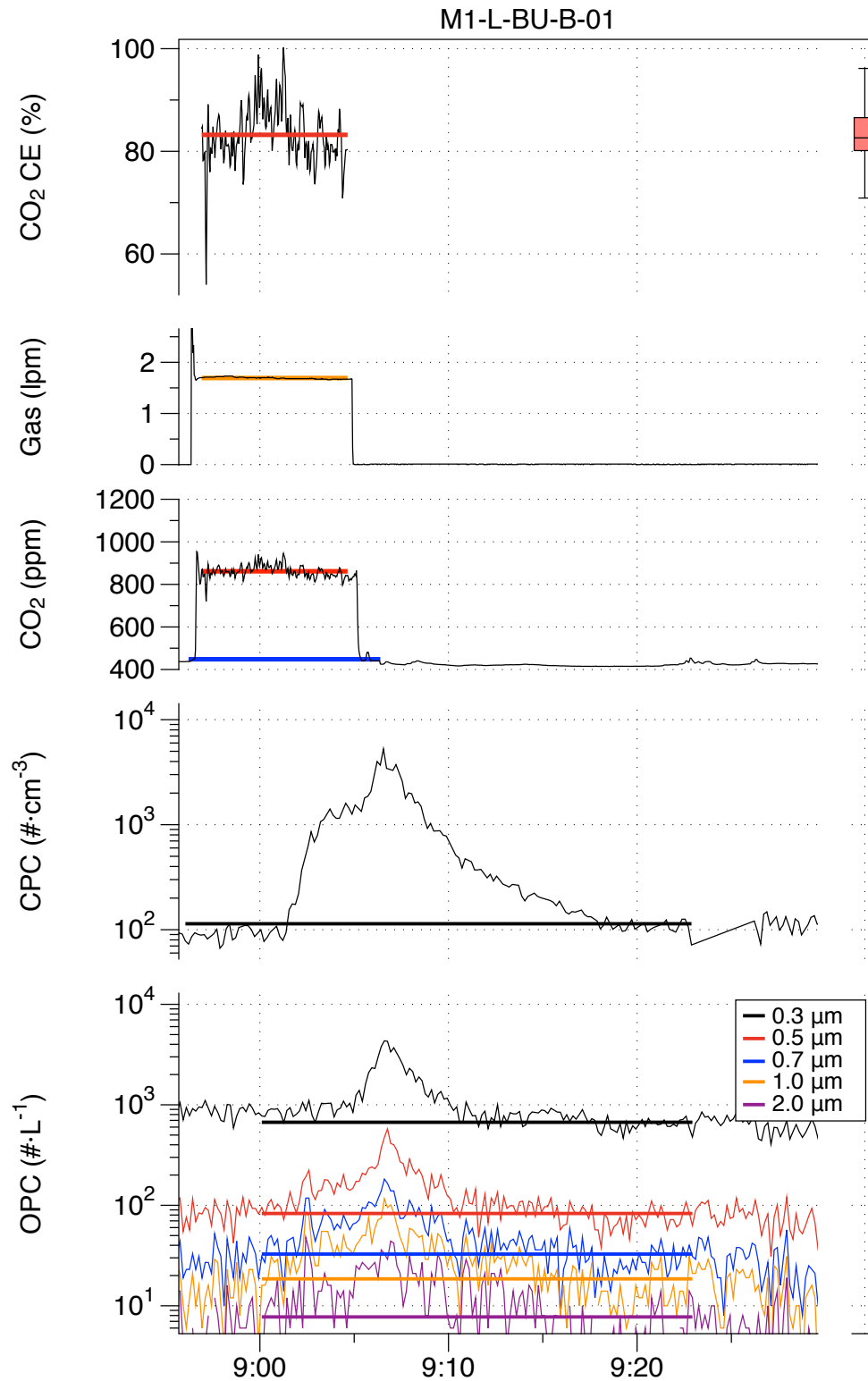


Figure G- 1. Results from experiment M1-L-BU-B-01: burger on back burner, Hood M1 on low speed.

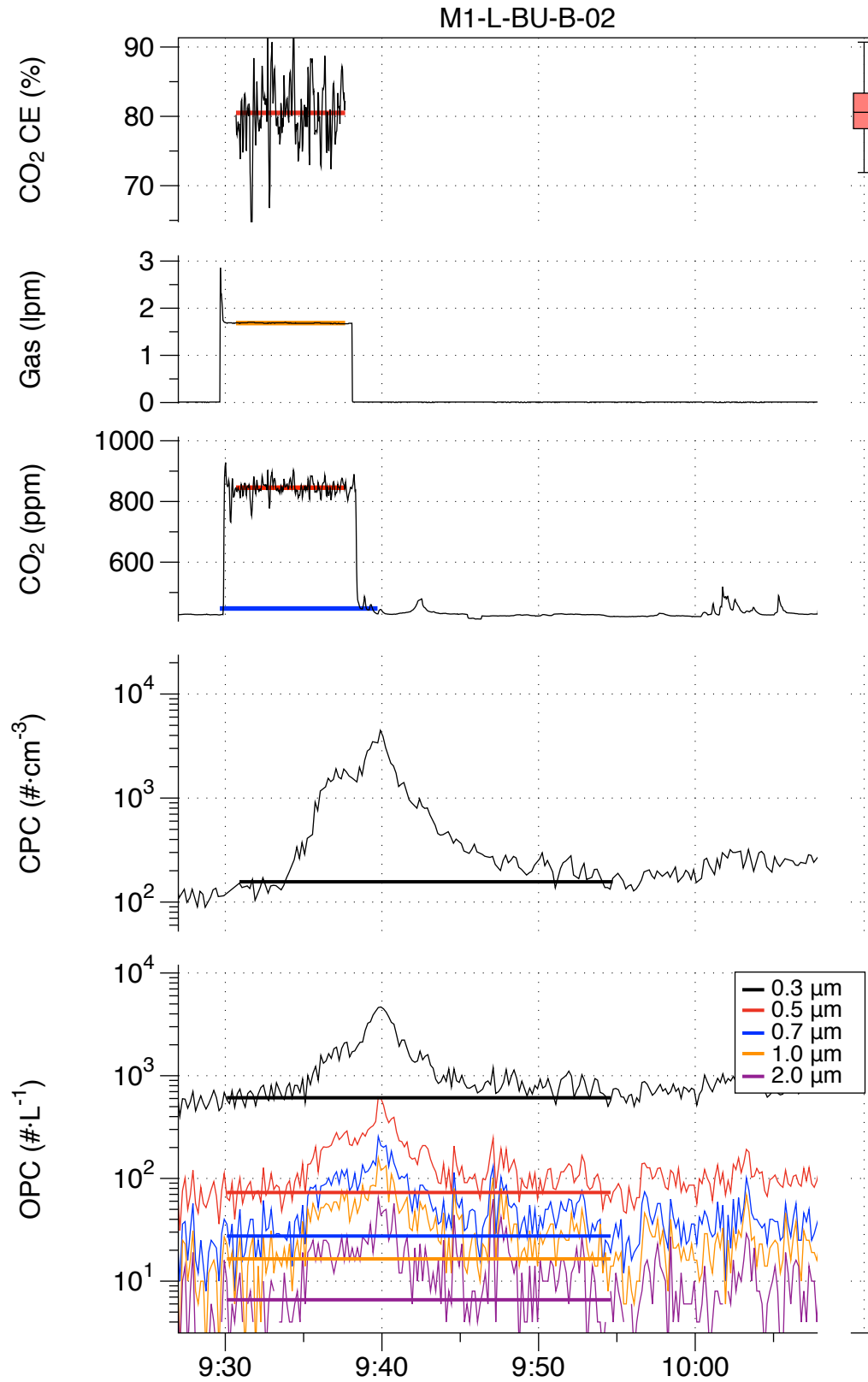


Figure G- 2. Results from experiment M1-L-BU-B-02: burger on back burner, Hood M1 on low speed.

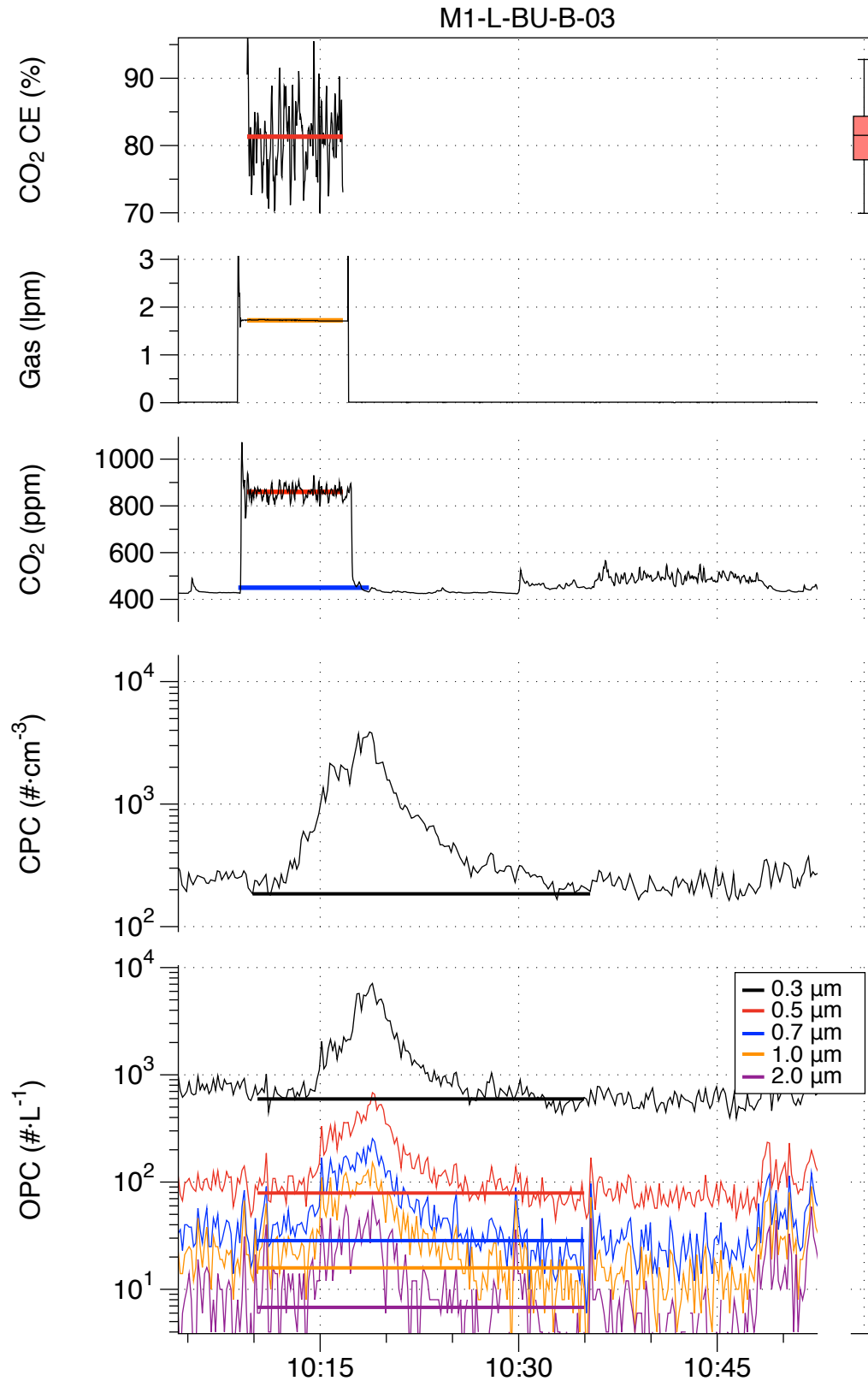


Figure G- 3. Results from experiment M1-L-BU-B-03: burger on back burner, Hood M1 on low speed.

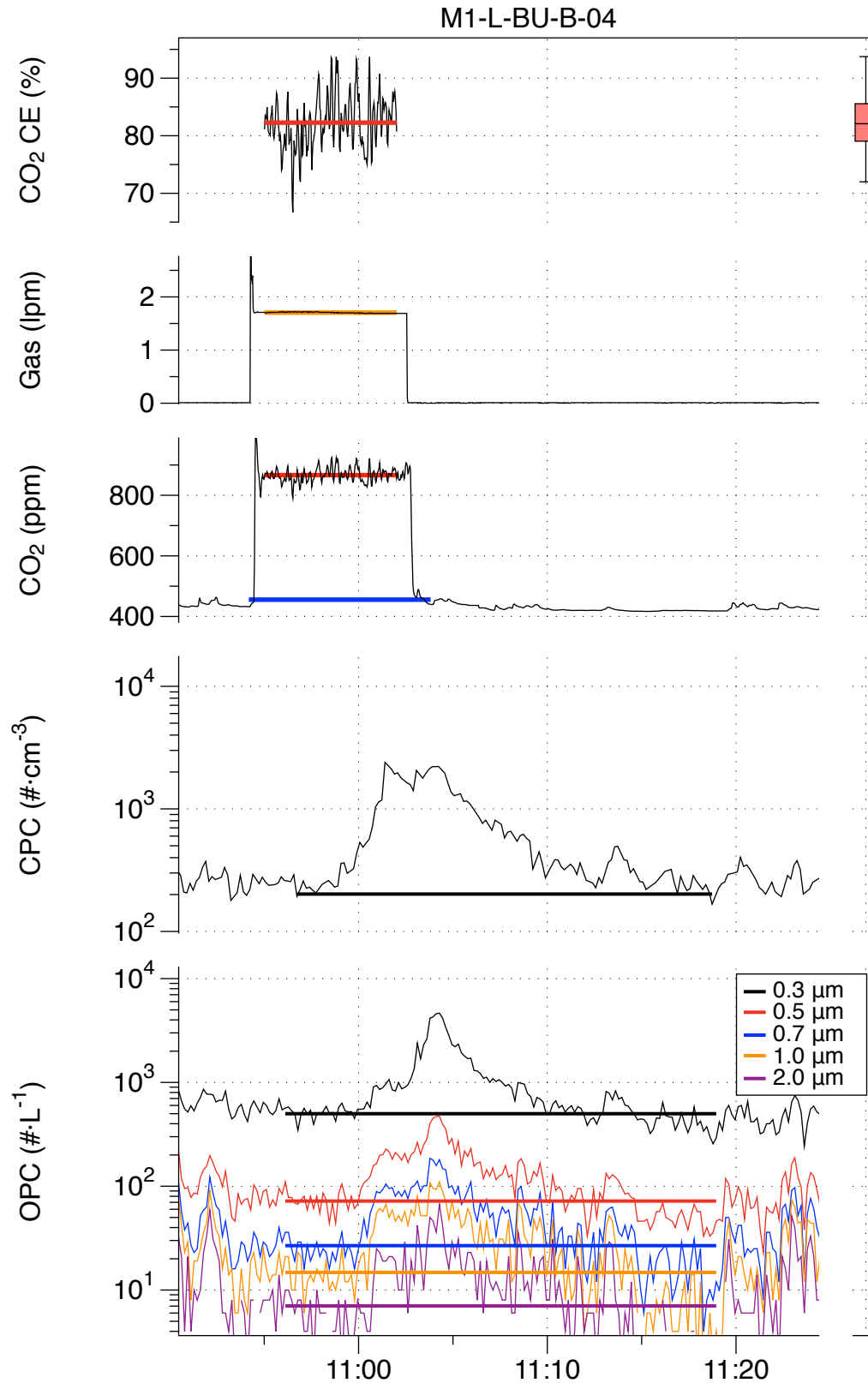


Figure G- 4. Results from experiment M1-L-BU-B-04: burger on back burner, Hood M1 on low speed.

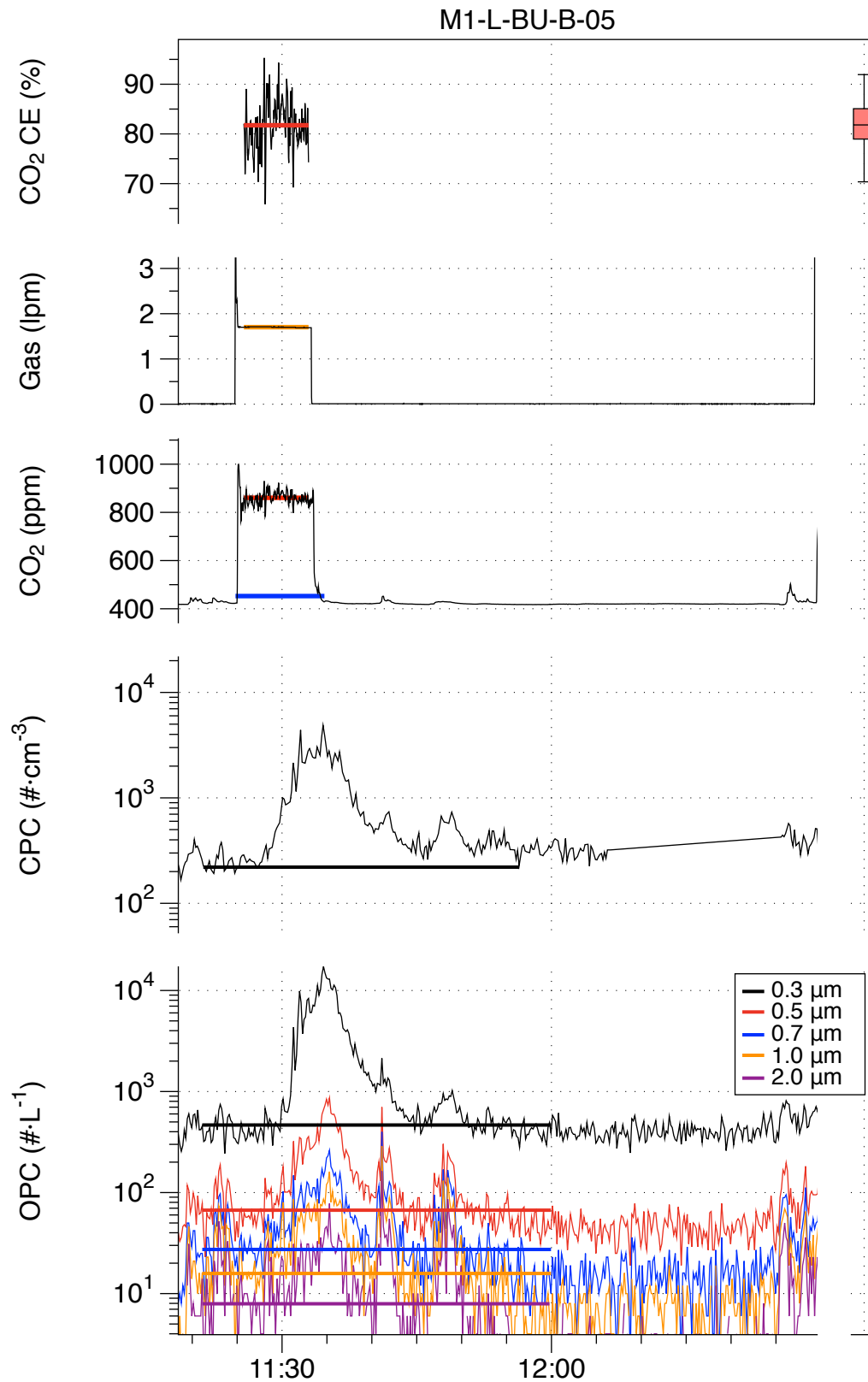


Figure G- 5. Results from experiment M1-L-BU-B-05: burger on back burner, Hood M1 on low speed.

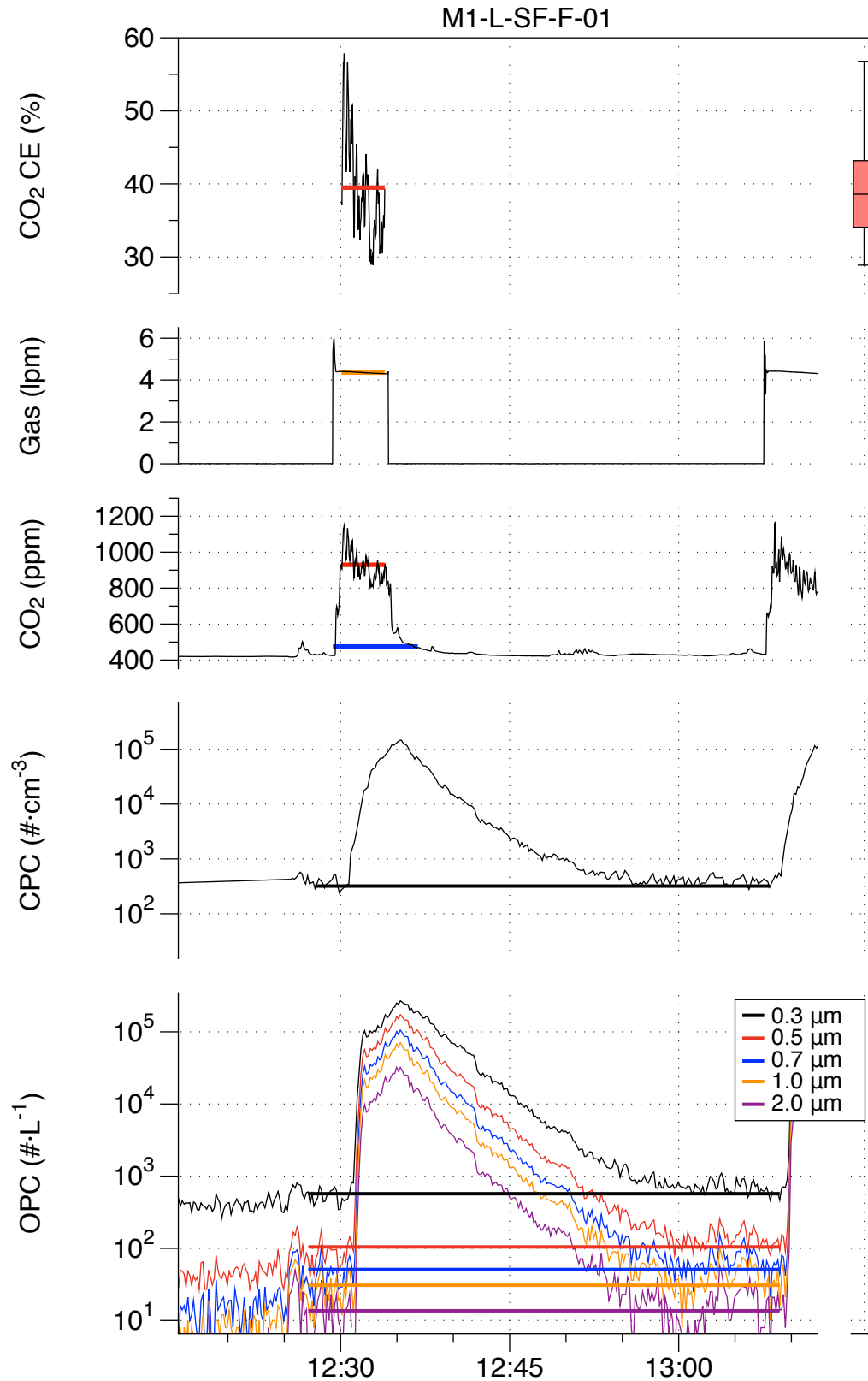


Figure G- 6. Results from experiment M1-L-SF-F-01: stir fry on front burner, Hood M1 on low speed.

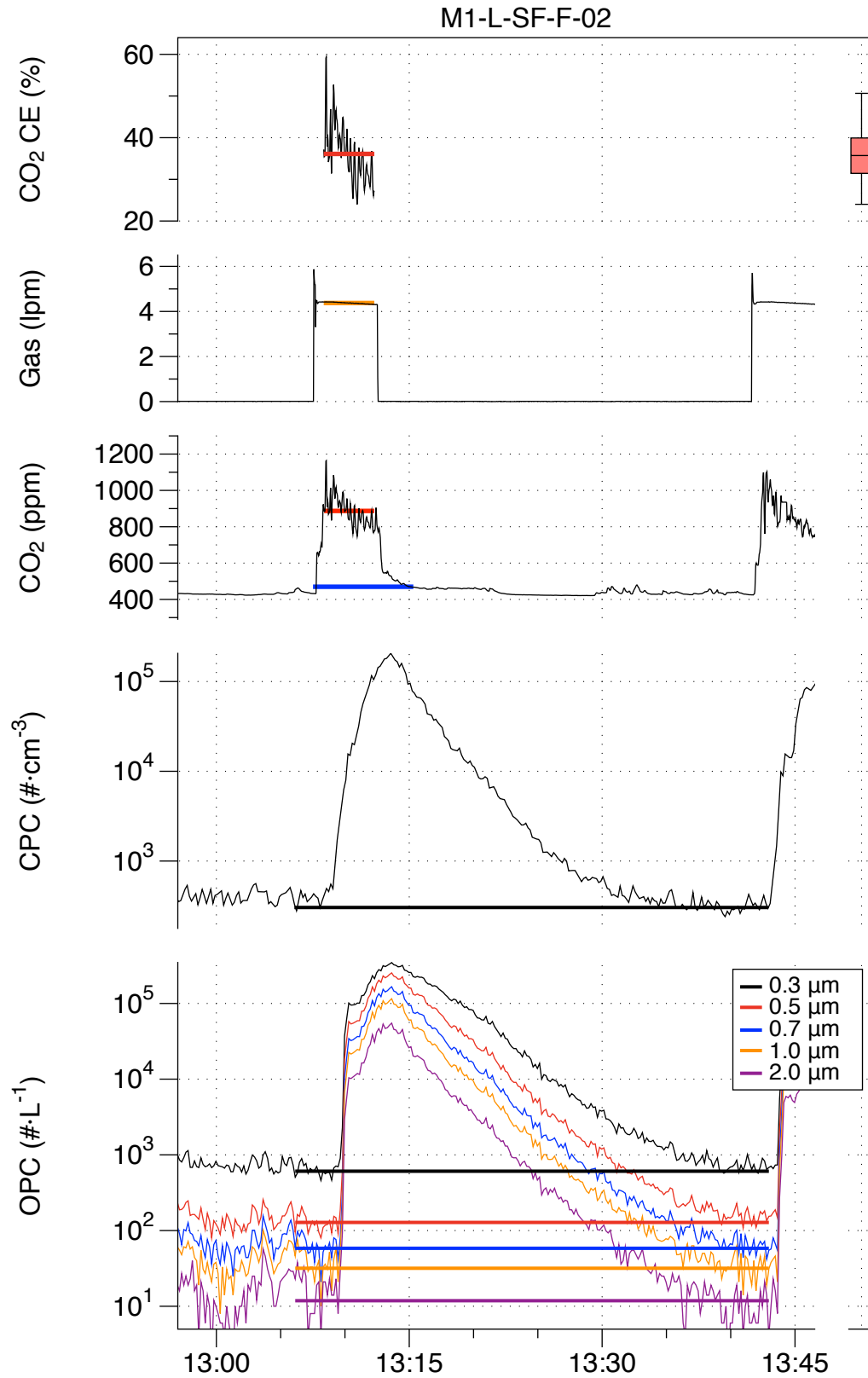


Figure G- 7. Results from experiment M1-L-SF-F-02: stir fry on front burner, Hood M1 on low speed.

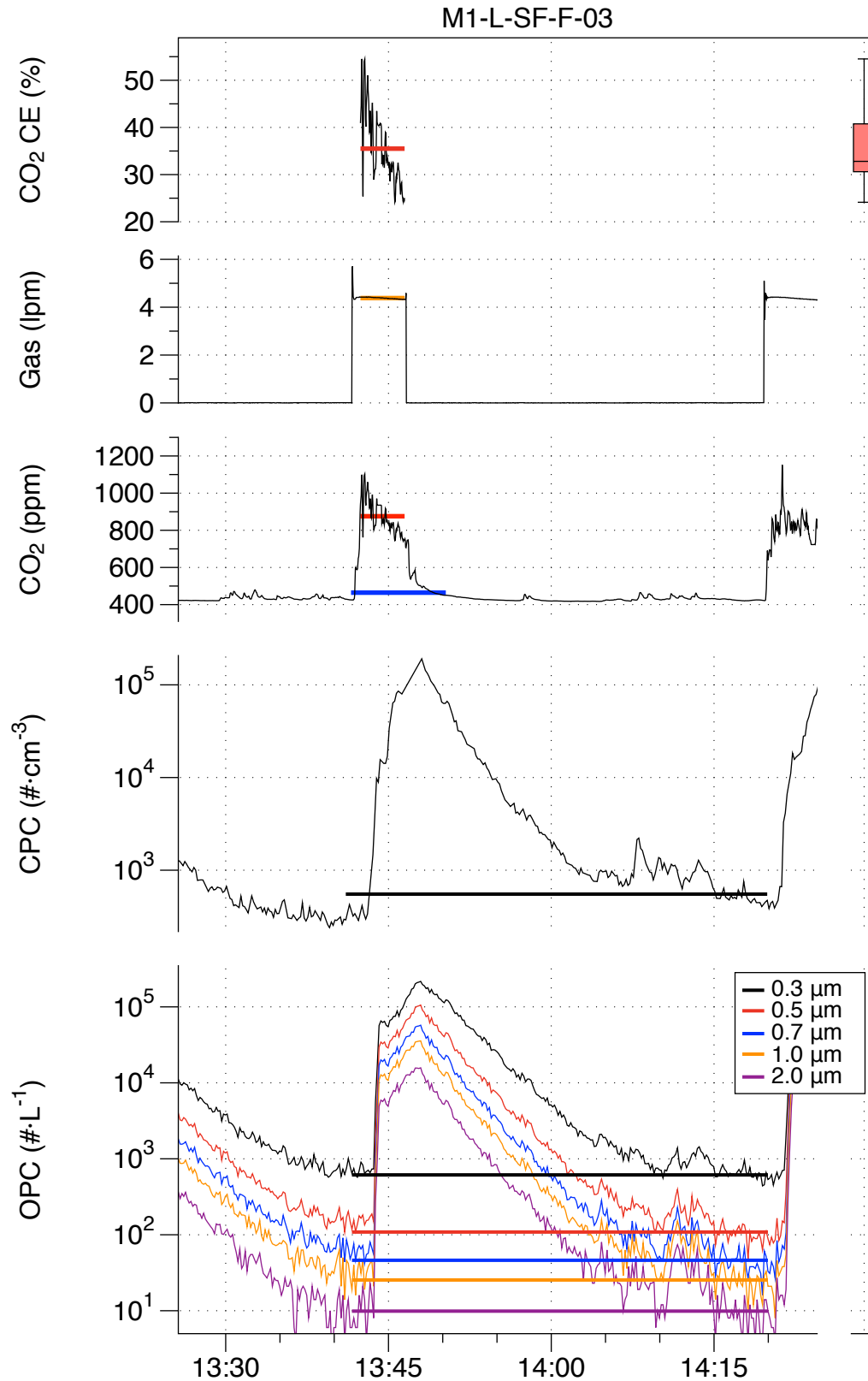


Figure G- 8. Results from experiment M1-L-SF-F-03: stir fry on front burner, Hood M1 on low speed.

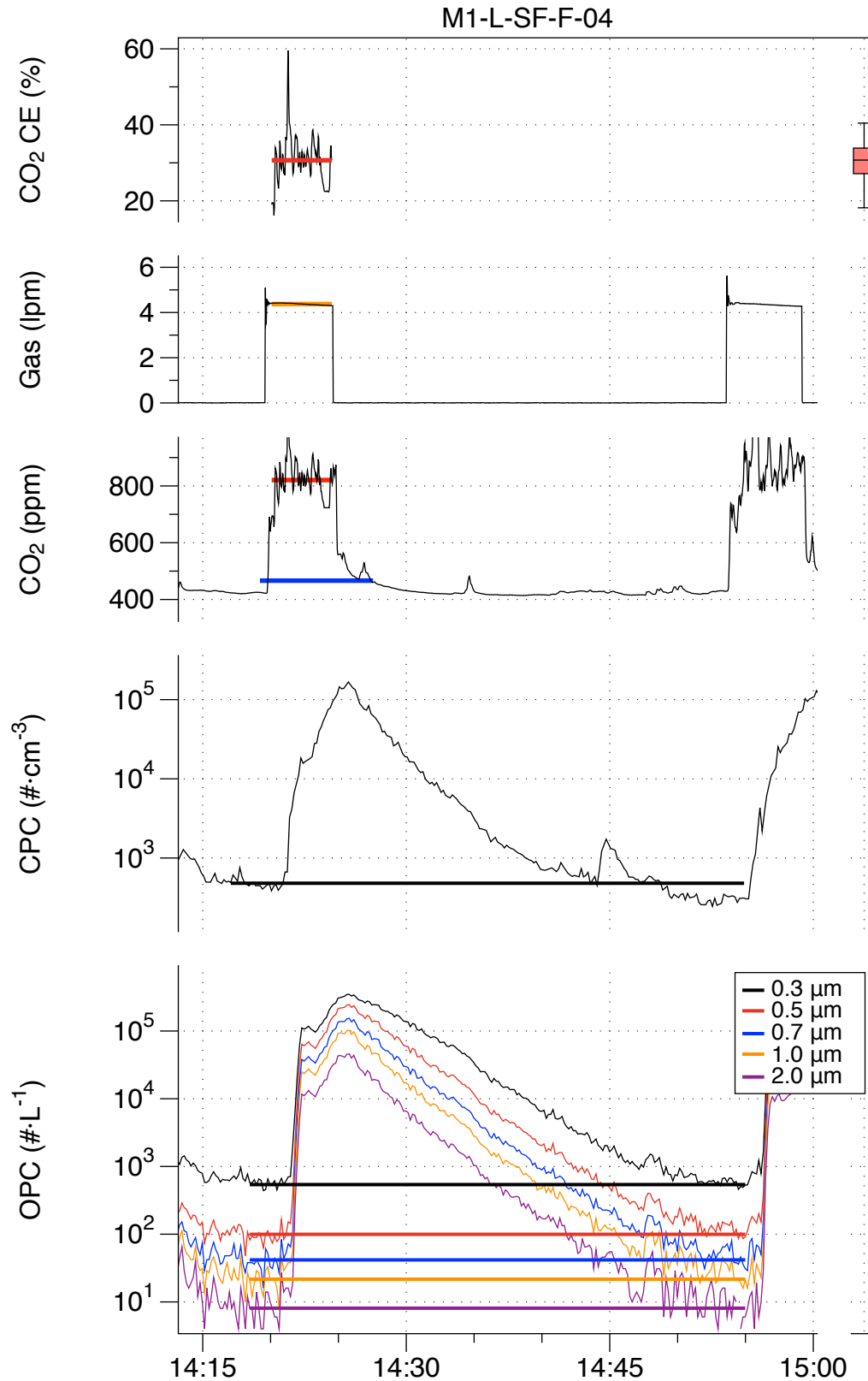


Figure G- 9. Results from experiment M1-L-SF-F-04: stir fry on front burner, Hood M1 on low speed.

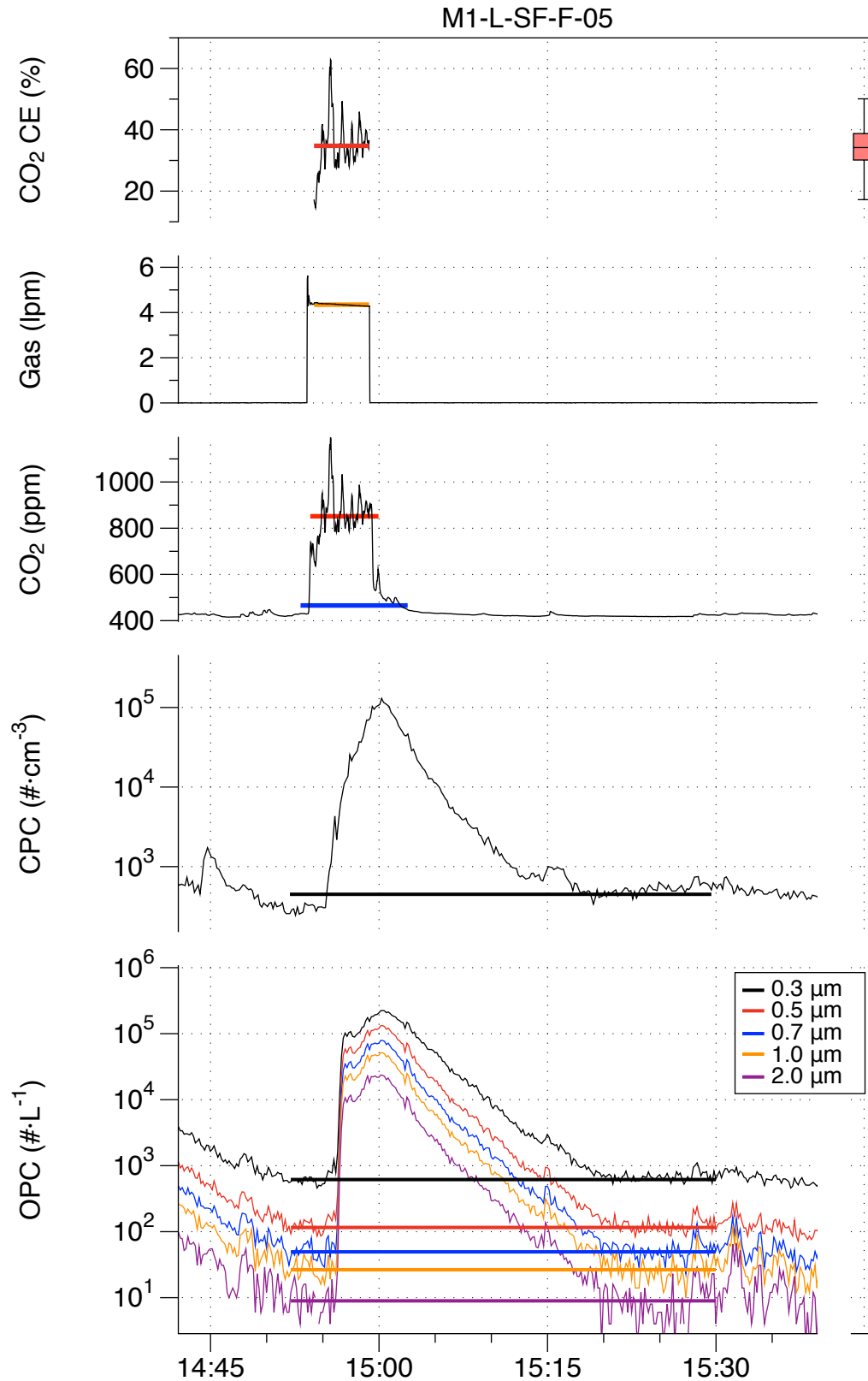


Figure G- 10. Results from experiment M1-L-SF-F-05: stir fry on front burner, Hood M1 on low speed.

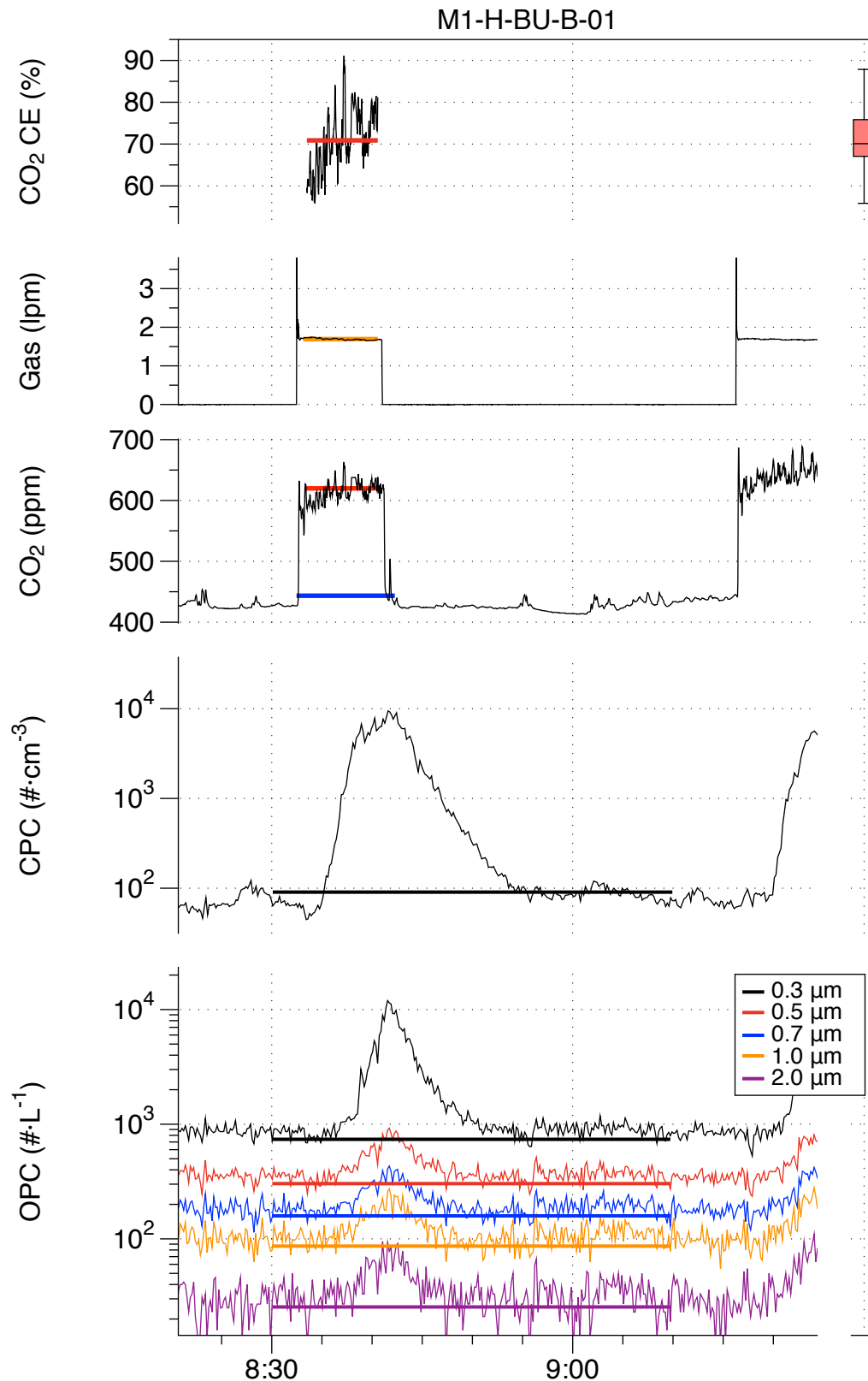


Figure G- 11. Results from experiment M1-H-BU-B-01: burger on back burner, Hood M1 on high speed.

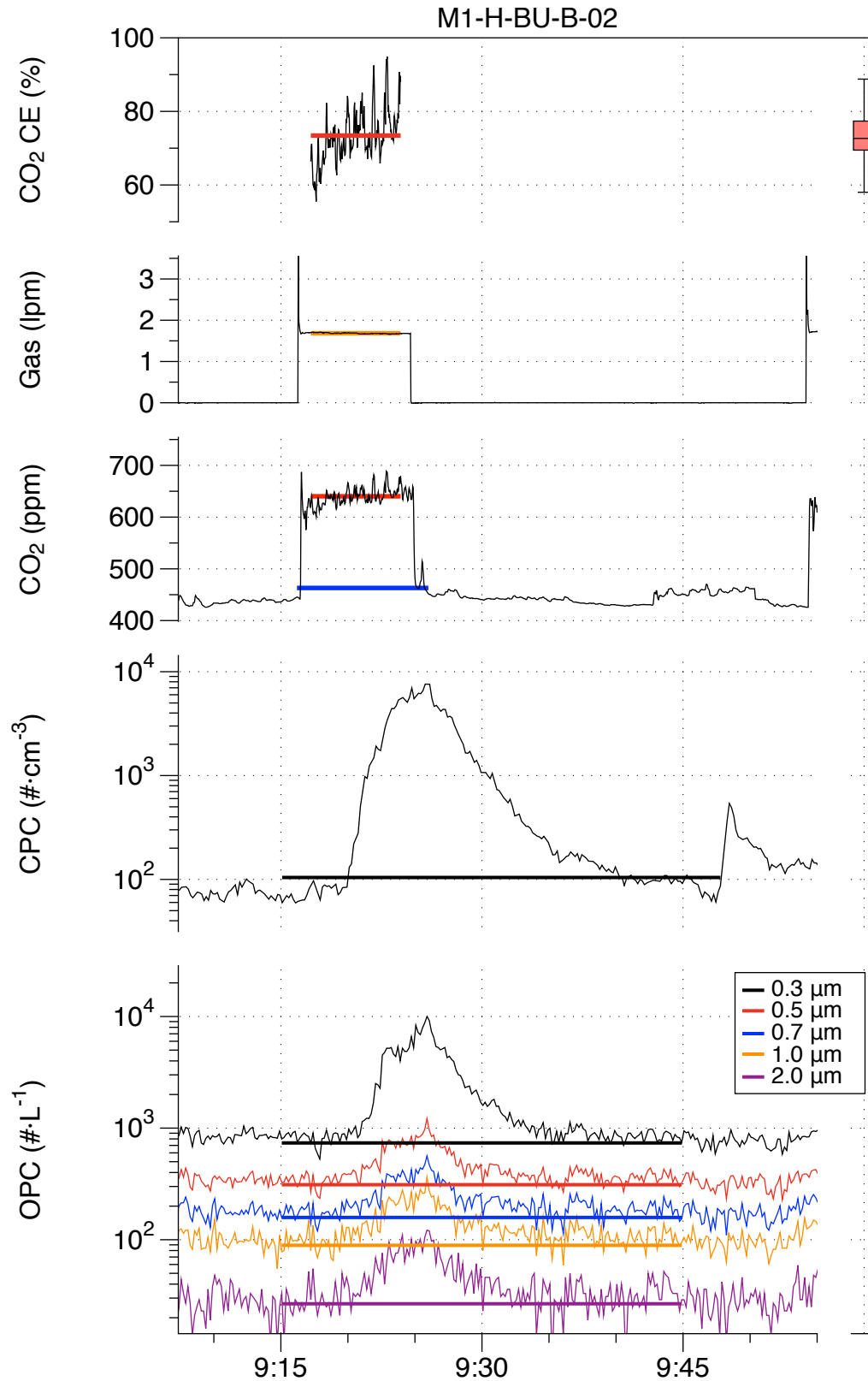


Figure G- 12. Results from experiment M1-H-BU-B-02: burger on back burner, Hood M1 on high speed.

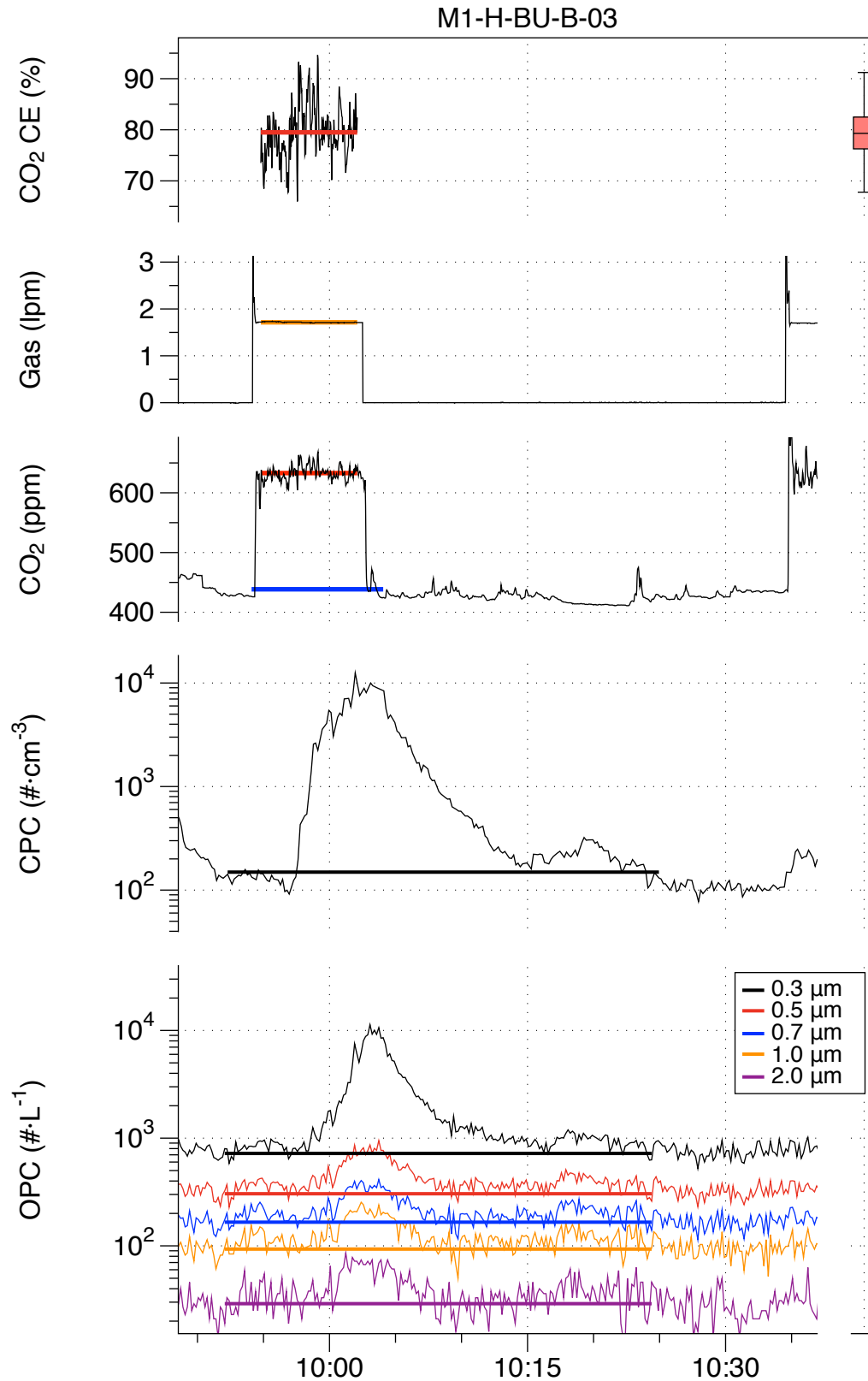


Figure G- 13. Results from experiment M1-H-BU-B-03: burger on back burner, Hood M1 on high speed.

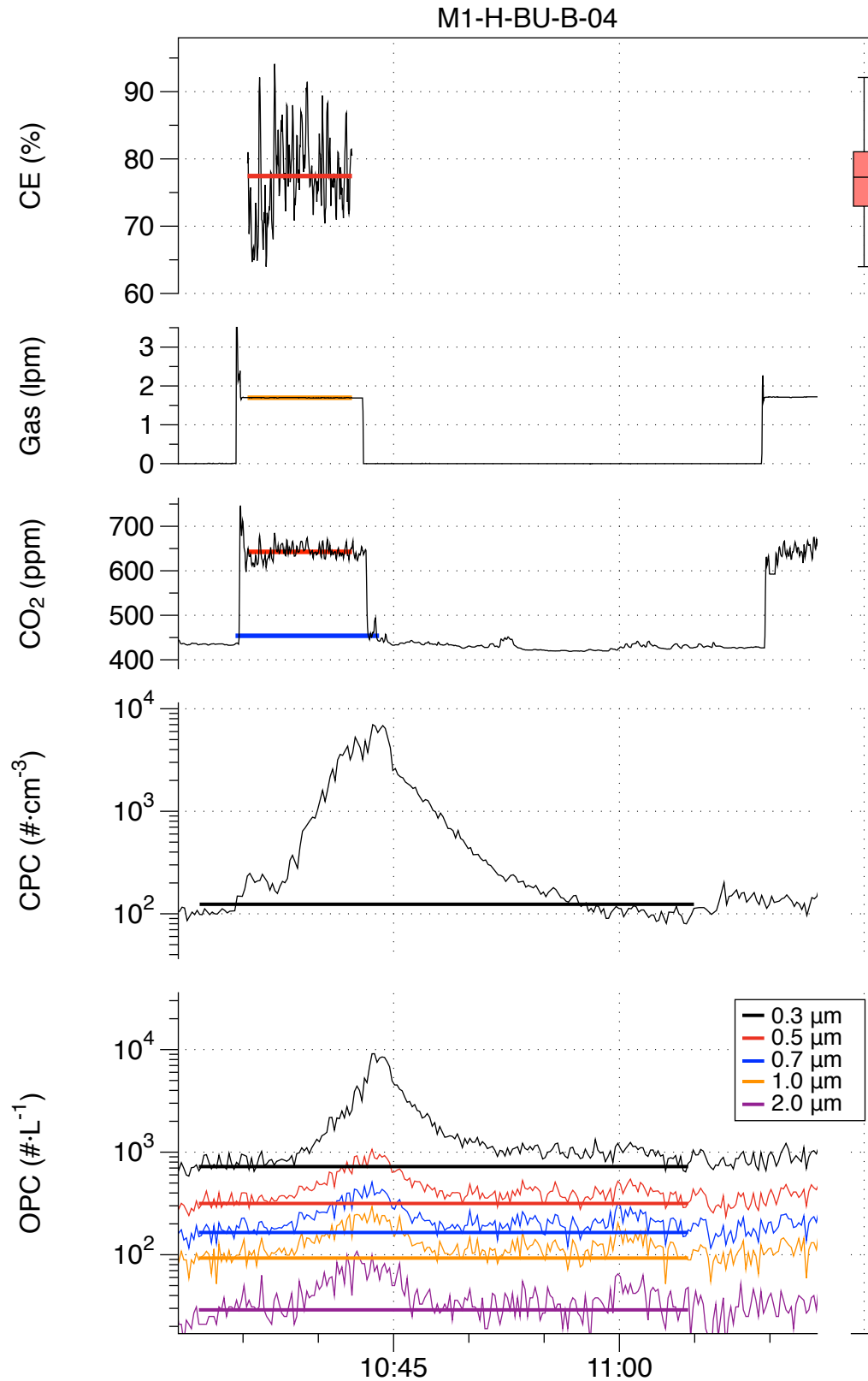


Figure G- 14. Results from experiment M1-H-BU-B-04: burger on back burner, Hood M1 on high speed.

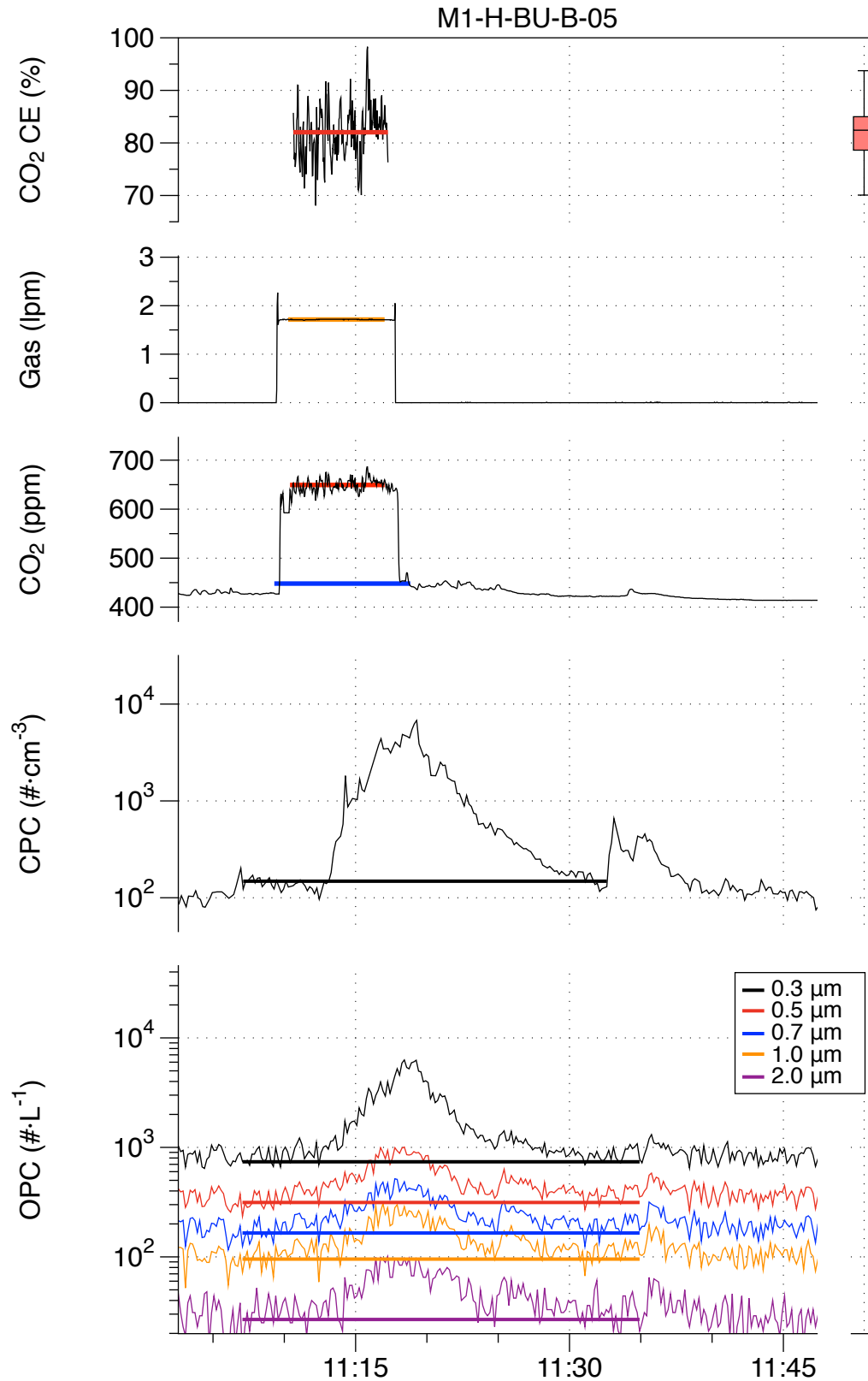


Figure G- 15. Results from experiment M1-H-BU-B-05: burger on back burner, Hood M1 on high speed.

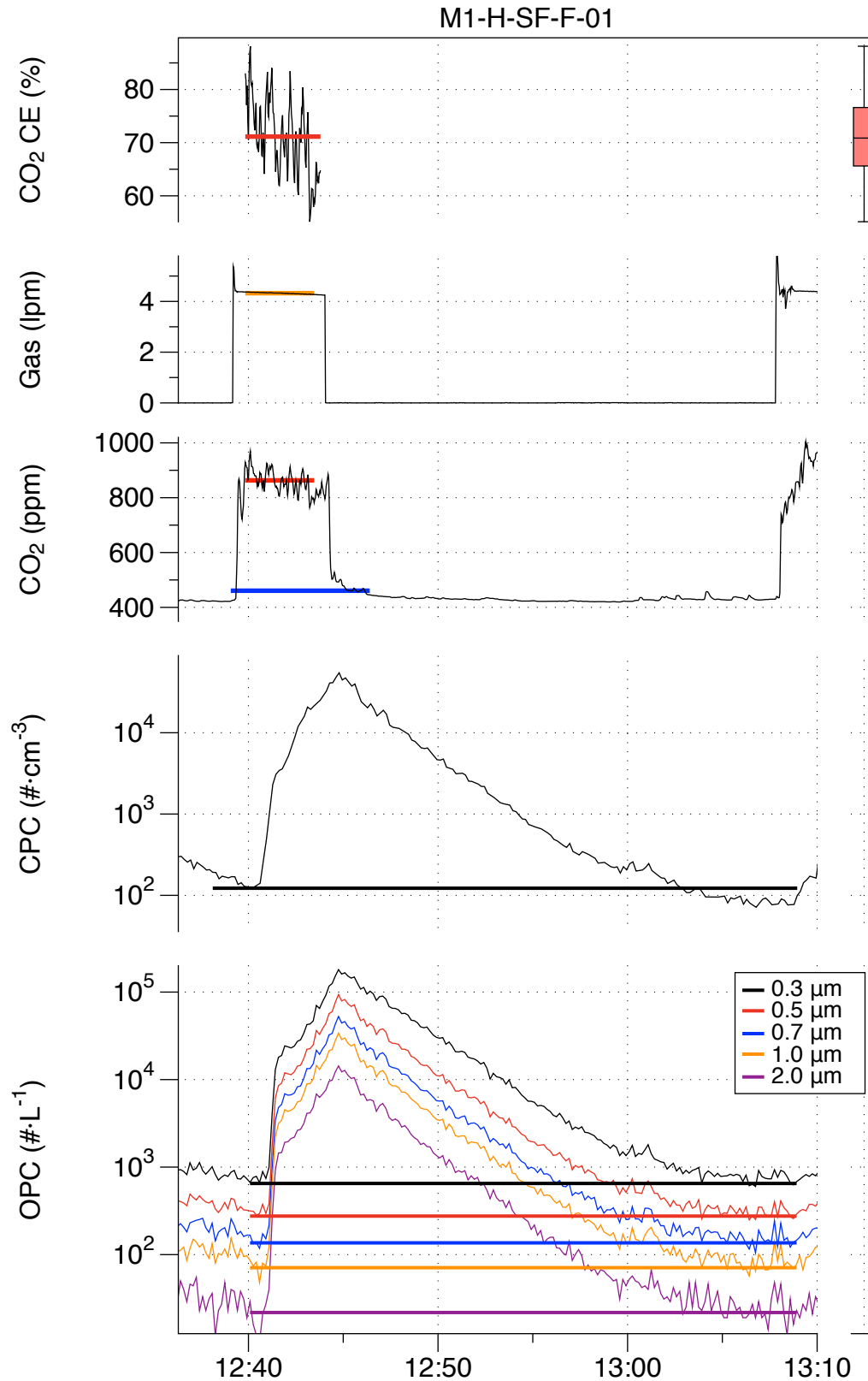


Figure G- 16. Results from experiment M1-H-SF-F-01: stir fry on front burner, Hood M1 on high speed.

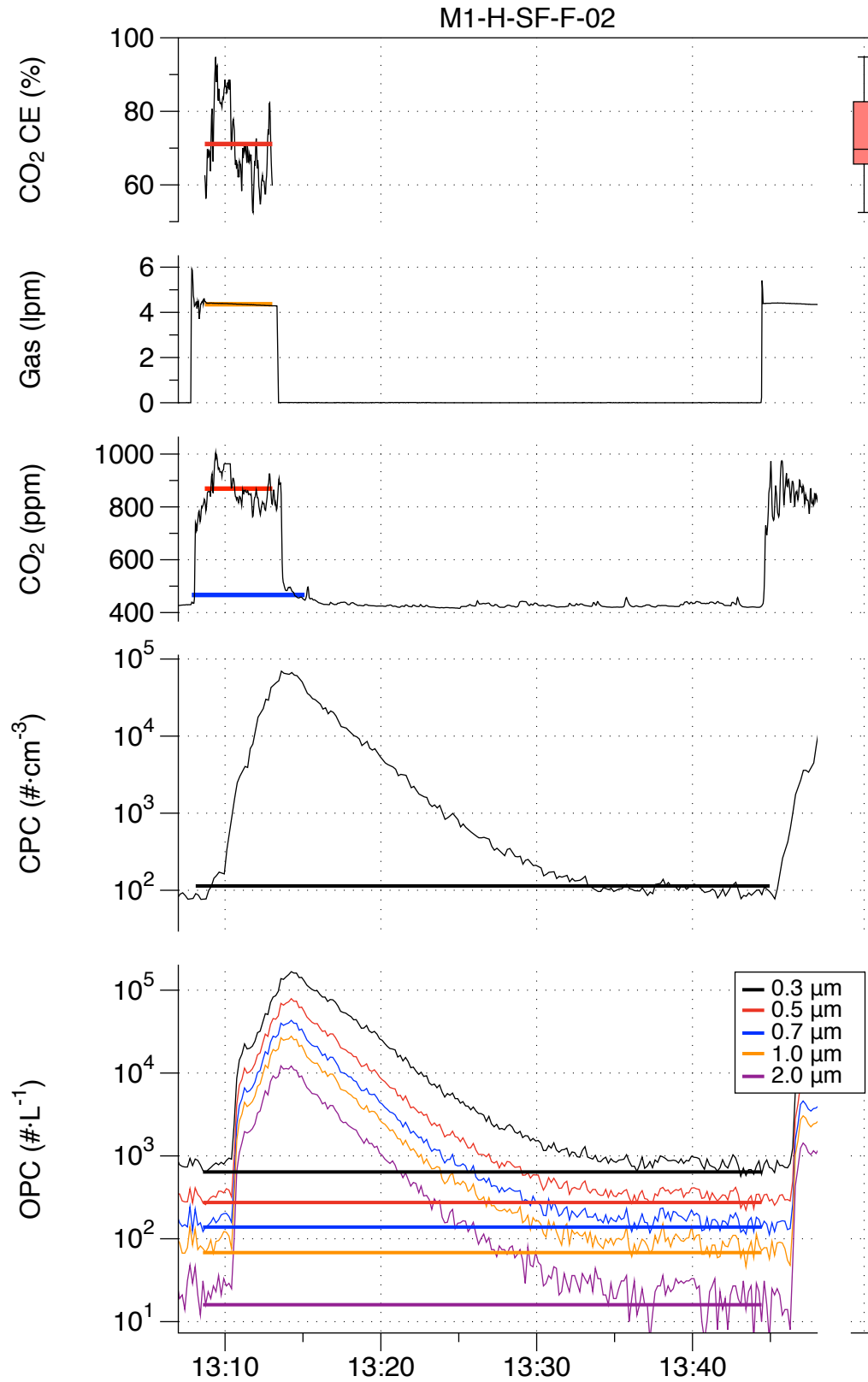


Figure G- 17. Results from experiment M1-H-SF-F-02: stir fry on front burner, Hood M1 on high speed.

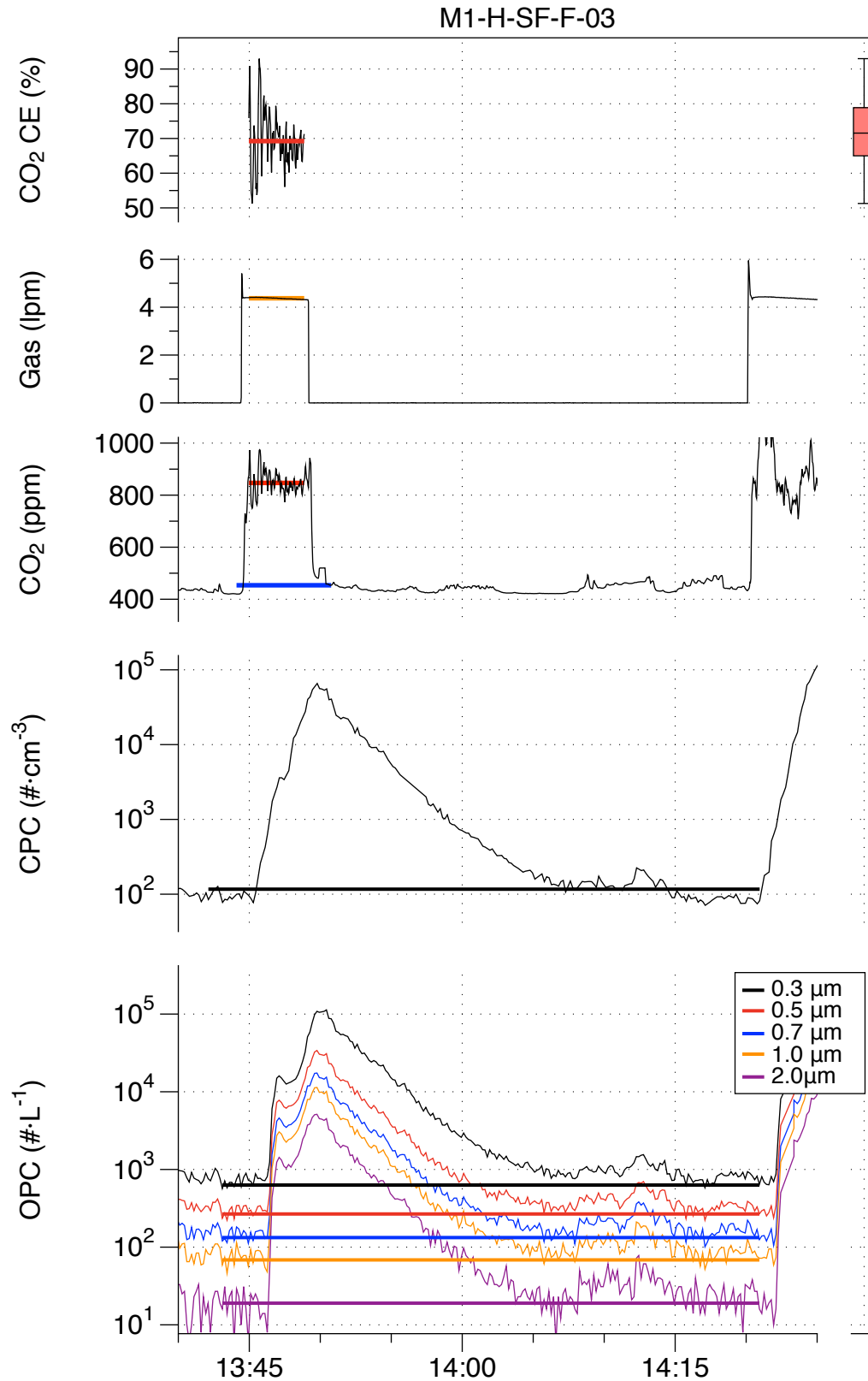


Figure G- 18. Results from experiment M1-H-SF-F-03: stir fry on front burner, Hood M1 on high speed.

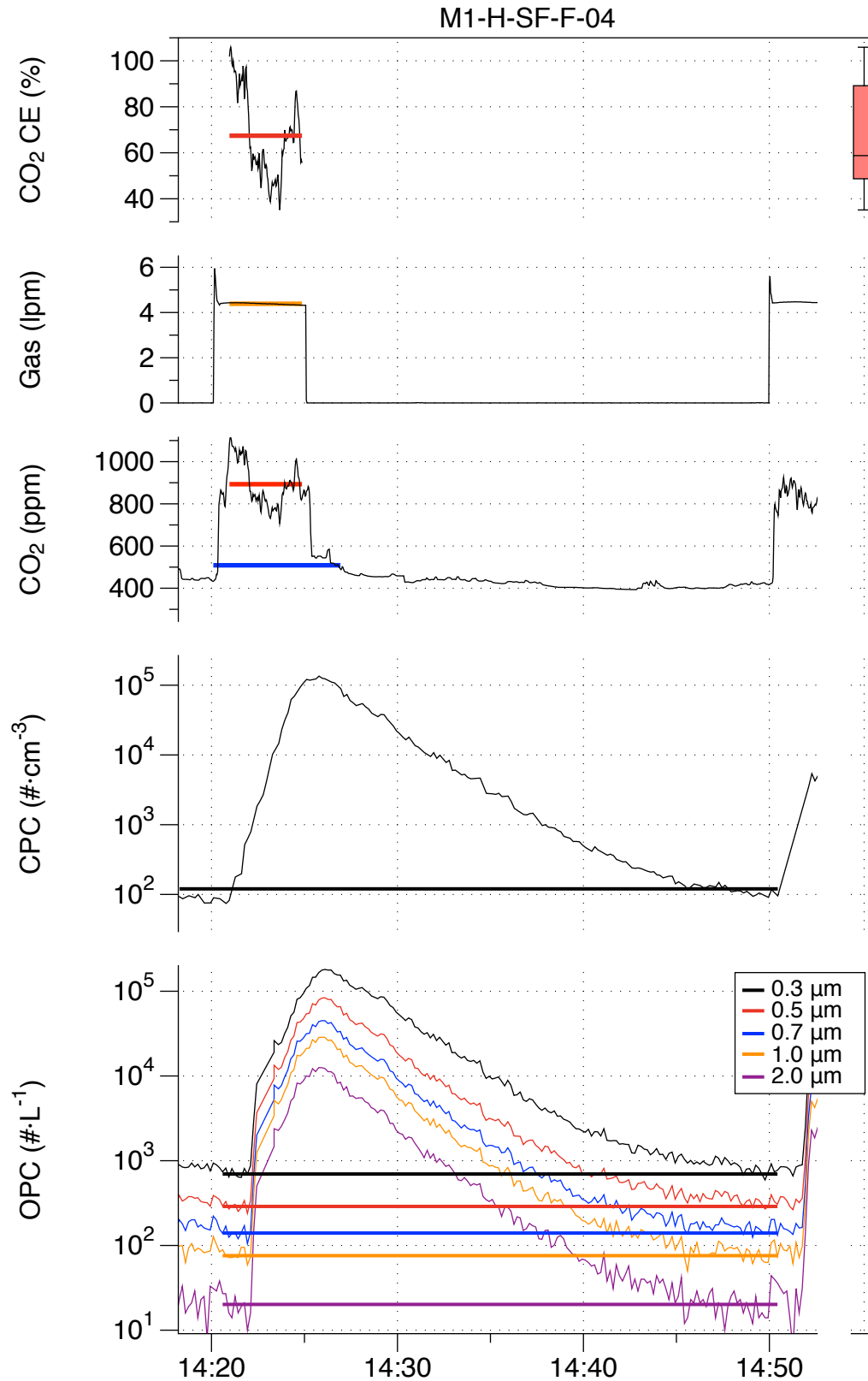


Figure G- 19. Results from experiment M1-H-SF-F-04: stir fry on front burner, Hood M1 on high speed.

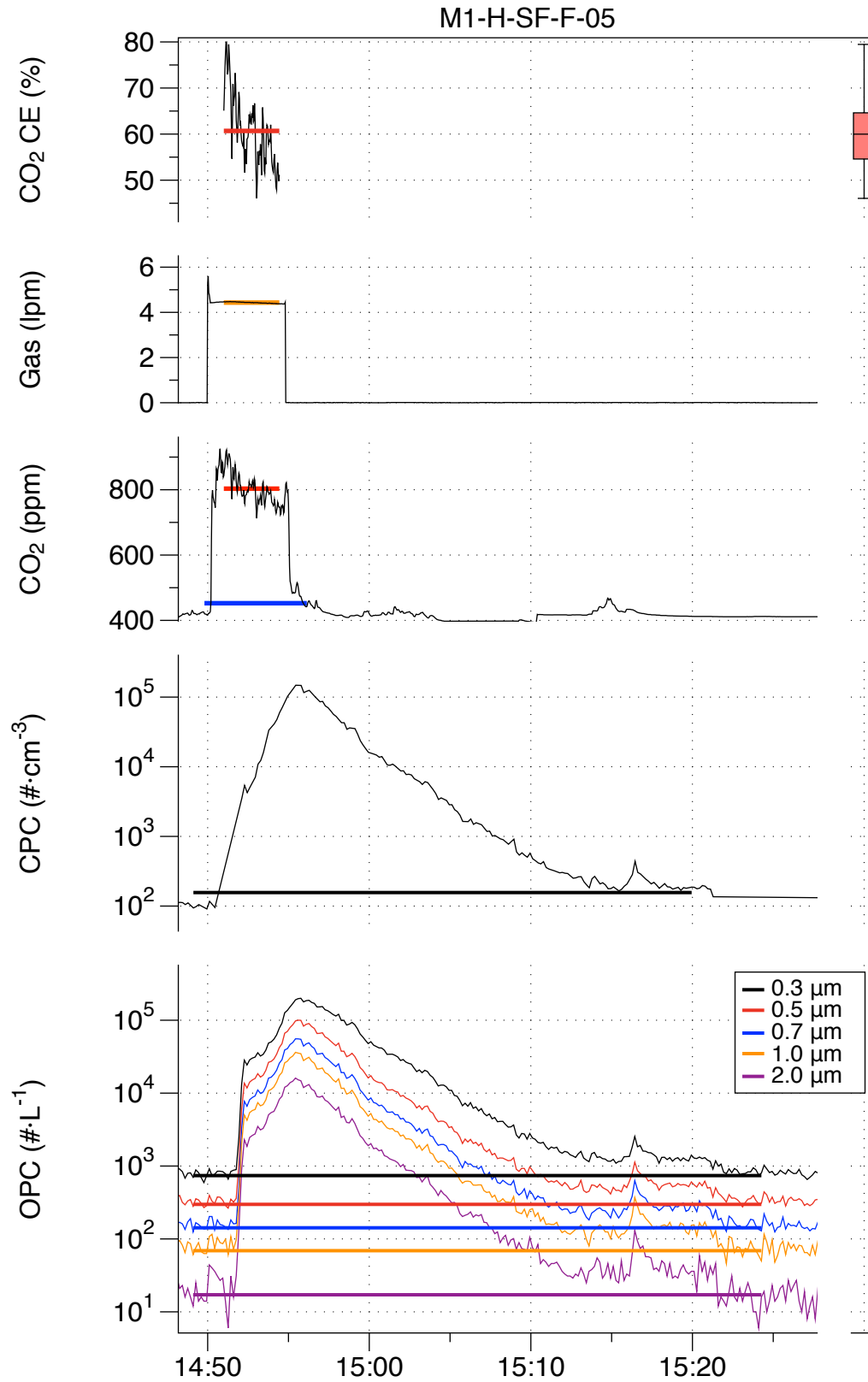


Figure G- 20. Results from experiment M1-H-SF-F-05: stir fry on front burner, Hood M1 on high speed.

Appendix H: Results of Experiments Conducted with Hood P1

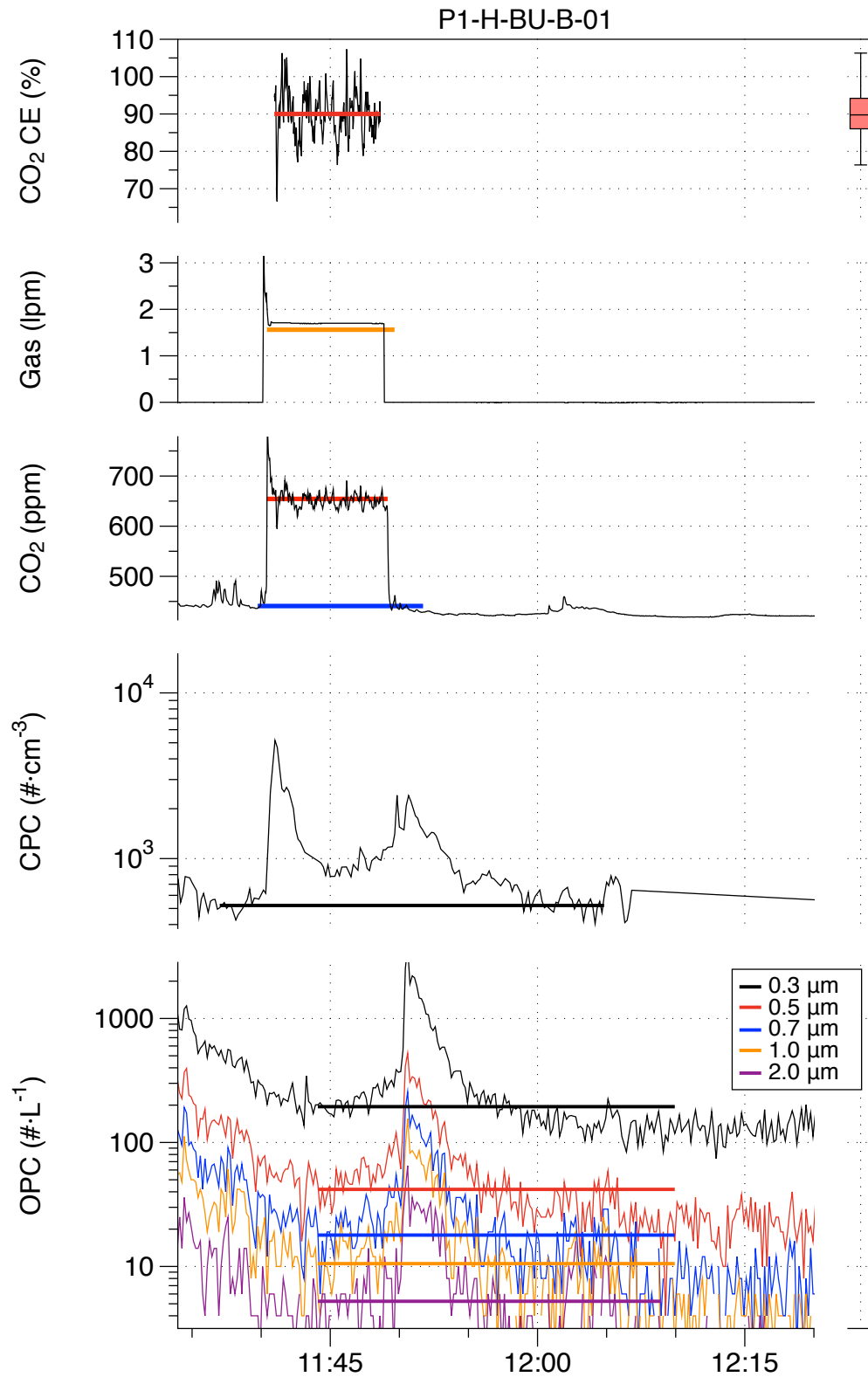


Figure H- 1. Results from experiment P1-H-BU-B-01: burger on back burner, Hood P1 on high speed.

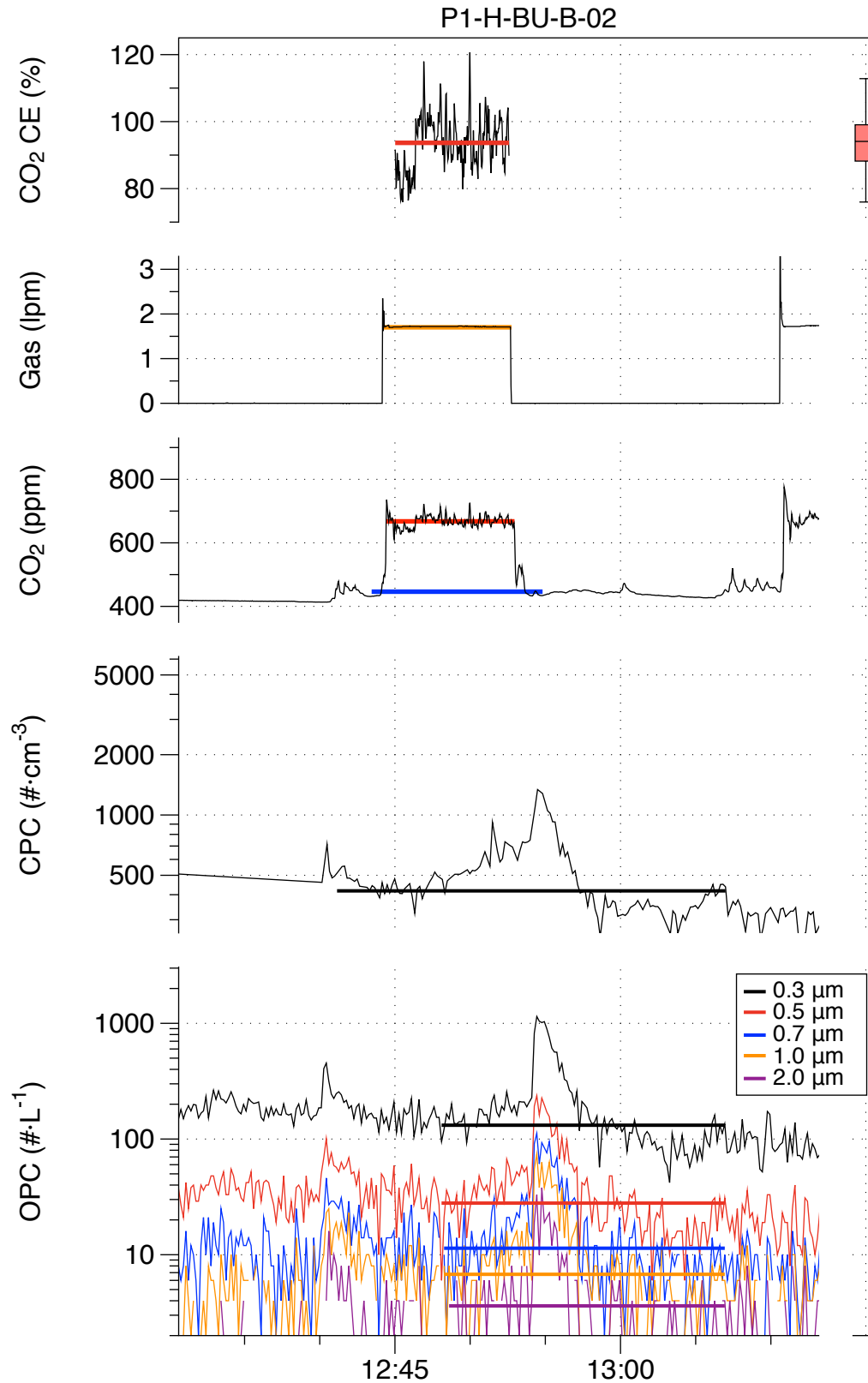


Figure H- 2. Results from experiment P1-H-BU-B-02: burger on back burner, Hood P1 on high speed.

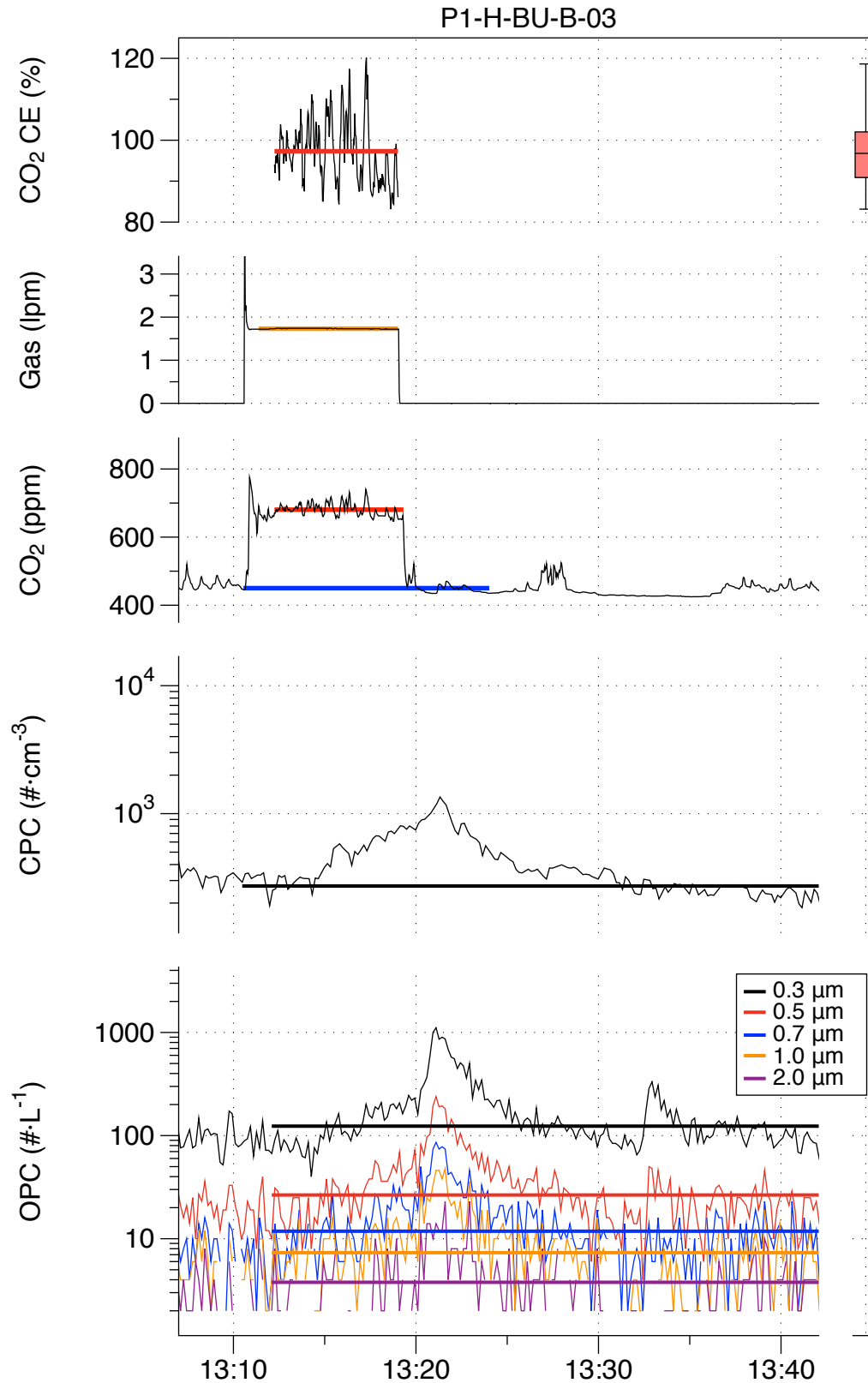


Figure H- 3. Results from experiment P1-H-BU-B-03: burger on back burner, Hood P1 on high speed.

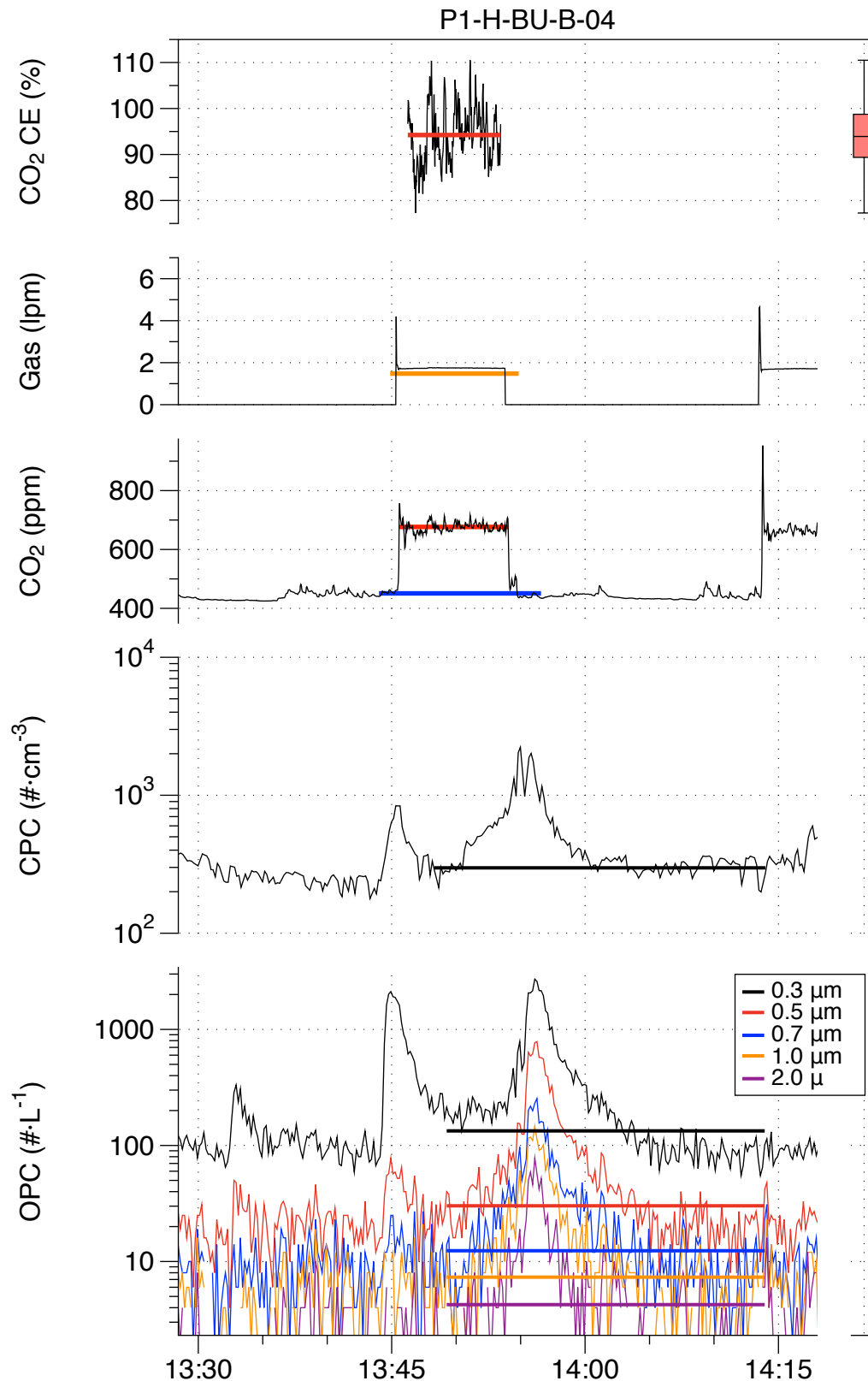


Figure H- 4. Results from experiment P1-H-BU-B-04: burger on back burner, Hood P1 on high speed.

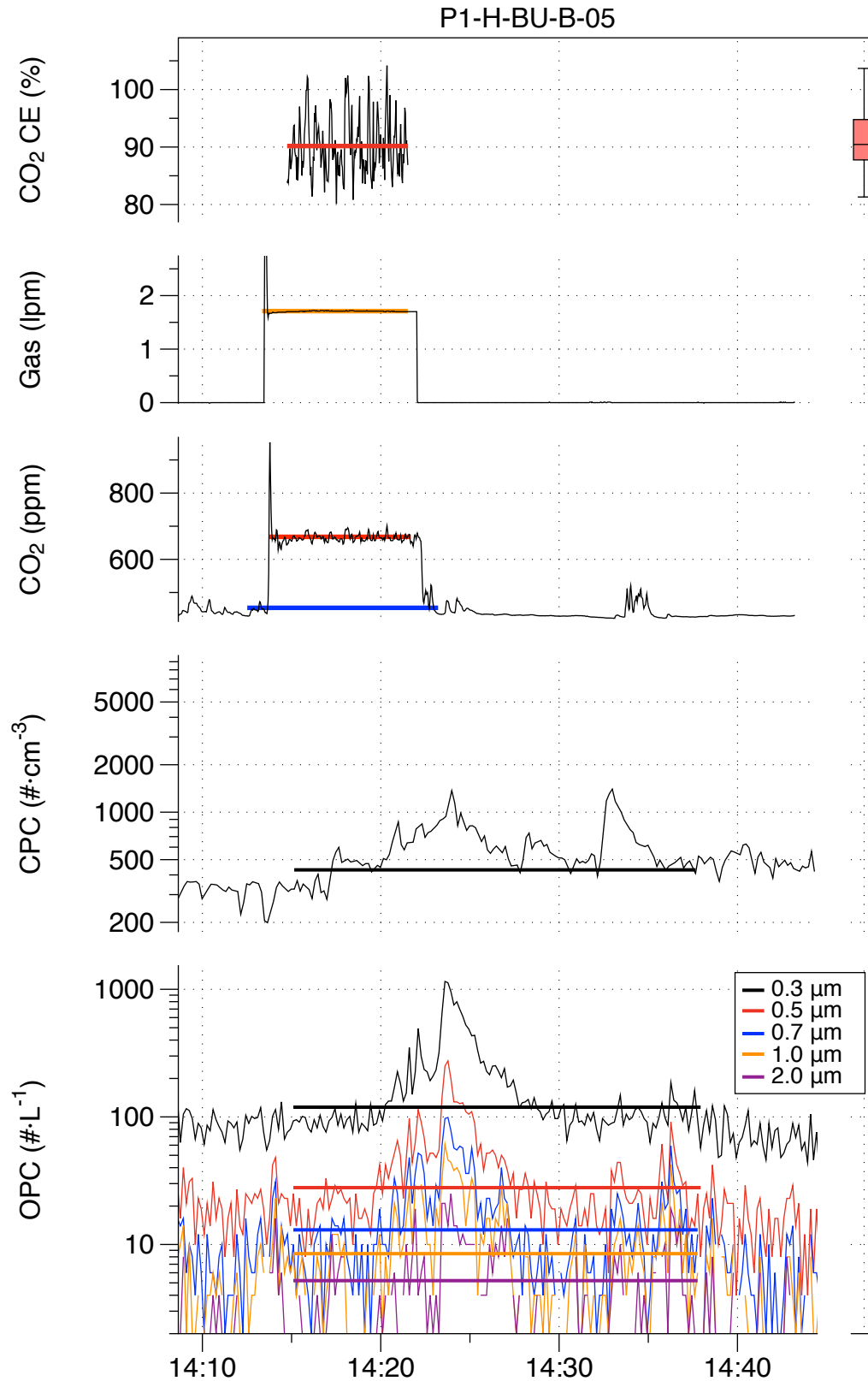


Figure H- 5. Results from experiment P1-H-BU-B-05: burger on back burner, Hood P1 on high speed.

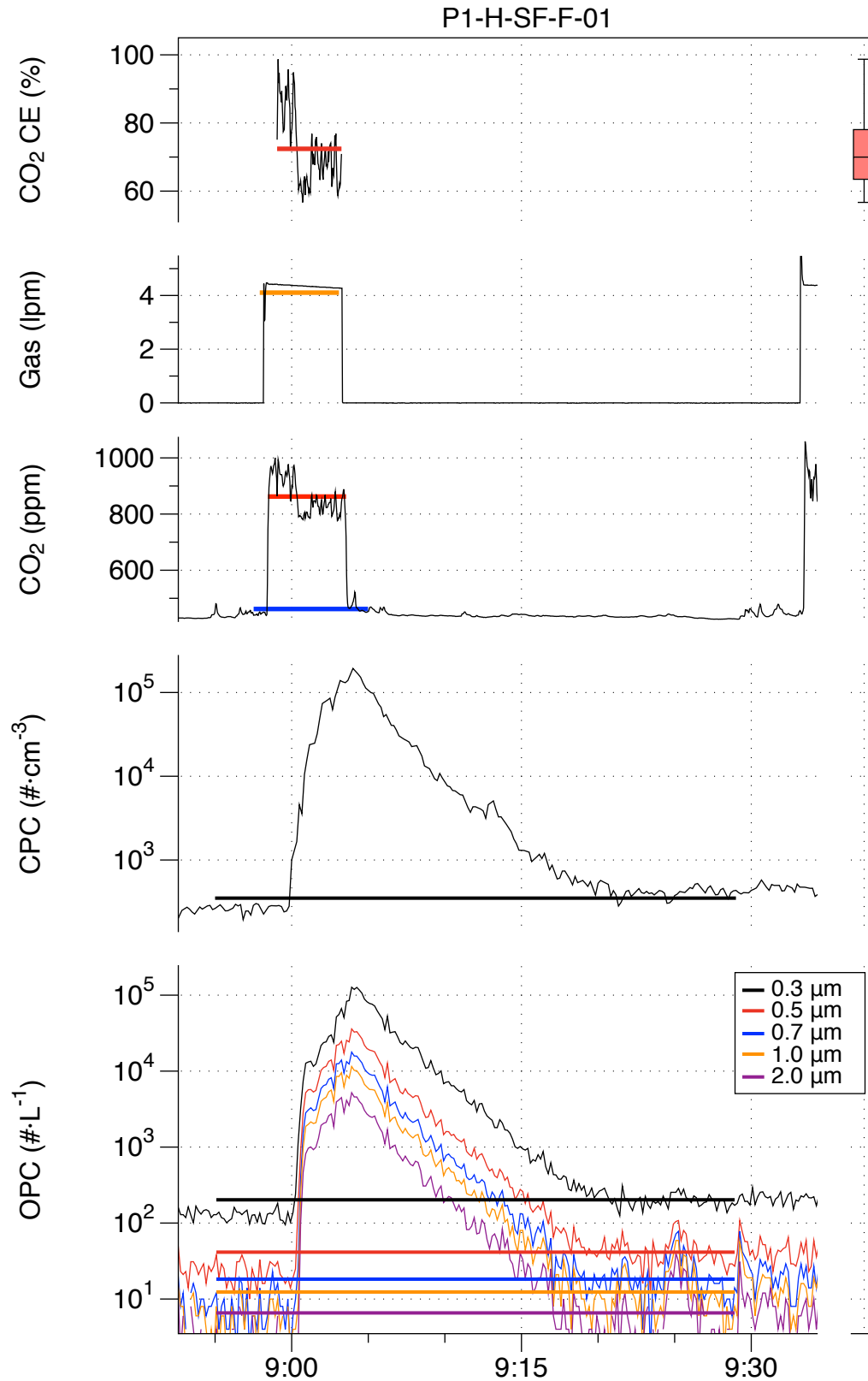


Figure H- 6. Results from experiment P1-H-SF-F-01: sir fry on front burner, Hood P1 on high speed.

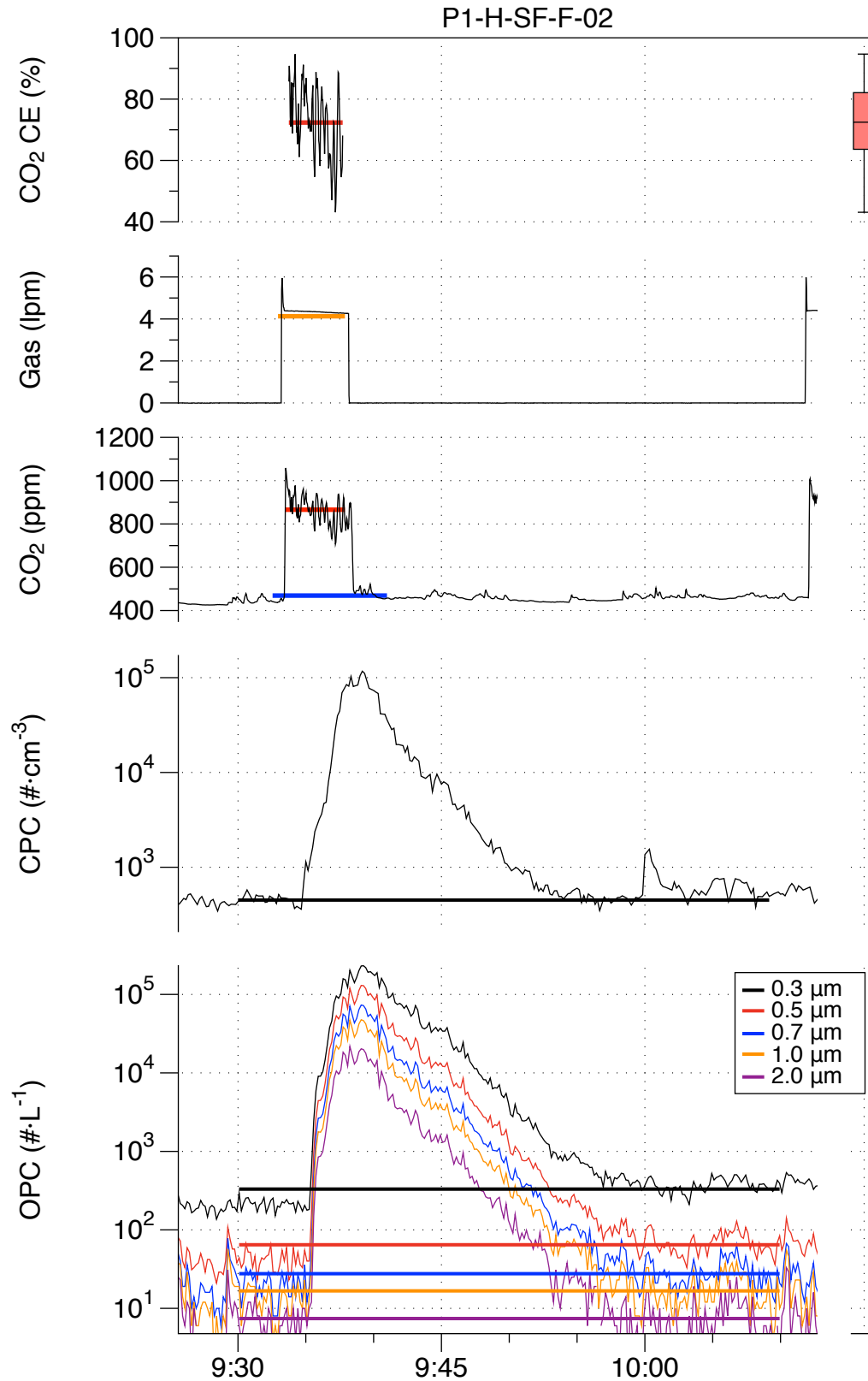


Figure H- 7. Results from experiment P1-H-SF-F-02: sir fry on front burner, Hood P1 on high speed.

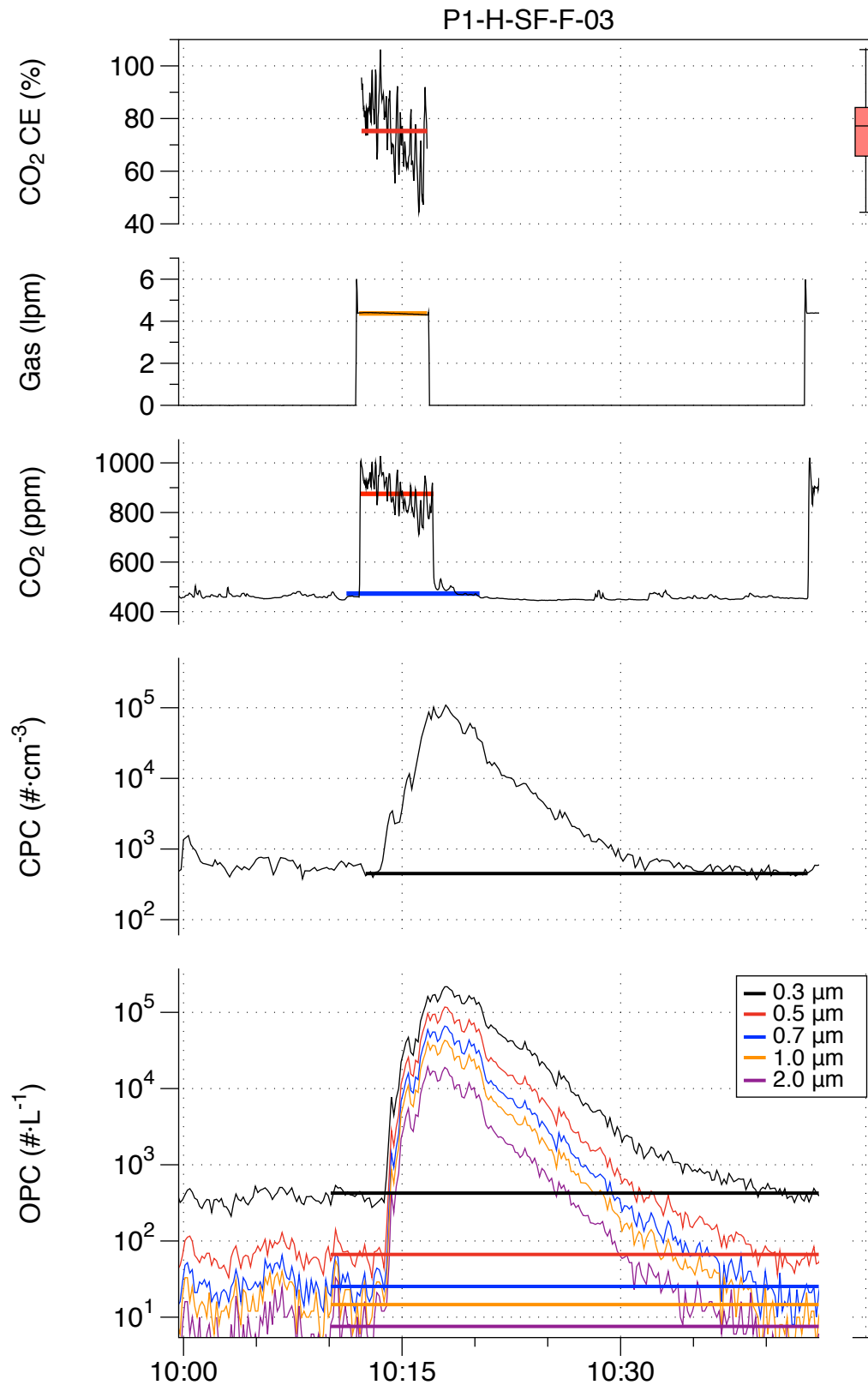


Figure H- 8. Results from experiment P1-H-SF-F-03: sir fry on front burner, Hood P1 on high speed.

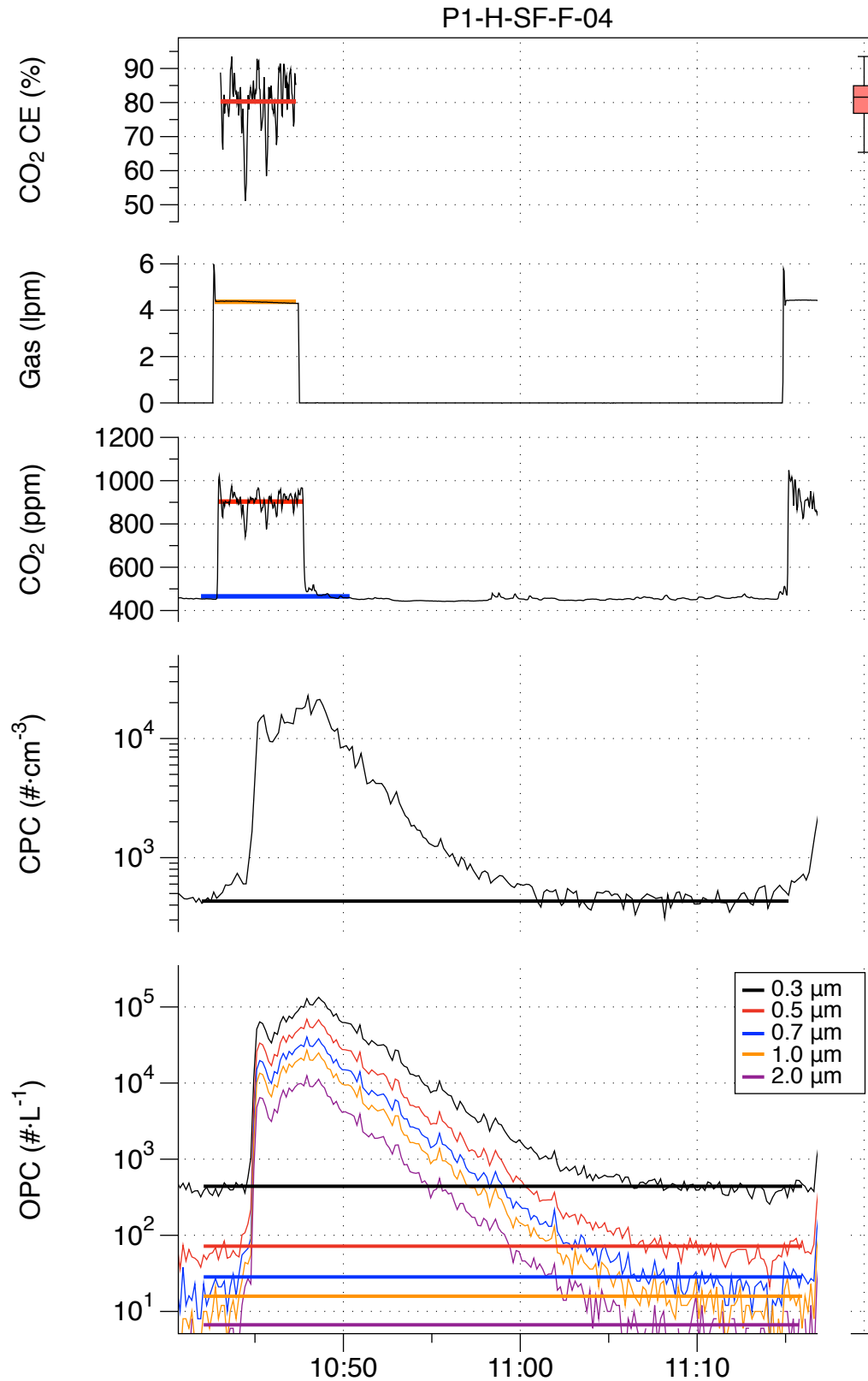


Figure H- 9. Results from experiment P1-H-SF-F-04: sir fry on front burner, Hood P1 on high speed.

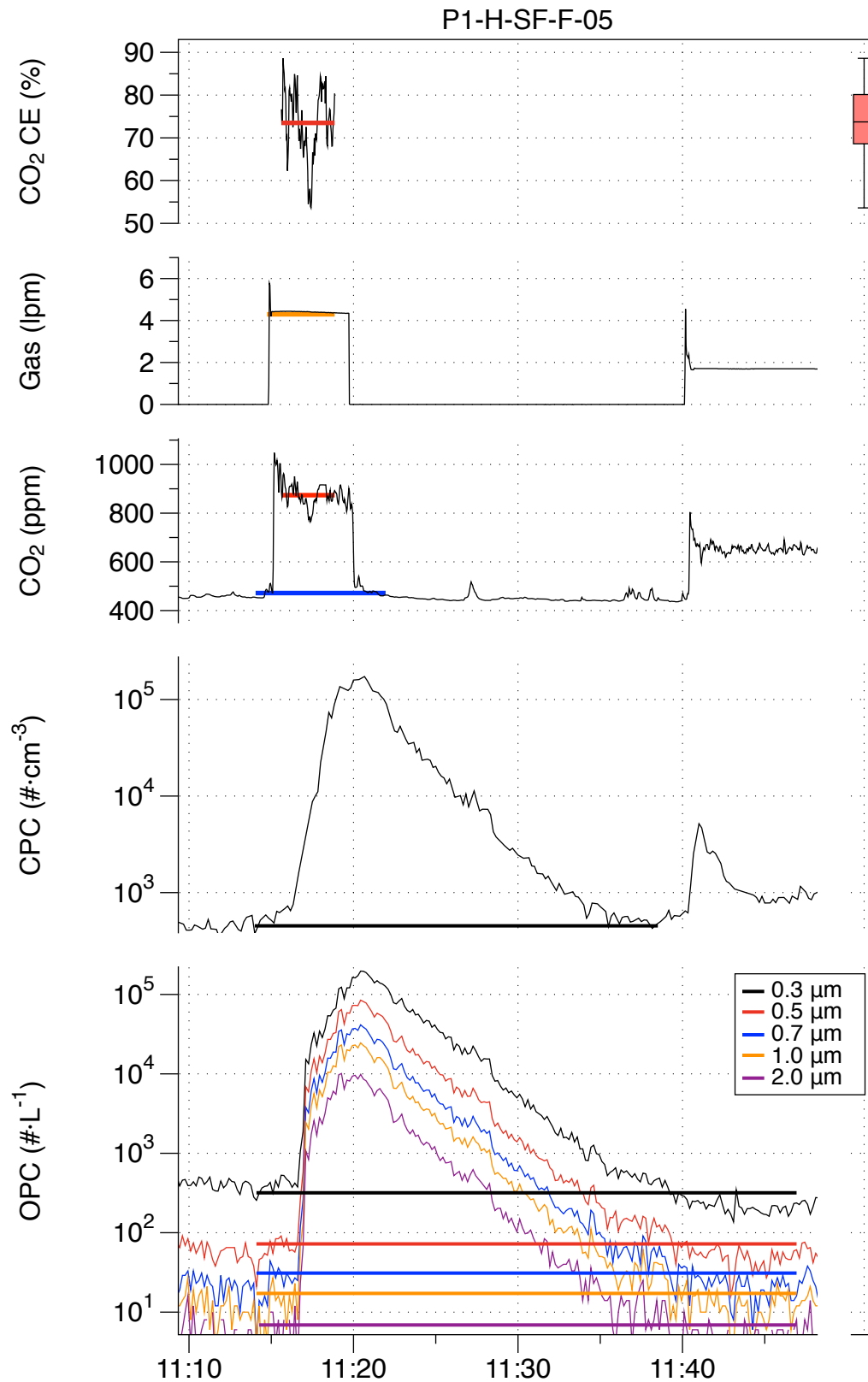


Figure H- 10. Results from experiment P1-H-SF-F-05: sir fry on front burner, Hood P1 on high speed.